

Stellingen behorende bij het proefschrift
'Classical and quantum charge dynamics in small tunnel junctions'
van Bart Geerligs

I

Daar de fundamentele relatie $I=e\dot{n}$ in een lang 1-dimensionaal array van tunneljuncties een gevolg is van de intrinsieke tijdsrelatie van tunnel gebeurtenissen, zal in de toekomst de nauwkeurigste stroomstandaard wellicht in een dergelijk systeem gerealiseerd kunnen worden.

II

Veelal is het voor de communicatie binnen een vakgroep aan te bevelen dat de leden minder tijd aan de communicatie naar buiten besteden.

III

Aangezien in tunneljuncties met een weerstand kleiner dan h/e^2 nog steeds Coulomb-blokkade optreedt, moet bij de interpretatie van metingen aan constricties in 2-dimensionale electronengassen, ook wanneer deze niet in pinch-off zijn rekening gehouden worden met het optreden van ladingseffekten.

IV

Net als ministers mogen co-auteurs om politieke redenen benoemd worden, hoeven ze niet in staat te zijn het gehele werk te verdedigen, maar aanvaarden ze wel verantwoordelijkheid voor de volledige inhoud.

V

Veel van de huidige experimenten aan ladingseffekten in kleine tunneljuncties zouden bij een geringe vermindering van de efficiëntie van elektron-fonon relaxatie niet goed uitvoerbaar zijn.

VI

Als de overheden er aan blijven hechten kerncentrales aan landsgrenzen te plaatsen, moet Europa 1992 vanuit dat oogpunt van harte verwelkomd worden.

VII

De Q in QPC (Quantum Punt Contact) is in de praktijk vaak een overbodige toevoeging: In veel experimenten blijkt het quantum karakter van de elektronen slechts uit de opdeling van de geleidingsband in kanalen en bewegen de elektronen in een kanaal (schijnbaar) klassiek door het puntkontakt.

VIII

Teneinde de eenzame filerijder uit zijn isolement te verlossen en daarmee mogelijk een meer sociaal rijgedrag te bevorderen verdient invoering op ruime schaal van de autotelefoon aanbeveling.

IX

De interpretatie van een gap in de I-V karakteristiek van een enkele junctie als zijnde een gevolg van Coulomb-blokkade van Cooper-paar tunneling [(M. Iansiti et al., Phys. Rev. Lett. **60**, 2414 (1988))] is slecht te verdedigen, daar blokkade van elektron tunneling niet waargenomen is en een klassieke verklaring beschikbaar is in de vorm van omgevings-resonanties.

X

De zogenaamde vrije wil kan slechts beperkt fluctueren om een statistisch genetisch bepaald gedrag (Richard Dawkins, The selfish gene, chapter 11).

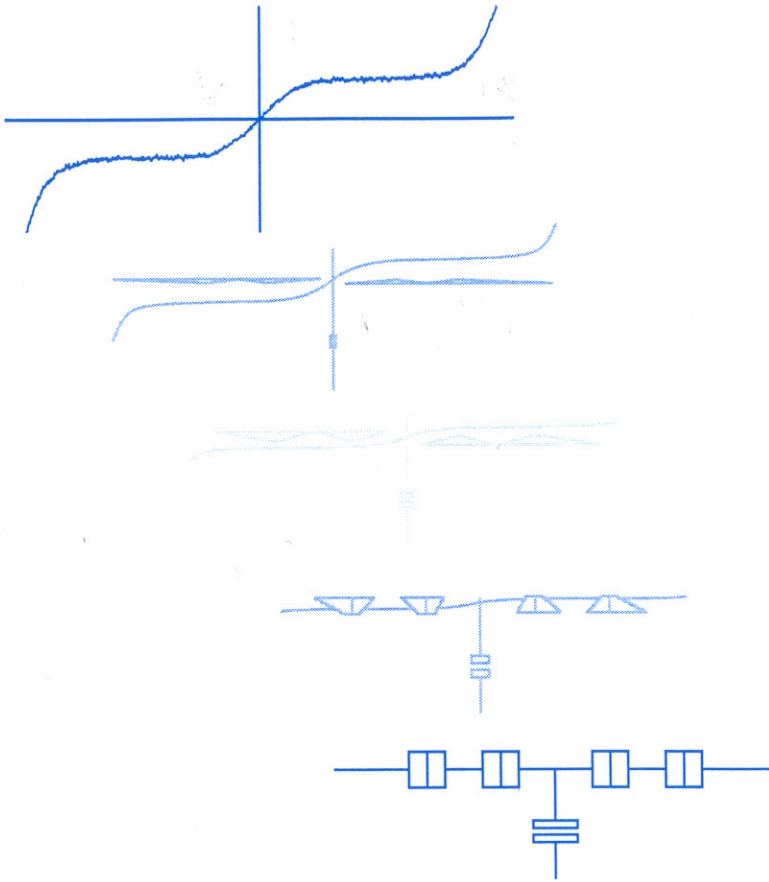
XI

De door Giordano [Phys. Rev. Lett. **63**, 2417 (1989)] waargenomen resonanties in de I-V karakteristiek van een submicron lijntje hebben waarschijnlijk meer met de korreligheid van zijn materiaal te maken dan met resonant tunnelen.

XII

In een quantum-dot gedefinieerd tussen twee puntkontakten, kan door uit-fase modulatie van de puntkontakten ook zonder ladingseffekten een door de modulatie-frekwentie bepaalde stroom gerealiseerd worden.

CLASSICAL AND QUANTUM CHARGE DYNAMICS IN SMALL TUNNEL JUNCTIONS



Bart Geerligs

**CLASSICAL AND QUANTUM CHARGE DYNAMICS
IN SMALL TUNNEL JUNCTIONS**

*Voor mijn ouders
en mijn grootouders*

**CLASSICAL AND QUANTUM CHARGE DYNAMICS
IN SMALL TUNNEL JUNCTIONS**

Proefschrift ter verkrijging van de graad van doctor
aan de Technische Universiteit Delft,
op gezag van de Rector Magnificus, prof. drs. P.A. Schenck,
in het openbaar te verdedigen ten overstaan van een commissie
aangewezen door het College van Dekanen, op

dinsdag 6 november 1990 te 16.00 uur

door

Lambert Johan Geerligs

geboren te Rotterdam

doctorandus in de natuurkunde

Dit proefschrift is goedgekeurd door de promotor prof. dr. ir. J.E. Mooij

Het onderzoek beschreven in dit proefschrift is financieel ondersteund door de
Stichting voor Fundamenteel Onderzoek der Materie (FOM)

TABLE OF CONTENTS

Chapter 1	Introduction	1
Chapter 2	Charge dynamics in normal metal tunnel junctions	5
I	Introduction	5
II	Classical theory for Coulomb blockade	8
III	Practical use of Coulomb blockade of electron tunneling	19
IV	Perturbative correction to the classical theory for Coulomb blockade	30
V	Quantum charge fluctuations in a non-perturbative approach	36
VI	Conclusions	40
	References	41
Chapter 3	Charge and phase dynamics in Josephson tunnel junctions	45
I	Introduction	45
II	Experimental techniques and junction characterization	50
A	Experimental techniques	50
B	Junction characteristics	53
III	Experimental results for voltage biased systems	57
A	Single junctions	59
B	Double junctions	63
C	Three junctions in series	69
D	Five junctions in series	71
E	Magnetic field effects	73
IV	Discussion of the results	74
A	Environmental resonances	74
B	Coherent tunneling for small voltages	76
C	Alternating Cooper-pair and quasiparticle tunneling for high voltages	78
D	Frequency-dependent damping in the phase-regime	80
V	Single junctions in a high impedance environment	81
VI	Frequency-controlled Cooper-pair tunneling	83

A	Theory	84
B	Preliminary measurements	89
VII	Conclusions	91
	References	91
Chapter 4	Frequency-locked turnstile device for single electrons	95
	Deviation of current quantization due to quantum leakage	104
Chapter 5	Observation of macroscopic quantum tunneling of the electric charge	107
Chapter 6	Influence of dissipation on the Coulomb blockade in small tunnel junctions	116
Chapter 7	Single Cooper-pair tunneling in small capacitance junctions	125
Chapter 8	Unbinding of charge-anticharge pairs in two-dimensional arrays of small tunnel junctions	134
Chapter 9	Charging effects and quantum coherence in regular Josephson junction arrays	143
	Correction due to capacitance renormalization on the superconductor-insulator phase transition	152
	Summary	154
	Samenvatting	156
	Vitals	159

CHAPTER 1

INTRODUCTION

The research described in this thesis started in Delft in 1986, as part of the research program of the Solid State Physics group at the Department of Applied Physics. At that time, renewed interest had arisen in tunnel junctions with very small capacitance [1]. Long before, several investigations [2] had shown the effect of small capacitance on tunneling of electrons in granular material. However, it was only when tunnel junctions of sufficiently small capacitance could be fabricated artificially, that this field gained intensive attention. Practical considerations certainly played a role. Likharev realized that time correlation of tunneling events, enforced by the small capacitance, would yield a practical possibility of observation of the fundamental relation $I=ef$. It was and is also becoming increasingly clear that single electron charging effects may be very important in future integrated circuit technology [3].

The group of Hans Mooij in Delft, with large experience in the fabrication of tunnel junctions and facilities for submicron lithography available in the Centre for Submicron Technology nearby, was the obvious place to start examining these effects experimentally. At the same time a theoretical group around Gerd Schön was set up at the same Department, focussing on the same subject. Delft has now obtained a good position for playing an important role in the future development of this field, which will attract increasing attention in the coming years.

The following two chapters of this thesis cover a broad range of charging effects in normal metal and in superconducting tunnel junctions, respectively. They are intended as an introduction to nearly all the consequences of small junction capacitance which have so far turned out to be experimentally accessible. For the normal metal junctions, good quantitative agreement with theory is obtained, both for classical charge dynamics and for quantum charge fluctuations due to a low tunnel resistance. The chapter on superconducting tunnel junctions is more intended as the author's qualitative view on how to understand the observed behavior of these junctions. It emphasizes the importance of more theoretical work on realistic model systems. The following chapters consider more detailed several topics of the first two chapters. Chapter four covers the single-electron turnstile device that creates a frequency-locked current or charge source, by transferring one single electron for each cycle of an external control voltage. Chapter five provides evidence of higher order perturbative contributions to tunneling of the electric charge in turnstile-like junction arrays of high tunnel resistance. Chapter six considers the effects of low tunnel

resistance on charge fluctuations, again in normal metal junctions. It also shows the destructive influence of a low-impedance environment on charging effects in single junctions. In chapter seven, linear arrays of superconducting junctions are found to obey classical charge dynamics for sufficiently low capacitance. The final two chapters cover charging effects in large 2-dimensional junction arrays. Arrays of small normal metal junctions are a system where the excess charges on the islands interact logarithmically. Since these excess charges are quantized, the arrays are a representation of a two-dimensional Coulomb gas, and will thus exhibit a Kosterlitz-Thouless phase transition. Below the transition temperature, the charges are bound in pairs, and cannot provide electrical conduction. Therefore, these arrays are isolating at very low temperature. This phase transition between isolating and resistive behavior is the subject of chapter eight. In the superconducting state a similar transition may occur for Cooper-pair charge-anti charge pairs, again resulting in isolating behavior at low temperatures. However, in the superconducting state charge fluctuations due to the Josephson coupling can produce free charges and result in conduction. Again a phase transition occurs, but now as a function of Josephson coupling energy relative to Coulomb energy, and separating superconducting and isolating low temperature behavior. This is the subject of chapter nine. Actually in chapter eight a similar phase transition is discussed, with the barrier transparency as the critical parameter. In chapter eight it is also shown that the charge excitations cause a spatially decaying charge polarization of the neighboring junctions. Moving charges therefore cause a sort of spiky current bias of the junctions in the array. This may be the reason that the I-V curves of superconducting arrays, as reported in chapter nine, have features that are predicted for single current-biased junctions. Where macroscopic quantum interference has not yet been observed in single junctions, probably due to the problems of realizing a current bias for a single junction, the arrays so far provide the only indications for exciting phenomena like Bloch oscillations and Zener tunneling of macroscopic variables.

The reader may, like the author, feel surprised by the difference between normal and superconducting state as far as fit of theories to experiments is concerned. In the low voltage regime of normal junction arrays, a nearly perfect agreement with the theory seems to be rule. In contrast, the superconducting arrays exhibit a wealth of phenomena which are so far at best qualitatively understood. Several reasons account for more complicated results in the superconducting state. The non-linear quasiparticle resistance, strongly temperature dependent, is one of them. The presence of both Cooper-pairs and quasiparticles, with different dependences of the tunneling rate on the charging energy change, is another. The fact that Cooper-pairs do not only tunnel through a single junction but, due to their condensation in a macroscopic coherent

wave function, can often tunnel through several junctions at a significant rate, is also a complicating feature. The ac Josephson relation makes the junction dynamics strongly dependent on the resonance modes in the environment. Since we did not pay much attention to control of these environmental modes, at least until some recent experiments, this sensitivity makes the reported experiments certainly also more difficult to interpret. An awarding direction of future research may focus on arrays of junctions in the superconducting state, in a controlled environment. Also in the normal state, one possible next step in fundamental research concentrates on the interaction with the environment. To indicate some other open fields of research, one may search for the single-junction SET or Bloch oscillations, concentrate on the superconducting equivalent of the turnstile, or examine device applications.

Most of the time I felt very fortunate to be able to do research on charging effects, for several reasons. It is attractive to start experimental work in a new field, where very few results are yet present but many theoretical predictions have been made and theoreticians are anxious for experimental confirmation of their work [4]. For an experimentalist the project offered the perfect blend of fascinating physics, state of the art technology and a fair amount of competition, with prospects of very rewarding results. One could even convince oneself that the work was really worth to spend so much time on, both from the viewpoint of fundamental physics (as a testcase for macroscopic quantum mechanics) and applications (a new current standard, a new class of submicron electronics devices).

Many people have contributed to this research, first of all of course Hans Mooij. I thank Kees van der Jeugd, Michiel Peters, Valérie Anderegg, Edwin Lenderink, Jeroen Walta and Peter Plooij for pleasant collaboration in the experiments, and everything around it. Special thanks go to the people from the Groupe Quantronique in Gif-sur-Yvette, Hugues Pothier, Daniel Esteve, Cristian Urbina and Michel Devoret. They are great physicists and have had a very important part in making this research successful. I have profited much from the experience of my room-mates Peter van der Hamer and Sjaak Schellingerhout. Dima Averin is gratefully acknowledged for his contributions to chapters five and seven. I am indebted to Huub Appelboom, Rosario Fazio, Uli Geigenmüller, Peter Hadley, Kees Harmans, Leo Kouwenhoven, Kostya Likharev, Dick van der Marel, John Martinis, Gerd Schön, Bart van Wees, Mark van Wees and Herre van der Zant for valuable advice and discussions. Finally, I would like to thank Chris Gorter, Bram Huis and Jan Kortlandt for their much appreciated technical assistance.

The Centre for Submicron Technology in Delft, now part of the Delft Institute for Microelectronics and Submicron Technology (DIMES), has provided essential facilities for the lithography.

REFERENCES

1. Widom *et al.*, J. Phys. A **15**, 3877 (1982) and K.K. Likharev and A.B. Zorin, in Proc. 17th Int. Conf. on Low Temp. Phys., eds. U. Eckern *et al.* (North-Holland, Amsterdam, 1984), p. 1153. See also various contributions in SQUID'85, eds. H.D. Hahlbohm and H. Lübbig (Walter de Gruyter, Berlin, 1985).
2. C.J. Gorter, Physica **17**, 777 (1951); I. Giaever and H.R. Zeller, Phys. Rev. Lett. **20**, 1504 (1968); J. Lambe and R.C. Jaklevic, Phys. Rev. Lett. **22**, 1371 (1969).
3. See, e.g., the proceedings of the NATO Advanced Study Institute on Granular Nanoelectronics, Il Ciocco, Italy, July 1990 (Plenum, New York, to be published).
4. Or should they at most hope for invalidation of competing theories? [M.H. Devoret, J.M. Martinis and J. Clarke, Phys. Rev. Lett. **63**, 212 (1989)]

CHAPTER 2

CHARGE DYNAMICS IN NORMAL METAL TUNNEL JUNCTIONS

I INTRODUCTION

In materials consisting of small metal grains, coupled by tunnel barriers, at low temperatures the electrical properties are strongly influenced by charging effects resulting from the small capacitance of the grains. Because charge is transferred in discrete units (e for normal metal junctions, $2e$ or e for superconducting tunnel junctions), the energy change of the system during tunneling can be significant. If the energy of the system would increase, the tunneling is forbidden at zero temperature. This phenomenon is called Coulomb blockade of (electron) tunneling. Typical energy changes are of order $E_C \equiv e^2/2C$, so that the temperature must be below E_C/k_B to observe charging effects. Already in 1951 this effect of small grain capacitance was appreciated as well as observed experimentally (Gorter 1951, see also Giaever and Zeller 1968, 1969, Lambe and Jaklevic 1969).

With the advance of submicron lithography it has become possible to artificially produce planar tunnel junctions with capacitance as small as 10^{-16} F, for which charging effects can be observed at liquid helium temperatures (although for most experiments the lower temperatures attainable in a dilution refrigerator are still useful). Many experiments have confirmed the basic theoretical description of these charging effects. We will present this basic theory and the related experiments on artificial tunnel junctions in section II. We will not discuss the experiments on granular systems (Kuzmin and Likharev 1987, Barner and Ruggiero 1987, van Bentum *et al.* 1988a and 1988b, Kuzmin and Safronov 1988, Wilkins *et al.* 1989) that have also provided convincing confirmation of the basic theory. Especially the recent possibility of using a scanning tunneling microscope on granular material allowed for observation of charging effects at much higher temperatures ($C \approx 10^{-18}$ F, or $E_C/k_B > 100$ K). However, this configuration is less flexible in device design and control of parameters.

In section III we will discuss the applicability of small tunnel junctions for practical purposes. As an example the single electron turnstile that has recently been developed together with the CEN Saclay (Geerligs *et al.* 1990) will be discussed in more detail, since it shows the possibility of controlling charge transfer at the single electron level.

Coulomb blockade of electron tunneling is not absolute. Passing of an electron through several

junctions in one process may be energetically favorable, even if the intermediate states where the electron resides on the electrodes between the junctions, have a high energy. This process is predicted to occur at a rate inversely proportional to the product of the junction resistances. It has been named macroscopic quantum tunneling of the charge, since this tunneling of a single electron corresponds to tunneling of the charge state of the total system through an energy barrier. This extension of the basic theory, which is valid only for high junction tunnel resistance (compared to the resistance quantum h/e^2), will be discussed in section IV, together with experiments. These results are important for practical applications based on high-resistance junctions, especially single-electronic logic circuits like the turnstile.

Finally, in section V we discuss the role of highly dissipative environments, that cause the breakdown of Coulomb blockade in single tunnel junctions or junctions of low tunnel resistance.

In this chapter we will consider some examples of the macroscopic quantum effects that arise from the non-commutivity of phase and charge. However, the presented experiments remain restricted to junctions of normal metal. In superconducting tunnel junctions, more prominent macroscopic quantum phenomena are expected to arise. Experimental results are presented in the next chapter. We also refer to two reviews, by Averin and Likharev (1990), and Schön and Zaikin (1990) that provide a thorough, mostly theoretical, overview of this subject. We also only mention here that Coulomb blockade effects have probably been observed recently in split-gate confined GaAs-AlGaAs heterostructures (Scott-Thomas *et al.* 1989, van Houten and Beenakker 1989, Meirav *et al.* 1989, Field *et al.* 1990, Kouwenhoven 1990, Brown *et al.* 1990). However, in these systems the description is necessarily more complicated due to e.g. the discreteness of single-particle levels.

The experiments that will be presented have all been performed on aluminum tunnel junctions. These junctions have been brought in the normal state by applying a high magnetic field (typically 2 T). We have found no reason to suspect that the field affects the physics of the Coulomb blockade in a measurable way.

A junction area of $(100 \text{ nm})^2$ yields a capacitance of about 10^{-15} F , depending on the barrier thickness. The smallest planar junctions that have been produced so far (Fulton and Dolan 1987, Kuzmin *et al.* 1989, Geerligs *et al.* 1989) were all fabricated from aluminum. For such a small junction area, useful tunnel resistances (of around $100 \text{ k}\Omega$) are obtained if the aluminum is thermally oxidized at room temperature in oxygen at a pressure of about 1 mbar to create the tunnel barrier. Together with the requirement of high purity metal electrodes this low oxidation pressure means that the total junction be preferably fabricated in one vacuum cycle. This is

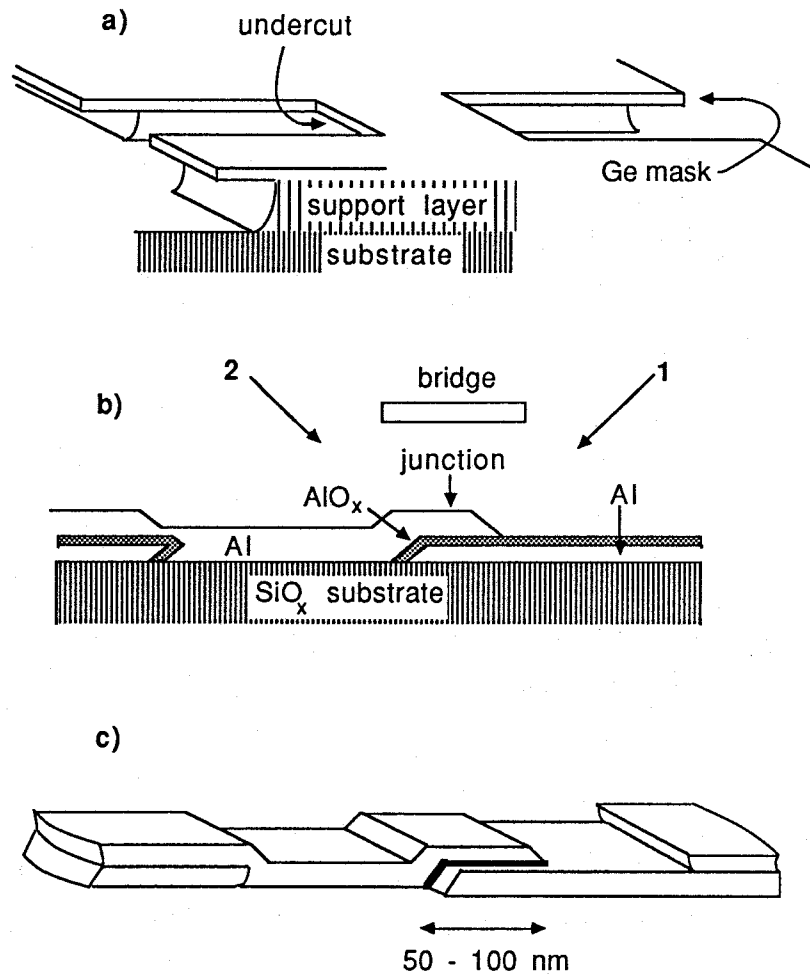


Fig. 1. Processing steps for shadow evaporation of a tunnel junction. (a) Suspended mask. (b) Oblique angle evaporation. (c) The resulting planar junction.

conventionally done by shadow evaporation (Fig. 1). A mask is suspended at around 200 nm above the (oxidized silicon) substrate. The mask is patterned by conventional submicron lithography. The supporting layer for the mask is an organic material (e.g. resist) that can be undercut by isotropic etching, either wet or with reactive ion etching. The two electrodes of a junction are evaporated from two angles. A mask patterned with a small channel interrupted by a bridge, thus results in a junction because of the interruption of the aluminum strips by the bridge shadow. On both sides of the junction the leads are actually also composed of a double aluminum layer with oxide barrier in between, i.e. the leads are large junctions. This creation of large junctions in series with the small ones can be partly avoided by using a slightly different geometry (see e.g. Fulton and Dolan 1987 or Kuzmin *et al.* 1989). A photograph of a two-dimensional array of junctions fabricated in this way is given in Fig. 2. This fabrication procedure has proven

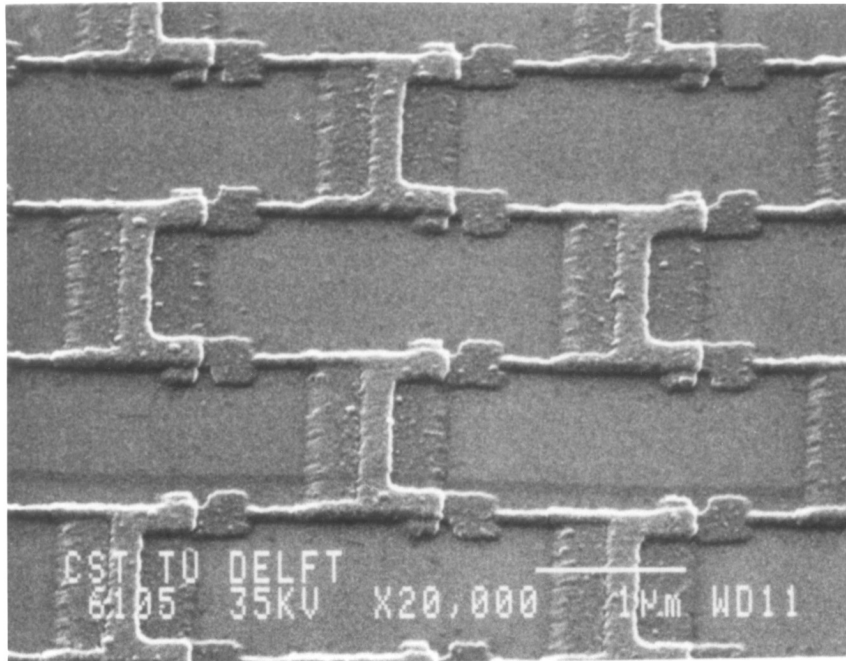


Fig. 2. Scanning electron microscope photograph of an array of small tunnel junctions produced by shadow evaporation. The white bar is 1 μm long.

to be sufficient for creating junctions with area down to $(30 \text{ nm})^2$. For significantly smaller dimensions, probably new methods have to be developed.

II CLASSICAL THEORY FOR COULOMB BLOCKADE

In this section we consider tunnel junctions with high tunnel resistance, $R_t \gg \hbar/e^2$. The charge transport through the junction can then be calculated by treating the charge Q on the junction as a classical variable. The charge can change in a *continuous* way by applying a polarizing voltage to the junction. Trapped charges in the oxide barrier of the junction or in the substrate close to the junction likewise provide the possibility of the junction having an offset charge in the absence of an applied voltage. The junction charge can change stochastically due to tunneling events during which *discrete* charge units are transferred across the barrier.

The rate for a tunneling process is determined by the energy change $\Delta E = E_f - E_i$ during tunneling (Averin and Likharev 1986):

$$\Gamma(\Delta E, T) = \frac{\Delta E}{e^2 R_t} [\exp(\Delta E/k_B T) - 1]^{-1} \quad (1)$$

For $|\Delta E| \gg k_B T$:

$$\Gamma(\Delta E) \approx \begin{cases} -\frac{\Delta E}{e^2 R_t} & \text{for } \Delta E < 0 \\ 0 & \text{for } \Delta E > 0 \end{cases} \quad (1a)$$

The relevant energy change is the change in free energy, the sum of the capacitive energies in the system and the work performed by the voltage sources (Likharev 1988, Bakhvalov *et al.* 1989):

$$E = \sum_i \frac{Q_i^2}{2C_i} - \sum_j Q_{tj} V_j \quad (2)$$

The index i denotes summation over tunnel junctions as well as true capacitors, the summation in j is over all voltages sources in the system. Q_{tj} denotes the charge transferred through voltage source V_j . Note that a large stray capacitor on a chip can act as a voltage source and change an experimentally applied current bias for high frequencies into a voltage bias. This is often the case in experiments.

For a circuit consisting only of capacitors and voltage sources, eq. (2) can be reduced to a simpler form for each individual junction (Esteve 1990). Using Thevenin's rule the circuit to which the junction is coupled is reduced to an equivalent capacitor C_e in series with a voltage source V_e (Fig. 3). In the expression for ΔE , V_e and the charge on C_e cancel so that the energy change during tunneling depends only on junction charge Q and a critical charge Q_c (to be calculated for each junction individually):

$$\Delta E = -\frac{e}{C} (Q - Q_c) \quad (3)$$

with

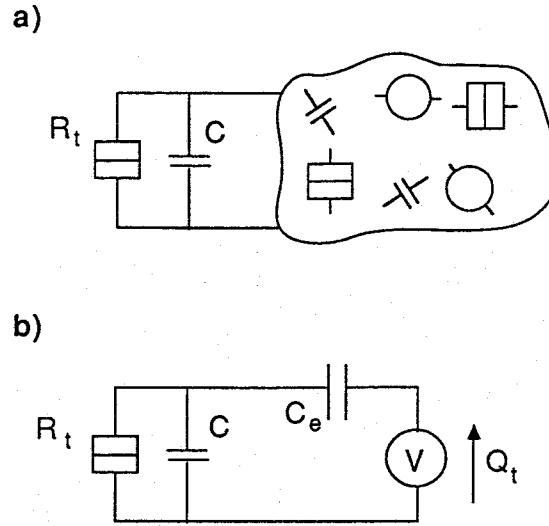


Fig. 3. The reduction of a junction environment consisting of voltage sources and capacitors (a) to an equivalent circuit with one equivalent capacitor C_e and one voltage source. The charge Q_t transferred through the voltage source is relevant for the energy change during tunneling.

$$Q_c = \frac{e}{2}(1 + C_e/C)^{-1} \quad (4)$$

At low temperature, an electron can tunnel only if $|Q| > Q_c$: the junction will show a Coulomb gap (threshold voltage for conduction) of Q_c/C . This concept of a critical charge is useful to calculate the tunneling characteristics of complicated systems subject to charging effects. Here we will use it to consider several simple cases. A single junction biased via a very small capacitor (e.g. Büttiker 1986) will show a Coulomb gap $e/2C$. Two equal junctions in series each have $Q_c=e/4$. A double junction will therefore show a total Coulomb gap $e/2C$. Likewise, n equal junctions in series have a Coulomb gap $(n-1)e/2C$. This Coulomb gap can be influenced by charging the metal islands between the junctions, a possibility that is discussed below.

First we consider a special case, the current biased single junction (Averin and Likharev 1986). In the bias scheme of Büttiker (1986), it could be realized by a series circuit of the junction with a very small classical capacitor C_e . Applying a linearly increasing voltage bias $V=\alpha t$, the junction is subject to a current $I_x=C_e(dV/dt)=\alpha C_e$. We can suppose $C_e \approx 0$ (keeping αC_e constant) so that $Q_c=e/2$. The externally applied current I_x induces a smooth time evolution of the charge on the junction:

$$\frac{dQ}{dt} = I_x + \left. \frac{dQ}{dt} \right|_{\text{tunneling}} \quad (5)$$

If the current is small compared to $e/R_t C$ a tunneling event will occur at a charge only slightly larger than $e/2$, changing the charge on the junction to about $-e/2$. Then it takes a time period e/I_x to recharge the junction for a new tunneling event. At $T=0$ and small current the resulting dc I-V curve has a parabolic shape:

$$\langle V \rangle = \sqrt{\frac{\pi I_x R_t e}{2C}} \quad (6)$$

At larger currents the I-V curve approaches a linear form with voltage offset $e/2C$ and slope $1/R_t$. At low currents the tunneling events are correlated in time. The voltage noise spectrum will peak at the Single Electron Tunneling frequency $f_{SET} = I_x/e$ and harmonics. By applying a high-frequency alternating current (frequency f) in addition to the dc current, resonances should occur in the I-V curve at currents $I = \frac{n}{m} e \cdot f$. This has not yet been observed, but a similar phenomenon has been observed in long 1-dimensional arrays of tunnel junctions (Delsing *et al.* 1989b), where for a different reason also time correlation of tunneling events occurs (Likharev *et al.* 1989, Bakhvalov *et al.* 1989). In a chain of junctions the current is carried by mutually repulsing charge solitons. A charge soliton consists of a charged metal island between two junctions, together with the associated polarization of the neighboring junctions. Due to the repulsion the charge is transferred in a train of regularly spaced solitons. On a given junction, a tunneling event occurs each time a soliton passes. Therefore the tunneling events are again correlated in time. Delsing *et al.* (1989b) have observed that under high frequency irradiation the I-V curve of such an array shows resonances in the differential resistance at $I=e \cdot f$ and $I=2e \cdot f$.

The ratio of the junction capacitance to the self-capacitance C_0 of the islands between the junctions determines the size of a soliton. The junction charge in a soliton decays as

$$Q = \frac{e}{\sqrt{1 + 4C_0/C}} [1 - \exp(-1/\Lambda)] \exp(-d/\Lambda) \quad (7)$$

where d is the distance, in number of junctions, from the soliton center (the charged island) and

the decay length is given by $\Lambda^{-1} = \text{arccosh}(1 + C_0/2C)$. On a given junction the charge increases in small steps if the soliton approaches, decreases by e if the soliton passes, and after tunneling again increases smoothly in time if one soliton moves away and a new approaches. Therefore chains of tunnel junctions, but also 2-D arrays of junctions (Mooij *et al.* 1990) can be used to provide a current bias in a single junction. Fig. 4 shows the I-V curve of a single junction in a 4-wire measurement. In each lead close to the junction a 90×9 junction array was incorporated to ensure current bias or (for the voltage leads) decouple the junction from the environment. The I-V curve shows the asymptotic linear behavior (inset) from which junction resistance and capacitance can be determined. With these two parameters the experimental I-V curve can be compared to the theory without fitting. The agreement is very good, showing that normal metal junction arrays can indeed provide a good current bias and decoupling from the environment.

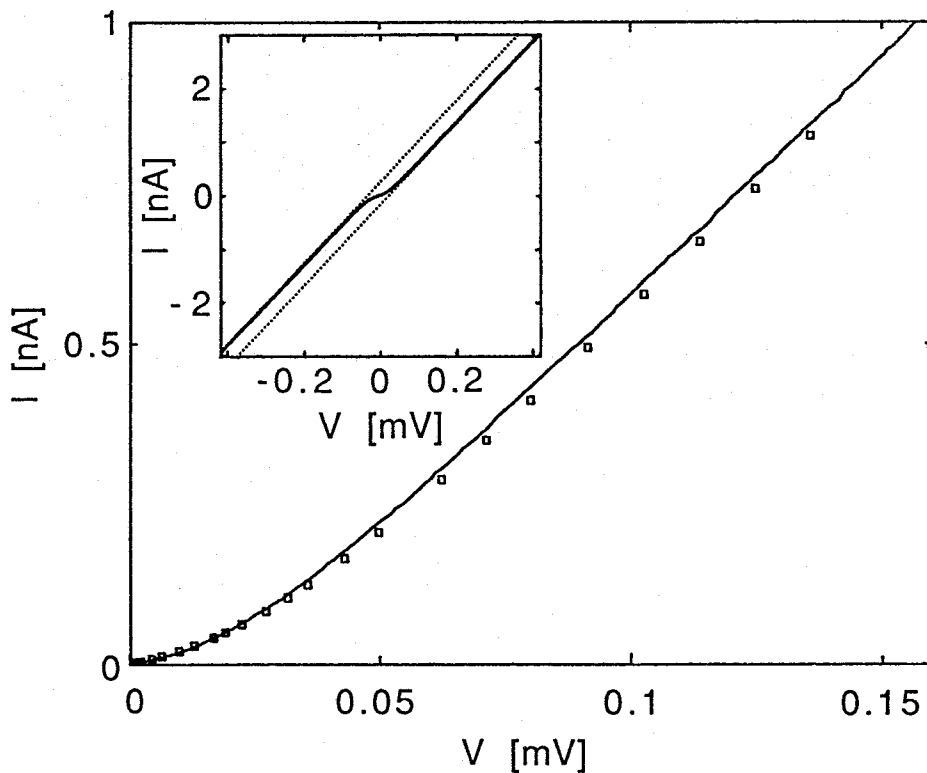


Fig. 4. I-V curve of a small current biased tunnel junction at a temperature of 55 mK. The current bias is possible because the junction is decoupled from the environment by 2-D junction arrays (90 junctions long, 9 wide) in the leads. The junction resistance and capacitance as determined from the I-V curve asymptote (inset) are $R_1 = 132 \text{ k}\Omega$ and $C = 2.9 \text{ fF}$. These parameters yield a theoretical prediction for the small-signal I-V curve (open boxes) in good agreement with the measurement.

For the rest of the chapter we restrict ourselves to voltage biased systems of two or more junctions (Fulton and Dolan 1987, Mullen *et al.* 1988, Likharev 1988). These are configurations that are easily realized experimentally. In addition they provide possibility for extra control of electron motion. The metal islands between the junctions always have a self-capacitance, i.e. a capacitance to ground. They can also be purposely coupled capacitively to a gate electrode. This provides an extra possibility to charge the junctions, apart from a bias voltage directly applied to the junctions. In a double junction the central metal island can be polarized by a gate voltage, shifting charge from junction capacitance to the gate capacitor. We denote this shifted 'island charge' by Q_0 : $Q_0 = C_g V_g + \text{const.}$ For example, an island charge $Q_0 = e/2$ on the gate capacitor results in a charge $\pm e/4$ for each of the junctions, in addition to the charge $CV/2$ provided by the bias voltage. Since for these junctions $Q_c = e/4$, the Coulomb gap is completely suppressed. Fig. 5

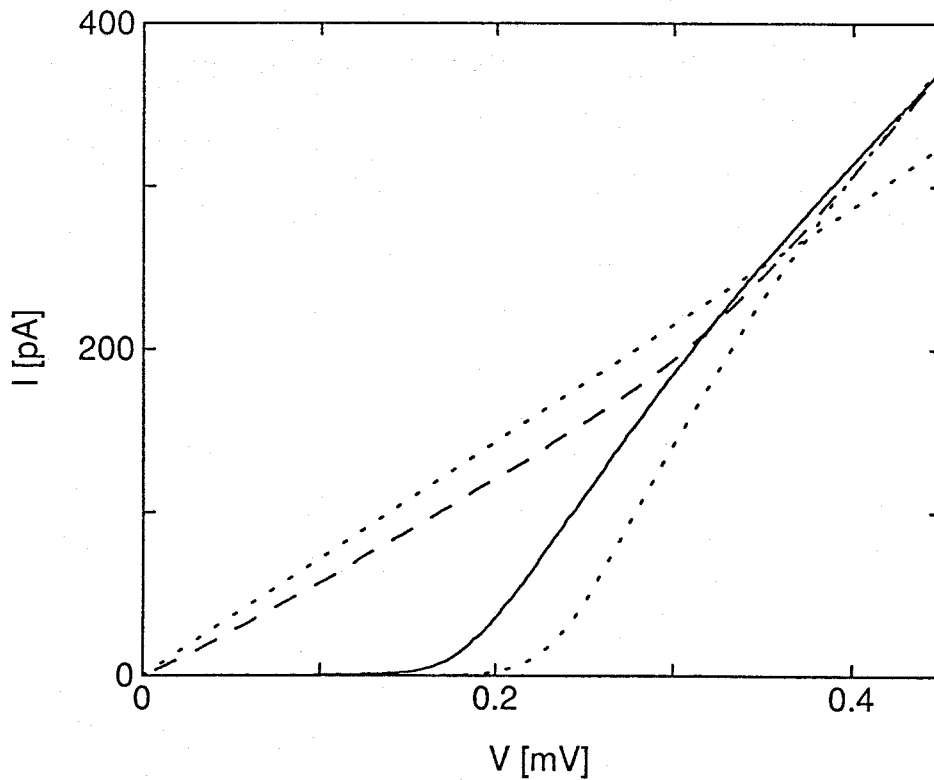


Fig. 5. I-V curve for a double tunnel junction with nominal $R_t = 347 \text{ k}\Omega$ and $C \approx 0.32 \text{ fF}$ at two gate voltages, corresponding to an island charge $Q_0 \approx 0$ (solid curve) and $Q_0 \approx e/2$ (dashed curve). The temperature is 15 mK. Also plotted (dotted curves) are the two corresponding theoretical predictions for the I-V curves at 60 mK. The discrepancy between theory and experiment may be due to several factors, such as imperfect symmetry of the voltage bias or inequality of the two junctions.

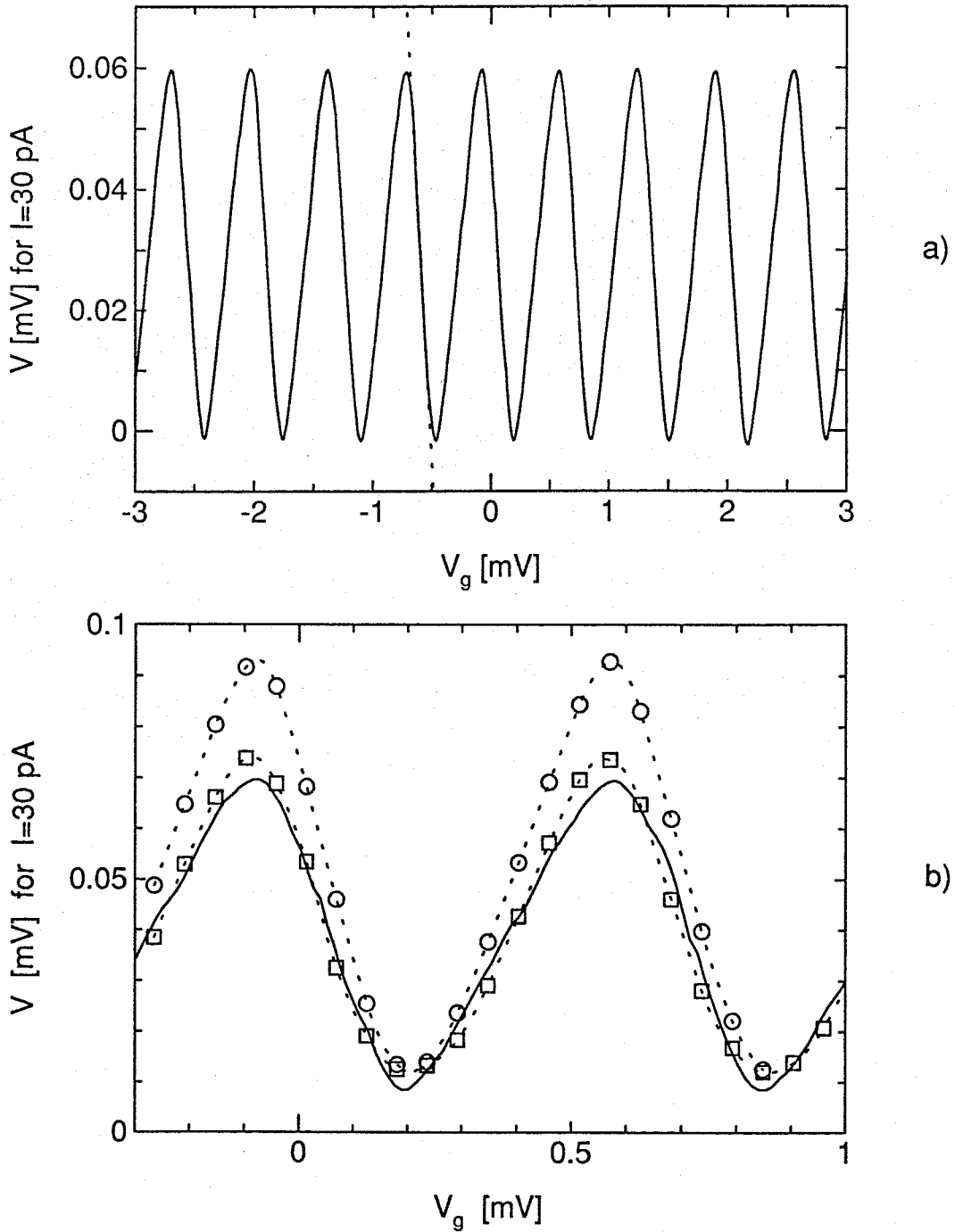


Fig. 6. $V-V_g$ curve for a double tunnel junction with dc current fixed at 30 pA, $T \approx 15$ mK. (a) Over a large range of V_g , showing the highly regular periodic behavior, following from the discreteness of charge transfer to the central island. The maximum voltage gain (dV/dV_g) is about 0.35 (slope of dotted curve). (b) Expansion in V_g -direction, comparing the measurement (solid curve) with calculated curves (dashed) for the estimated junction parameters (105 k Ω , 0.6 fF). The temperatures in the calculations are 60 and 90 mK for the circles and squares, respectively.

gives the measured I-V curve for a double junction for the two gate charges where the Coulomb gap is maximum and minimum. In the case of the maximum Coulomb gap (solid curve) the conduction below the threshold voltage is very low, although not completely zero. We will consider the charge-MQT that causes the leakage in this device in section IV. With gate charge the Coulomb gap can be completely suppressed to an almost Ohmic curve (dashed curve). At high voltages the same voltage offset $e/2C$ is recovered. As a function of gate voltage the I-V curve evolves continuously between the two extremes shown. With the average current through the device fixed at a low level, the voltage versus gate voltage can be recorded. An example is given for a similar double junction in Fig. 6. The curve is periodic because gate charges V_g and V_g' are equivalent if $C_g(V_g - V_g') = e$. This is a clear proof of the possibility to store charges for long times on the metal islands between tunnel junctions, without noticeable ohmic leakage. At the same time the continuous evolution of the I-V curve as a function of gate voltage proves the possibility of a continuous charging of a tunnel junction.

In Fig. 7 we show the current through linear arrays of 2, 3 or 5 junctions for a fixed bias voltage, again as a function of gate voltage. Of course this shows the same periodic behavior as the previous Figure. For 3 junctions the gate voltage is applied via two gate capacitors to the two islands between the junctions, for 5 junctions via 4 capacitors to 4 islands. Within the main period of e/C_g , a total of $n-1$ dips can be observed for n junctions. Fig. 7 illustrates an important aspect of experiments with gate voltages. Most curves show a minimum in the current which does not occur for the expected zero gate voltage but instead for a seemingly random value. Curve b shows telegraph noise: the current jumps between two positions corresponding to two I- V_g curves which are slightly offset in V_g -direction. The curves for arrays of 5 junctions all differ in their fine structure, whereas theory predicts one pattern for any device of 5 equal junctions. All these results show that the junctions have a random offset charge, probably caused by trapped charges near the junctions. The impossibility to predict even approximately the gate voltage that is necessary to maximize or minimize the Coulomb gap, might limit the usefulness of these junctions in large scale integrated applications.

As is expected from eq. (1), the charging effects are suppressed if the energy of thermal fluctuations $k_B T$ becomes of the order of E_C . In Fig. 8 this is shown for a double junction, with two different values of the gate voltage. Although the gap voltage is about halved for an island charge $Q_0=e/4$, the characteristic temperature for smearing of the Coulomb gap is approximately the same as in the situation with $Q_0=0$. In Fig. 9 we show similar curves for an array of 5 junctions. The characteristic non-linear gap feature mostly disappears between 25 and 200 mK,

i.e., far below E_C/k_B (≈ 0.6 K). In the same temperature range the structure in the $I-V_g$ curves also disappears.

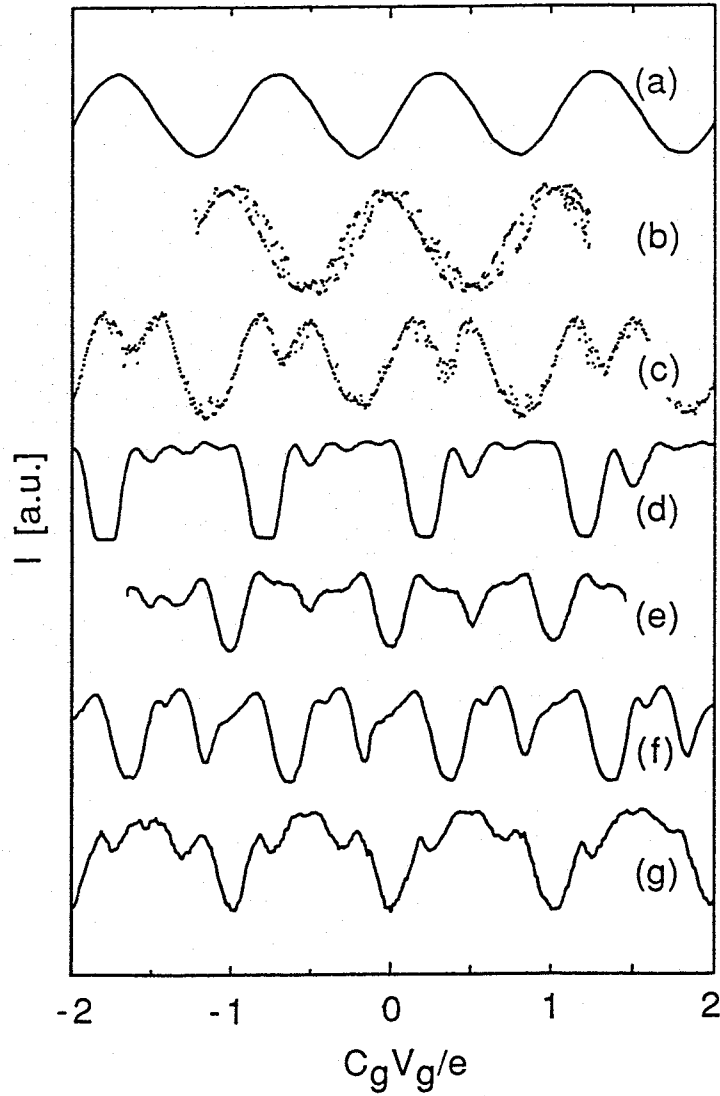


Fig. 7. $I-V_g$ curves for linear arrays of 2 (a,b), 3 (c) and 5 (d-g) junctions at fixed bias voltage, $T \approx 15$ mK. (d) and (e) are for the same device with V_g offset by 10 periods. It shows beating due to differing gate capacitances.

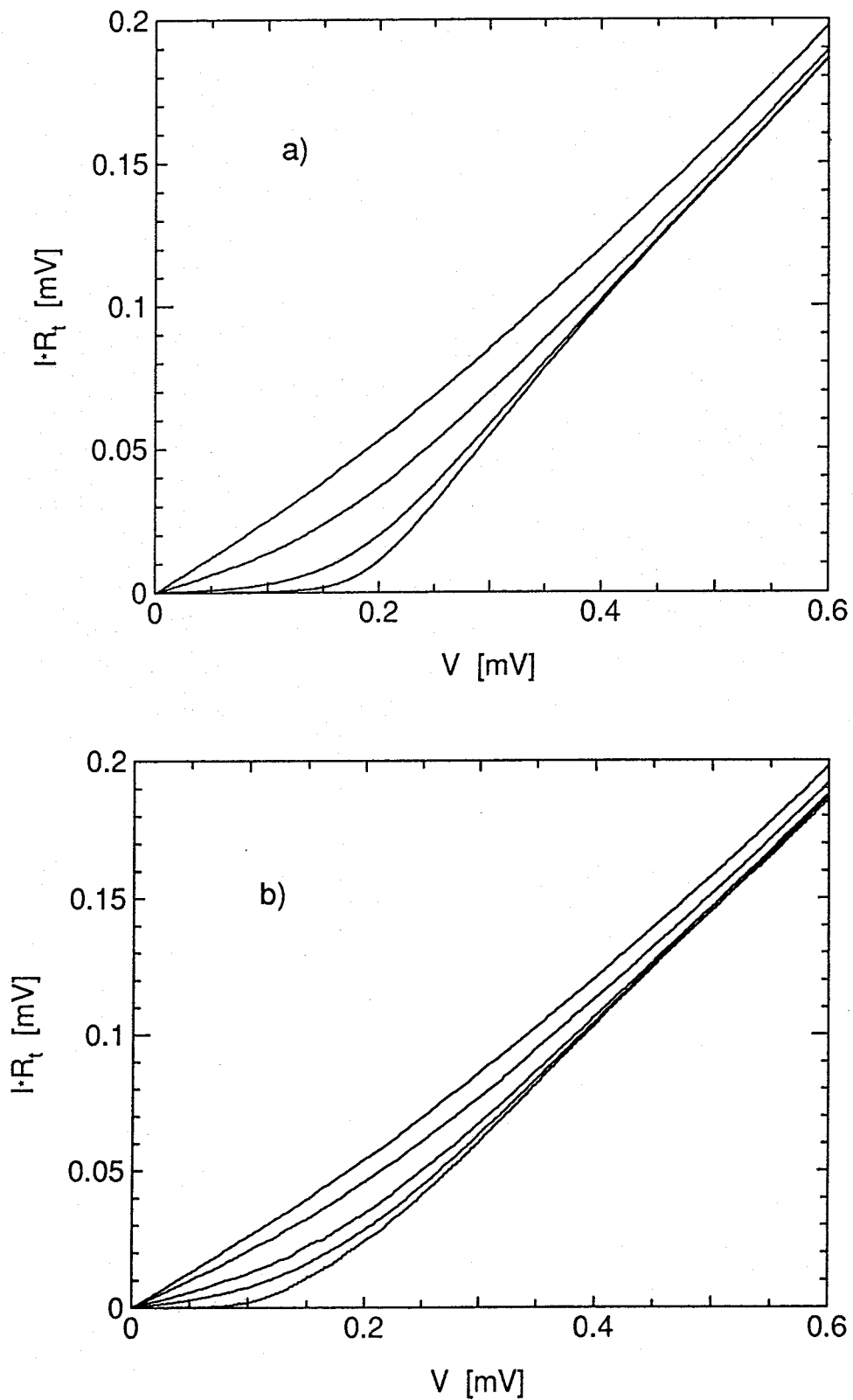


Fig. 8. I - V curves for a double junction with $R_t = 117 \text{ k}\Omega$ as a function of temperature. (a) For an island charge $Q_0 \approx 0$, $T = 25, 200, 400$ and 700 mK . (b) For an island charge $Q_0 \approx e/4$, $T = 40, 200, 300, 500, 700 \text{ mK}$. The estimated $E_C \approx 3 \text{ K}$.

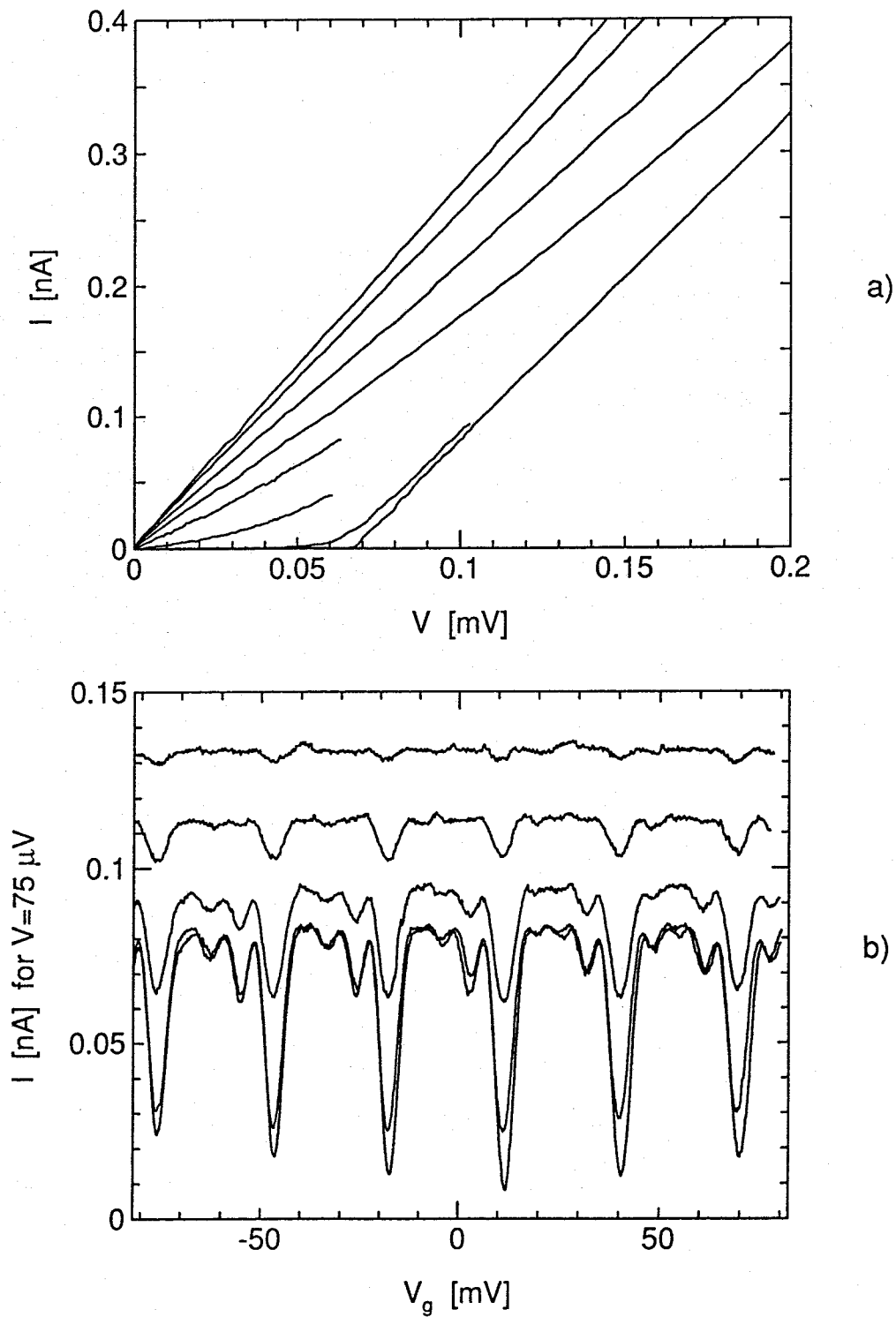


Fig. 9. (a) I - V curves for an linear array of 5 junctions with $R_t=58 \text{ k}\Omega$ as a function of temperature. $T=25, 50, 100, 150, 200, 300, 500, 700 \text{ mK}$. The estimated $E_C \approx 0.6 \text{ K}$. The strongest suppression of the Coulomb gap takes place between 25 and 200 mK. (b) The I - V_g curves for $T=25, 50, 100, 150, 200 \text{ mK}$, also losing structure in this temperature range.

III PRACTICAL USE OF COULOMB BLOCKADE OF ELECTRON TUNNELING

Various applications of the Coulomb blockade in small junctions have been proposed (e.g. Likharev 1987 and 1988, Yoshikawa *et al.* 1989). Some possible advantages of these circuits are the extreme integration level, the high speed (the typical operating frequency should be measured in $(R_t C)^{-1}$) and the low dissipation. Here we will present some experimental results that give a feeling of the possibilities and problems. As mentioned above one serious problem seems to be the presence of offset charging of junctions by trapped charges. In many applications this may in future be circumvented by using a resistive gate instead of a gate capacitance (Likharev 1987). The low temperature necessary to work with junctions with the presently attainable capacitance also forms a limitation. All experiments presented here have been performed in a dilution refrigerator, with the devices at temperatures down to 10 mK. We have found that low-pass filtering of the leads to the devices is important. The filters need to be cooled to low temperatures in order to suppress their own thermal noise. The filtering and attenuation of the gate voltage line also turned out to be crucial, especially in the experiments on the turnstile device to be discussed below.

Obviously, a double junction is a sensitive detector for charge on the gate electrode. It can be used to count electrons, like a DC SQUID is used to count flux quanta. Like the SQUID the sensitivity is higher than the electron charge. In preliminary measurements we have found that the gate charge fluctuations corresponding to the measured current noise in curves like Fig. 7(a), is about $10^{-4} e/\sqrt{\text{Hz}}$ between 10 and 200 Hz (Fig. 10). Compared to the SQUID a severe problem is the application of the charge to the gate. The input line needs to have a small capacitance compared to C_g . Otherwise much of the charge that should polarize the gate capacitor is lost to the parasitic lead capacitance.

A double junction can also be used as a high quality switch. The difference in resistance of the two states of the device of Fig. 5 is for low voltages almost infinite. Apart from conventional applications in digital circuits, it would be interesting to evaluate the use of such a double junction for experiments on mesoscopic circuits. As an example, with this switch these circuits could perhaps at will be coupled and decoupled from a part of the environment, in one experiment. Similarly, it could be used as a very high impedance voltmeter (by using the gate electrode as the voltage probe) very close to a mesoscopic circuit.

The maximum slope of the $V-V_g$ curve in Fig. 6 is 0.35, corresponding approximately to the ratio of C_g to C . By increasing the gate capacitance to a value larger than the junction capacitance, an amplifying element would be obtained, be it with a very small input voltage range.

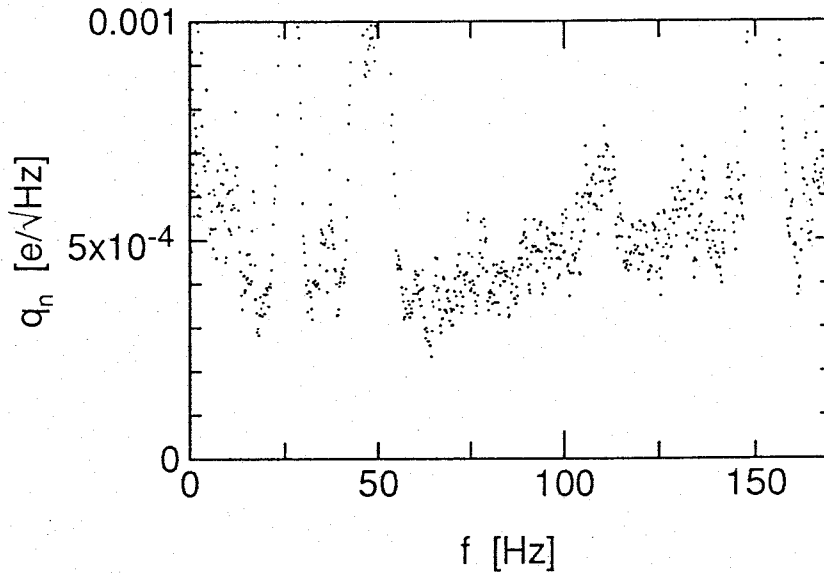


Fig. 10. Gate charge fluctuations versus frequency for a double junction with $R_T=62 \text{ k}\Omega$ and $C=1 \text{ fF}$. The charge noise (in $e/\sqrt{\text{Hz}}$) was derived from the measured current noise by multiplying with $C_g(dV_g/dI)$. Apart from peaks at harmonics of the line-frequency, the noise is about $4 \cdot 10^{-4} e/\sqrt{\text{Hz}}$.

Other, more complicated circuits have been proposed. Some of those belong to the class of single-electronic devices, such as the memory cell of Yoshikawa *et al.* In these devices the information is stored not as a voltage but as an excess charge (e.g. one electron). The operation of such devices requires the control of motion of single electrons at high frequencies. That this is indeed possible has recently been shown by the successful operation of single electron turnstile devices in Delft and Saclay (Geerligs *et al.* 1990). In these devices two or more junctions on each side of a central gate capacitor are used to block electron tunneling during part of a clock cycle. The clocking signal consists of a high frequency alternating voltage (added to a dc voltage) applied to the central gate capacitor. Only once per cycle an electron can tunnel across one arm and only once per cycle can it tunnel across the other arm. Coulomb blockade is used to ensure that precisely one electron tunnels. The turnstile creates a very accurate current or charge source.

The working principle can be conveniently illustrated using the concept of the critical charge. It is shown in Fig. 11 for a device with four junctions. For simplicity we consider a square wave gate voltage modulation. The gate capacitance is close to $C/2$ so that each junction has the same critical charge of $e/3$. In the first part of the cycle the critical charge is exceeded for the junctions in the left arm but not for those in the right arm. If a tunneling has occurred in one junction, the second will follow almost immediately. If the electron has reached the central island, it will mainly

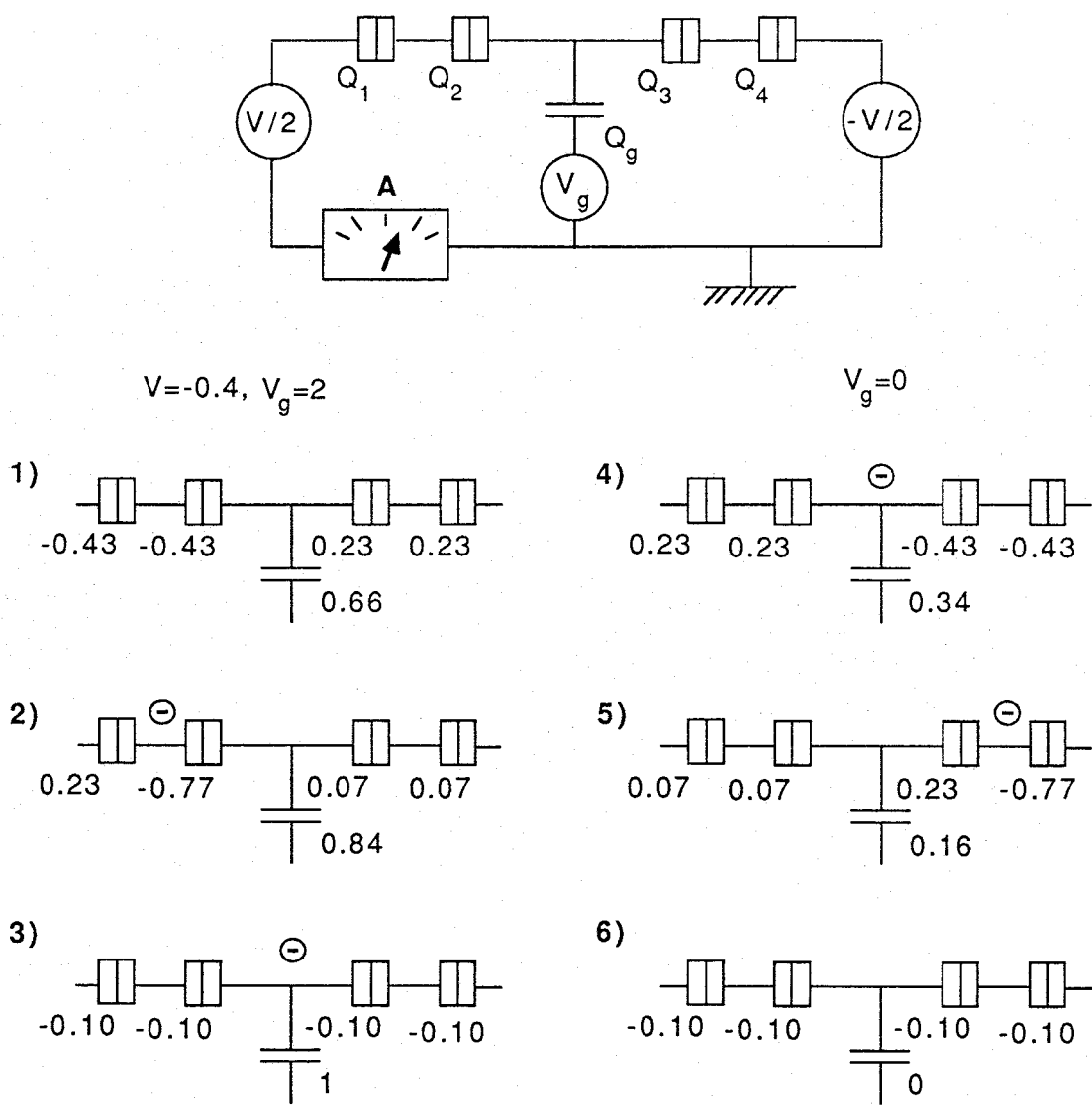


Fig. 11. Working principle of a turnstile for single electrons. An ac plus dc voltage is applied to the central gate between the 4 junctions. The numbers denote consecutive moments in one ac cycle. Junctions are denoted by double boxes. $C_g = C/2$, hence $Q_c = e/3$ for all junctions. The momentaneous charges are indicated in units of e .

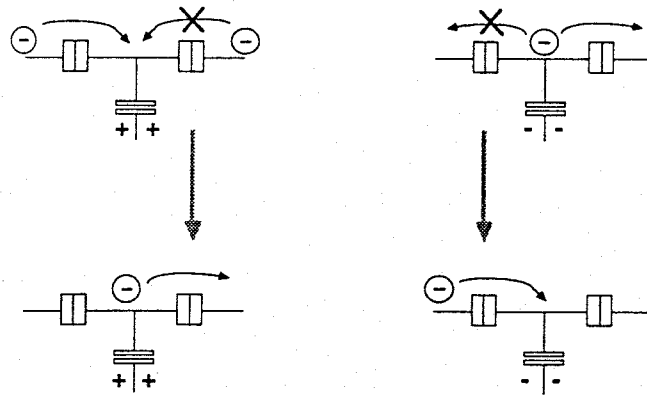


Fig. 12. The turnstile is probably the simplest system that operates with one rf modulation voltage. For a double junction the constraint of sending the electron in a specific direction is in conflict with the need to trap the electron on the central island.

polarize the relatively large gate capacitor and all junction charges will be lower than the critical charge. No other tunneling events occur until the gate voltage is decreased in the second half of the cycle. Then the critical charge is exceeded for the junctions in the right arm but not for those in the left arm (for the gate voltage amplitude within a certain window). Consequently, the electron leaves on the other side of the device. After this event no tunneling can happen until the start of the next cycle. In absence of the ac component of the gate voltage no tunneling is possible, i.e. the conduction is zero. Thus, after switching on the ac gate voltage, at each moment in time the passed charge is known up to at most a single electron.

At least two junctions are needed in each arm of the device, to avoid unwanted entering or leaving of electrons. Fig. 12 exemplifies that forcing the electron to enter from the left, and thus forbidding a tunneling through the right junction *onto* the central island, makes it possible for an electron to leave from the island to the right. Thus, the constraint of making the direction of tunneling deterministic is in conflict with the need to trap an electron during part of the cycle. The 4-junction turnstile is probably the simplest system that works with one rf drive. The electrodes with small self-capacitance in each arm can block electron transfer. Of course, if it is possible to control the junction barrier itself, e.g. with a split-gate confined quantum dot in a heterostructure, it should be possible to obtain controlled electron transfer in a two-barrier system (Odintsov 1990). (See also Guinea and Garcia 1990 for a specific example with a scanning tunneling microscope) Also, more complicated control schemes with two-junction devices are expected to work (see, e.g., the last section of the next chapter) and a three-junction electron-pump has been operated at Saclay.

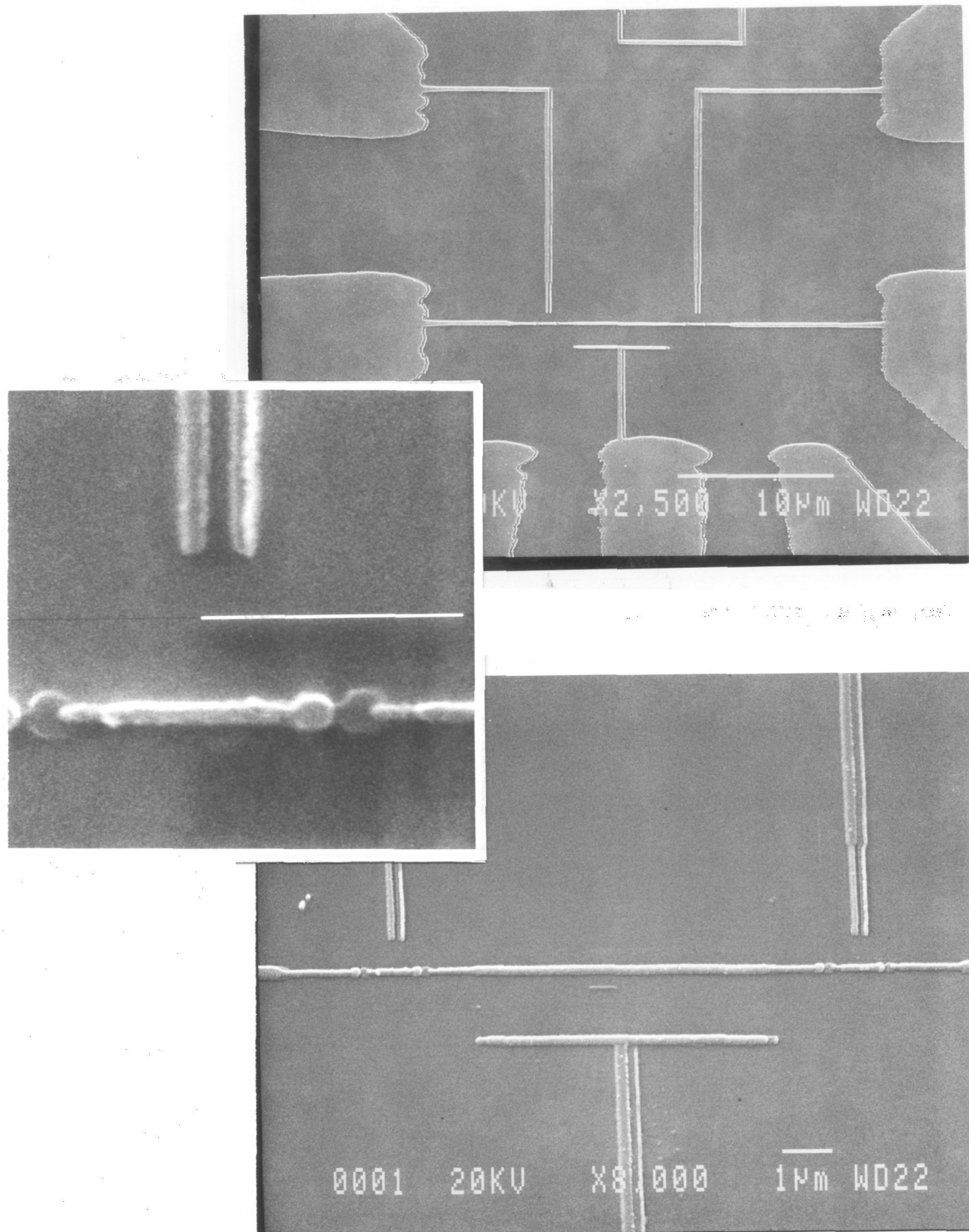


Fig. 13. (a) Scanning electron microscope photograph of the turnstile device as realized with aluminum junctions. The main difference from Fig. 11 is the addition of auxiliary gate electrodes. The ac line is guarded. (b) Enlargement. Inset: Detail of one arm with two junctions and an auxiliary gate electrode. The white bars are 1 or 10 μm long.

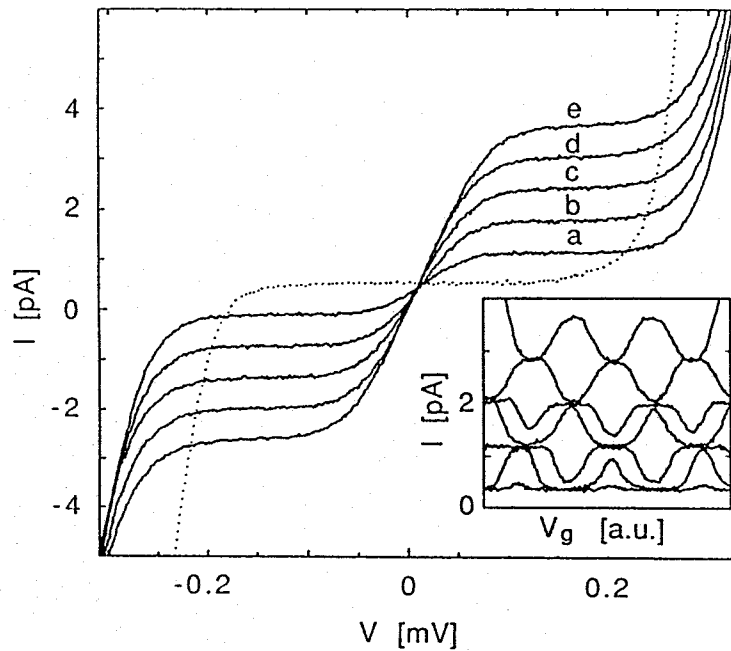


Fig. 14. I - V curves of the turnstile device of Fig. 13 without ac gate voltage (dotted) and with ac gate voltage of frequency 4 to 20 MHz in steps of 4 MHz (a-e). The inset shows the I - V_g curves for an ac gate voltage (5 MHz) of increasing amplitude (top to bottom), taken at a bias voltage of about 0.15 mV. $R_t=340$ k Ω , $C=0.4$ fF, $C_g=0.3$ fF.

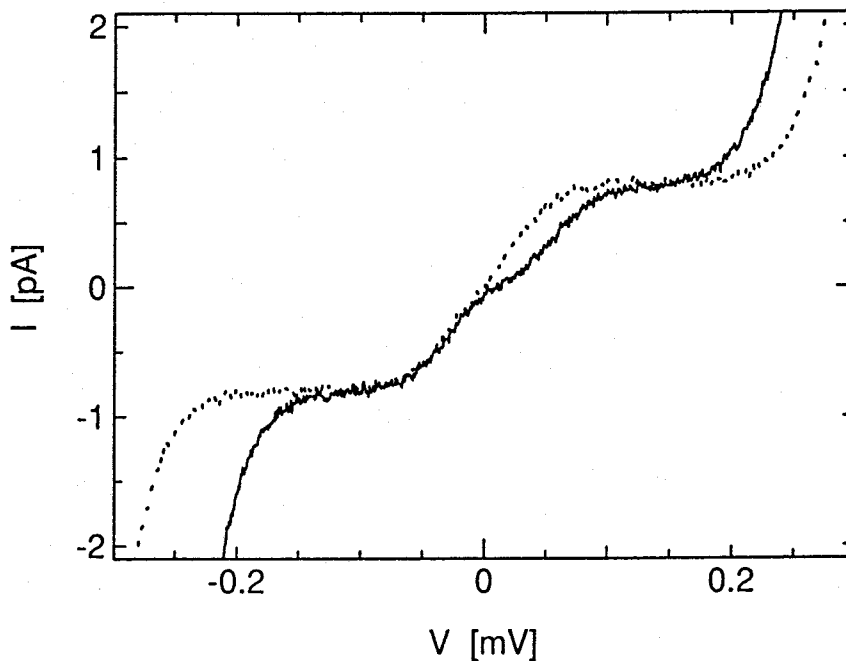


Fig. 15. Effect of offset charges on the current plateau. The dotted curve is the best plateau at 5 MHz that could be obtained by adjusting rf amplitude and auxiliary gates. The solid curve is for the worst plateau that could be produced (by trial and error) with misadjustment of the auxiliary gates.

As Fig. 13 shows the physical layout of the turnstile device is very close to the schematic. An important difference is the addition of small additional gate electrodes to tune out offset charges on the two metal islands in the left and right arm of the device.

Fig. 14 shows I-V curves of the device without ac gate voltage (dotted) and with ac gate voltage at a set of frequencies f between 4 and 20 MHz. The zero current Coulomb gap in the absence of the ac voltage (dotted) is lifted to a plateau $I=e\cdot f$ if the ac voltage is applied. The width of the plateaus is dependent on the amplitude of the ac signal but the height is not. To obtain wide flat plateaus it was necessary to tune the auxiliary gate electrodes. However, qualitatively similar I-V curves have been obtained without these gates. An example of rather serious deterioration of the plateaus due to island charges is shown in Fig. 15. The auxiliary gate electrodes were used to try to destroy the plateaus on purpose. The inset of Fig. 14 shows I- V_g curves in the presence of ac signals of various amplitudes (at a frequency $f=5$ MHz) for a bias voltage in the middle of the plateaus. The curves tend to be confined between consecutive multiples of $e\cdot f$. This shows that the device can also pass several electrons per cycle in a controlled way. At higher ac amplitude it is possible to fill the central island with more than one electron. On decreasing the gate voltage these trapped electrons are released one by one through the other arm. It has been possible to obtain quantization (although less accurate) at levels as high as $8e\cdot f$ (Pothier *et al.* 1990). Fig. 16 gives both the measured and the calculated dependence of the I-V curves on the gate voltage amplitude, with calculations based on eqs. (1-4). Since the junction capacitance and resistance can be measured from the I-V curve asymptote, and the gate capacitance from the period of gate voltage modulation, in principle no parameters need to be fitted. However, the asymptote can still be identified with either $\approx(n-1)e/2C$ or with $\approx ne/2C$ ('global' versus 'local' rule, see e.g. Geigenmüller and Schön 1989). In a previous publication (Geerligs *et al.* 1990) we determined C with global rule. This was probably unjustified due to too low bias voltage or current. For the calculations shown, local rule determination of C yields an almost perfect agreement with theory with only marginal fitting of temperature and gate voltage attenuation. Only 1 dB attenuation of the ac signal in the transmission lines and a sample temperature slightly higher than the mixing chamber temperature were assumed. A slightly less satisfactory correspondence is obtained between calculated and observed temperature dependence of the plateaus (Fig. 17). However, the general correspondence of theory and experiment that is present here too, gives convincing evidence that the behavior of circuits of small high resistance tunnel junctions can indeed be very well described by simple theory.

In the experiment, deviations of the current quantization from the relation $I=ef$ were smaller

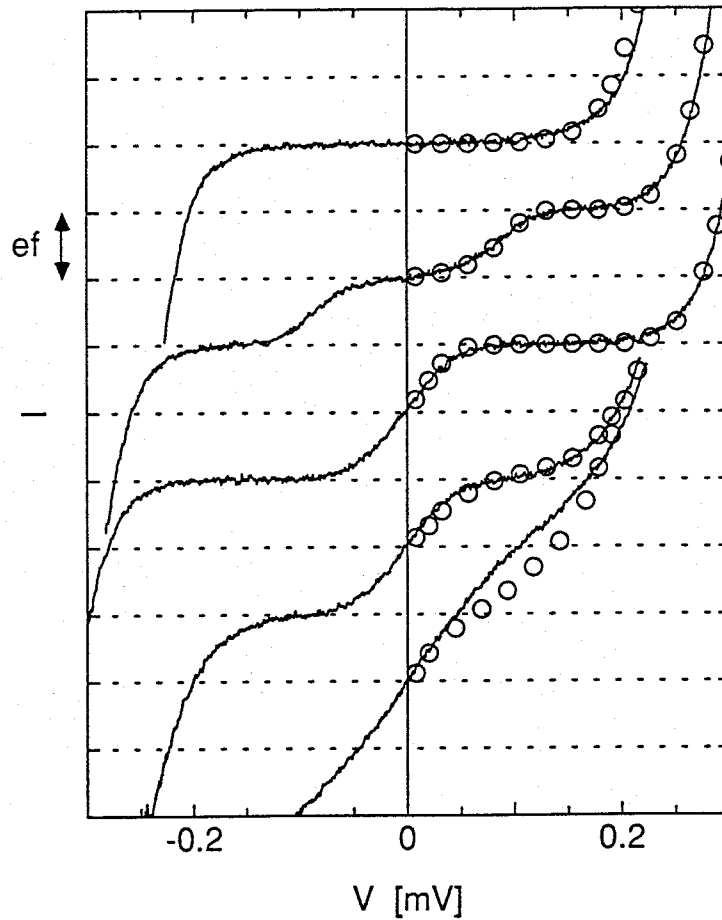


Fig. 16. I-V curves at $f=5$ MHz for different amplitudes of ac gate voltage, increasing from top to bottom. The dotted horizontal lines are at intervals $ef=0.80$ pA. The corresponding calculated I-V curves (at 60 mK, or 115 mK for the bottom two curves) are indicated by circles. For these calculations, 1 dB extra attenuation was assumed. The rf amplitudes in the calculations are 0, 0.41, 0.65, 1.03 and 1.30, in units of $e/C=0.40$ mV.

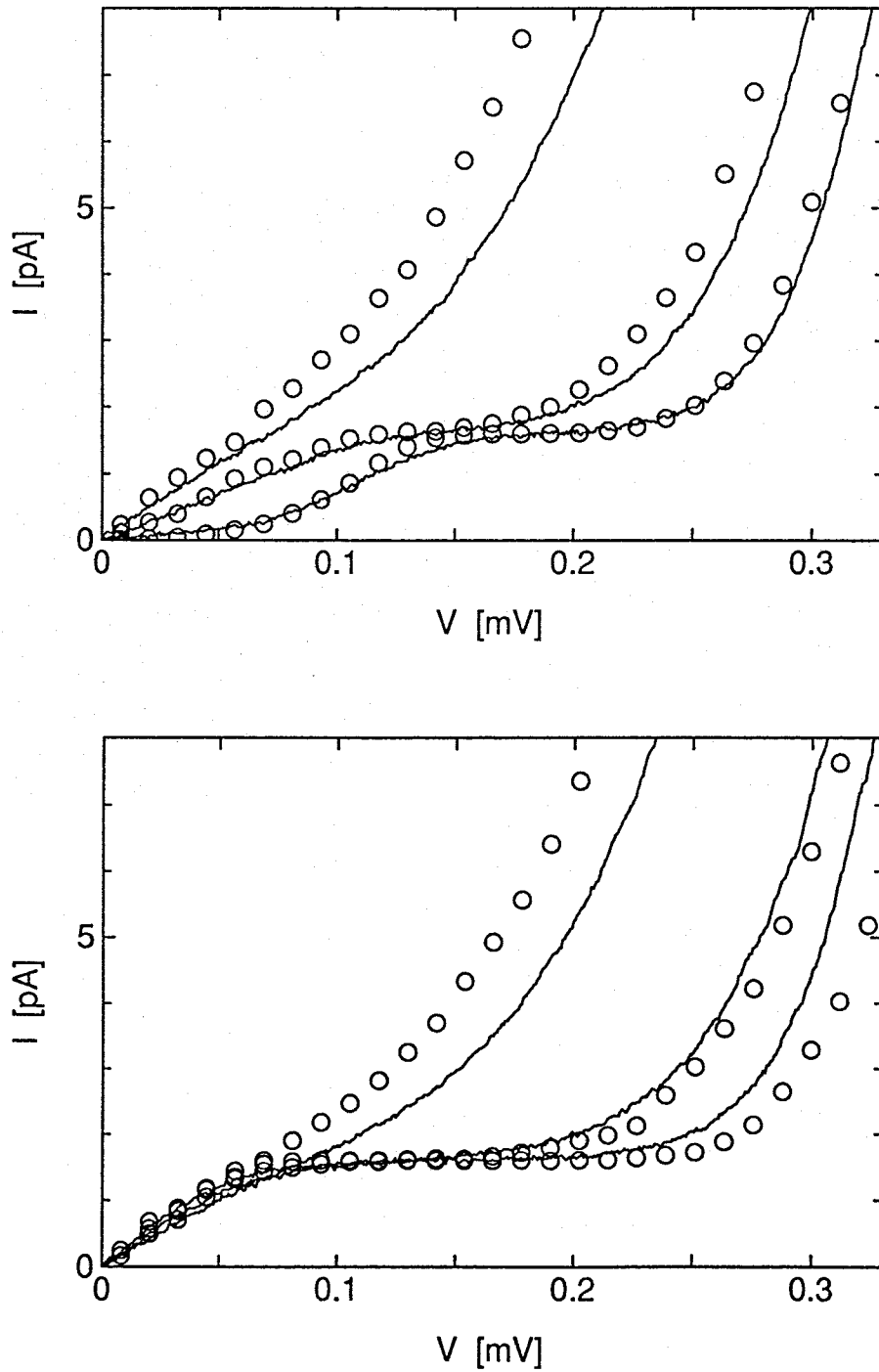


Fig. 17. The temperature dependence of the current plateaus, for $f=10$ MHz and at two different rf amplitudes (differing by 4 dB). The temperature in the experiments is 20, 100 and 200 mK (solid curves). The temperature for the calculations is 60, 100 and 200 mK (circles). The attenuation of the rf line is the only fit parameter (10 MHz is beyond the experimental low-pass cutoff frequency of about 6 MHz), the fitted value is about 10 dB attenuation.

f (MHz)	I_s (fA)	σ_m (fA)	$ef-I_s$ (fA)
4.012	635	2	8
6.011	967	2	-4
8.031	1287	2	0
10.040	1610	2	-1
12.029	1930	2	-3
14.028	2243	2	5
16.026	2560	3	7
18.063	2890	3	4
20.011	3196	3	10
30.036	4856	3	-44

Table 1. Accuracy of the current quantization in the turnstile device of Fig. 14. The measured current plateau I_s is compared with the relation $I_s=ef$. σ_m is the standard deviation of I_s , as determined from averaging about 50 data points, well inside the current plateau.

than the accuracy of the current measurement. This amounts to a few fA's or about 0.3 % for the plateaus at frequencies below 20 MHz. For higher frequencies the plateaus do not show a part that is flat within the current noise. The determination of the level of the current plateau as the current at the inflexion point then causes larger errors. Experimental results on the accuracy of the current quantization are given in Table 1. It is easy to estimate the expected intrinsic accuracy of the current quantization in this device from the simple theory. To obtain a high accuracy of the relation $I=ef$, the ac cycle should last long enough to let tunneling to and from the central island happen with high probability, i.e. f must be much smaller than $(R_1C)^{-1}$ to avoid cycles being lost. On the other hand an electron trapped on the central electrode should have a negligible probability to escape by a thermally assisted transfer. At finite temperature there is a trade-off between the two requirements: a thermally assisted escape will be more probable for lower frequencies. For an electron transfer in the situation shown in Fig. 11 the first tunnel event of each half of the cycle ($\Delta E=0.1e^2/C$) can occur in two junctions with a rate $\Gamma=(10R_1C)^{-1}$. For a square wave modulation

this yields a probability to miss a cycle of about $\exp(-\Gamma/f)=\exp(-1/10fR_tC)$. For the device used in the experiments, $(R_tC)^{-1}\approx 5$ GHz, so at 5 MHz this probability is $\exp(-100)\approx 10^{-44}$, while at 50 MHz it is already about 10^{-5} . Obviously, the required accuracy puts an upper limit to the allowed frequency. To estimate the effect of thermal fluctuations, we compare the rate for unwanted tunneling events, $\tilde{\Gamma}$, with the one for favorable events, Γ . From eq. (1) we find that the ratio is of order $\exp(-\Delta E/k_B T)$. For an accuracy of e.g. 10^{-8} , it is necessary to have $\tilde{\Gamma}/f\approx 10^{-8}$, which combined with the requirement $\Gamma/f=10^3$ yields $\exp(-\Delta E/k_B T)=10^{-11}$, or $k_B T\approx \Delta E/25$. Since typically ΔE is on the order of $0.1e^2/C$, for the present device this corresponds to temperatures of about 15 mK. Comparable problems with unwanted transitions could arise from insufficient screening from noise and interference in the experiments. The simulations in Fig. 16,17 suggest that in the present experiment these disturbances seem to be described well by a temperature of not more than 60 mK, which is already close to the temperature requirement derived above. More careful screening is possible. These limitations are relaxed by the use of smaller junctions. For junctions of 0.1 fF with the same resistance, the requirement that $f < 10^{-3}/R_tC$ corresponds to $f < 30$ MHz and $k_B T < 0.1e^2/C$ to $T < 75$ mK.

A third cause for accuracy degradation is the already mentioned macroscopic quantum tunneling (MQT) of the charge. This amounts to the escape (at zero temperature) of a trapped charge on the central electrode, through both junctions in one event. The rate is proportional to the product of the junction conductances. The addition of junctions to each arm of the device would decrease the rate of this process. This addition would not significantly increase the chance of cycles being lost, since the tunneling of an electron through the wings is an avalanche process, where the first tunnel event takes most of the time. Below we will consider charge MQT more detailed and present experiments that confirm the higher order perturbative description. With this description, if we denote the rate for unwanted transitions again by $\tilde{\Gamma}$, it turns out that $\tilde{\Gamma}/f=10^{-8}$ together with $\Gamma/f=10^3$ corresponds to the approximate condition $(R_t/R_q)^{n-1} < 10^{13-n}$ where n is the number of junctions in each arm and $R_q=h/4e^2 \approx 6.5$ k Ω . This is e.g. fulfilled for wings of 5 junctions of $R_t\approx 650$ k Ω . Averin and Odintsov (1990, See also chapter 4) have recently performed a rough calculation of the effect of q-MQT on the accuracy of the turnstile. They expect for the 4-junction turnstile device as presented above, a leakage current of at best about 10^{-3} times the value $I=ef$. However, for turnstile devices with longer arms (e.g. 4 junctions in each arm), the leakage current should be easily suppressed to acceptable values.

A practical complication when using a turnstile device to create a current standard is the presently very low current level of around 1 pA. The usual technique for high-accuracy

multiplication of a dc current uses a cryogenic current comparator (Sullivan and Dziuba 1974). The primary current (e.g. from a turnstile device) and the multiplied current are sent in opposite direction through ratio windings. An rf SQUID senses the ampere-turn unbalance. The SQUID control electronics adjust a slave-current source in a feedback loop to produce a secondary (multiplied) current for zero unbalance. For the usual current magnitudes of μA 's or higher, a transfer accuracy of 10^{-8} can be easily reached. However, for multiplying the turnstile current the bottle-neck for the accuracy is the very small flux that can be produced with the primary current, even compared to the typical SQUID sensitivity of $10^{-4} \Phi_0/\sqrt{\text{Hz}}$. It will prove hard in practice to obtain a high ratio of primary ampere-turn product and the SQUID sensitivity. As an example, the cryogenic current comparator that is presently in use at the Van Swinderen laboratory in Delft for the Quantum Hall resistance standard (van der Wel, Mooij and Harmans 1988) would only give a transfer sensitivity of about 10%.

IV PERTURBATIVE CORRECTION TO THE CLASSICAL THEORY FOR COULOMB BLOCKADE

In this section we will discuss several examples of macroscopic quantum tunneling of the electric charge (q-MQT). In this process small quantum fluctuations of the charge on a junction yield a finite probability for tunneling of an electron despite Coulomb blockade. Due to the Coulomb energy, all free electrons in the metal electrodes participate in such a process, making it a macroscopic event. (See also chapter 5). We have experimentally observed q-MQT in linear arrays of tunnel junctions. We note, however, that the effect could also arise in a single junction, which might be realized in future experiments.

A single voltage biased tunnel junction can show a Coulomb gap if it is well decoupled from the environment. The charge dynamics of this system is in several respects similar to the phase-dynamics of a single current biased superconducting junction. The system can be represented by a particle of mass L (L is the inductance in series with the junction), moving in a piecewise parabolic potential in Q -space, $E(Q) = (Q - ne)^2/2C - QV$ (Fig. 18), where n is the number of electrons passed through the junction. A resistor R_e in series with junction and inductor causes damping of the particle: $d^2Q/dt^2 = V - (Q - ne)/C - R_e(dQ/dt)$. Trapping of the particle in the metastable state at $Q = CV + ne$, which is possible for $V < e/2C$, corresponds to Coulomb blockade of electron tunneling. As Devoret *et al.* (1990) showed, the zero-point oscillations of the LC-circuit will provide a possibility to escape from the metastable Coulomb blockade state. The mass

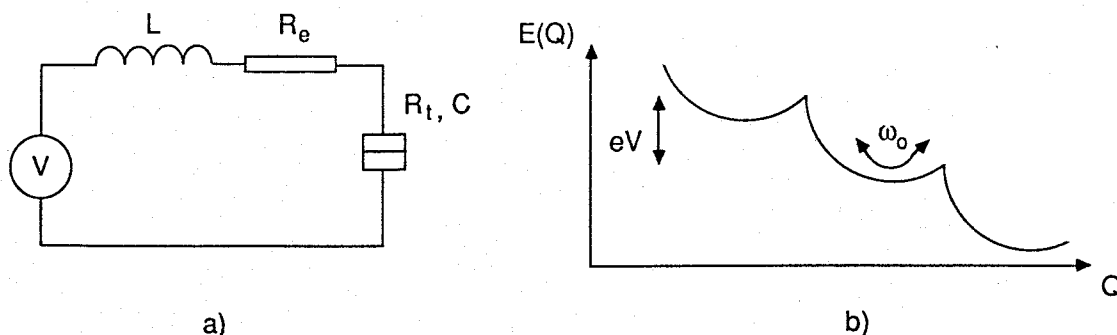


Fig. 18. A voltage biased series circuit of junction, inductor L and resistor R_e (a), can be represented by a particle of mass proportional to L and damping proportional to R_e^{-1} , with coordinate Q . It moves in a piecewise parabolic potential with a slope proportional to V (b). The charge is a continuous variable, and can tunnel out of the metastable state through the charging energy barrier.

(inductance) ensures a hysteretic response to this event, i.e. a current starts to flow. Thus, the macroscopic quantum tunneling experiments in phase space (φ -MQT, see e.g. Martinis, Devoret and Clarke 1987) could be repeated for the charge. Rough estimates show, however, that an experiment will be hard to realize. The problem is that the quantum fluctuations of the charge are usually by far too large and completely suppress the Coulomb blockade for any voltage below $e/2C$. The typical energy barrier in the metastable state will be smaller than E_C , which should therefore in an experiment be much larger than the harmonic oscillator ground state $\hbar/2\sqrt{LC}$. This amounts to $\sqrt{L/C} \gg R_q \equiv h/4e^2$. Since C will not be much smaller than 10^{-16} F, an inductor much larger than 10^{-4} H is required on a μm -scale. The typical geometric inductance of small metal wires, about 10^{-12} H/ μm , is clearly not sufficient. By using low electron-density materials, which have high kinetic inductance ($L' = m/ne^2S$ per unit length, where n is the electron density and S the cross-section, e.g. Mooij and Schön 1985) one could hope to reach this requirement. In dirty superconductors the necessary charge carrier densities n_s of order 10^{20} m^{-3} can be attained.

As expected from the duality to the current biased Josephson junction, a low shunt resistance enhances charge fluctuations and increases q -MQT (Averin and Odintsov 1989). For this single junction, the charge evolves continuously during the tunneling. Therefore the q -MQT rate depends exponentially on the characteristic impedances like R_e , R_t or $\sqrt{L/C}$, and can be strongly suppressed by increasing these impedances.

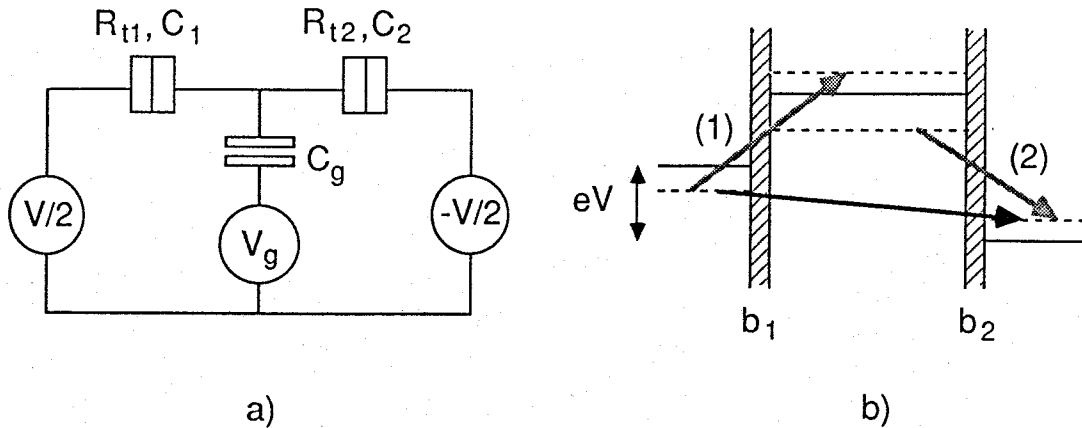


Fig. 19. Macroscopic quantum tunneling of the charge in a double junction (a) is a combination of two discrete tunneling events, indicated by (1) and (2) in (b), with a virtual intermediate state of higher charging energy. The rate of the net tunneling process (solid arrow) is linearly suppressed by increasing the junction resistances.

In an array of junctions with low bias voltage, electrons residing on the central metal islands increase the energy of the total system. This produces a barrier for electron transport across the system. Thermal fluctuations of the charge on the junctions can cause passage of this barrier. At low temperatures electron transport is exponentially (in $E_C/k_B T$) suppressed, giving rise to the Coulomb gap and the possibility of trapping an electron in the turnstile. However, here too quantum fluctuations of the charge can cause the system to change the charge distribution to a state where one electron charge has passed through the complete array. Effectively virtual tunneling events have occurred to the intermediate forbidden states. It need not be the same electron that crosses the various junctions. Indeed, as Fig. 19 shows for a double junction, it is an inelastic process in which an electron-hole excitation is created on the central island(s). Averin and Odintsov (1989) have shown that for high tunnel resistances the rate for this process is proportional to the junction conductances and proportional to V^{2N-1} , where N is the number of junctions:

$$\Gamma \propto \frac{V^{2N-1}}{h} \prod \frac{\alpha_i}{\pi^2} \quad (8)$$

$\alpha_i = R_Q/R_t$ for junction i , and the product is over all junctions. In Fig. 20a we show experimental I-V curves of the Coulomb gap of a 2-, 3- and 5-junction array. It is clear that the Coulomb gap sharpens considerably for the longer arrays, in agreement with this equation. In particular, in Fig.

20b the $\log(I)$ - $\log(V)$ curves for the 2-junction and 3-junction array are close to the expected slopes of 3 and 5, respectively.

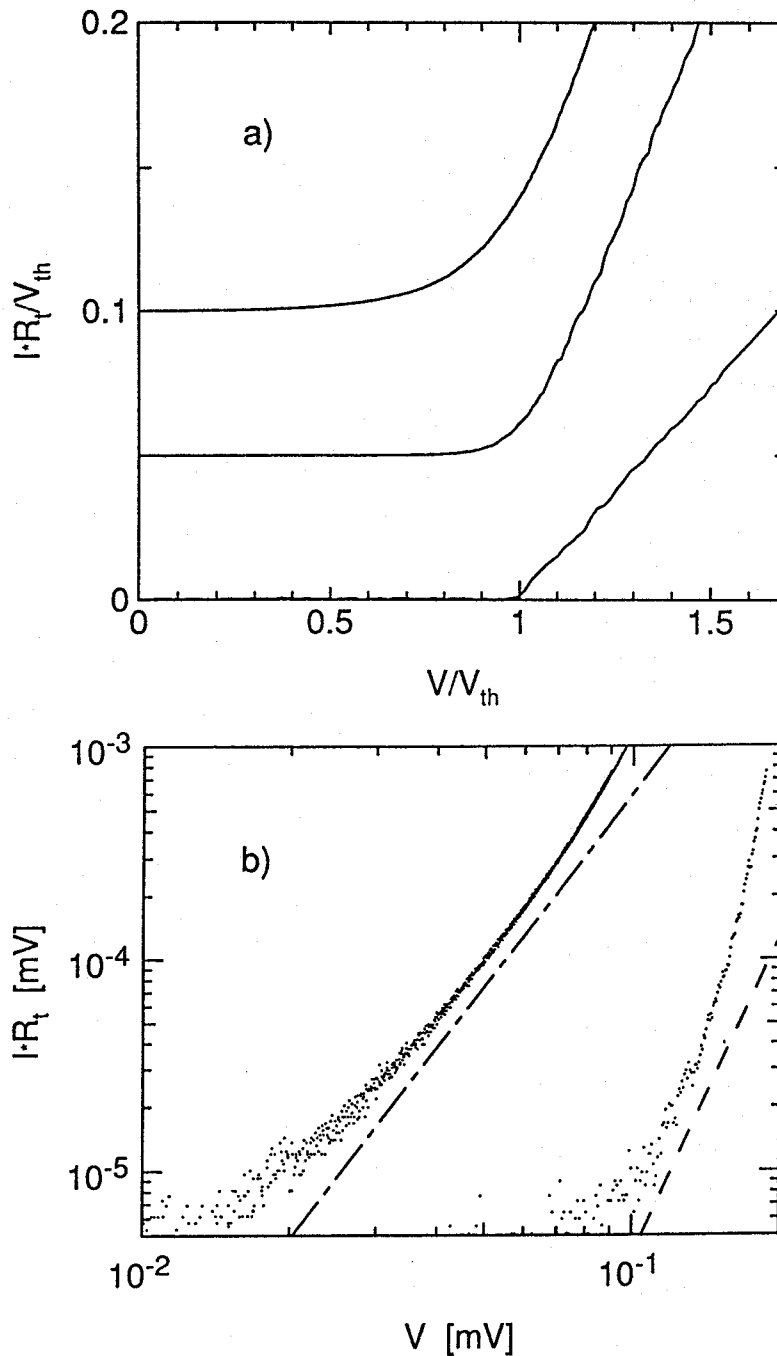


Fig. 20. (a) The Coulomb gap sharpens up significantly for longer arrays (top to bottom: 2,3 and 5 junctions, all with R_t around $70 \text{ k}\Omega$). The curves have been scaled to the threshold values V_{th} of (top to bottom) 0.13, 0.20 and 0.068 mV. The I - V curves have been offset in y -direction for clarity. (b) In $\log(I)$ - $\log(V)$ curves, the slopes are in agreement with the expected values; 3 (left, for a double junction) and 5 (right, for 3 junctions).

To study the effect of R_t on q-MQT, the double junction is the most favorable system, since it has the highest q-MQT rate with the weakest voltage dependence. For a double junction, the rate is for voltages inside the Coulomb gap

$$\Gamma = \frac{h}{(2\pi)^2 e^4 R_{t1} R_{t2}} \left\{ \left[1 + \frac{2E_1 E_2}{eV(E_1 + E_2 + eV)} \right] \left[\ln \left(1 + \frac{eV}{E_1} \right) \left(1 + \frac{eV}{E_2} \right) \right] - 2 \right\} eV \quad (9)$$

E_1 and E_2 are the energies of the (virtual) intermediate state if the first tunnel event occurs in the left junction and the right junction, respectively;

$$E_1 = \frac{e}{C_\Sigma} (e/2 + Q_0 - (C_2 + C_g/2)V) \quad (10a)$$

$$E_2 = \frac{e}{C_\Sigma} (e/2 + Q_0 - (C_2 + C_g/2)V) \quad (10a)$$

$$C_\Sigma = C_1 + C_2 + C_g \quad (10c)$$

In Fig. 21 we compare measurements of the I-V curves of 4 double junctions (with maximum Coulomb gap, so $Q_0 \approx 0$) with the theoretical prediction from classical theory and q-MQT respectively. The measurements have been scaled to dimensionless voltage VC_Σ/e and current $IR_t C_\Sigma/e$ to allow for easy comparison. R_t is determined from the I-V curve asymptote. C_Σ is used as a fit parameter. There is very good agreement with q-MQT theory. We note that the correspondence of the slope (3, both in experiment and theory) is independent of the fitted C_Σ . Further, we will show below that the fitted value for C_Σ is very reasonable. In contrast, to obtain rough agreement with the predictions from thermal fluctuations (eqs. (1-4)), it is necessary to introduce some *ad hoc* corrections. A high temperature of 100 mK is used to obtain a curve that is at least in the range of the measurements. In addition it is necessary to assume a misadjustment of the gate charge, that is systematically larger for low resistance samples. In Table 2 the fitted C_Σ is compared to two independently measured values. Both the asymptote offset V_{of} and the threshold voltage V_{th} of the Coulomb gap should be equal to e/C_Σ . In actual I-V curves this is not the case. V_{th} may be suppressed, due to asymmetric voltage bias, thermal effects, etc. The asymptotic value V_{of} is possibly more reliable. In Table 2, the fitted value of C_Σ lies between e/V_{of} and e/V_{th} . We

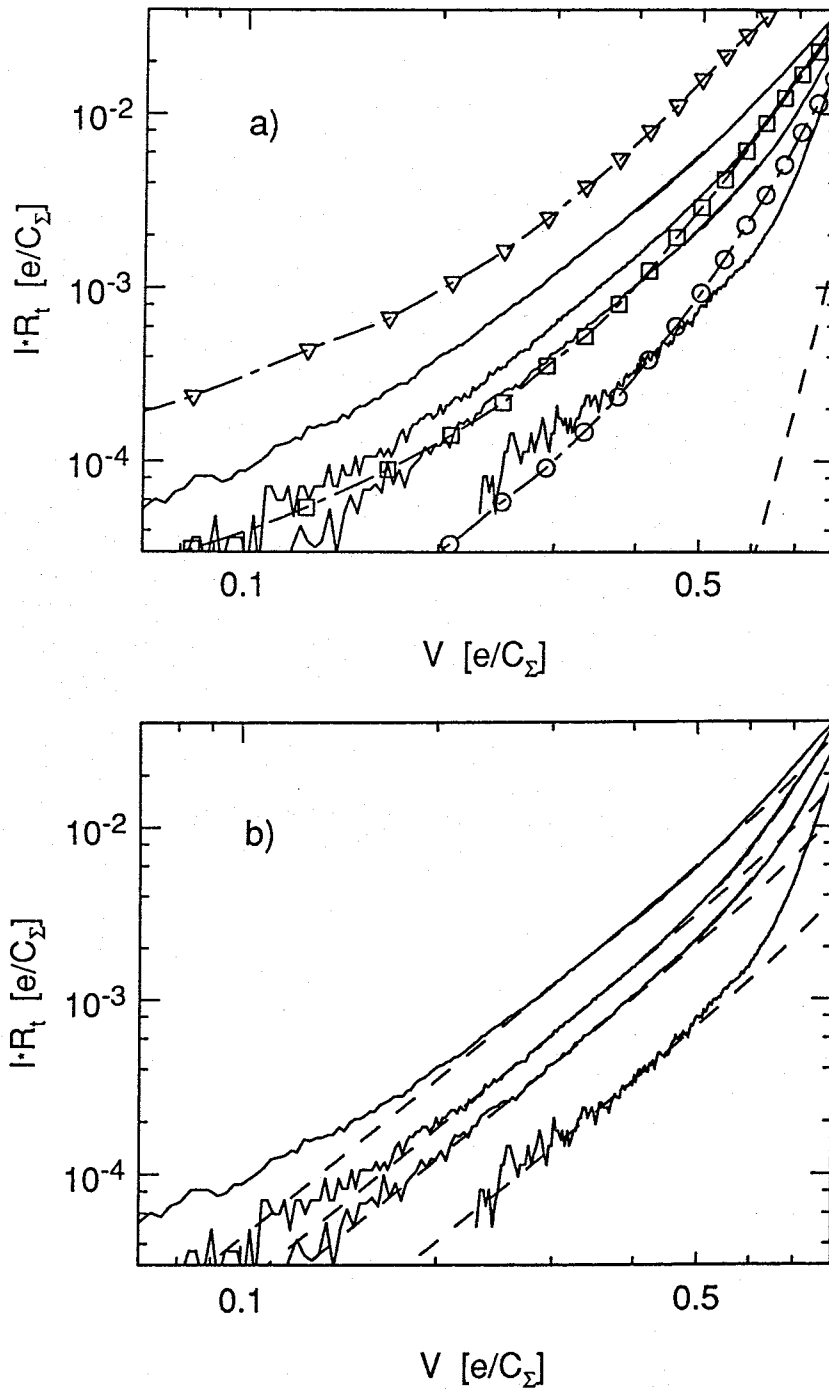


Fig. 21. I-V curves of 4 double junction devices, with $R_t=41, 77, 117$ and 347 k Ω (top left curve to bottom right curve). The Coulomb gap was maximized with V_g . (a) Comparison with classical theory (thermally assisted tunneling according to eq. (1)) for $k_B T=0.02 e^2/C_\Sigma$ (dashed curve) and $0.04 e^2/C_\Sigma$ (dash-dotted curves). Circles: $Q_0=0$; boxes: $Q_0=0.1e$; triangles: $Q_0=0.2e$. (b) Comparison with q-MQT theory (dashed curves). The curves have been fit with C_Σ , the fitted values are close to the values following from the Coulomb gap (Table 2).

R_t (k Ω)	$C_{\Sigma=e/V_{of}}$ (fF)	$C_{\Sigma=e/V_{th}}$ (fF)	$C_{\Sigma, \text{ best fit}}$ (fF)
41	0.92	1.38	1.19
78	0.77	1.21	0.95
117	0.63	0.88	0.71
347	0.68	0.91	0.72

Table 2. The parameters of the four double junctions in the q -MQT experiment.

note that for the two highest resistance devices, the fitted C_{Σ} is close to e/V_{of} . For the other two devices it is smaller. This may indicate a breakdown of the perturbative approach yielding eq. (9).

We conclude that quantum leakage is a relevant factor in the description of devices based on tunnel junctions with realistic values of R_t (below or of order of 1 M Ω). As already mentioned by Averin and Odintsov, for single-electron logic circuits like the turnstile it is therefore advisable to use more than two junctions to block electron tunneling reliably.

V QUANTUM CHARGE FLUCTUATIONS IN A NON-PERTURBATIVE APPROACH

A systematic approach to the description of tunneling in small junctions has been developed on the basis of microscopic theory (Ambegaokar *et al.* 1982, Ben-Jacob *et al.* 1983, Eckern *et al.* 1984). With this technique in principle high tunnel conductances and strong coupling to a dissipative environment, both giving rise to quantum charge fluctuations on the junctions, can be treated. An effective action can be obtained in which all microscopic degrees of freedom have been traced out and only the macroscopic degrees of freedom, the junction charge Q and a generalized phase difference $\varphi = (e/\hbar)\int V dt$, remain. In this section we will consider the effect of quantum charge fluctuations on the I-V curves, especially the conductance in the linear response regime of junctions with low R_t . The effect of the environment, causing a strong suppression of the Coulomb gap in single junctions, will also be shortly considered.

For low R_t the charge on a junction is no longer a well-defined quantity. Qualitatively one might say that the wavefunctions of the electrons leak too strongly through the barrier. Brown and Simánek (1986) obtained a closed-form expression for the conductance of a tunnel junction for arbitrary R_t . In a variational approach they replaced the effective action with a new one with

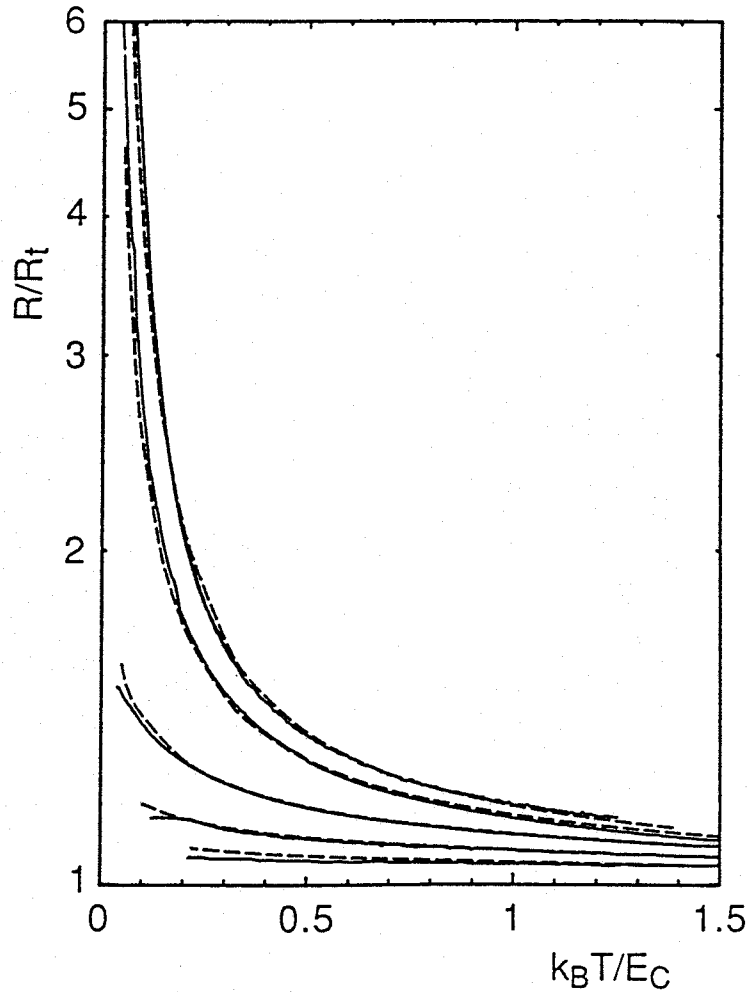


Fig. 22. Resistance versus temperature in the linear response regime for linear junction arrays. The solid curves are the measurements, the dashed curves give the theoretical predictions from Brown and Simánek. From top to bottom the devices are: double junction, $R_t=82 \text{ k}\Omega$, $C=1.1 \text{ fF}$; 5 junction array, $5.4 \text{ k}\Omega$, 1.0 fF ; 10 junction array, $1.3 \text{ k}\Omega$, 0.8 fF ; 10 junction array, $0.52 \text{ k}\Omega$, 2.3 fF ; 10 junction array, $0.24 \text{ k}\Omega$, 3.7 fF .

effective ohmic dissipation. The current-current time correlation function was used to calculate the junction resistance with the Kubo formula, for arbitrary temperature. Also Odintsov (1988) replaced quasiparticle dissipation by an effective Ohmic one to calculate the I-V curve for a very low R_t junction. Here we compare measurements of the linear response of junction arrays with the Brown and Simánek theory. The use of arrays is necessary to fix the junction capacitance and exclude the parasitic capacitance of the leads. In Fig. 22 we give for several arrays the resistance normalized to the tunnel resistance as a function of temperature. R_t varies between 0.24 and 82

k Ω . The sharp (actually exponential) resistance increase at low temperature for the high resistance samples is strongly suppressed in the low resistance samples. The agreement with the theory from Brown and Simánek is good if the capacitance is allowed to be used as a fit parameter. In principle it should be equal to the capacitance determined from the asymptote of the I-V curve. For the devices with $R_t > 1$ k Ω the fitting adjustment is within a factor 2. At low temperatures the measured R(T) curves for high R_t samples are dependent on the gate voltage. In this case the fit with theory is less satisfactory.

Much attention is being given at this moment to the influence of the environment on Coulomb blockade. Generally, the capacitance between leads to a single junction is very large compared to the junction parallel plate capacitance. This results in the absence of a Coulomb gap in a single junction without special precautions (Delsing *et al.* 1989a, Geerligs *et al.* 1989). By using high impedance leads the effect of parasitic lead capacitance can be effectively avoided. One possibility to realize high impedance leads is to use arrays of junctions (Fig. 4, see also Delsing *et al.* 1989a). Cleland *et al.* (1990) showed that leads in the form of narrow strips of high sheet resistance material also cause a clear Coulomb gap to appear in single junctions. Although these may seem trivial results, until recently there was some controversy about this subject. It was argued by Büttiker and Landauer (1986) and supported by van Bentum *et al.* (1988a) that due to the short tunneling time a Coulomb gap should be observed also in a single junction. The reasoning is that only the capacitance within a small radius given by the product of speed of electromagnetic field and electron barrier traversal time (approximately $(10^8 \text{ ms}^{-1}) \cdot (10^{-15} \text{ s}) = 100 \text{ nm}$) can contribute to the capacitance for charging effects - a 'relativistic horizon' argument (Geigenmüller and Schön, 1989). Recently this problem has been treated by various authors (Nazarov 1989a and 1989b, Devoret *et al.* 1990, Cleland *et al.* 1990, Averin and Schön 1990). The results vary in the basic assumptions, but describe similar results for most practical cases that have been examined so far. The models consider the influence of an arbitrary frequency dependent shunt impedance on the tunneling process in a junction. The electromagnetic field in the shunt geometry is influenced by but also has a backinfluence on the tunneling process. Devoret *et al.* showed that a Coulomb gap is due to inelastic tunneling; i.e. it arises if during tunneling low frequency modes can be excited in the environment. If only elastic tunneling is possible (due to small coupling to environmental modes, e.g. in a low impedance environment) no Coulomb gap arises. These authors as well as Cleland *et al.* showed that the Coulomb gap in a single junction can also be understood to be washed out by quantum fluctuations in the environment. Calculating these fluctuations from the fluctuation-dissipation theorem for a well-controlled experimental impedance Cleland *et al.* found

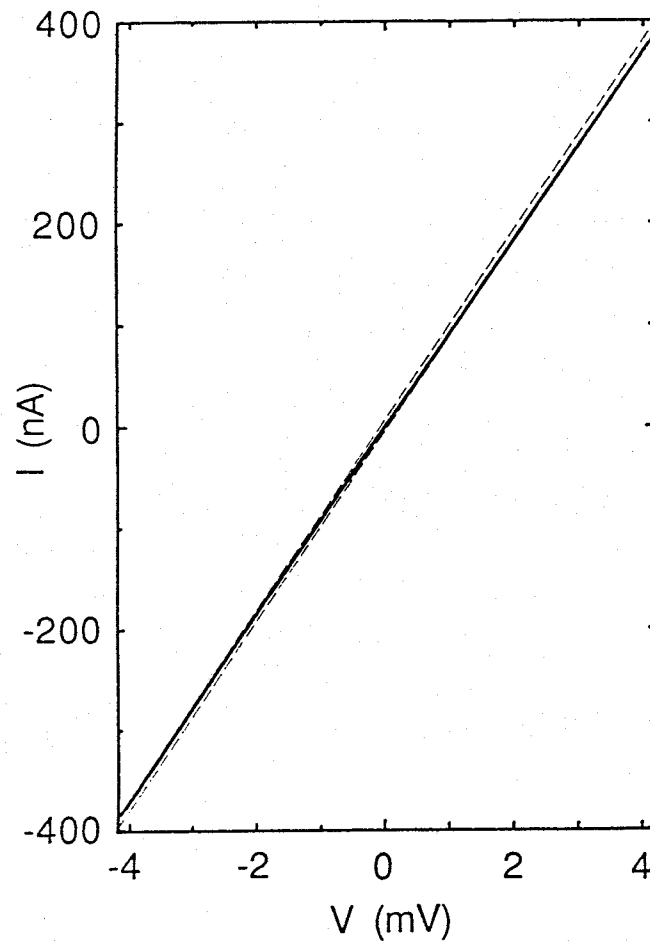


Fig. 23. I-V curve of a single junction at high current. The asymptotes (dashed lines) yield $R_t=10.7\text{ k}\Omega$ and $C=1.3\text{ fF}$, the capacitance being in agreement with the $0.01\text{ }\mu\text{m}^2$ junction area.

agreement between theory and observed suppression of the Coulomb gap. Note that these authors take the charge fluctuations due to the environment to be incoherent. Features of macroscopic quantum mechanical behavior of the environment are not present in this approach, such as for example quantization of the energy levels in the case of a large series inductance, resulting in quantized conductance as a function of voltage (Devoret *et al.* 1990).

The solution to the relativistic horizon paradox is that two timescales are important in this problem. In addition to the Büttiker-Landauer traversal time the inverse of the energy change during tunneling is important (following from the energy-time uncertainty). The important one is the longer of the two, which is for not too high voltages in these experiments the latter one. Thus for high voltages (where this time is shortened or, in the alternative Devoret *et al.* formalism,

inelastic tunneling is possible), it is expected that the Coulomb gap appears. This has not been conclusively observed. An alternative way to cut off the effective tunneling time is to increase the current to a level where the mean time between tunneling events - e/I - becomes short. We have observed a Coulomb gap in single junctions (Fig. 23) with the current rather than the voltage apparently being the relevant quantity.

VI CONCLUSIONS

An important result from the presented experiments is the good agreement of theory with the observed charging effects in arrays of junctions, for bias voltages not much larger than e/C .

For devices constructed of high resistance junctions, the behavior is in quantitative agreement with very simple calculations, based on straightforward engineering concepts like ideal parallel plate capacitors and voltage sources. It is apparently unnecessary to take into account non-equilibrium effects like creation of hot electrons or sample heating. The experimental expertise is advanced enough to start working on practical applications. One important aspect should then be born in mind, namely the possible presence of background charging of the junctions.

In the same low voltage regime the effects of charge fluctuations due to low tunnel resistance are also in good agreement with theory. For not too low resistance, electrons can leak through a Coulomb blockade barrier in an act of macroscopic quantum tunneling of the charge. For our relatively large systems it is, as expected, the inelastic process of successive incoherent electron tunneling events which dominates. For low tunnel resistance (compared to $h/4e^2$) the Coulomb blockade effects are strongly suppressed. The charge on the junctions is no longer a (semi-) classical variable, but fluctuates strongly. The resulting junction impedance follows the fluctuation-dissipation theorem.

This is roughly where at present most of the experimental knowledge ends. From the agreement of results with global rule, one can conclude that there is interaction of the junctions with the environment. This is clearly a subject to examine carefully. The high voltage behavior of a single junction could be used to test this interaction. For this regime, detailed theory has been developed. We would also like to point at the more neglected high current behavior, which seems to have an independent influence on the Coulomb blockade. The research on interaction with the environment will benefit from development of fabrication techniques of extremely high sheet-resistance materials, which are also of great advantage for several applications.

REFERENCES

- Ambegaokar, V., U. Eckern and G. Schön, 1982, *Quantum dynamics of tunneling between superconductors*, Phys. Rev. Lett. **48**, 1745.
- Averin, D.V., and K.K. Likharev, 1986, *Coulomb blockade of single-electron tunneling, and coherent oscillations in small tunnel junctions*, J. Low Temp. Phys. **62**, 345.
- Averin, D.V., and A.A. Odintsov, 1989, *Macroscopic quantum tunneling of the electric charge in small tunnel junctions*, Phys. Lett. A **140**, 251.
- Averin, D.V., and A.A. Odintsov, Comment on "*Frequency-locked turnstile device for single electrons*", submitted to Phys. Rev. Lett.
- Averin, D.V., and K.K. Likharev, 1990, *Single-Electronics*, to be published in "Quantum Effects in Small Disordered Systems", eds. B.L. Al'tshuler, P.A. Lee and R.A. Webb (Elsevier, Amsterdam).
- Averin, D.V., and G. Schön, 1990, *Single electron effects in small tunnel junctions*, to be published in the proceedings of the NATO Advanced Study Institute on Quantum Coherence in Mesoscopic Systems, Les Arcs, April 1990.
- Bakhvalov, N.S., G.S. Kazacha, K.K. Likharev and S.I. Serdyukova, 1989, *Single-electron solitons in one-dimensional tunnel structures*, Zh. Eksp. Teor. Fiz. **95**, 1010 [Sov. Phys. JETP **68**, 581].
- Barner, J.B., and S.T. Ruggiero, 1987, *Observation of the incremental charging of Ag particles by single electrons*, Phys. Rev. Lett. **59**, 807.
- Ben-Jacob, E., E. Mottola and G. Schön, 1983, *Quantum shot noise in tunnel junctions*, Phys. Rev. Lett. **51**, 2064.
- Brown, R., and E. Simánek, 1986, *Transition to Ohmic conduction in ultrasmall tunnel junctions*, Phys. Rev. B **34**, 2957.
- Brown, R.J., M. Pepper, H. Ahmed, D.G. Hasko, D.A. Ritchie, J.E.F. Frost, D.C. Peacock and G.A.C. Jones, 1990, *Differential negative resistance in a one-dimensional mesoscopic system due to single electron tunnelling*, J. Phys.: Condens. Matter **2**, 2105.
- Büttiker, M., 1986, *Quantum oscillations in ultrasmall normal loops and tunnel junctions*, Physica Scripta T **14**, 82.
- Büttiker, M., 1987, *Zero-current persistent potential drop across small-capacitance Josephson junctions*, Phys. Rev. B **36**, 3548.
- Büttiker, M., and R. Landauer, 1986, *Traversal time for tunneling*, IBM J. Res. Develop. **30**,

451.

- Cleland, A.N., J.M. Schmidt, and J. Clarke, 1990, *Charge fluctuations in small-capacitance junctions*, Phys. Rev. Lett. **64**, 1565.
- Delsing, P., K.K. Likharev, L.S. Kuzmin and T. Claeson, 1989a, *Effect of high-frequency electrodynamic environment on the single-electron tunneling in ultrasmall junctions*, Phys. Rev. Lett. **63**, 1180.
- Delsing, P., K.K. Likharev, L.S. Kuzmin and T. Claeson, 1989b, *Time-correlated single-electron tunneling in one-dimensional arrays of ultrasmall tunnel junctions*, Phys. Rev. Lett. **63**, 1861.
- Devoret, M.H., D. Esteve, H. Grabert, G.-L. Ingold, H. Pothier and C. Urbina, 1990, *Effect of the electromagnetic environment on the Coulomb blockade in ultrasmall tunnel junctions*, Phys. Rev. Lett. **64**, 1824.
- Eckern, U., G. Schön and V. Ambegaokar, 1984, *Quantum dynamics of a superconducting tunnel junction*, Phys. Rev. B **30**, 6419.
- Esteve, D., 1990, private communication.
- Field, S.B., M.A. Kastner, U. Meirav, J.H.F. Scott-Thomas, D.A. Antoniadis, H.I. Smith and S.J. Wind, 1990, *Conductance oscillations periodic in the density of one-dimensional electron gases*, preprint.
- Fulton, T.A., and G.J. Dolan, 1987, *Observation of single-electron charging effects in small tunnel junctions*, Phys. Rev. Lett. **59**, 109.
- Geerligs, L.J., V.F. Anderegg, C.A. van der Jeugd, J. Romijn and J.E. Mooij, 1989, *Influence of dissipation on the Coulomb blockade in small tunnel junctions*, Europhys. Lett. **10**, 79.
- Geerligs, L.J., V.F. Anderegg, P.A.M. Holweg, J.E. Mooij, H. Pothier, D. Esteve, C. Urbina and M.H. Devoret, 1990, *Frequency-locked turnstile device for single electrons*, Phys. Rev. Lett. **64**, 2691.
- Geerligs, L.J., D.V. Averin and J.E. Mooij, 1990, *Observation of macroscopic quantum tunneling of the electric charge*, submitted to Phys. Rev. Lett.
- Geigenmüller, U., and G. Schön, 1989, *Single-electron effects in arrays of normal tunnel junctions*, Europhys. Lett. **10**, 765.
- Giaever, I., and H.R. Zeller, 1968, *Superconductivity of small tin particles measured by tunneling*, Phys. Rev. Lett. **20**, 1504.
- Gorter, C.J., 1951, *A possible explanation of the increase of the electrical resistance of thin metal films at low temperatures and small field strengths*, Physica **17**, 777.

- Guinea, F., and N. Garcia, 1990, *Scanning tunneling microscopy, resonant tunneling, and counting electrons: a quantum standard of current*, Phys. Rev. Lett. **65**, 281.
- Kouwenhoven, L., 1990, unpublished, observed a Coulomb staircase and field-independent conductance oscillations in a chain of quantum dots.
- Kuzmin, L.S., and K.K. Likharev, 1987, *Direct experimental observation of discrete correlated single-electron tunneling*, Pis'ma Zh. Teor. Eksp. Fiz. **45**, 389 [JETP Lett. **45**, 495].
- Kuzmin, L.S., and M.V. Safronov, 1988, *Observation of one-electron Coulomb effects in end-type tunnel junctions*, Pis'ma Zh. Teor. Eksp. Fiz. **48**, 250 [JETP Lett. **48**, 272].
- Kuzmin, L.S., P. Delsing, T. Claeson and K.K. Likharev, 1989, *Single-electron charging effects in one-dimensional arrays of ultrasmall tunnel junctions*, Phys. Rev. Lett. **62**, 2539.
- Lambe, J., and R.C. Jaklevic, 1969, *Charge-quantization studies using a tunnel capacitor*, Phys. Rev. Lett. **22**, 1371.
- Likharev, K.K., 1987, *Single-electron transistors: electrostatic analogs of the dc SQUIDs*, IEEE Trans. Magn. **23**, 1142.
- Likharev, K.K., 1988, *Correlated discrete transfer of single electrons in ultrasmall tunnel junctions*, IBM J. Res. Develop. **32**, 144.
- Likharev, K.K., N.S. Bakhvalov, G.S. Kazacha, and S.I. Serdyukova, 1989, *Single-electron tunnel junction array: an electrostatic analog of the Josephson transmission line*, IEEE Trans. Magn. **25**, 1436.
- Martinis, J.M., M.H. Devoret and J. Clarke, 1987, *Experimental tests for the quantum behavior of a macroscopic degree of freedom: The phase difference across a Josephson junction*, Phys. Rev. B **35**, 4682.
- Meirav, U., M.A. Kastner, M. Heiblum and S.J. Wind, 1989, *One-dimensional electron gas in GaAs: Periodic conductance oscillations as a function of density*, Phys. Rev. B **40**, 5871.
- Mooij, J.E., and G. Schön, 1985, *Propagating plasma mode in thin superconducting filaments*, Phys. Rev. Lett. **55**, 114.
- Mooij, J.E., B.J. van Wees, L.J. Geerligs, M. Peters, R. Fazio and G. Schön, 1990, *Unbinding of charge-anticharge pairs in two-dimensional arrays of small tunnel junctions*, Phys. Rev. Lett. **65**, 645.
- Mullen, K., E. Ben-Jacob, R.C. Jaklevic and Z. Schuss, 1988, *I-V characteristics of coupled ultrasmall-capacitance normal tunnel junctions*, Phys. Rev. B **37**, 98.
- Nazarov, Yu. V., 1989a, *Coulomb blockade of tunneling in isolated junctions*, Pis'ma Zh. Eksp. Teor. Fiz. **49**, 105 [JETP Lett. **49**, 126].

- Nazarov, Yu. V., 1989b, *Anomalous current-voltage characteristics of tunnel junctions*, Zh. Eksp. Teor. Fiz. **95**, 975 [Sov. Phys. JETP **68**, 561].
- Nazarov, Yu.V., 1990, *Influence of the electrodynamic environment on the electron tunneling at finite traversal time*, preprint.
- Odintsov, A.A., 1988, *Effect of dissipation on the characteristics of small-area tunnel junctions: application of the polaron model*, Zh. Eksp. Teor. Fiz. **94**, 312 [Sov. Phys. JETP **67**, 312].
- Odintsov, A.A., 1990, unpublished, independently proposed this same experiment.
- Pothier, H., D. Esteve, C. Urbina, P.F. Orfila, M. Devoret, L.J. Geerligs, V.F. Anderegg, P.A.M. Holweg and J.E. Mooij, 1990, *Ecluse mono-electron pilotée par radio-fréquence*, internal report CEN Saclay. They also consider more detailed the explanation of the $V-V_g$ plot.
- Schön, G., and A.D. Zaikin, 1990, *Quantum coherent effects, phase transitions, and the dissipative dynamics of ultra small tunnel junctions*, to be published in Physics Reports.
- Scott-Thomas, J.H.F., S.B. Field, M.A. Kastner, H.I. Smith and D.A. Antoniadis, 1989, *Conductance oscillations periodic in the density of a one-dimensional electron gas*, Phys. Rev. Lett. **62**, 583.
- Sullivan, D.B., and R.F. Dziuba, 1974, *Low temperature direct current comparators*, Rev. Sci. Instrum. **45**, 517.
- van Bentum, P.J.M., H. van Kempen, L.E.C. van de Leemput and P.A.A. Teunissen, 1988a, *Single-electron tunneling observed with point-contact tunnel junctions*, Phys. Rev. Lett. **60**, 2543.
- van Bentum, P.J.M., R.T.M. Smokers and H. van Kempen, 1988b, *Incremental charging of single small particles*, Phys. Rev. Lett. **60**, 2543.
- van der Wel, W., J.E. Mooij and C.J.P.M. Harmans, 1988, *Cryogenic current comparator with increased resolution*, Rev. Sci. Instrum. **59**, 624.
- van Houten, H., and C.W.J. Beenakker, 1989, Comment on "*Conductance oscillations periodic in the density of a one-dimensional electron gas*", Phys. Rev. Lett. **63**, 1893.
- Wilkins, R., E. Ben-Jacob and R.C. Jaklevic, 1989, *Scanning-tunneling-microscope observations of Coulomb blockade and oxide polarization in small metal droplets*, Phys. Rev. Lett. **63**, 801.
- Yoshikawa, N., M. Sugahara and T. Murakami, 1989, *The circuits of phase-quantum-tunneling device*, IEEE Trans. Magn. **25**, 1286.
- Zeller, H.R., and I. Giaever, 1969, *Tunneling, zero-bias anomalies, and small superconductors*, Phys. Rev. **181**, 789.

CHAPTER 3

CHARGE AND PHASE DYNAMICS IN JOSEPHSON TUNNEL JUNCTIONS

*May the New Year bring us ... fewer but more
successful theories*

Editorial Phys. Rev. Lett. January 1, 1959.

I INTRODUCTION

In this chapter we present measurements on superconducting tunnel junctions (Josephson junctions) with small capacitance. These measurements, mainly current-voltage (I-V) characteristics, provide information about the dynamics of two macroscopic degrees of freedom, the junction charge and phase difference. These degrees of freedom are not independent. The phase difference can only be well-defined if there is the possibility of a free exchange of Cooper-pairs across the junction (e.g. Ferrell and Prange 1963, Anderson 1964, De Gennes 1966). If this exchange, or the accompanying charge fluctuations, are for any reason inhibited, the phase becomes uncertain and the charge becomes the well-defined variable. This is obvious for the extreme limit of two distant pieces of bulk superconductor. In this work we are concerned with the quenching of charge fluctuations due to the small capacitance of junctions: Transfer of a Cooper-pair across a junction of capacitance C will typically yield an energy change of order $E_C \equiv e^2/2C$. At temperatures far below E_C/k_B energetically unfavorable events will be forbidden, so that the junction charge is well-determined. Since the junction states that differ by a Cooper-pair are mixed by a tunneling matrix element of magnitude $E_J/2$, the important parameter in the balance of charge and phase fluctuations is the ratio E_J/E_C . For large E_J/E_C , the junction behavior is in practical cases well-described by classical dynamics of the phase. For small E_J/E_C , a classical charge is better suited to describe a Josephson junction (see, e.g., the review by Schön and Zaikin 1990).

An interesting feature of tunnel junctions is that the dynamics of phase and charge, as macroscopic degrees of freedom, are subject to quantum mechanics. The variables do not commute; $[\phi, q] = 2ei$, so that they obey an uncertainty relation $\delta\phi\delta q > e$. Various fascinating phenomena for small Josephson junctions, such as tunneling, Bloch oscillations and Zener tunneling of the macroscopic degrees of freedom have been predicted. However, until recently

only macroscopic quantum tunneling in phase space (ϕ -MQT) had been observed. In a recent publication (Geerligs *et al.* 1989, chapter 9) we reported on experiments in 2-D arrays of small junctions that show behavior that can be very well explained by Bloch oscillations and Zener tunneling of the constituent junctions. We also reported experiments on normal metal tunnel junctions that show macroscopic quantum tunneling of the charge degree of freedom (Geerligs, Averin and Mooij 1990, chapter 5). Here we consider superconducting junctions with E_J/E_C varying from much larger than unity, with accordingly phase as the well-defined degree of freedom, to much smaller than unity, with the charge well-defined. However, although our experiments are concerned with quantum mechanics of the macroscopic degrees of freedom of the junctions, this often coincides with tracking the behavior of single Cooper-pairs or electrons. The reader should bear in mind that this is consistent, though perhaps confusing. The significant Coulomb energy implies that all free electrons and Cooper-pairs participate in the dynamics of a single charge carrier, making this a macroscopic event.

After a short introduction of the Josephson junction as a quantum particle, in section II we will describe the experimental apparatus and techniques. In section III, measurements are presented on single junctions and short linear arrays in a low impedance environment. In that section, we will also mention the more straightforward interpretations of the measurements. A more elaborate discussion is given in section IV. In section V, we show results for single junctions which are decoupled from the environment by large 2-D arrays. A discussion of possible high-frequency experiments with small capacitance junctions is given in section VI, with some intriguing first results. Finally, conclusions are summarized in section VII.

The Hamiltonian of an isolated Josephson junction reads, if quasiparticle conduction is neglected

$$H_0 = \frac{q^2}{2C} - E_J \cos \phi \quad (1)$$

Here ϕ is, as mentioned above, the phase difference of the condensate wave functions on both sides of the barrier. It is conjugate to the number of Cooper-pairs that have tunneled through the junction, $q/2e$. This Hamiltonian is equivalent to the one describing a quantum harmonic oscillator (Condon 1928). The eigenstates are the 2π -periodic Mathieu-functions (Abramowitz and Stegun 1965). For the junction, the 2π -periodicity results directly from the discreteness of the charge on the junction. Although the operators q and $-2ei(\partial/\partial\phi)$ are identical, the commutation relation between q and ϕ is best written as $[e^{i\phi}, q/2e] = e^{i\phi}$ since ϕ is not an observable quantity (Peierls

1979). In experiments a junction is not isolated but can be charged from an external source by an amount q_x (a classical parameter), so that the Hamiltonian changes into

$$H_{q_x} = \frac{(q - q_x)^2}{2C} - E_J \cos\varphi \quad (2)$$

As noted by Büttiker (1986, 1987), this charge can e.g. be introduced by the use of a small capacitor in series with the junction, and voltage biasing this system. The charge q_x can also be introduced by a perfect current source, as is seen from a gauge transformation to an equivalent Hamiltonian

$$H_I = \frac{q^2}{2C} - E_J \cos\varphi - \frac{\hbar}{2e} I \varphi \quad (3)$$

where the bias current is equal to the time rate of change of q_x : $\partial q_x / \partial t = I$. For the junction on which an external charge is induced, the eigenstates of H_0 (or approximately of H_I) are Bloch functions $\exp(-i\varphi q_x / 2e) u_{n, q_x}(\varphi)$. In the gauge of H_{q_x} the eigenstates are just the $u_{n, q_x}(\varphi)$. However, the eigenvalues in both cases form a band energy-spectrum, with q_x as coordinate. For low E_J / E_C , well inside the Brillouin zone the band is close to parabolic: $E = q_x^2 / 2C$ for the lowest band. At the Brillouin zone edges, which are found at $q_x = \pm e, \pm 3e$, etc., a bandgap of width E_J arises due to Cooper-pair tunneling. Sweeping the external charge q_x , by means of an external current source or via the small capacitor, sweeps the junction through the band. This produces Bloch oscillations, i.e. coherent Cooper-pair tunneling with fixed time intervals $I/2e$ (Widom *et al.* 1982, Ben-Jacob and Gefen 1985, Likharev and Zorin 1985). At high sweep rates, Zener tunneling can occur, which means that a Cooper-pair tunneling event is missed (e.g. Geigenmüller and Schön 1988, Mullen, Ben-Jacob and Schuss 1988). Note that, if the work performed by the source of q_x is taken into account, the Hamiltonian is no longer 2π -invariant. This is always so if dissipation in the junction (due to shunt conductance) gives rise to an additional term

$$\frac{\hbar}{2e} I_{qp} \varphi \quad (4)$$

with I_{qp} the dissipative current, carried by quasiparticles. However, whether phases differing by a multiple of 2π are distinguishable or not, usually does not have physical consequences (see e.g. Zwerger 1987, Schön and Zaikin 1988).

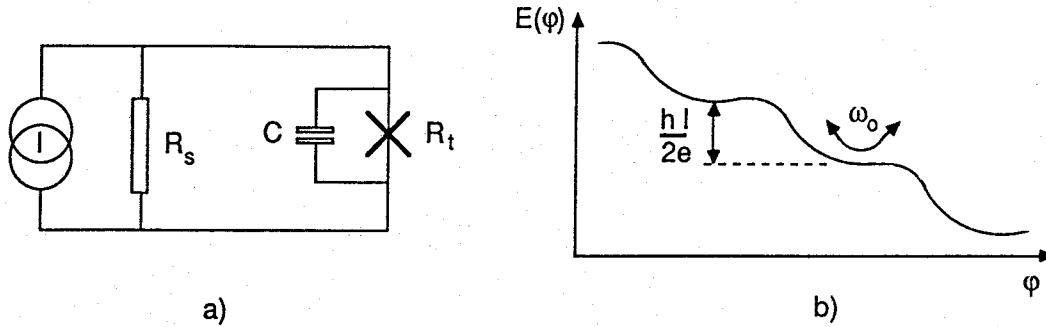


Fig. 1. The analogue of a classical Josephson junction (left) is a point particle in a sloped cosine-potential (right), with coordinate ϕ . The mass of the particle is proportional to the junction capacitance, the height of the potential wells to the Josephson coupling and the friction to the junction shunt conductance.

The hamiltonian (3)+(4) yields for classical phase the well-known picture of a point particle in a sloped washboard potential, subject to friction (Fig. 1). The Hamilton equation of motion for q is just the current balance of the junction. It contains the Josephson pair current term $I_S = I_C \sin \phi$. The equation of motion for ϕ yields the ac Josephson relation $q/C = V = \hbar \dot{\phi} / 2e$. The quantum mechanical description is likewise analogous to that of a particle in a periodic potential, subject to a driving field $\hbar I / 2e$. (Although for zero current bias the eigenstates are delocalized in ϕ -direction, in high E_J / E_C junctions in practical situations the phase is localized, see e.g. Nagai and Kondo 1980 or Schön and Zaikin 1990). One interesting feature of this macroscopic quantum system is the interaction between macroscopic quantum degrees of freedom and the underlying microscopic degrees of freedom, which can be identified with dissipation (Caldeira and Leggett, 1981, Ambegaokar, Eckern and Schön 1983, Schön and Zaikin 1990). This subject has received much theoretical research. The general outcome is that strong dissipation, which coincides with a large single electron conductance in the junction, quenches phase fluctuations. Several experiments, most convincingly ϕ -MQT (Esteve *et al.* 1989), but possibly also the observation of phase transitions in granular or regular 2-D Josephson junction arrays (Mooij and Schön 1988), have shown this effect of dissipation. We will consider the effects of dissipation on the quantum dynamics mainly in section VI.

With the advance of submicron fabrication techniques, the fabrication of junctions for studying macroscopic quantum effects seems to have become trivial. However, a serious practical problem is encountered if one attempts to realize the current bias. Without special care, at high frequencies the junction will be shunted by the low impedance environment from its bias leads, which is of the order of the free space impedance. This problem was realized, but not completely solved, in previous experiments on Josephson junctions in the quantum regime by Iansiti *et al.* (1988, 1989). Later Martinis and Kautz (1990) showed the effect of the high frequency impedance on the characteristics of classical junctions in a carefully designed environment. The usual way to circumvent the problem of a low impedance environment has become the use of several junctions in series. In the limit of long arrays this can realize a current bias, but even for two junctions there is the advantage that at least the capacitance of the junction is reasonably well defined. The impedance of the neighbouring junctions will generally also decrease the damping of a given junction. Therefore in our experiments we concentrated mostly on short arrays of junctions.

As Fulton *et al.* (1989) pointed out, important features of the behavior of these short arrays under voltage bias can be understood from a description based on the simple tunneling hamiltonian for Cooper-pairs:

$$H = H_L + H_R + H_T + H_Q \quad (5)$$

where H_T couples states differing by one Cooper-pair, via a matrix element of magnitude $E_J/2$ (Josephson 1962, Ambegaokar and Baratoff 1963). H_L and H_R describe the electrodes, H_Q the charging energy. Of course, this Hamiltonian is also the basis of (1)-(4), but as Fulton *et al.* showed it can often be conveniently interpreted in terms of single Cooper-pair motion. Since Cooper-pairs are condensed at the Fermi level, mixing of electrode charge states differing by one Cooper-pair is strong only if they are at approximately the same energy. Due to Coulomb blockade effects, for small capacitance junctions this requires generally a significant voltage on the junction (e/C for an isolated junction). This aspect of Cooper-pair tunneling is similar to single electron tunneling in normal metal tunnel junctions. However, the single electron tunneling is stochastic. In the normal state, the probability that a tunneling event occurs in a short time interval is proportional to the energy change during tunneling ΔE . In contrast, in the superconducting state a coherent charge oscillation across the tunnel barrier arises, with amplitude decreasing with increasing $|\Delta E|/E_J$. In the adiabatic approximation, sweeping the junction state through the resonance condition $\Delta E=0$, will always result in Cooper-pair tunneling (a Bragg reflection occurs

at the band edge).

For the short arrays of junctions which are considered in this chapter, we find for low E_J/E_C a regime of classical charge. We can explain the results with single Cooper-pair dynamics, subject to Coulomb blockade effects. In the intermediate and large E_J/E_C regime, the description is more complicated. For high E_J we can use the familiar description in ϕ -space, although this description is quite complicated due to frequency-dependent damping. For intermediate E_J/E_C , this description is affected by the presence of quantum fluctuations of the phase.

II EXPERIMENTAL TECHNIQUES AND JUNCTION CHARACTERIZATION

A Experimental techniques

All junctions described in this work are fabricated from aluminum. They are evaporated together with the connecting circuit on 0.4 mm thick silicon substrates, usually on a 0.4 μm silicon oxide isolating top layer. Aluminum junctions have several advantages for this research, the only disadvantage probably being the low critical temperature. They can be easily and reliably fabricated, since the condensation heat of aluminum is not very large and does not affect our evaporation mask. The grain size is fairly small, and the condensed metal has low mobility, features that are necessary in order to define a small junction area. The junction quality is very high, for a wide range in linear dimension (from at least μm 's to tens of nm's).

The junctions were produced by shadow evaporation, as illustrated in Fig. 2. The advantage of this method is the fabrication of a complete junction in one vacuum cycle. This ensures a high quality tunnel barrier, for reasonable current densities. For this technique, a suspended mask has to be created. In our case this mask is made of Ge, suspended 200-1000 nm above the substrate by a layer of organic resist. On top of the Ge, a high resolution e-beam resist is applied for patterning of the circuit. The coarse circuit (connection leads) can be exposed with deep-UV. After that, the actual junction pattern is written with a modified SEM with a spot size of about 8 nm, at 50 kV beam voltage and about 5 to 10 pA current. After developing, this pattern is transferred into the Ge by reactive ion etching. The suspending organic material is removed by a combination of anisotropic reactive ion etching and isotropic wet etching. In this way, a free hanging bridge is created, that is used for evaporating the junction. Typically a first layer of 25 nm Al is evaporated, followed by oxidation of the barrier and evaporation of a 50 nm counter electrode from a different angle. The barrier thickness is controlled by the oxidation pressure. Values between 0.02 and 10

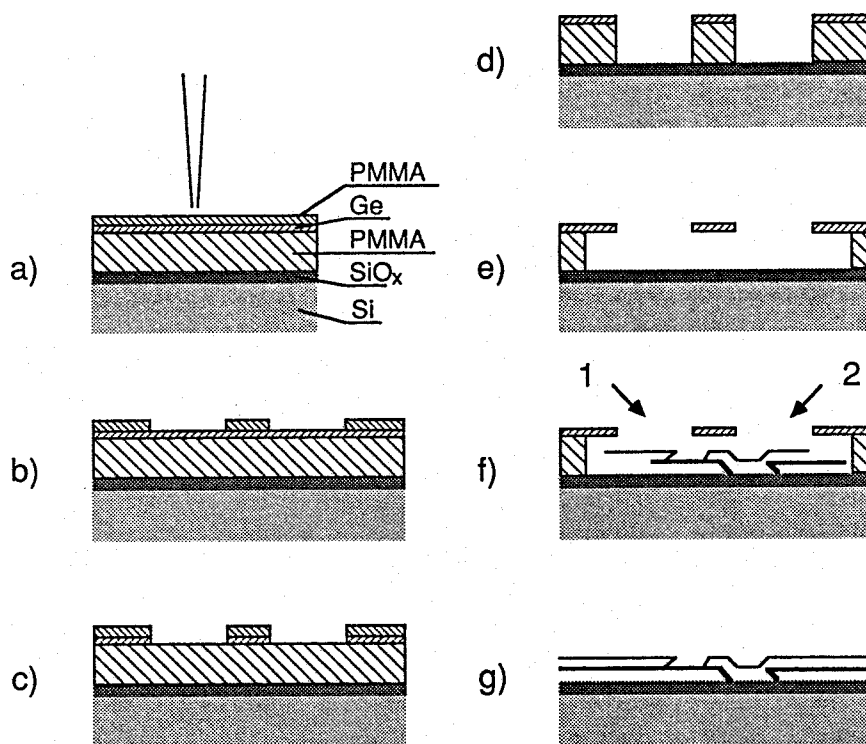


Fig. 2. Schematic side-view of shadow evaporation of small junctions. (a) A pattern is defined in the upper layer of a three-layer resist by U-V and e-beam exposure, and subsequently developed (b). (c) The pattern is transferred into an intermediate Ge-layer by reactive ion-etching with SF_6 . (d) This pattern is again transferred into the bottom layer by reactive ion etching with O_2 . (e) An undercut is created by wet (isotropic) etching of the bottom layer. (f) In one vacuum-cycle two aluminum electrodes are evaporated from two angles, with an oxidation step in between to create the barrier. A suspended Ge-bridge thus results in a small junction. (g) Liftoff in acetone clears the unused silicon-oxide surface.

mbar yield reliable barriers for a critical current density between 10^4 and 10^7 A/m². After evaporation, the mask is lift-off with acetone. The resulting junctions are typically very stable. They survive storage in normal air for a period of up to several years. The tunnel resistance does not change significantly over this time, except for high current density barriers and junctions with dirty aluminum electrodes.

All measurements were performed with the junctions thermally anchored to the mixing chamber of a dilution refrigerator. We found that glueing the substrate with vacuum grease to a copper sample holder provided sufficient thermal contact. The leads were also thermally anchored close to their connection with the sample. The electrical setup is carefully designed to prevent radio-

frequency interference and ground loops reaching the sample or affecting the measurements. It is divided in two parts. The primary part consists of the cryostat, with separate ground, the sample and a minimal amount of measurement circuitry. The latter consists of the voltage preamplifier and active current source, or alternatively the voltage source with current sensing virtually shorted FET-input opamp, all powered by floating power supplies. This circuitry is shielded in closed metal boxes that are grounded to the cryostat via the shields of the measurement cables. The secondary part of the circuitry, consisting of e.g. oscilloscope, ramp generator, and lock-in amplifier, is powered by line power, with a clean separate ground. The connection between the two parts is formed by two high level voltage lines: the first is a control voltage for the bias source, the second line carries the output voltage of the pre-amp or current sensing opamp. These two signals are optically decoupled by high-accuracy (0.1 %) analog optical isolation-amplifiers. As a result, in case of noise problems only a very simple circuit on the primary side has to be debugged.

All lines into the cryostat are shielded, twisted, and filtered by 1 MHz low-pass filters at the cryostat entrance. However, for experiments on superconducting tunnel junctions at these low temperatures it is usually necessary to add low-pass filters which are thermally anchored to the mixing chamber (Martinis, Devoret and Clarke 1987). This is probably due to the sensitivity of the junctions to high-frequency room temperature noise, which can e.g. develop in the leads inside the cryostat. If this cryogenic filtering is omitted, in our case usually the I-V curves (or I_C -histogrammes, etc.) do not change below about 300 mK. Cold RC-filters already improved the measurements, but in most experiments we used RC filters in combination with special microwave filters, with the sample in a tightly closed, conducting box. The special filters consisted of a long length of signal lead, coiled inside a tube filled with tightly packed copper powder (<30 μm grainsize). High frequency signals (above about 1 GHz) are very effectively attenuated in these filters by skin effect damping in the small copper grains. Measurements on small-capacitance junctions obtained in this way showed significant changing of the I-V curves, below 100 mK. To test this filtering, we also performed standard phase-MQT experiments, which are reputedly very sensitive to high frequency room-temperature noise. Results are in good agreement with theory for ϕ -MQT and will be given in later sections. Although many measurements are recorded at or below 20 mK mixing chamber temperature, we avoid to attribute any special significance to this temperature compared with, say, 50 mK, to be on the safe side with respect to e.g. filtering, sample heating or non-equilibrium effects. This is also the reason that we like to study charging effects in junctions with capacitance of order 10^{-15} F ($E_C/k_B \approx 1$ K)

even though junctions with $C \approx 10^{-14}$ F of high enough resistance (about 100 k Ω) have E_J/E_C of order 1, and should therefore show strong charging effects below 100 mK.

B Junction characteristics

For interpretation of the measurements, it is important to have an accurate estimate of junction parameters like the Josephson coupling energy E_J , the capacitance C (or the charging energy E_C), the quasiparticle supgap resistance and possible ohmic leakage of the junctions. The devices which are discussed in this chapter are listed in Table 1.

The capacitance of small junctions can be determined from the normal state Coulomb gap. It is related to the voltage offset of the asymptote of the I-V curve (see chapters 5 and 6). We have taken the offset ΔV of the linear part of the I-V curve, not very far outside the Coulomb gap, to be given by the 'global rule' (Geigenmüller and Schön 1989) as $\Delta V = (n-1)e/2C$, where n is the number of junctions in the array. This was determined at a voltage of around 3-4 mV and a current below 100 nA. For high currents (of order 1 μ A) or voltages (50 mV) we expect an offset consistent with 'local rule', i.e. equal to $ne/2C$. The latter determination was used for low resistance arrays or small single junctions, where a sharp Coulomb gap is absent. Note that unequal junction capacitances affect the quoted equations for the offset voltage. For large junctions ($\geq 0.5 \mu\text{m}^2$), we have assumed the capacitance to scale with the junction area. This seems plausible given the results for the small junctions, for which the junction capacitance roughly follows the parallel plate formula $C = \epsilon_0 A/t'$, where A is the junction area and $t' = t/\epsilon_r$ is about 1-1.5 \AA (chapter 6). The barrier thickness t is dependent on oxidation pressure, and varies by about a factor 2 in the range that we use.

The Josephson coupling energy E_J is related to the critical current I_c of a junction by $E_J = \hbar I_c / 2e$. However, in our experiments for all but the largest junctions the supercurrent is significantly less than I_c because of thermal or quantum fluctuations. Therefore we determine E_J from the Ambegaokar-Baratoff (1963) relation $I_c(T) = (\pi\Delta/2eR_n) \tanh(\Delta/2k_B T)$, where R_n is the normal state resistance in the absence of charging effects of the junction. In this equation the temperature dependent quasiparticle excitation gap $\Delta(T)$ appears. We have checked for several junctions, large as well as small ones, that this gap follows the BCS relation (e.g. Mühlischlegel 1959), both for the dependence on T/T_c and for the relation $\Delta(0) = 1.76 k_B T_c$ (Fig. 3). For a 3 μm^2 junction of low resistance, we have checked that the critical current also follows the Ambegaokar-Baratoff prediction, both in absolute value and in temperature dependence (Fig. 4). (Note,

sample	R_n (k Ω)	C (fF)	E_J/k_B (K)	E_C/k_B (K)	E_J/E_C
1A	0.14	200	54	0.005	$1.1 \cdot 10^4$
1B	0.57	50	13	0.02	$7 \cdot 10^2$
1C	4.5	1.5	1.7	0.9	2.7
1D	140	1	0.05	0.9	2.7
1E	14	2.7	0.53	0.34	1.6
1F	132	2.9	0.06	0.32	0.18
2A	58	1	0.13	0.9	0.14
2B	41	0.43	0.18	2.1	0.09
2C	110	0.6	0.07	1.6	0.04
2D	117	0.28	0.064	3.3	0.02
3A	2.7				
3B	73	1.4	0.10	0.7	0.15
5A	5.5	1	1.4	0.9	1.6
5B	58	2	0.13	0.45	0.3
5C	64	1	0.12	0.9	0.13

Table 1. Devices discussed in this chapter. The digit in the name gives the number of junctions in series. Samples 1E and 1F are single junctions with 2-D arrays in the leads for decoupling from the environment. The capacitance determination was performed in various ways, as discussed in the text. For single junctions 1B to 1D the quoted value for E_J/E_C is probably not very realistic due to shunting by parasitic capacitance in the environment.

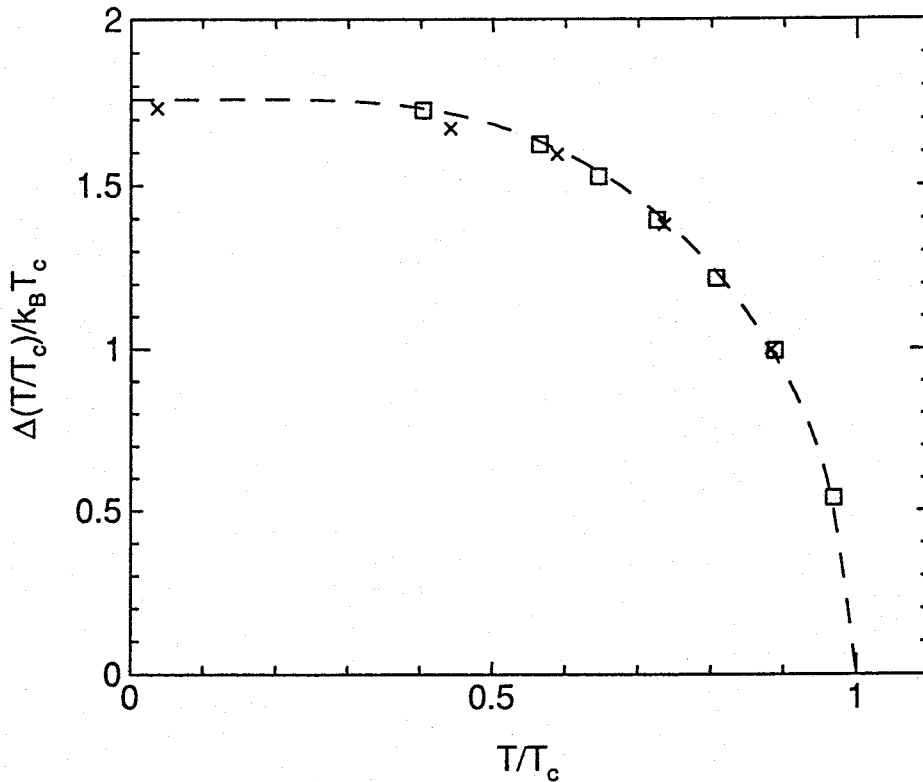


Fig. 3. Measured gap voltage (from the I-V curves) versus reduced temperature for two single junctions. Boxes are for junction 1A ($3 \mu\text{m}^2$, $R_n=140 \Omega$, $C \approx 200 \text{ fF}$). Crosses are for junction 1D ($0.01 \mu\text{m}^2$, $R_n=140 \text{ k}\Omega$ and $C \approx 1 \text{ fF}$). The dashed curve gives the BCS-expression for the gap as a function of temperature. For junction 1A the fitted T_c is equal to 1.24 K, for 1D it is 1.36 K.

however, that the $\Delta(0)$ and fitted T_c in Fig. 3 for this junction are suppressed compared to the $I_c(T)$ fit). Since this junction was fabricated with the same procedure as the smaller ones, we assume that the Ambegaokar-Baratoff relation also describes $E_J(T)$ for the smaller junctions. The critical temperature of the aluminum varies around 1.35 K. This is higher than the literature value for bulk aluminum of ≈ 1.2 K. The T_c is correlated to the film thickness. We found for 100 nm thick aluminum $T_c=1.30$ K, increasing for thinner films to 1.52 K at 20 nm.

The small signal quasiparticle resistance R_{qp} of two arrays of three small capacitance junctions was measured directly from the I-V curve. The critical current was suppressed by a magnetic field of 0.4 Tesla. In Fig. 5 we have plotted the quasiparticle resistance together with the prediction of Bol *et al.* (1985), which can be closely approximated by

$$R_{qp}/R_n = \exp[\Delta(0)(1/T - 1/T_c)/k_B] \quad (6)$$

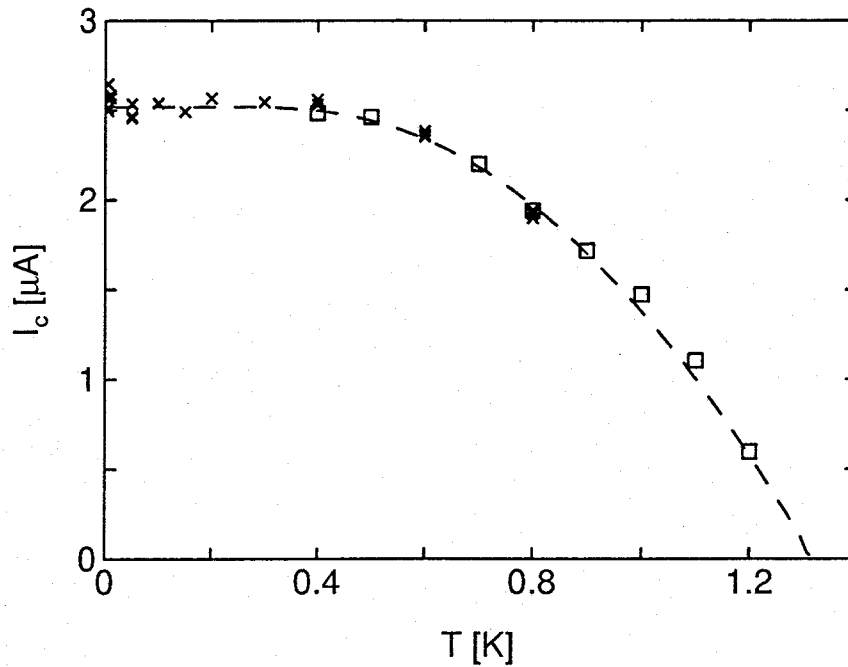


Fig. 4. Critical current from switching distributions (crosses) and I-V curves (boxes) for junction 1A. The fitted T_c is 1.32 K, the corresponding $I_c(T)$ is in good agreement with the Ambegaokar-Baratoff equation (dashed curve).

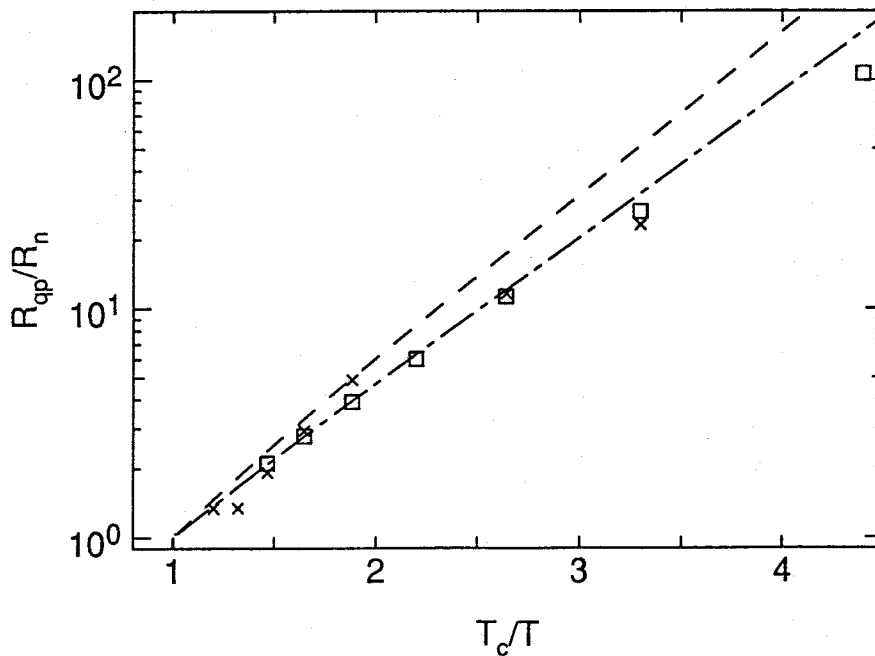


Fig. 5. Subgap resistance relative to normal state resistance for array 3A (three small capacitance junctions) (boxes) and single junction 1A (crosses), versus inverse reduced temperature. The lines give the theoretical prediction, which can be closely approximated by $R_{qp}/R_n = \exp[\Delta(0)(1/T - 1/T_c)/k_B]$. For the dashed line $\Delta(0) = 1.76k_B T_c$, for the dashdotted line $\Delta(0) = 1.6k_B T_c$.

The agreement is good, if $\Delta(0) \approx 1.6k_B T_c$ instead of the BCS value $\Delta(0) = 1.76k_B T_c$ is used. A very small part of the exponential resistance increase in this experiment will have been due to the Coulomb blockade. An alternative way to determine the quasiparticle resistance uses measurements of the so-called retrapping current in the I-V curve (Stewart 1968, McCumber 1968). On decreasing the bias current, a classical junction that is in the running state in the washboard potential, will eventually switch back from high voltage to a supercurrent. The current at which this occurs is dependent on the quality factor $Q = \omega_p RC$, where the plasma frequency $\omega_p = \omega_0(1 - (I/I_c)^2)^{1/4}$, $\hbar\omega_0 = \sqrt{8E_J E_C}$ and R is the damping resistance at high voltage, which is essentially the DC resistance R_{qp} . The R_{qp} determined in this way for a classical single junction is also plotted in Fig. 5. It too fits satisfactorily to the expression (6), which we therefore assume to be valid at least for the temperature range of these measurements (down to 0.3 K).

The ohmic shunt conductance of these junctions is very low. This follows from two types of measurements on small junctions. First, in the normal and superconducting state for high R_n it is possible to induce a gate charge on a metal island between two junctions in an array for apparently indefinite time (except for special cases where the charge jumps between two or more discrete values). The fact that this charge does not leak away notably, shows that only discrete charge transfer is possible from these islands. In addition, in the superconducting state for low E_J/E_C generally a Coulomb gap develops with very high resistance. The lower limit on the determination of the resistance inside the gap is posed by the experimental current noise. For the associated low voltages it is a few $G\Omega$'s. Ohmic conductance would show up inside the Coulomb gap, unaffected by the Coulomb blockade.

III EXPERIMENTAL RESULTS FOR VOLTAGE BIASED SYSTEMS

In this section we will present results for junctions which are capacitively shunted by the measurement leads, so that they are voltage biased for high frequencies. Even if a current bias is applied externally, the current only buffers the shunt capacitance and determines the accessible part of the I-V curve. The relevant frequencies change with the state and parameters of the junction. However, due to the high internal impedance of the junctions and the very low specific inductance of our leads we can say that the junctions are voltage biased roughly from 100 MHz up to frequencies larger than the gap frequency of aluminum. However, the voltage bias is not perfect; resonances and neighbour junctions still affect the junction dynamics. This will be considered in section IV.

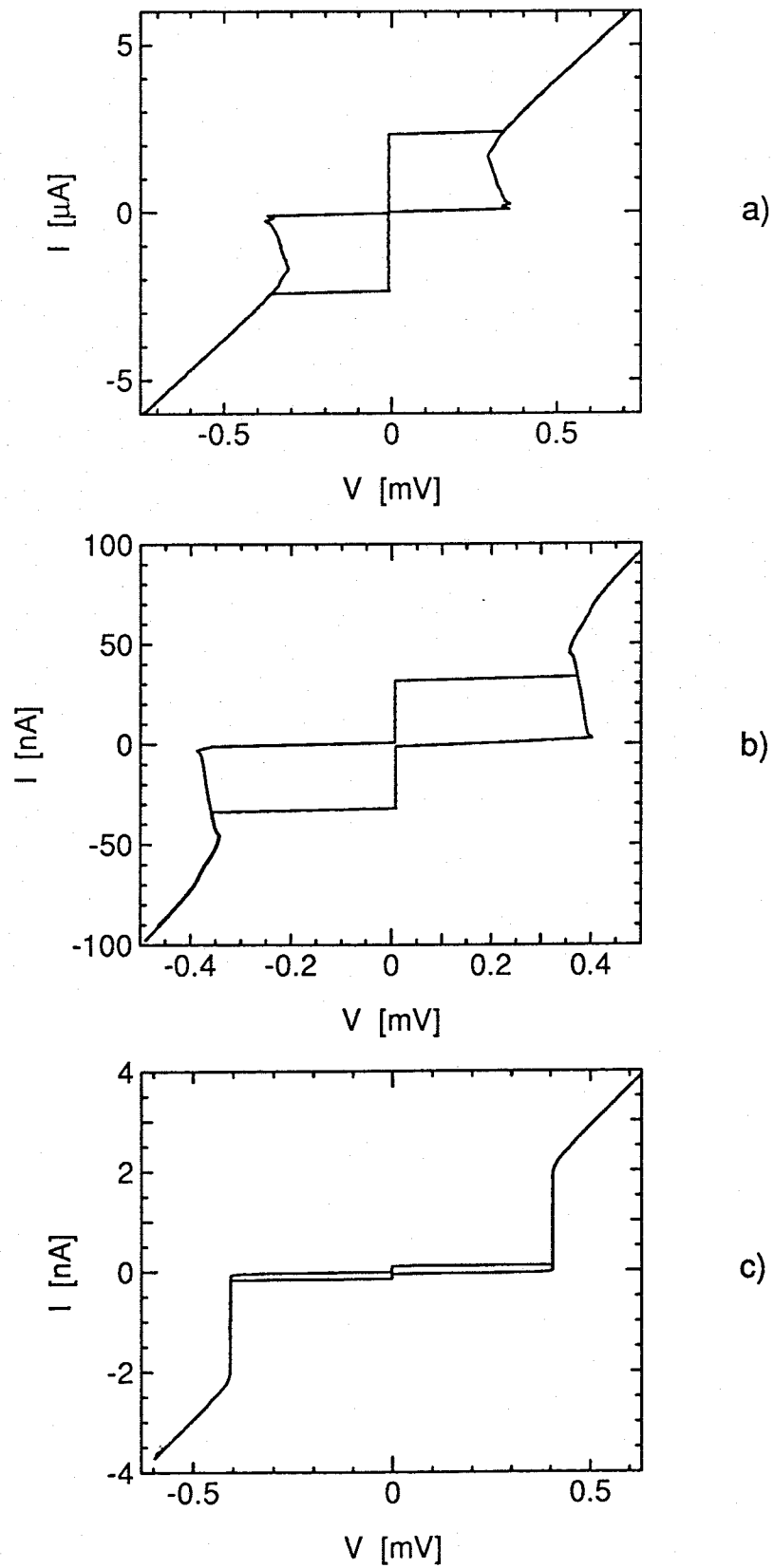


Fig. 6. *I-V* characteristics for single junctions. (a) 1A ($R_n=140 \Omega$, $C\approx 200 \text{ fF}$); (b) 1C ($R_n=4.5 \text{ k}\Omega$, $C=1 \text{ fF}$); (c) 1D ($R_n=140 \text{ k}\Omega$, $C=1 \text{ fF}$).

A Single junctions

Single junctions will typically be biased from a source impedance of about 50 Ω . This is already sufficient to predict that charging effects must be strongly suppressed (e.g. Nazarov 1990, Devoret *et al.* 1990). We will describe experimental results for junctions with area between 3 and 0.01 μm^2 , resistance varying between 140 Ω and 140 k Ω , and capacitance between about 200 fF and 1 fF. The junctions with the lowest resistances show classical phase dynamics. The small junctions show some unconventional features, which can however still be explained with semi-classical phase dynamics. For the largest junction, the environment has negligible effect on the I-V curve, in contrast to the smaller ones, for which it is very crucial to take the environment into account.

In Fig. 6 we show current-voltage characteristics of these junctions. They all show classical underdamped hysteretic I-V curves, with a zero resistance supercurrent. The supercurrent is equal to a large fraction of the Ambegaokar-Baratoff critical current, except for the 140 k Ω junction. In some cases the gap edge has a negative differential resistance, which is probably a result of the increasing heating of the junction (and thus suppression of the gap) for increasing current at the gap voltage. The measured voltage on this negative resistance part is the average of low-frequency oscillations between finite- and zero-current state.

We have recorded distributions of the current at which switching out of the zero voltage state occurs. Two series are shown in Fig. 7. For all junctions the critical current increases if the temperature is decreased. However, whereas for the largest junction the width of the distribution decreases with temperature, for the small junctions it *increases*. The decreasing width for the large junction is expected from thermal activation theory. The switching distribution is determined by the escape rate Γ from the zero-voltage state. For moderately damped junctions (Kramers 1940),

$$\Gamma = \frac{\omega_p}{2\pi} \exp[-\Delta U/k_B T] \quad (7)$$

where ΔU can be approximated by $(4\sqrt{2}/3)E_J(1-I/I_c(T))^{3/2}$. Therefore, if $[\ln(\omega_p/2\pi\Gamma(I))]^{2/3}$ is plotted versus I , it should yield a straight line with slope proportional to $T_{\text{esc}}^{-2/3}$, where T_{esc} is the so-called escape temperature (Martinis, Devoret and Clarke 1987). In Fig. 8 these plots are given. The intersection with the current axis yields the critical current, which was plotted in Fig. 4. The inset shows the escape temperature versus mixing chamber temperature T . At high temperature,

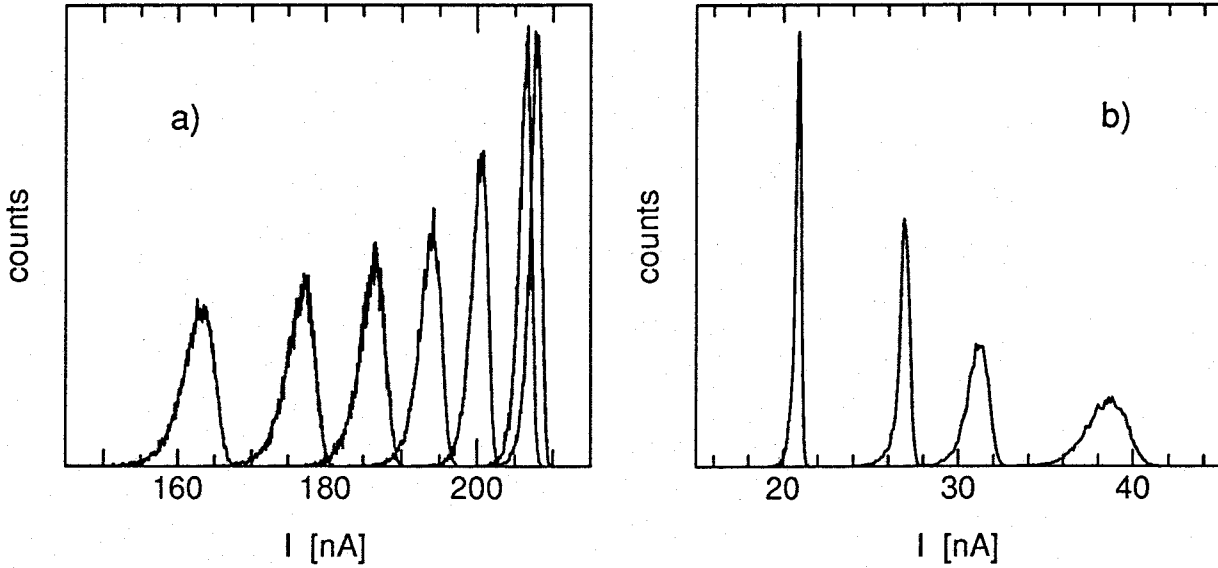


Fig. 7. Distributions of switching currents out of the zero-voltage state for single junctions (a) 1A ($R_n=140 \Omega$, $C \approx 200$ fF), from left to right, the temperature is 0.6, 0.5, 0.4, 0.3, 0.2, 0.1, 0.01 K; (b) 1C ($R_n=4.5$ k Ω , $C=1$ fF), from left to right the temperature is 0.6, 0.4, 0.2, 0.06 K.

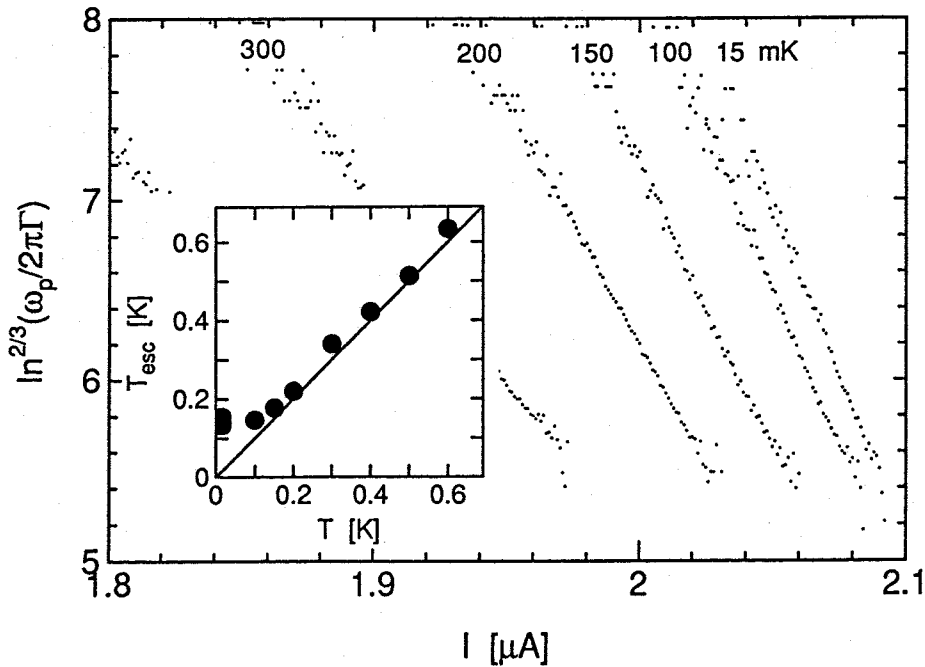


Fig. 8. Switching rate out of the zero-voltage state Γ , from the measurements in Fig. 7a, plotted in such a way that a straight line is obtained with slope scaling as $T_{esc}^{-2/3}$. The inset shows the T_{esc} thus obtained, versus the actual mixing chamber temperature.

there is generally good agreement with the prediction $T=T_{\text{esc}}$, within about 20 mK, but below about 150 mK T_{esc} becomes constant. This is the effect of macroscopic quantum tunneling out of a well of the washboard potential, the first indication of quantum phase fluctuations. The crossover temperature of 150 mK, from thermal activation to phase-MQT, is in agreement with theory.

The increasing width of switching distributions for the smaller junctions can also be explained with semi-classical theory. It results from the sensitivity of the phase dynamics to the high frequency impedance of the environment. We will return to this in section IV. Here we will give one example of the classical phase dynamics of the junction with $R_n=4.5 \text{ k}\Omega$ and area $0.01 \mu\text{m}^2$ (a parallel plate capacitance of $C\approx 1 \text{ fF}$). Under irradiation of microwaves on this junction, Josephson current steps develop in its I-V curve. These are shown in Fig. 9. Josephson steps result from phase locking of junction motion in the washboard potential. However, although the relation $\dot{\phi}=2eV/\hbar$ is also valid for operators, the amplitude of oscillation of relevant expectation values like $\langle \sin\phi \rangle$ vanishes for strong phase fluctuations (Likharev and Zorin 1985). We also note that even

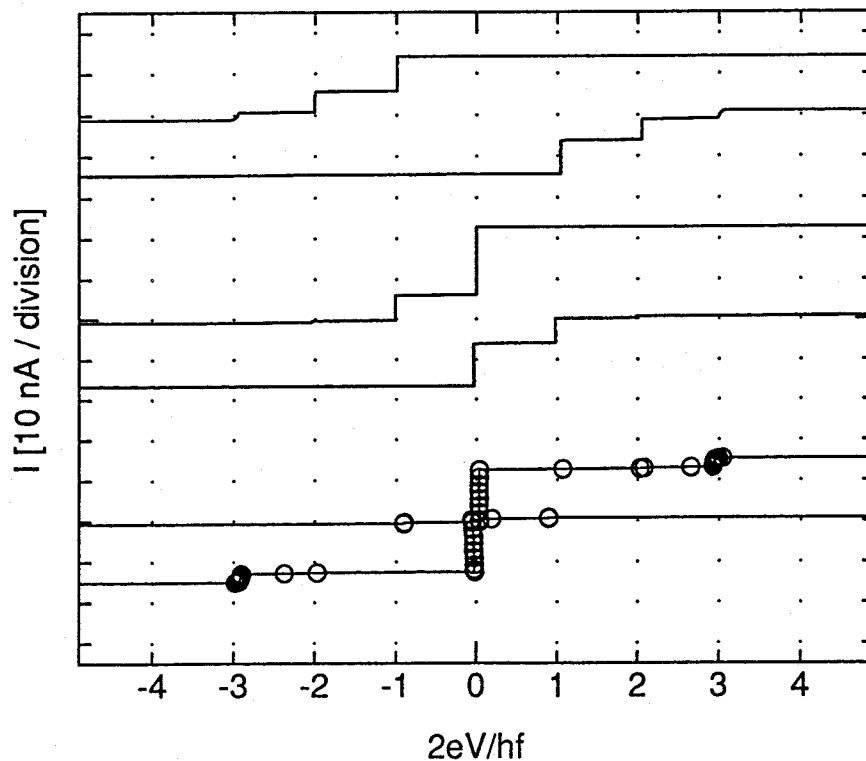


Fig. 9. I-V characteristics in the presence of microwave radiation for single junction IC ($R_n=4.5 \text{ k}\Omega$ and $C\approx 1 \text{ fF}$). The voltage has been scaled to the Josephson step value of $hf/2e$. From top to bottom the frequencies are 11.4, 8.87, 3.9 GHz.

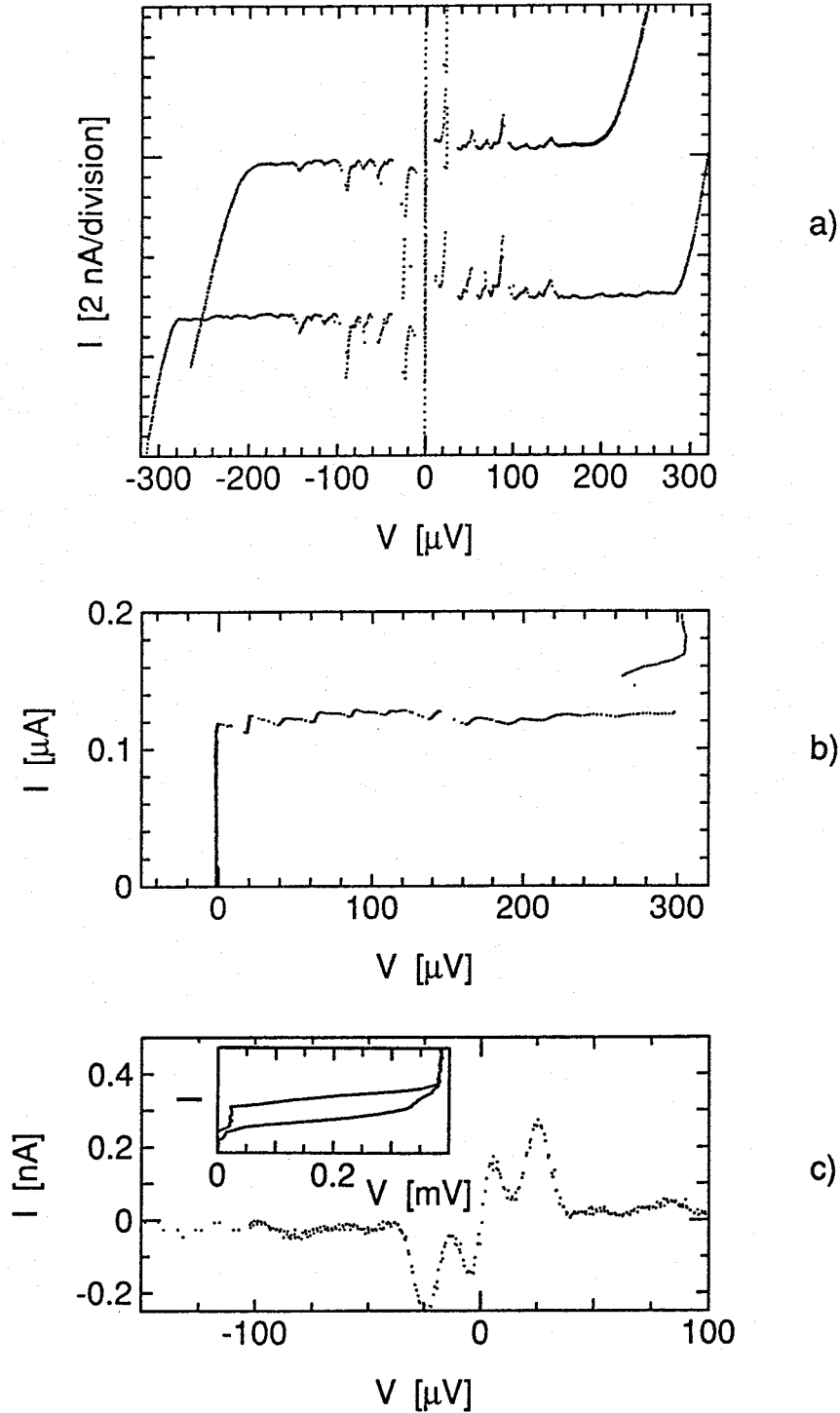


Fig. 10. Voltage biased I - V characteristics of single junctions. Current resonances occur at device-independent voltages. (a) junction 1C ($R_n=4.5$ k Ω and $C\approx 1$ fF). The bottom curve is in zero-magnetic field, for the top curve a field of 0.15 T is applied, giving a significant suppression of the quasiparticle excitation gap. (b) junction 1B ($R_n=540$ Ω , $C\approx 50$ fF). (c) junction 1D ($R_n=140$ k Ω , $C\approx 1$ fF). For this device the current biased I - V curve shows a constant voltage step of ca. 20 μ V (also clear from the inset, which is for $T=0.6$ K).

the smallest junctions, with parallel plate capacitance about 1 fF, do not show a Coulomb gap in the normal state (except for high currents, of order 1 μA). This also shows that there is no suppression of charge fluctuations by Coulomb blockade.

The suppression of phase fluctuations is due to the coupling to the environment. In Fig. 10 there is another direct indication of such coupling. It appears in the form of current resonances in the I-V curve at voltages about equal to multiples of 20 μV . For current bias the resonances are mostly hidden inside the hysteresis loop of the I-V curve. This effect has been observed before in junctions coupled to an external resonating load (Kuzmin, Olsson and Claeson 1985, Kistenev *et al.* 1985). Note that the position of the resonances is not affected if the superconducting excitation gap is significantly suppressed by a magnetic field. We will show in the next section that resonances also occurred, at the same voltages, in double junctions in the charging regime.

From the inset of Fig. 10c it is clear that the first current resonance can be larger than the supercurrent. In such a case a current biased I-V curve shows a gap, with a width which is independent of temperature. We note that this looks similar to a phenomenon observed by Iansiti *et al.* (1988, 1989) in similar small single junctions. These authors did not interpret the gap with environmental modes, but instead gave an explanation that relied on the quantum behavior of such junctions.

B Double junctions

In double junctions, in contrast to single junctions, the capacitance is certainly of about the magnitude that is expected from the junction area. This follows for instance from the occurrence of a Coulomb gap in the normal state. Therefore double junctions are probably the simplest systems where the effect of decreasing E_J/E_C can be studied reliably.

In Fig. 11 the voltage biased I-V curve is shown for a double junction with $E_J/E_C \approx 0.09$. On a large scale the curve is clearly asymmetric, with the BCS sumgap at approximately the usual value of 0.8 mV (for two junctions). Inside the gap a resonance is present at about 0.5 mV, which is also asymmetric. On an expanded current scale (inset of Fig. 11) we observe a smaller gap, with a width of approximately 0.35 mV. In Fig. 12 we compare the small scale I-V curves of various double junctions with Coulomb gap measurements in the normal state. The remarkable feature is that they all show a smaller gap, with the gap voltage close to two times the normal state Coulomb gap of the same device. The Coulomb gap is the lowest voltage where tunneling of an electron can occur across one of the two junctions with zero energy difference (see, e.g., chapter 2).

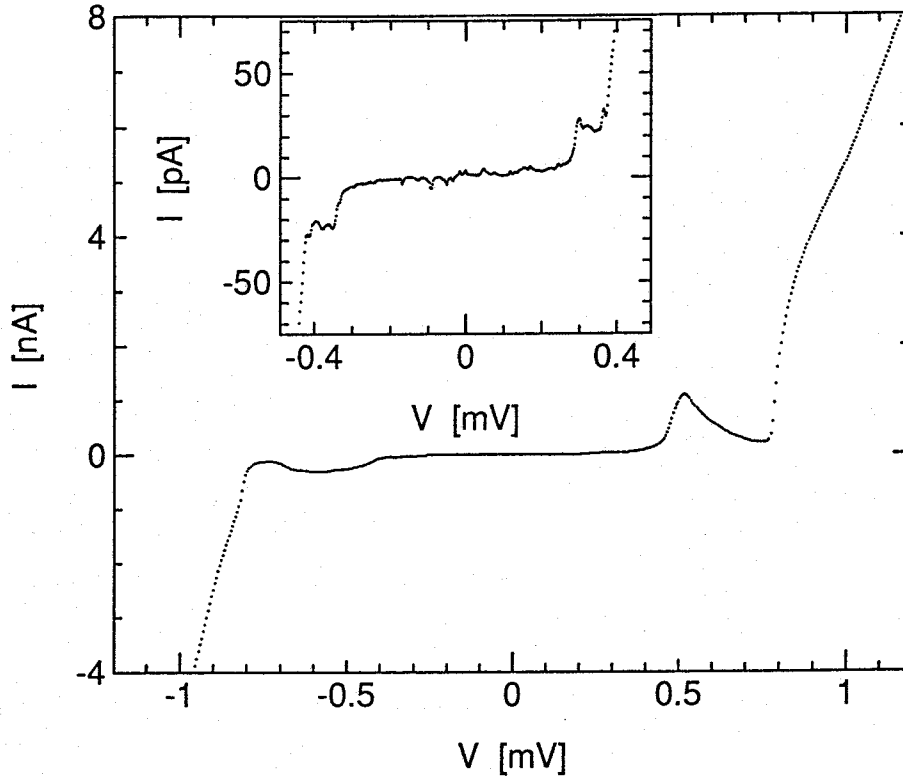


Fig. 11. I-V characteristic of double junction 2B with $R_n=42 \text{ k}\Omega$, $C\approx 0.47 \text{ fF}$ ($E_J/E_C\approx 0.09$). The inset shows the current plateau starting at about 0.35 mV (the Cooper-pair gap), and a strong current increase at 0.4 mV.

Consequently, the double voltage is the lowest voltage where one junction can pass a Cooper-pair with zero energy difference. We will call this gap a Cooper-pair gap, and return on this interpretation in the next section.

In the normal state, the Coulomb gap can be strongly suppressed by the gate voltage. This is not so much the case in the superconducting state. In Fig. 13 we give I-V curves of a Cooper-pair gap for different gate voltages. The gap can be somewhat modulated in width, and depending on gate voltage a resonance at the gap voltage may arise. For somewhat higher E_J/E_C current peaks in the I-V curve almost mask the Cooper-pair gap. These current peaks are shown more detailed in Fig. 14. They occur at the same position as the peaks of the single junctions of Fig. 10. One peak is centered around $V=0$. For convenience, we will call this a supercurrent without meaning that the resistance is truly zero. Fig. 14 gives the I-V curves of one device in two situations. The first curve was measured with the usual external on-chip circuit. For the second curve, the superconducting leads on the chip were interrupted and bridged by normal metal. Clearly, this did not affect the position of the peaks very strongly. We have found that the geometry of the on-chip

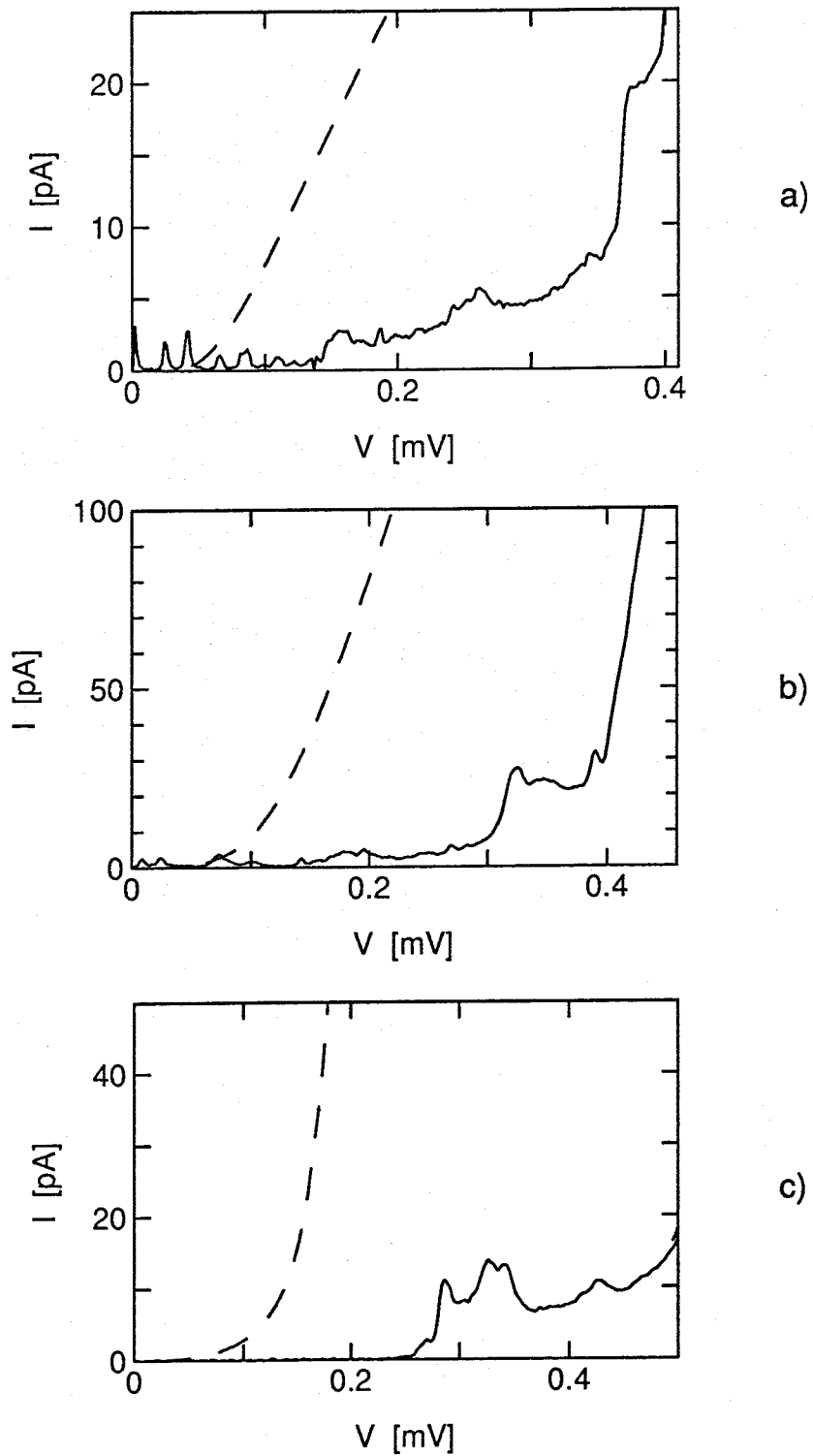


Fig. 12. Comparison of normal state Coulomb gap (dashed) and superconducting state Cooper-pair gap (solid line) for several double junctions. (a) 2A ($R_n=62$ k Ω , $C=1$ fF, $E_J/E_C\approx 0.13$); (b) 2B ($R_n=42$ k Ω , $C=0.47$ fF, $E_J/E_C\approx 0.09$); (c) 2D ($R_n=117$ k Ω , $C=0.3$ fF, $E_J/E_C\approx 0.02$). For (a) and (b) the current in the normal state is divided by 10.

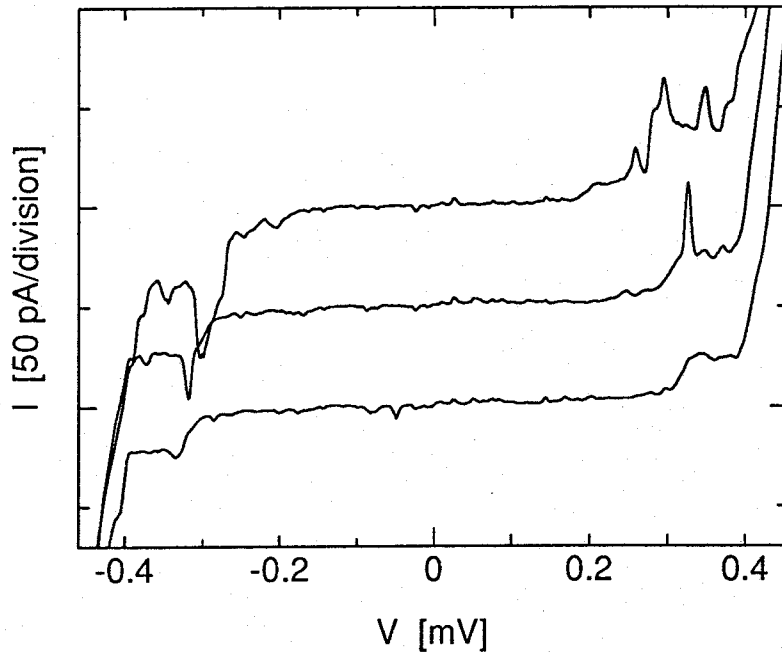


Fig. 13. I-V characteristics of double junction 2B ($R_n=41 \text{ k}\Omega$, $C=0.47 \text{ fF}$) for three different gate voltages, showing influence on the width of, and a resonance at the Cooper-pair gap.

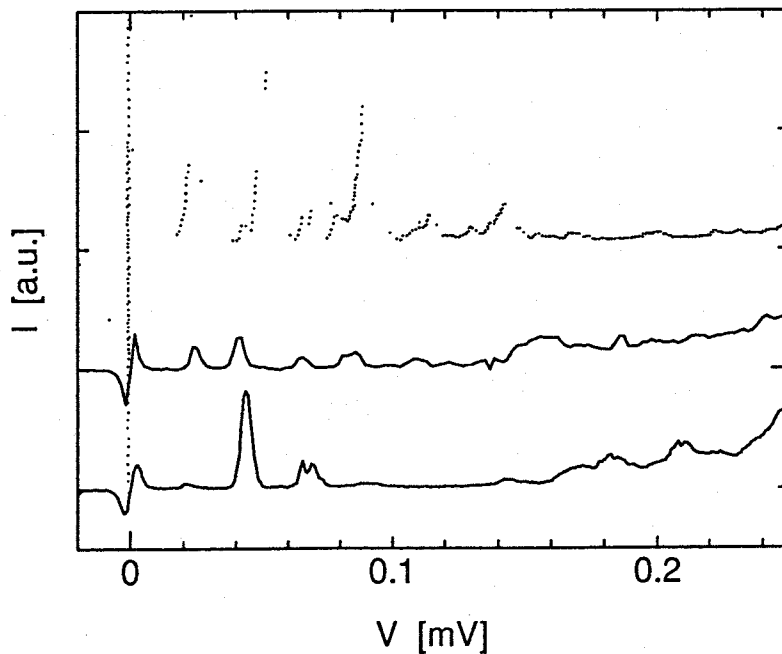


Fig. 14. Current peaks in the I-V curve for double junction 2A ($R_n=62 \text{ k}\Omega$, $C=1 \text{ fF}$, bottom two curves, 10 pA/division) compared with those for single junction 1C (top curve, 10 nA/division). The devices were patterned with the same on-chip connecting circuit. For the lower curve of device 2A, part of the superconducting lead to the junctions was replaced by normal metal.

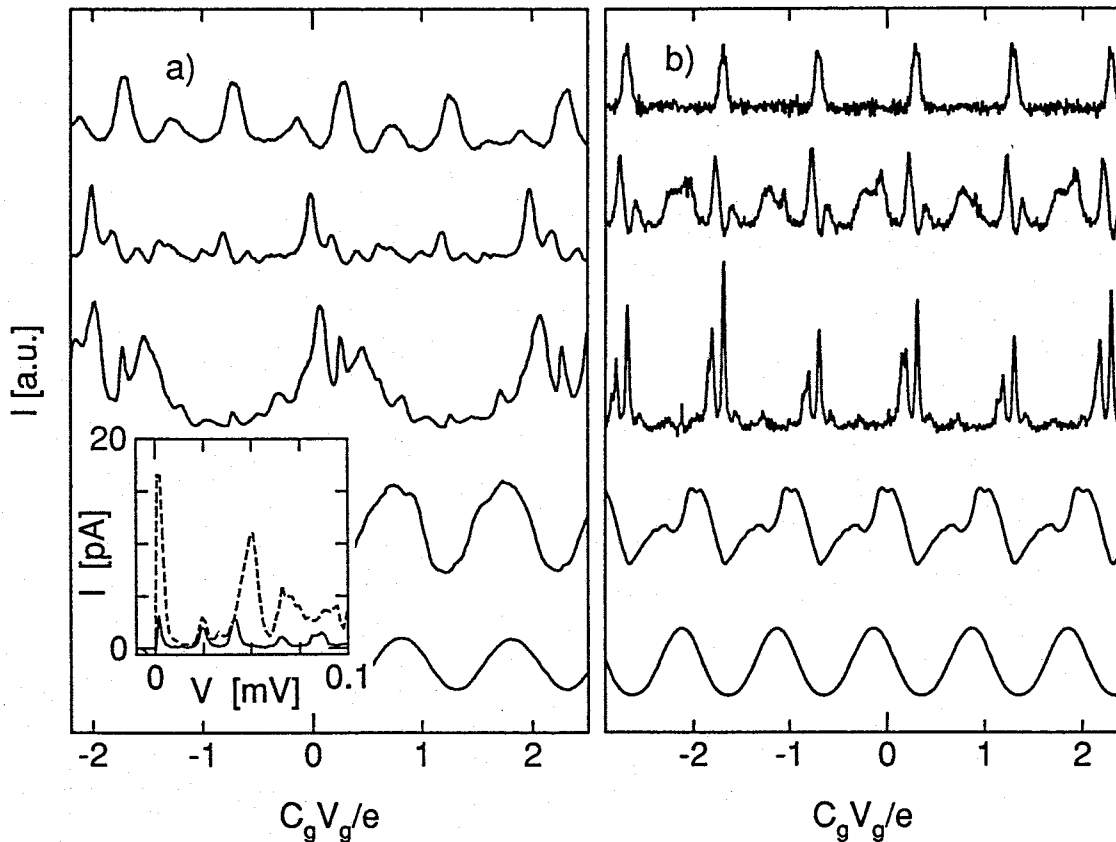


Fig. 15. Gate voltage modulation of the current peaks in the superconducting state, and the Coulomb gap in the normal state. Shown are (top to bottom) $I-V_g$ curves for the supercurrent, the $20 \mu\text{V}$ and $40 \mu\text{V}$ resonance, for a bias voltage on the flank of the BCS gap, and in the normal state. (a) device 2A ($E_J/E_C=0.13$), (b) device 2B ($E_J/E_C=0.09$). The inset of (a) shows the maximum and minimum supercurrent in $I-V$ curves for two gate-voltages (solid and dashed curves).

circuit has some influence on the position of the peaks. The peaks disappear for low E_J/E_C . As for the single junctions, they are probably a result of a resonance with environmental modes. However, although in a single junction the phase dynamics is classical, in this case the current resonances are influenced by gate voltage. This shows the presence of charging effects in these junctions. Modulation of the current peaks at several values of voltage bias is shown in Fig. 15 for two samples. For reference, the modulation is given of the current just outside the Coulomb gap in the normal state, of which we know that the period corresponds to an electron charge divided by the gate capacitance. In the superconducting state there is mostly an e -periodic modulation of the height of the current peaks, but in one case for the resonances at 20 and $40 \mu\text{V}$, a $2e$ period can be observed. It should also be noted that the supercurrent and resonances are

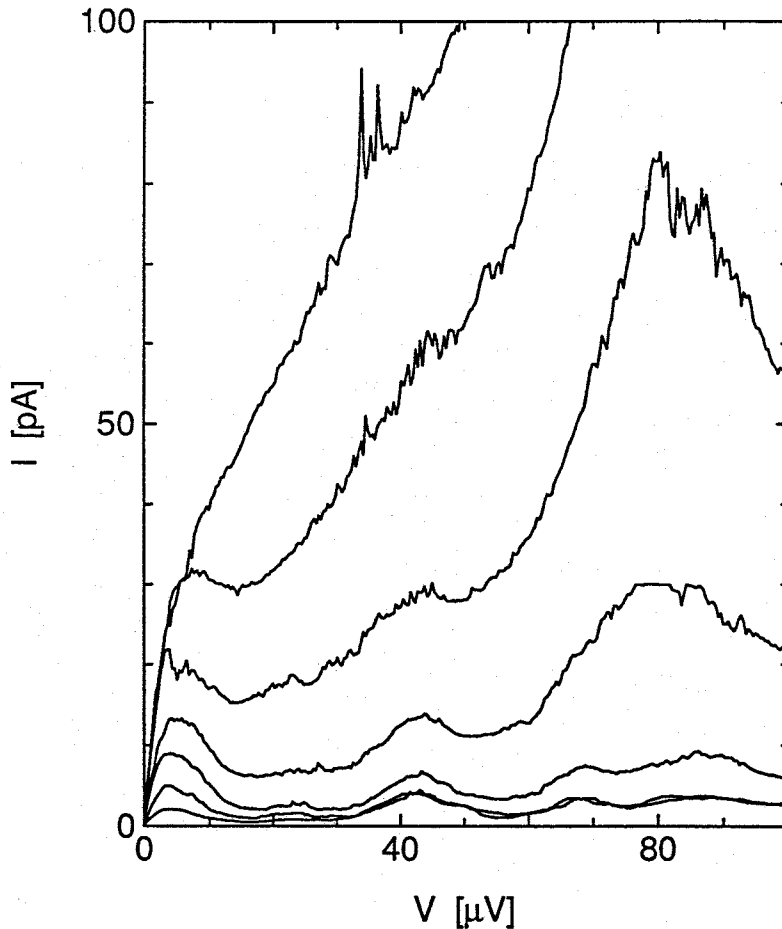


Fig. 16. Temperature dependence of the small-voltage I-V characteristic of double junction 2A. The temperature increases from 0.1 to 0.7 K in steps of 0.1 K (bottom to top).

maximum when the normal state Coulomb gap is maximized, which occurs for island charges equal to an integer times e . Fig. 15a shows that the gate voltage does not affect the position of the peaks.

For all devices, the current peaks strongly increase with increasing temperature. This is shown in Fig. 16. The current peak at about the BCS sumgap is generally less strongly dependent on temperature, the behavior varying from device to device and with gate voltage. At voltages where both small junctions are in the voltage carrying state, i.e. larger than about 0.8 mV, the I-V curve shows the presence of a third junction in the circuit, which we identify with the metal island between the two small junctions. Since this island is also a double metal layer with barrier in between, it is also a junction, but of about 10 times larger capacitance and higher E_J .

C Three junctions in series

The three junction device of low E_J/E_C that is presented in this section shows cross-over behavior between the two-junction and five-junction devices that we have examined. We will only shortly describe the results. Fig. 17 shows I-V curves for three junctions of small E_J/E_C in series, with the same general features as the double junctions, except that a supercurrent is absent. The Cooper-pair gap is hardly visible due to the current resonances at small voltage. With increasing temperature the gap is washed out in favour of a supercurrent. On a larger scale again current resonances appear at about 2Δ and 4Δ . These increase in height for increasing voltage and with increasing temperature.

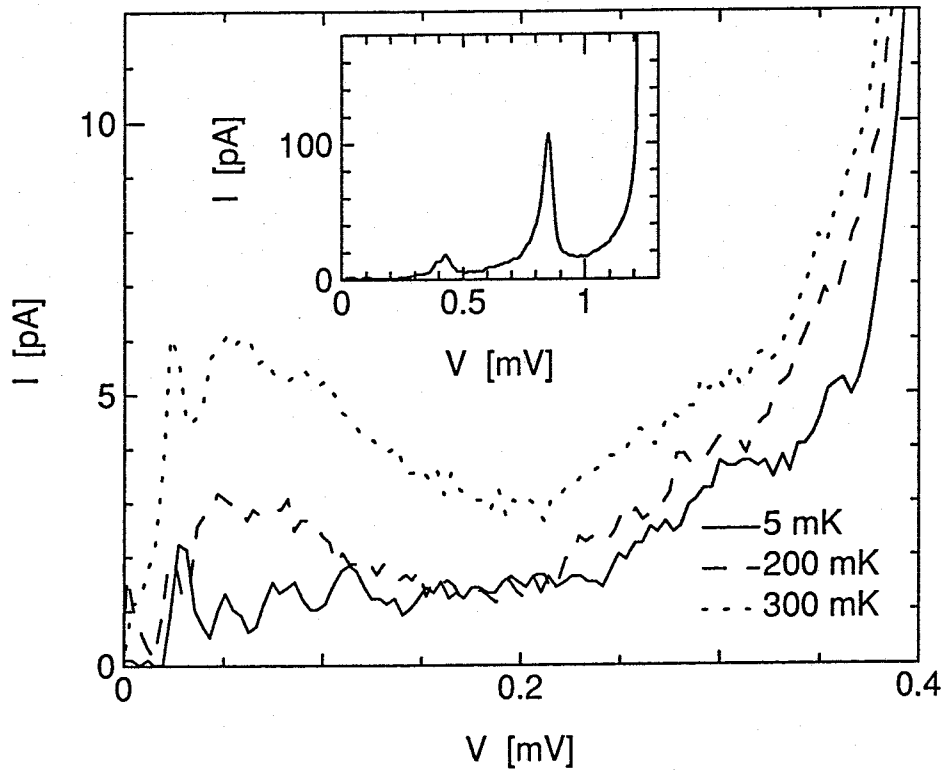


Fig. 17. I-V characteristic of 3-junction array 3B ($E_J/E_C \approx 0.15$) at 10, 100, 200 and 300 mK. At the lowest temperature a Cooper-pair gap is visible. The inset shows the large-scale characteristic.

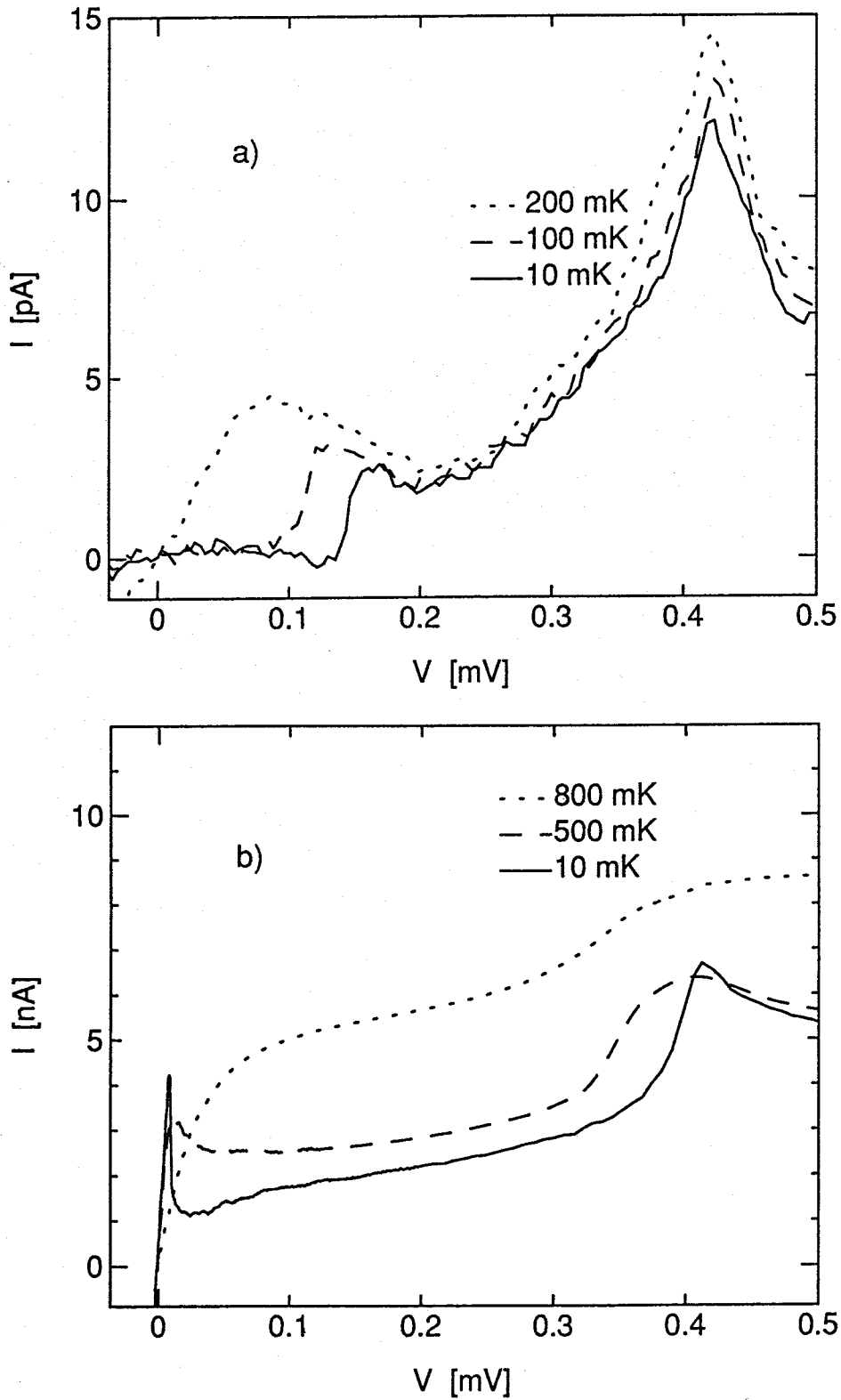


Fig. 18. *I-V* characteristics at low temperature for 5-junction arrays. (a) array 5B ($E_J/E_C=0.3$). At the lowest temperature a Cooper-pair gap arises. (b) array 5A ($E_J/E_C=1.6$). A true supercurrent develops at low temperature.

D Five junctions in series

Arrays of five junctions turn out to have much less detailed structure in the I-V curves at small voltages. Instead they provide a clear superconductor-insulator phase transition as a function of E_J/E_C . As an example we show in Fig. 18 I-V curves for two arrays of five junctions, with E_J/E_C equal to 0.3 and 1.6. There is a crossover from a clear supercurrent to a large Cooper-pair gap. In Fig. 19 we show for one device that the Cooper-pair gap is again about equal to two times the threshold voltage for onset of conduction in the normal state. The Cooper-pair gap can be slightly modulated by a gate voltage. The current just outside the Cooper-pair gap is modulated with the same period and structure as the normal state Coulomb gap.

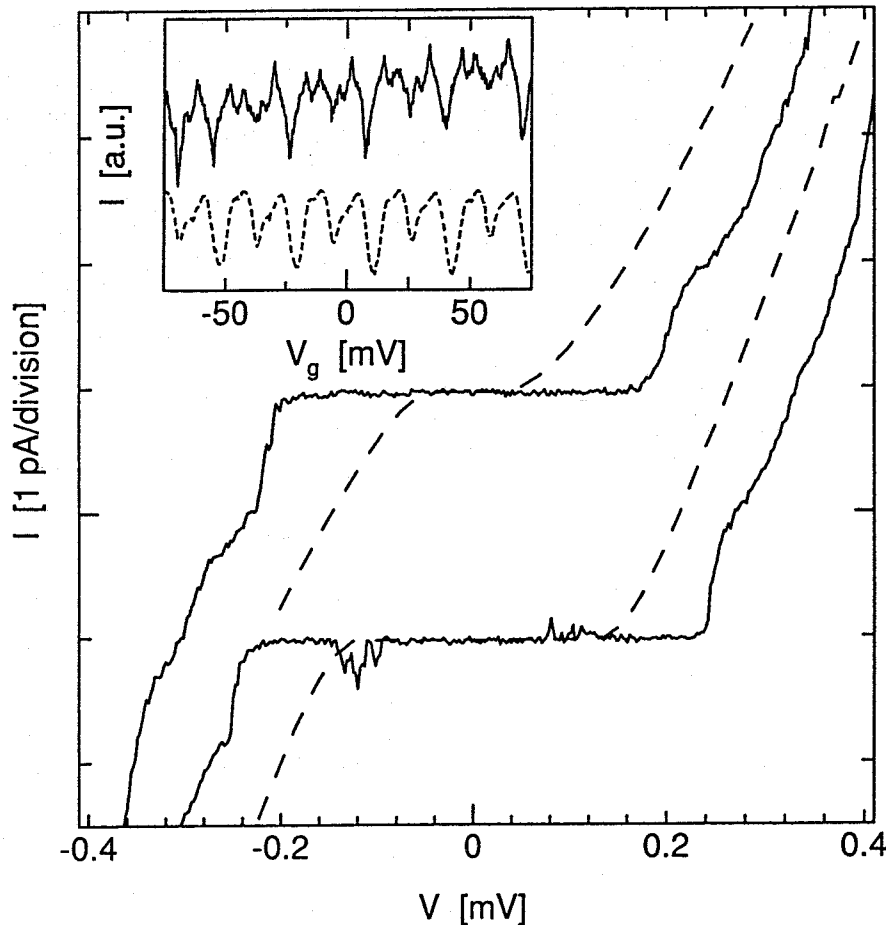


Fig. 19. Comparison of normal Coulomb gap (dashed) and superconducting Cooper-pair gap (solid line) for array 5C ($E_J/E_C \approx 0.13$). The approximately minimum and maximum gaps are shown (not for the same V_g in normal and superconducting state). The curves have been offset in I-direction for clarity. The inset shows the gate voltage modulation of the current just outside the gaps.

On a large scale, the arrays all exhibit I-V curves with current resonances at voltages somewhat larger than multiples of the BCS sumgap. All show a step-like pattern for these resonances, the height increases for increasing voltage. However, the effect of temperature on these large scale I-V curves depends on E_J/E_C . Whereas for high E_J/E_C there is little effect of temperature on the current resonances, for low E_J/E_C the current increases stronger with temperature (Fig. 20). The effect of increasing temperature on the Cooper-pair gap is quite similar for all devices. First the gap decreases in width, but remains rather sharp with a clear plateau outside the gap. For higher temperatures an increasing supercurrent arises.

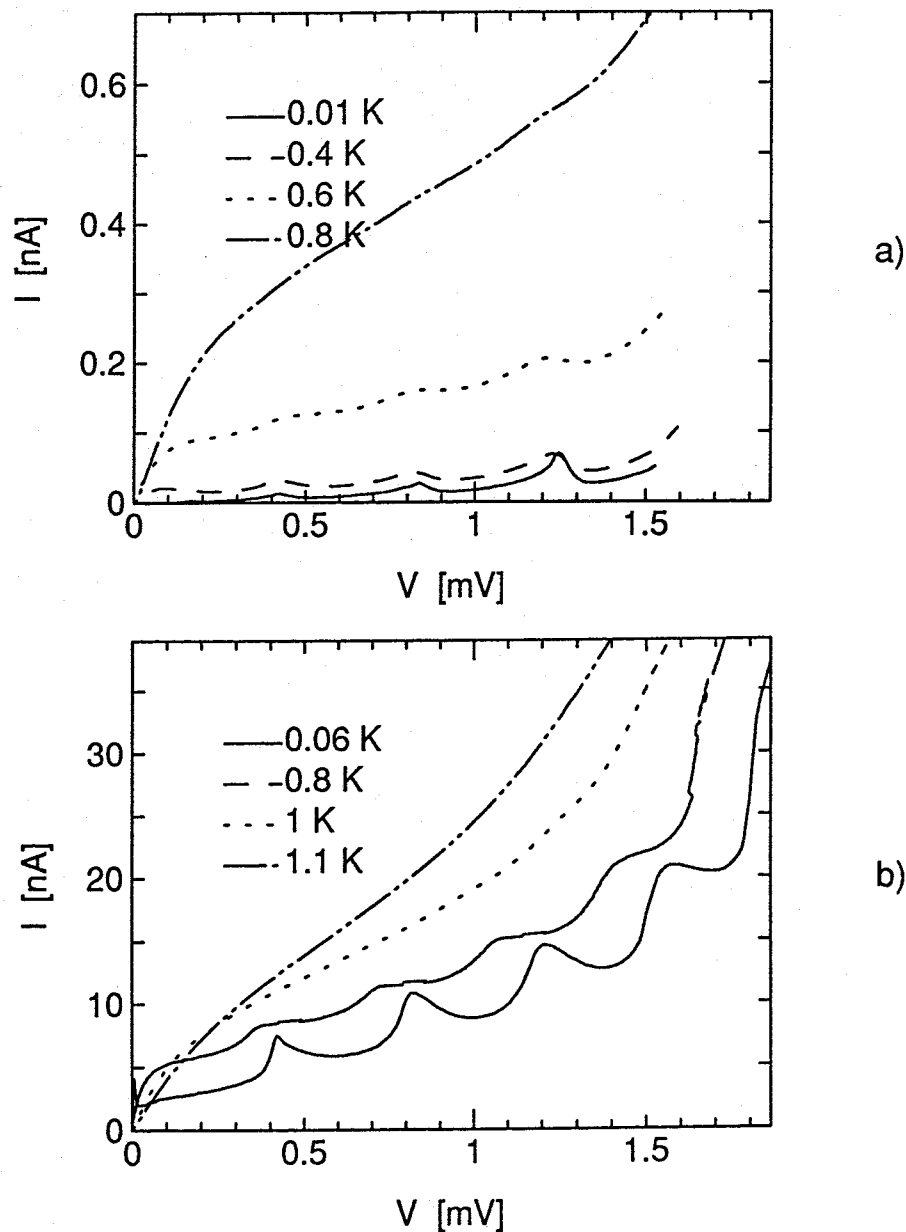


Fig. 20. Influence of temperature on the large scale I-V curves for arrays 5B (a) and 5A (b).

E Magnetic field effects

A magnetic field suppresses both the Josephson coupling and the quasiparticle excitation gap. Both these effects influence the I-V curves of junctions. In Fig. 21 we show the I-V curves of a double junction ($E_J/E_C=0.09$) for small magnetic fields. The field is applied in the plane of the junction and the aluminum strips. Therefore the critical field for suppression of superconductivity is significantly larger than the roughly 100 Gauss for bulk aluminum. As the field increases the quasiparticle excitation gap is clearly suppressed from its zero-field value. Both the gap edge at 0.8 mV and the current peak at about 0.5 mV shift to lower voltages. The current peak initially increases in height and then disappears. On a small scale the Cooper-pair gap is also slightly suppressed, without changing significantly in height. The supercurrent peaks at a field that is slightly smaller than the field at which the 0.5 mV resonance is maximum (0.15 versus 0.2 Tesla). The penetration depth of the field in the aluminum is much larger than the electrode thickness of a few tens of nm. Therefore the field penetrates the total cross-section of the junction, of the order of $(100 \text{ nm})^2$. One fluxquantum is induced in this area for a field of about 0.2 Tesla.

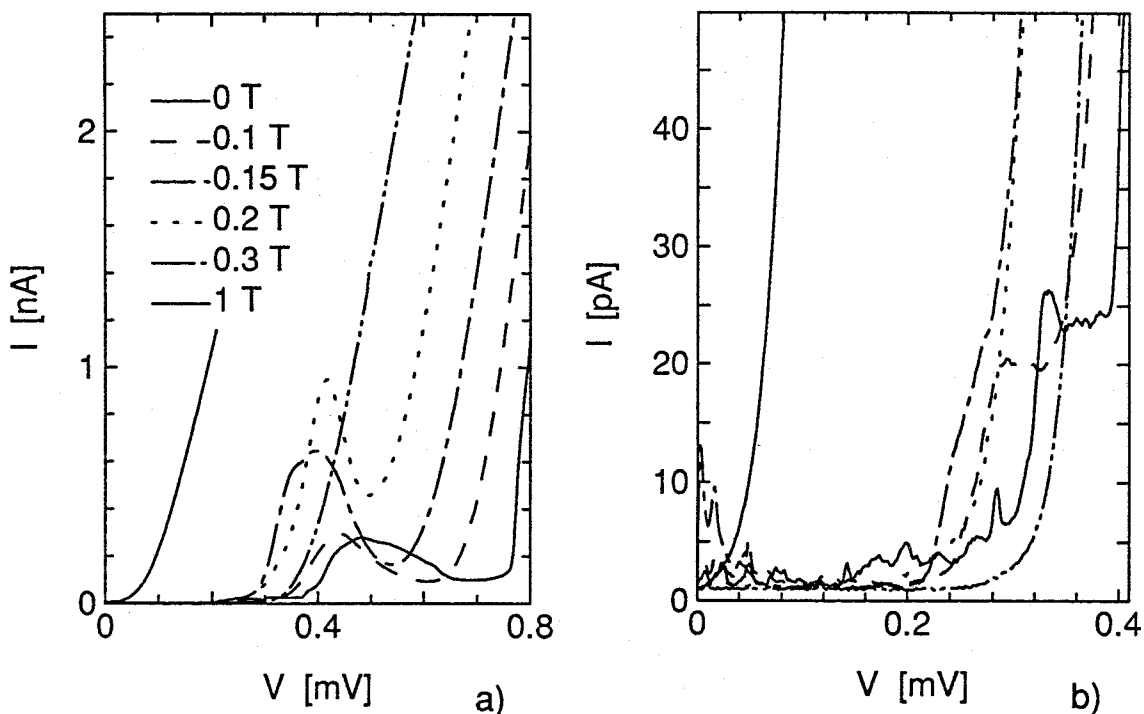


Fig. 21. Influence of a magnetic field on the I-V characteristics of a double junction 2B. (a) large scale; (b) expanded current scale, for the same field values.

IV DISCUSSION OF THE RESULTS

In this section we will discuss the results of the previous section in two main lines of argumentation. First, various features of the observed I-V curves can be explained by considering the frequency dependent damping of a junction in its environment. This is applicable to single junctions, where the damping is due to the on-chip circuit. It is also important for arrays, where the impedance of the neighbours often determines the damping of a junction. The argumentation will be mostly classical, i.e. based on a description of a phase-particle. Second, we have observed clear charging effects in the I-V curves of junction arrays. We will explain these from two complementary viewpoints. Under certain circumstances, despite charging effects, a Cooper-pair can be transferred coherently through an array. This leads to a picture of the array as a single equivalent junction. Mostly, however, charging effects strongly influence the rate of Cooper-pair tunneling in a way that can be described rather analogous to the picture of single electron tunneling as presented in the previous chapter.

A Environmental resonances

Interaction with the environment is present in the I-V curves of most systems that we have measured. This may look somewhat surprising, since for multi-junction arrays the individual junctions are for the purpose of charging effects well-decoupled from the environment. However, as we will discuss below, multi-junction arrays in the superconducting state can in some circumstances be regarded as an equivalent single junction with weak Josephson coupling. For a (true or equivalent) single junction, we can understand the influence of the environment on the I-V curve better.

The I-V curve of a single junction is strongly dependent on damping (e.g. Stewart 1968, McCumber 1968, Likharev 1986). For perfect voltage bias the dc current at non-zero voltage is zero. Alternating supercurrent with the Josephson frequency $2eV/h$, and amplitude of order $2eE_J/h$ is flowing. For non-ideal voltage bias, e.g. when there is a non-zero impedance in the environment, the alternating supercurrent becomes anharmonic and the average yields dc supercurrent. If the bias impedance is frequency dependent, the dc current of the I-V curve will mainly follow the damping at the Josephson frequency, and thus trace the spectrum of environmental modes. This has been observed for junctions in a specially designed resonating circuit (Kuzmin, Olsson and Claeson 1985, Kistenev *et al.* 1985). Because of the small

capacitance and very low internal damping, our systems are very sensitive to loading by the environment, even without being meant to.

From the measurements, clearly an important resonance frequency is the Josephson frequency at approximately $20 \mu\text{V}$, i.e. about 10 GHz. For our roughly 3 mm long on-chip leads, which can be regarded as striplines with a propagation velocity of the electromagnetic field of about 10^8 m/s , this is close to the frequency of $\lambda/4$ standing waves. However, avoiding the on-chip stripline configuration, by changing from narrow leads to very wide, high capacitance pads, does not prevent the occurrence of the resonances. This could lead one to consider soliton oscillations in the leads as possible source of the resonances. The leads are, as the junctions, made of two overlapping aluminum layers with barrier in between. Indeed, the zero-field step voltage (e.g. Pedersen 1983) of these long Josephson junctions turns out to be about $20 \mu\text{V}$, and to be inversely proportional to the length of the leads. However, since replacement of part of the leads by normal metal did not affect the resonances very strongly (cf. Fig. 14), it seems that they are indeed due to standing waves. The voltage bias will be improved by further increasing the mutual capacitance between the leads. For this, an on-chip configuration with interdigitated leads has been designed. No reliable results are yet available for this circuit.

Of course an imperfect voltage bias is equivalent to a current bias with a large shunt. Therefore, a single junction in a low impedance environment can be described by the particle in a washboard potential (essentially a current biased picture), subject to strong friction (Martinis and Kautz 1990, Devoret 1989). At very low voltages, the high frequency harmonics of the Josephson frequency become increasingly dominating with a peak around the plasma frequency ω_p . In typical circuits, the impedance at these high frequencies is very low, lower than the free space impedance of 377Ω . Therefore, many escapes from the zero voltage state result in retrapping in a nearby potential well. Switching to the voltage carrying state can only occur for bias currents high enough to accelerate the particle through this first stage impeded by the retrapping due to high frequency damping. Consequently there is a rather sharp threshold current for escape (the retrapping current), and the switching distributions yield a narrow histogram. For decreasing temperatures, the escape events shift to higher bias currents, where there is a stronger acceleration to the voltage carrying state. Therefore as the switching distribution shifts to higher currents, it also becomes wider, i.e. closer to the actual thermal or quantum width.

B Coherent tunneling for small voltages

A tunneling matrix element of magnitude $E_J/2$ couples charge states differing by one Cooper-pair. For a single large capacitance junction this means that at zero voltage bias the degenerate charge states with a Cooper-pair left and right are mixed, yielding new energy eigenvalues which are E_J apart. For an isolated single junction the same occurs at the Brillouin zone edge, $V=e/C$. If the junction could be prepared in a definite charge state, with Cooper-pair left or right, this would result in a coherent charge oscillation with frequency E_J/\hbar , giving the possibility to carry a maximum dc supercurrent $I_c = 2eE_J/\hbar$.

In a double junction, there are three possible charge states that are coupled by Cooper-pair tunneling, those with a Cooper-pair left, centered, or right. For small junctions, the Coulomb energy of the central position, E_i , may be large compared to E_J . This decreases the coupling of the left and right states, compared to a single junction (for zero bias voltage, e.g., by a factor $E_J/2E_i$). Thus the maximum supercurrent is decreased by a factor of order (E_J/E_C) . Only if the charging energy E_i of the central state vanishes by the presence of an island charge e , all three states are degenerate and the coupling becomes of order E_J . Averin and Likharev (1990) found that the maximum supercurrent that can be obtained by varying the gate voltage is about half the supercurrent of the individual junctions. For an array of n small-capacitance junctions, the coupling for coherent transfer through the array will likewise be decreased by a factor $(E_J/E_C)^{n-1}$. Again the coupling will be influenced by gate charge.

For low voltages the process of coherent Cooper-pair transfer through arrays can explain various experimental observations. In double junctions there will be the possibility of a supercurrent for not too low values of E_J/E_C . This shows that the double junction behaves as a single weakly coupled classical junction. Likharev and Zorin (1987) have shown that the sum of the phase differences across the two junctions, ϕ_Σ , is a classical variable that follows the ac Josephson relation $\hbar\dot{\phi}_\Sigma=2eV$. Therefore, at finite voltages we observe the same resonances with environmental modes as for the single junctions.

The Josephson coupling of the equivalent single junction is determined by the island charge, and can thus be controlled by the gate voltage. Experimentally, the supercurrent and resonances peak regularly at all integer island charges. Theoretically, only for odd island charges, $\pm e, \pm 3e$, etc., the charging energy change during Cooper-pair tunneling vanishes, yielding a peak in supercurrent. However, all island charges larger than $e/2$ are not energetically stable against quasiparticle tunneling, since by a single electron tunneling event a lower energy state can be

reached. Therefore, taking into account the likely presence of at least a few quasiparticles on the superconducting electrodes, on experimental time scale all integer island charges relax to zero island charge. From this charge state, a thermally assisted quasiparticle tunneling can for a limited duration create an island charge e , and thus catalyze conduction by Cooper-pair tunneling. This explains the observed e -periodicity instead of $2e$ -periodicity of the supercurrent modulation. It also explains the strong suppression of the maximum supercurrent compared to the prediction of Averin and Likharev (1990) (about 20 pA instead of $I_c/2 \approx 2700$ pA) because this supercurrent is predicted for absence of quasiparticle tunneling, i.e. relies on the possibility of a stable island charge e . We note that from the standard equations for single electron tunneling, the rate of creation of the island charge e is about $\exp(-\Delta E/k_B T) \Delta E/e^2 R$, and the rate of decay of this charge is about $\Delta E/e^2 R$, where R is the quasiparticle tunneling resistance, and ΔE is the energy difference between the island charge e and island charge 0 situation. The ratio of the two, $\exp(-\Delta E/k_B T)$, gives the time fraction that is available for catalyzed Cooper-pair tunneling. For the 62 k Ω junction of Fig. 15a, $I_c = 5.5$ nA and $\Delta E = E_C/2 \approx 0.5$ K so that at 100 mK we would expect a maximum supercurrent of 18 pA, which is close to the measured current, maximized with gate voltage, at the lowest temperature. This high temperature may indicate residual noise in the experiments. However, macroscopic quantum tunneling of the charge is known to produce charged island states, analogous to thermal fluctuations. This might increase the occupation of the state that catalyzes Cooper-pair tunneling. For increasing temperature, the supercurrent indeed increases strongly. However, this is equally true for island charges that are non-integer, where the above discussion does not apply. The increase of Cooper-pair tunneling with increasing temperature, even for off-resonance condition, will be discussed in the next section.

For the five-junction devices with small E_J/E_C , the possibility of coherent Cooper-pair transfer at zero bias voltage is dependent on the application of equal gate charges of $\pm 2e/5$ on all four islands between the junctions. This is generally impossible to achieve without individual gate electrodes, because of the presence of non-integer offset charges on the islands. Therefore, for arrays with small E_J/E_C supercurrent is suppressed by a factor of order $(E_J/E_C)^4$. Only for $E_J \geq E_C$, there will be significant coherent transfer through the array despite charging effects.

As regards the effect of increasing temperature, this seems to enhance Cooper-pair tunneling through the array. First the Cooper-pair gap decreases in width. For higher temperatures, even in the devices with low E_J/E_C a supercurrent-like feature arises (cf. Fig. 18). This thermally assisted Cooper-pair tunneling is however not necessarily a coherent transfer through all junctions.

C Alternating Cooper-pair and quasiparticle tunneling for high voltages

In the above discussion charge transfer was due to coherent Cooper-pair transfer through all junctions of a multi-junction device, which in that respect could be regarded as an equivalent single junction. It required significant mixing of the various positions of a Cooper-pair in the array. However, for not too high E_J , and with the exception of some special gate charges, at most one junction is at resonance for Cooper-pair tunneling at any one bias voltage. On the other junctions charge fluctuations are suppressed and these can be regarded as classical capacitors. Although it is thus generally impossible to realize Cooper-pair tunneling through all junctions, there may still be tunneling current due to a combination of Cooper-pair tunneling with quasiparticle tunneling, across the *individual* junctions in an array. This was pointed out by Fulton *et al.* (1989) and Averin and Aleshkin (1989, 1990).

The quasiparticle tunneling is subject to the usual single electron tunneling rate equation (chapter 2), corrected for the nonlinear junction resistance. If $-\Delta E$ is smaller than the BCS sumgap, the rate is proportional to the subgap conductance R_{qp}^{-1} , at zero temperature $\Gamma_{SET} = -\Delta E / e^2 R_{qp}$ ($\Delta E < 0$). On the other hand, if $-\Delta E$ is larger than the BCS sumgap $2\Delta_{BCS}$, quasiparticles can be excited and the rate is proportional to the normal state conductance, at zero temperature $\Gamma_{SET} = (-\Delta E + 2\Delta_{BCS}) / e^2 R_n$.

For the Cooper-pair tunneling rate Γ_{CPT} , Averin and Aleshkin give in the limit E_C smaller than the BCS gap:

$$\Gamma_{CPT} = \nu E_J^2 / 2(\Delta E^2 + \hbar^2 \nu^2) \quad (8a)$$

where

$$\nu = \Sigma [\Gamma_{SET}^{\pm} + \tilde{\Gamma}_{SET}^{\pm}] \quad (8b)$$

This equation shows that the Cooper-pair tunneling rate is a function of the single electron tunneling rates for the charge distributions before (Γ_{SET}) and after ($\tilde{\Gamma}_{SET}$) tunneling of the Cooper-pair, summed over both junctions and in both directions. It shows that if charging energy of the intermediate state is important, the tunneling rate will decrease as $(E_J/E_C)^2$. The tunneling rate is appreciable only at resonance of the energies before and after tunneling, i.e. $\Delta E \approx 0$. For increasing temperature, due to the dependence of the single electron tunneling rates on

temperature, Cooper-pair tunneling can also increase.

The description is complicated by the possibility of catalyzed Cooper-pair transfer, like the supercurrent in the double junction was enhanced by the metastable presence of a charge on the central electrode. This was first pointed out by Fulton *et al.* for a double junction as the reason for the current peak at the BCS sumgap. In their interpretation, conduction starts by tunneling of a quasiparticle to the central metal island, which is followed by Cooper-pair tunneling across one junction. If the bias voltage $V > 2\Delta_{\text{BCS}}/e + e/4C$, then this will be followed by two quasiparticle tunneling events across the other junction with energy change so large, that the rate is determined by the normal state resistance. Thus a significant current can develop. (If the voltage is lower, the subgap resistance strongly reduces the quasiparticle tunneling rate.) Although the excess electron on the central island is in an unstable situation, the tunneling rate out of the island will be governed by the subgap resistance, and hence be very low, under the condition that $V < 2\Delta_{\text{BCS}}/e + 3e/4C$. As a result a current peak of width about $e/2C$ arises somewhat beyond the sumgap. How well the resonance condition for Cooper-pair tunneling is fulfilled for the charged island depends on the non-integer part of the island charge. Therefore the current peak is modulated by the gate voltage (Fig. 22). For longer arrays, as similar process occurs, which gives resonances at $V = n2\Delta_{\text{BCS}}/e + re/C$, where r increases with n and is of order 1.

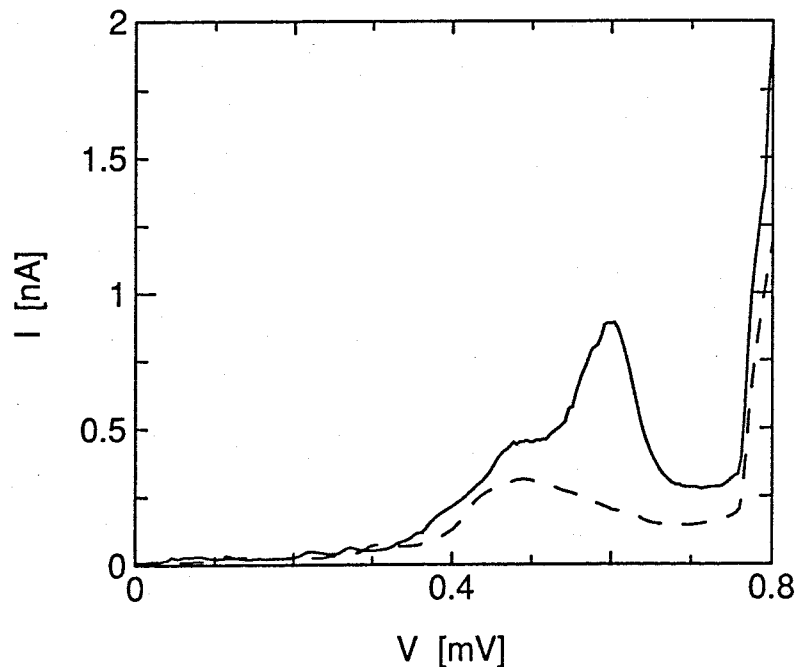


Fig. 22. The resonance arising from Cooper pair tunneling combined with excitation and tunneling of quasiparticles, for two different gate voltages. The sample is 2B ($E_J/E_C \approx 0.09$) at 400 mK.

For bias between $2\Delta_{\text{BCS}}/e+e/4C$ and $2\Delta_{\text{BCS}}/e-e/4C$, this catalyzing action of a permanent average charge on the central electrode is less efficient (only one of the quasiparticles will tunnel at a high rate), for still lower voltages it is completely absent. There only a combination of Cooper-pair tunneling with slow ($\Gamma \propto R_{\text{qp}}^{-1}$) quasiparticle tunneling is possible. The lowest voltage where the resonance condition for Cooper-pair tunneling is fulfilled, is the doubled normal state Coulomb gap (Cooper-pair gap). At this voltage conduction changes from being limited by only quasiparticle tunneling events, to a process of Cooper-pair tunneling across one junction, and quasiparticle tunneling across the other. Since typically E_J/h is much larger than $(R_{\text{qp}}C)^{-1}$, this increases the conduction by at least a factor two. (Although a current resonance rather than a plateau is expected when Cooper-pair tunneling comes in, a finite E_J and inequality of the junction capacitances will smear out the resonance.) In Fig. 12a we possibly observe both the Cooper-pair gap and the increase at $V=2\Delta_{\text{BCS}}/e-e/4C$. For Figs. 12b and c the interpretation as to what gap is observed is not so clear. Taking into account the slight suppression of the gap with magnetic field (Fig. 21), one might choose for the catalyzed Cooper-pair transfer starting at $V=2\Delta_{\text{BCS}}/e-e/4C$.

D Frequency-dependent damping in the phase regime

In the classical-phase picture each current peak at a multiple of the BCS sumgap corresponds to a given number of junctions in the normal state, and the others in the superconducting state. By taking into account a frequency-dependent damping of the junctions, the I-V curves can also be qualitatively explained in this classical picture.

In an array, the damping of a single junction is certainly frequency-dependent. The impedance of a superconducting neighbour is given by the parallel circuit of subgap resistance, capacitive impedance and the impedance of the superconducting inductance $L=\hbar/2eI_c\cos\phi$. The ac impedance of a neighbour that has switched to $V=2\Delta_{\text{BCS}}/e$ is very low, since $\delta V \approx 0$ for small signals. Therefore the shunt impedance at the plasma frequency, important for the retrapping events, is roughly proportional to the number of superconducting neighbours. This explains the steplike increase in current of the resonances in the I-V curves. Since the retrapping current increases with decreasing shunt, it predicts that the current peak height should scale as $1/N_s$, N_s being the number of superconducting neighbours. However, this prediction relies on equal ac impedance of all junctions, which is rather unlikely since the impedance will be very sensitive to small differences in plasma frequency between the junctions. As a function of temperature the damping does not change significantly, since the impedance should mainly be determined by the

temperature-independent capacitance and inductance. Thus it seems that this picture is valid for the high E_J/E_C array of Fig. 20b, where there is indeed little temperature effect on the current resonances. For voltages between the resonances, the damping at lower frequencies is more important, and here we probably see the decrease of subgap resistance with increasing temperature.

V SINGLE JUNCTIONS IN A HIGH IMPEDANCE ENVIRONMENT

In this section we will discuss results for single small capacitance junctions which are not trivially voltage biased. It was shown theoretically (Bakhvalov *et al.* 1989) and experimentally (chapter 2, Delsing *et al.* 1989) that arrays of normal metal tunnel junctions can be used to create a current bias. A single junction with, incorporated in the bias leads, four 2-D arrays of similar junctions (Fig. 23), can in this way be current-biased in the normal state (see chapter 2). However, below a certain temperature, I-V curves can not be recorded because of the high impedance of the arrays in the leads. This high impedance results from charging effects, yielding in the arrays a Coulomb gap in the normal state and a Cooper-pair gap (or Bloch nose) in the superconducting state. Above the critical temperature range where the arrays are isolating, in the

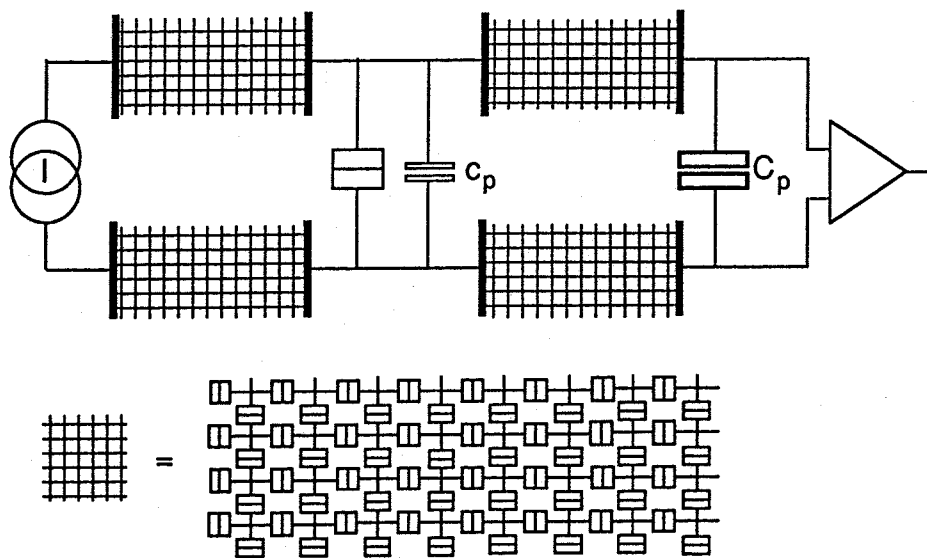


Fig. 23. Schematic of the configuration used to perform measurements on a single, isolated junction. The junction is decoupled from the environment (the large stray capacitance C_p) by arrays of $L \times W = 90 \times 9$ junctions in the leads, close to the junction.

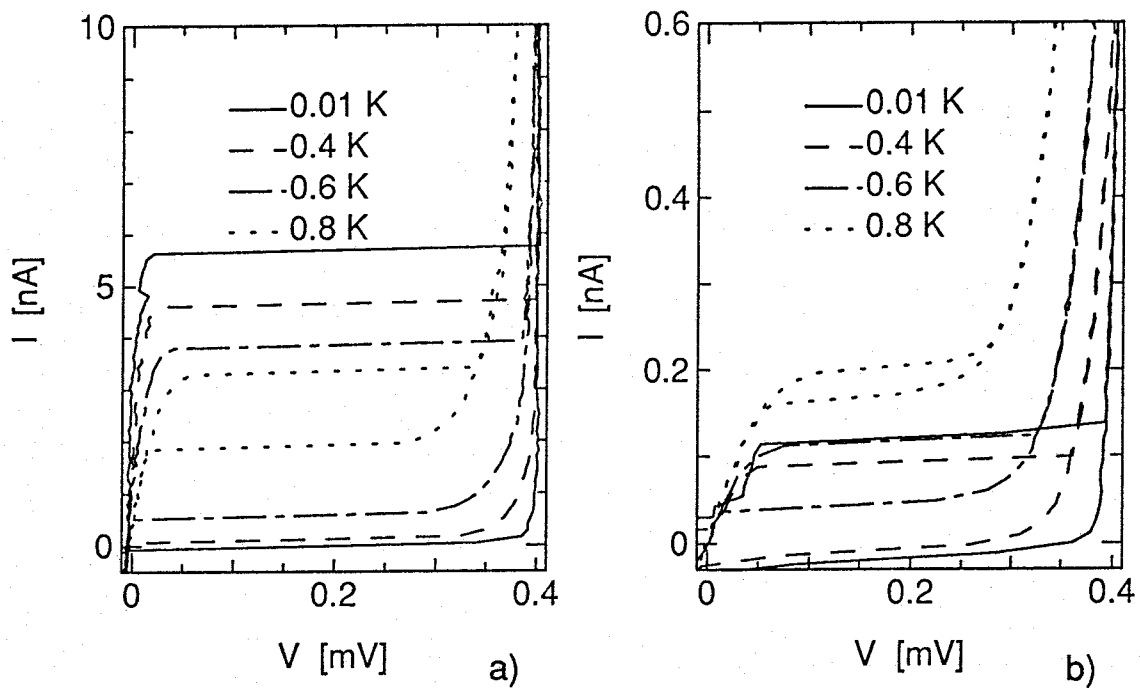


Fig. 24. *I-V characteristics of single junctions, in the configuration of Fig. 23. Both have a capacitance of about 2.8 fF. (a) junction 1D ($R_n=14\text{ k}\Omega$); (b) junction 1E ($R_n=132\text{ k}\Omega$). Curves are shown for temperatures of 0.8, 0.6, 0.4 and 0.01 K.*

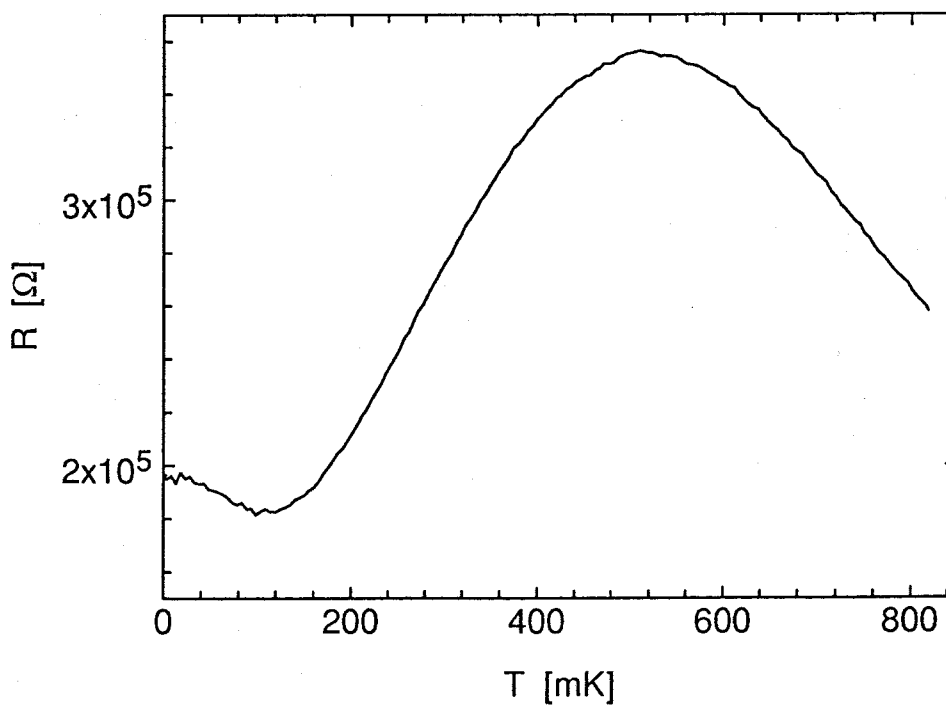


Fig. 25. *Small-signal resistance versus temperature for junction 1E.*

normal state a Coulomb gap is visible, but in the superconducting state an ordinary supercurrent is present. With arrays of junctions in which the charging energy is decreased, in the normal state for the single junction a Coulomb gap can be recorded down to lower temperatures. In the superconducting state however, neither the arrays nor the single junction develop clear charging effects. Note that if the arrays do not show charging effects, it is doubtful that the current can be described as being due to orderly moving, mutually repelling, charge solitons.

However, the junction is certainly to some extent decoupled from large shunt capacitances, so this technique may be useful to study junction dynamics with controlled damping. In particular, the arrays yield a significant inductance (of order $0.1 \mu\text{H}$) in series with the junction (e.g. McCumber 1968). Fig. 24 shows the I-V curves for two single junctions in this measurement configuration. In the normal state, both showed a Coulomb gap, with offset corresponding to a capacitance of about 2.8 fF . In the superconducting state both junctions show a classical hysteretic I-V curve. Note that these junctions both show a small voltage in the supercurrent, which is a sign of phase diffusion. From the observation that the voltage decreases with decreasing temperature, it can be concluded that this is predominantly thermally induced phase diffusion. However, even with careful cryogenic filtering, the resistance versus temperature of the lowest E_J junction (Fig. 25) shows at low temperatures flattening-off and even a small quasi-reentrant behavior. Although one should be careful with interpretation of these kind of observations, this might point at phase diffusion induced by quantum fluctuations. The quasi-reentrant behavior can be caused by decreasing damping at low temperatures, if the subgap resistance has a contribution to the damping. Since damping decreases the phase delocalization (Caldeira and Leggett 1981), a decreasing damping at low temperatures yields increasing phase diffusion. An alternative explanation is the direct effect of temperature on quantum phase diffusion. Occupation of higher energy levels at elevated temperatures tends to localize a quantum junction in phase space (e.g. Zwerger 1988).

VI FREQUENCY-CONTROLLED COOPER-PAIR TUNNELING

The work discussed in this section was instigated by and performed in cooperation with the Groupe Quantronique in Gif-Sur-Yvette. As was shown by the results on low E_J/E_C double junctions, the charge on these junctions is the classical variable. Moreover, these results showed that the tunneling of Cooper-pairs is indeed a resonant process, dependent on matching of energy levels of the charge states of the system. This suggests the possibility of control of Cooper-pair

transfer across the junctions by the use of bias voltage and gate voltage.

A Theory

In a double junction in the normal state, an electron cannot be trapped on the central island, if it can tunnel out with energy gain. In contrast, in a superconducting double junction, such an excited charged state is metastable if the energy levels are off-resonance. This yields extra possibilities for the control of Cooper-pair tunneling. In this section several procedures are described to realize synchronized Cooper-pair tunneling with a high frequency voltage, with the object to obtain a current equal to $2ef$ or a multiple. Which procedure might work depends on the precise charge dynamics, especially the occurrence of Zener tunneling. If a junction charge is swept through the resonance situation, and damping is low, a Cooper-pair will be transferred for low sweep speed. For high sweep speed Zener tunneling occurs. It is also known (Ao and Rammer 1990) that damping affects (increases) Zener tunneling probabilities. At low temperature the excitation transition probability is not enhanced by damping, whereas the decay transition is. The result is that at low temperature and for strong damping a Cooper-pair will tunnel at the Brillouin zone edge only if the system is in the lowest band (ground state).

We assume that to one junction, the other is just a true capacitor with classical charge as described by Büttiker. This is allowed for practical purposes if two conditions are met. First, coherent tunneling through the array should be negligible, i.e. E_J/E_C should be so low that for example a supercurrent is absent. Second, bias conditions for which both junctions are in resonance at the same time should be avoided (e.g. an island charge e at zero bias voltage). We also need a quasiparticle tunneling rate which is low enough to avoid fast decay of states in higher bands. For example, at a synchronization frequency of 10 MHz, R_{qp} should be much larger than $10\text{ M}\Omega$, for a decay probability of the excited state during one cycle to be much smaller than 1. This is probably valid for real junctions at low temperature. Finally, we will neglect interference of Zener tunneling events, which will at least be true for situations where damping is large and causes the Zener tunneling.

All operating principles can be illustrated with the same diagram in parameter space. In Fig. 26 we have plotted the resonance conditions for Cooper-pair tunneling, as lines in a (V, V_g) -plot. In a double junction of two equal capacitance junctions, and a low-capacitance gate, a Cooper-pair can tunnel at a junction charge equal to $\pm e/2$. This leads to very simple resonance conditions, depending on V , V_g and the number of Cooper-pairs on the central island n , as

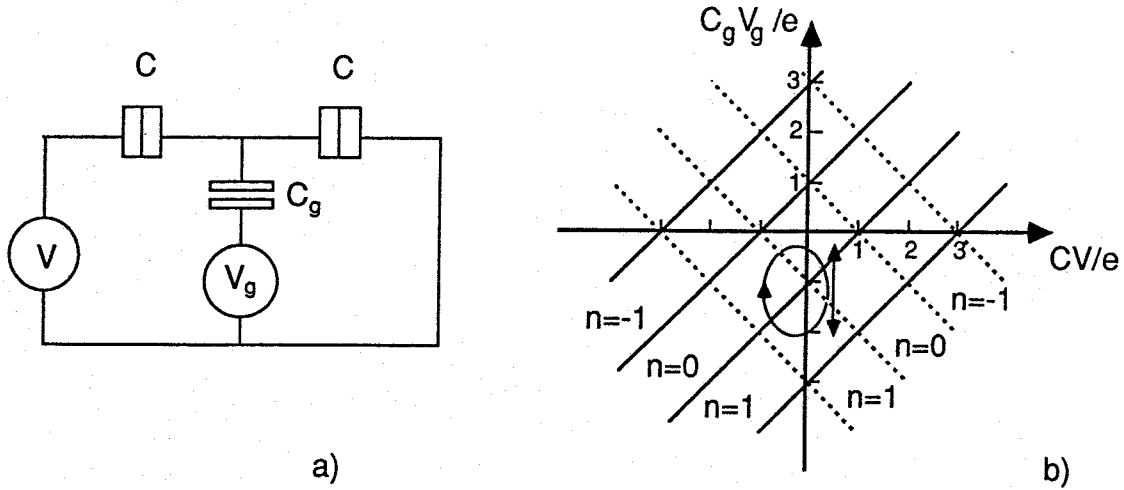


Fig. 26. (a) Double junction controlled by two voltages. (b) V - V_g diagram, showing resonance lines where Cooper-pair transfer may occur (solid: in the left junction; dotted: in the right junction). For both junctions the number of Cooper pairs n on the central island which gives the lowest charging energy as far as tunneling through that junction is concerned is indicated, between the resonance lines. Two modulation trajectories as discussed in the text are shown.

$$CV/e - C_g V_g/e = \pm 1 + 2n \tag{9a}$$

for the left junction (solid lines in Fig. 26), and

$$CV/e + C_g V_g/e = \pm 1 - 2n \tag{9b}$$

for the right junction (dotted lines). We have indicated in Fig. 26 the number of Cooper-pairs n for which a junction is in the ground state (plotted between the resonance lines for that junction). Of course these values of n change by unity precisely on the resonance lines (9a) and (9b). In the adiabatic approximation a Cooper-pair transfer will always take place on line crossing. In the high-damping limit, because the decay transition probability equals 1, on crossing a resonance line Cooper pair tunneling only takes place if the junction starts from the ground state. Note that only for regions along the V_g -axis both junctions can be in the ground state for the same value of n .

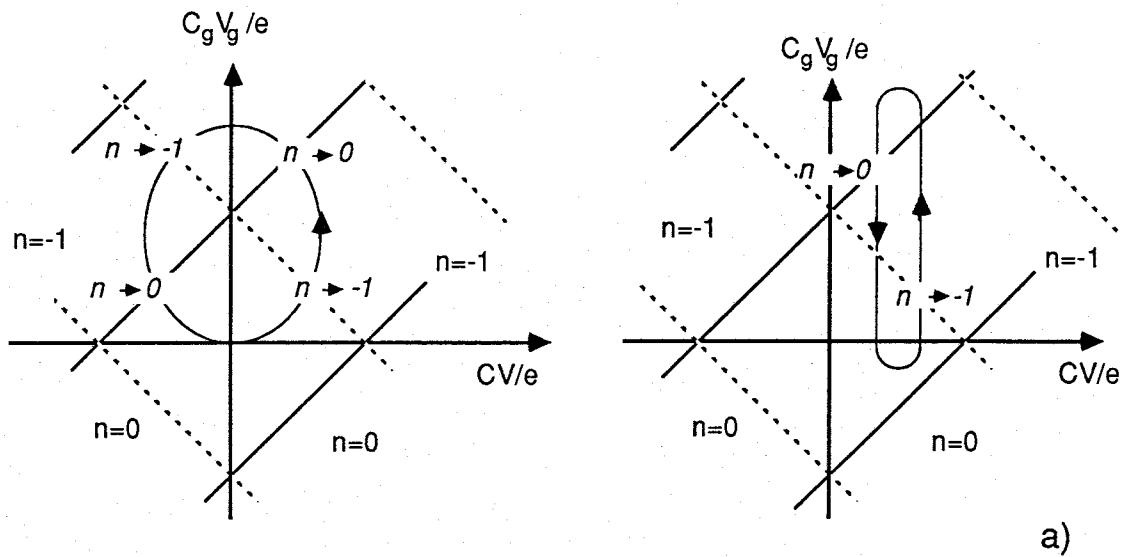


Fig. 27. Synchronized Cooper-pair transfer in the absence of interband transitions. Each line crossing yields one Cooper-pair transfer, so that two Cooper-pairs are transferred through the system per cycle.

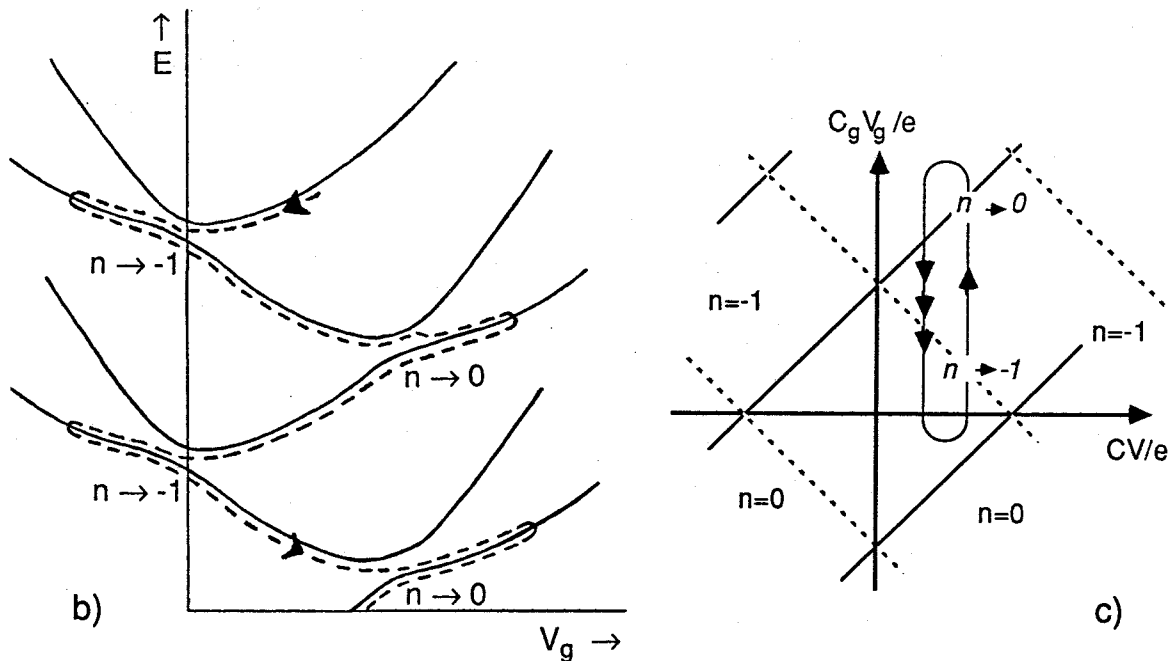


Fig. 28. Synchronized Cooper-pair transfer with one ac voltage, by using interband transitions. (a) High probability of decay transitions. (b) Same as (a), in system energy vs V_g diagram. (c) Selective Zener tunneling by sawtooth modulation.

If interband transitions do not occur, encircling an intersection point of resonance lines on the V_g -axis yields a current $\pm 4ef$. Such a circle can be realized in an experiment if both gate voltage and bias voltage are rf modulated, with amplitude approximately $e/2C_g$ and $e/2C$, and a phase difference of $\pi/2$. In addition a dc bias voltage on the gate is necessary. In Fig. 27, one possible centre-point for this rf cycle is illustrated. Starting at the $V_g, V \approx 0$ in the island state $n=0$, and going ccw, the following tunneling events occur (all with a charge $+2e$ tunneling to the right): junction 2 (bringing junction 1 in a higher band); junction 1 (bringing junction 2 in a higher band); junction 2 (relaxing junction 1); junction 1 (relaxing junction 2). Note that $3/4$ of the cycle is metastable, i.e. a Cooper-pair tunneling is energetically favorable, but cannot occur because of off-resonance condition. As Likharev (1990) noted, this cycle is very sensitive to sporadic interband transitions, because the current changes sign after each interband transition. Unless care is taken to correct for this effect, e.g. by dwelling long enough around $V, V_g \approx 0$ to let relaxation by quasiparticle tunneling happen, the net current will average to zero.

The second operating possibility is illustrated in Fig. 28. With a vertical oscillation and selective Zener tunneling, a current $2ef$ can be created. In Fig. 28a strong damping is assumed. The cycle starts again in the ground state of both junctions. Going up, first junction 2 tunnels, bringing junction 1 in an excited state. Increasing the gate voltage, junction 1 is relaxed by an interband transition. Next, decreasing the gate voltage, now that junction 1 is in the ground state a Cooper-pair tunnels at the resonance line between $n=0$ and $n=-1$. This brings junction 2 in a higher band, which relaxes again on going back to the initial situation. This principle would not have the instability against unwanted Zener tunneling that the double rf principle suffers from. By increasing the gate voltage modulation amplitude, higher multiples of $2ef$ can be realized. The approach of considering the junctions separately is just as valid or invalid as constructing the two-junction energy diagram by plotting the charging energy and introducing band splittings where Cooper pair tunneling across a single junction can occur. Such a diagram is given in Fig. 28b, to illustrate again the trajectory of Fig. 28a. Finally, a sawtooth V_g -modulation (Fig. 28c) can in principle also yield synchronized Cooper-pair tunneling by selecting Zener tunneling with sweep speed, but such an approach will be hard to realize in experiments.

Note that the dc experiments on double junctions are probably very sensitive to the presence of quasiparticle tunneling conductance, even if it is very small. High frequency experiments may be a more fruitful way to study the bare Cooper-pair tunneling and a better tool to test theories for small-capacitance superconducting junctions which disregard this quasiparticle tunneling.

From the work by Ao and Rammer we can make some remarks about the probability of decay

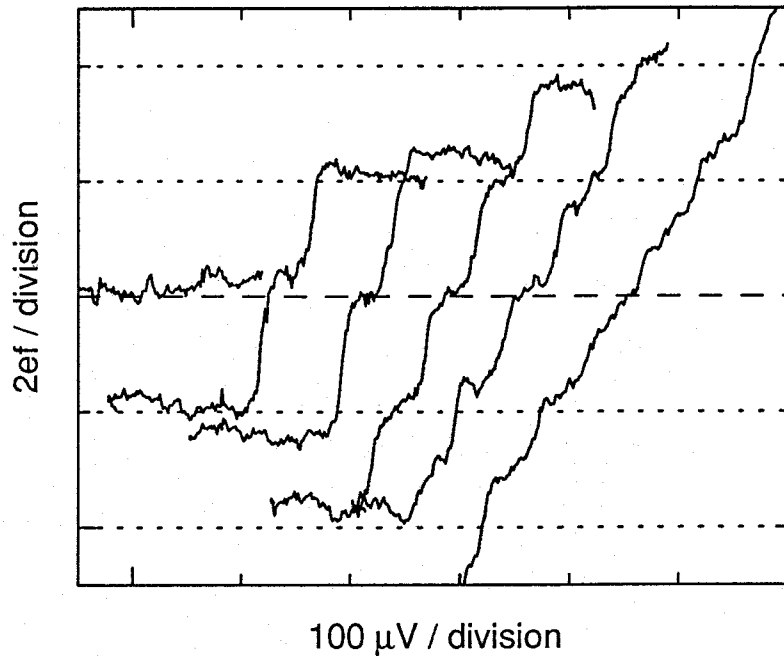


Fig. 29. I-V characteristics of double junction 2C ($E_J/E_C = 0.04$) at low bias voltage, in the presence of an alternating gate voltage of frequency 8 MHz. The measurements have been offset in voltage direction for clarity. The current offset is unknown, symmetry suggests that the dashed line is $I=0$. From left to right the rf amplitudes are 0.5, 1.4, 2, 2.8, 3.6 and 4 V, where eIC_g corresponded to roughly 2 V at DC. The dotted lines are spaced by $2ef$.

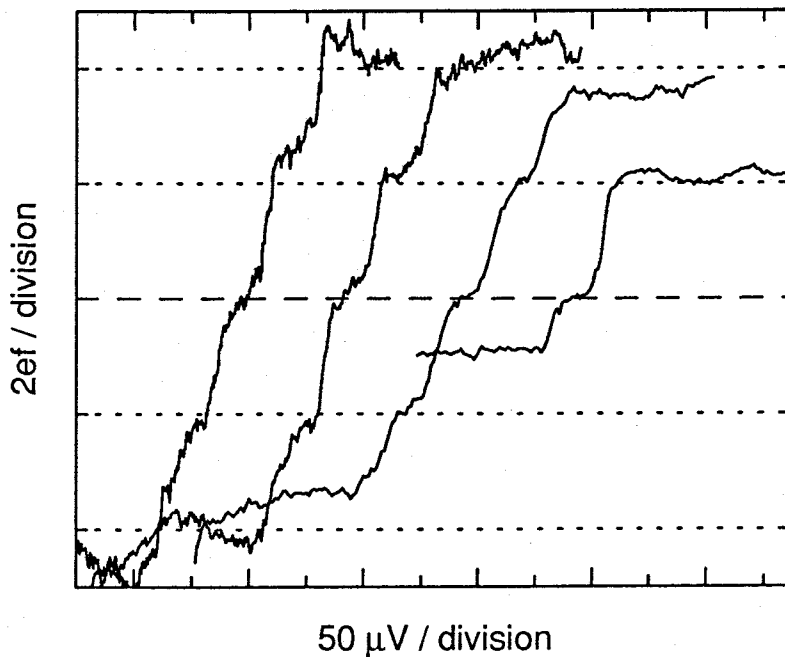


Fig. 30. I-V characteristics of device 2C for gate voltage frequency (from left to right) $f=4, 5, 10$ and 15 MHz. The amplitudes have been chosen for clearest step structure, and vary between 2.5 and 4 V. The current is scaled to $2ef$.

transitions in our systems, in which at first sight one would expect the damping to be small. For strong damping (e.g. an Ohmic shunt with $R < R_q/2\pi$) the decay probability is close to 1. For weak damping, the decay transition probability is proportional to the density of states in the dissipative bath (the usual dense set of harmonic oscillators, e.g. Caldeira and Leggett 1981) at a frequency E_J/\hbar . At this frequency the typical capacitive junction impedance is about $10R_q$, and we would expect the decay transition probability to be significantly smaller than 1. However, a quantitative evaluation of the damping and decay probability for our systems has not been performed, and the experiments presented in the next section suggest that the decay transition might be more probable than expected.

B Preliminary experiments

In Fig. 29 we show I-V curves of a double junction with $E_J/E_C=0.04$ ($R_n=110$ k Ω), with dc gate voltage adjusted to suppress the zero-voltage current. Without rf voltage on the gate, the current inside the BCS sumgap is negligible. With rf gate voltage applied, current is transferred through the device at low voltage. As the Figure shows, for low rf levels only one plateau tends to develop at equal positive and negative current, relatively independent of rf voltage amplitude. For increasing amplitude a step structure with two current plateaus develops. The plateaus are near $I=2ef$ and $I=4ef$. This behavior occurs for low frequencies, e.g. $f=8$ MHz in Fig. 29. In Fig. 30 we show the I-V curves for frequencies between 4 and 15 MHz, for rf levels that yield an optimum step structure. The current is normalized to $2ef$. For higher frequencies only a plateau at $I=2ef$ develops. It is clear that there is correlation between frequency and step height, although one cannot speak of clear synchronization of Cooper-pair transfer. Since these results were obtained with only gate voltage modulation, it seems to confirm the presence of decay transitions during sweeping of the junction charge. Nevertheless, the same device also transmitted current if two rf voltages were applied, with a clear effect of the phase difference on the sign of the current.

In Fig. 31 we give I- V_g curves obtained under comparable conditions for a double junction with $E_J/E_C=0.02$. For increasing rf amplitude, the current increases and also changes the sign of the modulation, i.e. maxima turn into minima and *vice versa*. There is a tendency for this inversion of the current modulation to occur at a current level $I=2ef$. This behavior is similar to that observed for the single electron turnstile device (chapter 2, inset of Fig. 14), and can be understood from similar arguments. The best conclusion based on these results is probably that there is a need for further experiments.

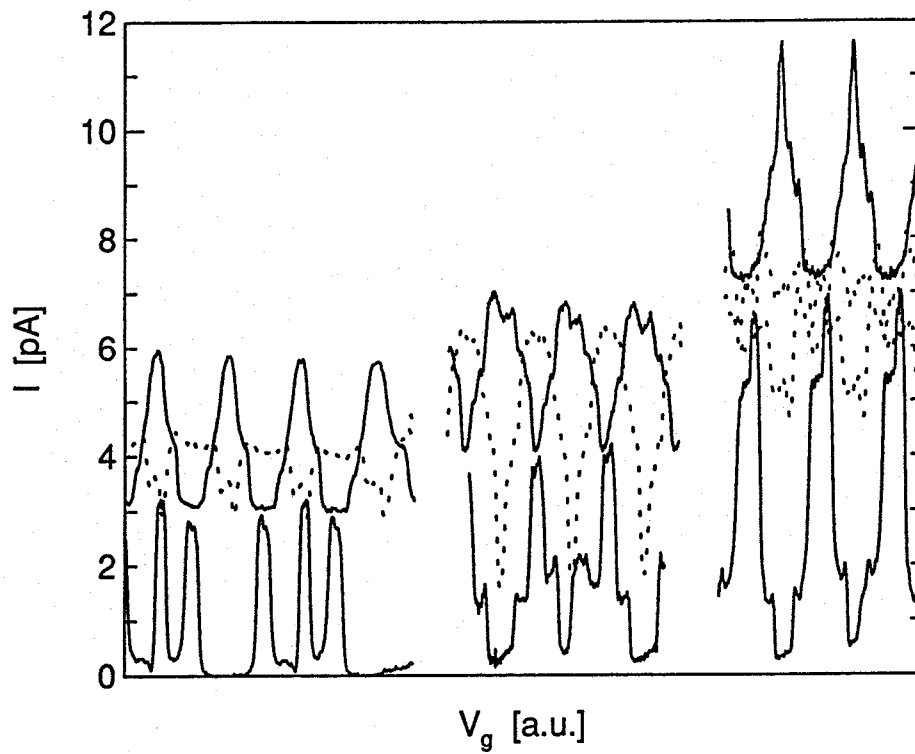


Fig. 31. I - V_g characteristics of double junction 2D ($E_J/E_C \approx 0.02$) for gate voltage modulation at $f=10, 12.5$ and 25 MHz (left to right). For each frequency, measurements are plotted for low and high modulation amplitude (solid curves) and intermediate amplitude (dotted curve). The I - V_g curves seem to mirror in the $I=2ef$ axis.

VII CONCLUSIONS

For single Josephson junctions in the usual low-impedance environment, we have observed semi-classical phase dynamics. This means that the junctions show behavior that fits well in the theories existing for conventional junctions, with only small modifications to allow for quantum phase fluctuations. Even if a junction is isolated from the low-impedance environment by arrays of junctions of small capacitance, the behavior is still apparently semi-classical as long as the arrays are superconducting. Since at low temperatures the arrays are either superconducting or insulating, this method seems of little use for research of strong charging effects in small superconducting junctions.

Charging effects show up strongly in linear arrays of small-capacitance junctions, if $E_J \ll E_C$. In that case, as for normal junctions, charge transfer is dominated by the Coulomb energy barrier associated with charging of the central electrodes. In the presented experiments, the behavior was complicated by resonating environmental modes and parasitic quasiparticle tunneling. There is a need for additional experiments, preferably on double junction systems, in a circuit where the environmental resonances are effectively shunted out. Individual determination of the junction parameters in a geometry as used by Fulton *et al.* will also help the comparison of theory with experiment.

High-frequency synchronized Cooper pair transfer through these systems is not only interesting from a practical point of view. It gives interesting possibilities to examine the dissipative quantum dynamics of this multi-band system, probably avoiding parasitic quasiparticle effects to a higher extent than is possible in dc experiments.

REFERENCES

- Abramowitz, M., and I.A. Stegun, 1965, eds., *Handbook of mathematical functions* (Dover, New York).
- Anderson, P.W., 1964, in *Lectures on the many-body problem*, ed. E.R. Caianiello, pp. 113 (Academic Press, New York).
- Aleshkin, V. Ya, and D.V. Averin, 1990, *Resonant tunneling of Cooper pairs in a double Josephson junction system*, to be published in the proceedings of LT19.
- Ambegaokar, V., and A. Baratoff, 1963, *Tunneling between superconductors*, Phys. Rev. Lett. **10**, 486.

- Ao, P., and J. Rammer, 1990, *Quantum dynamics of a two-state system in a dissipative environment*, submitted to Phys. Rev. B.
- Averin, D.V., and V.Ya Aleshkin, 1989, *Resonance tunneling of Cooper pairs in a system of two small Josephson junctions*, Pis'ma Zh. Eksp. Teor. Fiz. **50**, 331 (JETP Lett. **50**, 368).
- Averin, D.V., and K.K. Likharev, 1990, *Single-Electronics*, to be published in "Quantum Effects in Small Disordered Systems", eds. B.L. Al'tshuler, P.A. Lee and R.A. Webb (Elsevier, Amsterdam).
- Bakhvalov, N.S., G.S. Kazacha, K.K. Likharev and S.I. Serdyukova, 1989, *Single-electron solitons in one-dimensional tunnel structures*, Zh. Eksp. Teor. Fiz. **195**, 1010 [Sov. Phys. JETP **68**, 581].
- Ben-Jacob, E., and Y. Gefen, 1985, *New quantum oscillations in current driven small junctions*, Phys. Lett. **A108**, 289.
- Bol, D.W., J.J.F. Scheffer, W.T. Giele and R. de Bruyn Ouboter, 1985, *Thermal activation in the quantum regime and macroscopic quantum tunnelling in the thermal regime in a metastable system consisting of a superconducting ring interrupted by a weak junction*, Physica B **133**, 196.
- Büttiker, M., 1986, *Quantum oscillations in ultrasmall normal loops and tunnel junctions*, Physica Scripta **T14**, 82.
- Büttiker, M., 1987, *Zero-current persistent potential drop across small-capacitance Josephson junctions*, Phys. Rev. B **36**, 3548.
- Caldeira, A.O., and A.J. Leggett, 1981, *Influence of dissipation on quantum tunneling in macroscopic systems*, Phys. Rev. Lett. **46**, 211.
- Condon, E.A., 1928, *The physical pendulum in quantum mechanics*, Phys. Rev. **31**, 891.
- de Gennes, P.G., 1966, *Superconductivity of metals and alloys*, p. 119 (Benjamin, New York).
- Delsing, P., K.K. Likharev, L.S. Kuzmin and T. Claeson, 1989, *Time-correlated single-electron tunneling in one-dimensional arrays of ultrasmall tunnel junctions*, Phys. Rev. Lett. **63**, 1861.
- Devoret, M.H., 1989, private communication.
- Devoret, M.H., D. Esteve, H. Grabert, G.-L. Ingold, H. Pothier and C. Urbina, 1990, *Effect of the electromagnetic environment on the Coulomb blockade in ultrasmall tunnel junctions*, Phys. Rev. Lett. **64**, 1824.
- Esteve, D., J.M. Martinis, C. Urbina, E. Turlot, M.H. Devoret, H. Grabert and S. Linkwitz, 1989, *Observation of the temporal decoupling effect on the macroscopic quantum tunneling*

of a Josephson junction, Physica Scripta T29, 121.

- Ferrell, R.A., and R.E. Prange, 1963, *Self-field limiting of Josephson tunneling of superconducting electron pairs*, Phys. Rev. Lett. **10**, 479.
- Fulton, T.A., P.L. Gammel, D.J. Bishop, L.N. Dunkleberger and G.J. Dolan, 1989, *Observation of combined Josephson and charging effects in small tunnel junction circuits*, Phys. Rev. Lett. **63**, 1307.
- Geerligs, L.J., M. Peters, L.E.M. de Groot, A. Verbruggen and J.E. Mooij, 1990, *Charging effects and quantum coherence in regular Josephson junction arrays*, Phys. Rev. Lett. **63**, 326.
- Geerligs, L.J., A.V. Averin and J.E. Mooij, 1990, *Observation of macroscopic quantum tunneling of the electric charge*, submitted to Phys. Rev. Lett.
- Geigenmüller, U., and G. Schön, 1988, *Single electron effects and Bloch oscillations in normal and superconducting tunnel junctions*, Physica B **152**, 186.
- Iansiti, M., A.T. Johnson, C.J. Lobb and M. Tinkham, 1988, *Crossover from Josephson tunneling to the Coulomb blockade in small tunnel junctions*, Phys. Rev. Lett. **60**, 2414.
- Iansiti, M., M. Tinkham, A.T. Johnson, W.F. Smith and C.J. Lobb, 1989, *Charging effects and quantum properties of small superconducting tunnel junctions*, Phys. Rev. **B39**, 6465.
- Josephson, B.D., 1962, *Possible new effects in superconductive tunnelling*, Phys. Lett. **1**, 251.
- Kistenev, V.Yu., L.S. Kuzmin, A.G. Odintsov, E.A. Polunin and I.Yu. Syromyatnikov, 1985, *Properties of the lead-alloy Josephson tunnel junctions*, in: SQUID'85, eds. H.D. Hahlbohm and H. Lübbig (Walter de Gruyter, Berlin), p. 113.
- Kramers, H.A., 1940, *Brownian motion in a field of force and the diffusion model of chemical reactions*, Physica **7**, 284.
- Kuzmin, L., H. Olsson and T. Claeson, 1985, *Parametric effects in inductively compensated tunnel junctions*, in: SQUID'85, eds. H.D. Hahlbohm and H. Lübbig (Walter de Gruyter, Berlin), p. 1017.
- Likharev, K.K., and A.B. Zorin, 1985, *Theory of the Bloch-wave oscillations in small Josephson junctions*, J. Low Temp. Phys. **59**, 347.
- Likharev, K.K., and A.B. Zorin, 1987, *Simultaneous Bloch and Josephson oscillations, and resistance quantizations in small superconducting double junctions*, Jap. J. Appl. Phys. **26**, 1407.
- Likharev, K.K., 1990, private communication.
- Martinis, J.M., M.H. Devoret and J. Clarke, 1987, *Experimental tests for the quantum behavior*

- of a macroscopic degree of freedom: The phase difference across a Josephson junction*, Phys. Rev. B **35**, 4682.
- Martinis, J.M., and R.L. Kautz, 1989, *Classical phase diffusion in small hysteretic Josephson junctions*, Phys. Rev. Lett. **63**, 1507.
- McCumber, D.E., 1968, *Effect of ac impedance on dc voltage-current characteristics of superconductor weak-link junctions*, J. Appl. Phys. **39**, 3113.
- Mooij, J.E., and G.B.J. Schön, 1988, eds., *Proceedings of the NATO Advanced Research Workshop on Coherence in superconducting networks*, Delft, The Netherlands, December 1987 (Physica B **152**, 1-302).
- Mühschlegel, B., 1959, *Die thermodynamischen Funktionen des Supraleiters*, Z. Phys. **155**, 313.
- Mullen, K., E. Ben-Jacob and Z. Schuss, 1988, *Combined effect of Zener and quasiparticle transitions on the dynamics of mesoscopic Josephson junctions*, Phys. Rev. Lett. **60**, 1097.
- Nagai, S., and J. Kondo, 1980, *Electrons in infinite one-dimensional crystals in a uniform electric field*, J. Phys. Soc. Jpn. **49**, 1255.
- Nazarov, Yu.V., 1990, *Influence of the electrodynamic environment on the electron tunneling at finite traversal time*, preprint.
- Pedersen, N.F., 1983, in *Proceedings of the NATO Advanced Study Institute on Advances in Superconductivity*, eds. B. Deaver and J. Ruvalds, Erice (Italy) July 1982 (Plenum, New York, 1983), p. 149.
- Peierls, R., 1979, *Surprises in theoretical physics*, p. 14 (Princeton University Press, Princeton).
- Schön, G., and A.D. Zaikin, 1988, *Distinguishing phases in Josephson junctions and the choice of states*, Physica B **152**, 203.
- Schön, G., and A.D. Zaikin, 1990, *Quantum coherent effects, phase transitions, and the dissipative dynamics of ultra small tunnel junctions*, to be published in Physics Reports.
- Stewart, W.C., 1968, *Current-voltage characteristics of Josephson junctions*, Appl. Phys. Lett. **12**, 277.
- Widom, A., G. Megaloudis, T.D. Clark, H. Prance and R.J. Prance, 1982, *Quantum electrodynamic charge space energy bands in singly connected superconducting weak links*, J. Phys. A **15**, 3877.
- Zwerger, W., 1987, *Quantum effects in the current-voltage characteristic of a small Josephson junction*, Phys. Rev. B **35**, 4737.

CHAPTER 4

FREQUENCY-LOCKED TURNSTILE DEVICE FOR SINGLE ELECTRONS

L.J. Geerligs, V.F. Anderegg, P.A.M. Holweg,^(a) J.E. Mooij

Department of Applied Physics, Delft University of Technology
P.O. Box 5046, 2600 GA Delft, The Netherlands

H. Pothier, D. Esteve, C. Urbina, M.H. Devoret

Service de Physique du Solide et de Résonance Magnétique
Centre d'Études Nucléaires de Saclay, 91191 Gif-Sur-Yvette, France

*In the distant past, when the number of physicists
was small and hasty publication unknown, the new
names could be agreed upon by committees ...*

Editorial Phys. Rev. Lett. 3, 161 (1959).

ABSTRACT

We have fabricated an array of ultras-small tunnel junctions which acts like a turnstile for single electrons. When alternating voltage of frequency f is applied to a gate, one electron is transferred per cycle through the device. This results in a current plateau in the current-voltage characteristic at $I=ef$. The overall behavior of the device is well explained by the theory of Coulomb blockade of electron tunneling. We discuss the accuracy limitations of this device.

With present-day lithographic techniques it has become possible to fabricate tunnel junctions with capacitance C small enough to make the charging energy of a single electron, $E_C=e^2/2C$, much larger than thermal energies at dilution refrigerator temperatures. Typical capacitances are below 10^{-15} F for junction areas below $(100 \text{ nm})^2$, hence $E_C/k_B > 1$ K. Under this condition the discreteness of electron tunneling leads to new phenomena, charging effects, as reviewed by Averin and Likharev.[1] In a pioneering paper Fulton and Dolan [2] confirmed experimentally the existence of charging effects in small circuits of planar tunnel junctions. In linear arrays of small tunnel junctions charge is transferred by mutually repulsing charge-solitons,[3] resulting in time-correlated tunneling events with fundamental frequency I/e . Delsing et al. [4] demonstrated this effect by application of a signal with frequency f , leading to resonances at current levels $I=ef$ and $I=2ef$. The resonances show up in the differential resistance only. In this paper, we present a new device in which a single electron is transferred per cycle of an externally applied rf signal. In this voltage biased device a current flows which is equal to the frequency times the electron charge. The device is based on a turnstile effect resulting from the Coulomb blockade in linear arrays of tunnel junctions. It opens the possibility of a high accuracy, frequency-determined current standard. In many respects resembling a single electron shift register, the device exemplifies the prospects of using charging effects for practical logic circuits.[5]

The Coulomb blockade of single electron tunneling manifests itself in voltage biased linear arrays as a voltage gap in their current-voltage (I - V) characteristic. This Coulomb gap arises because for an electron to transfer through the array it has to occupy intermediate positions on the metal "islands" between the junctions. For bias voltages well below e/C (C being the junction capacitance) the energy of these intermediate states is higher than the energy of the initial state. Conduction is thus energetically suppressed. Consider the energy of a device constructed, like in our experiment, of both tunnel junctions and true capacitors, biased from several voltage sources. The energy associated with a given electron position is the sum of the capacitive energy for the resulting charge distribution and the work performed by the bias voltage sources.[3] If, under the influence of particular bias conditions, the absolute value of the charge on a junction of the array exceeds a critical charge, an electron can tunnel across this junction. The difference ΔE_k between the final and initial energy for the tunnel event across junction k of the array can be expressed as:

$$\Delta E_k = -e(|Q_k| - Q_{ck})/C_k \quad (1)$$

where Q_k and C_k are the charge and capacitance of junction k , respectively. The critical charge

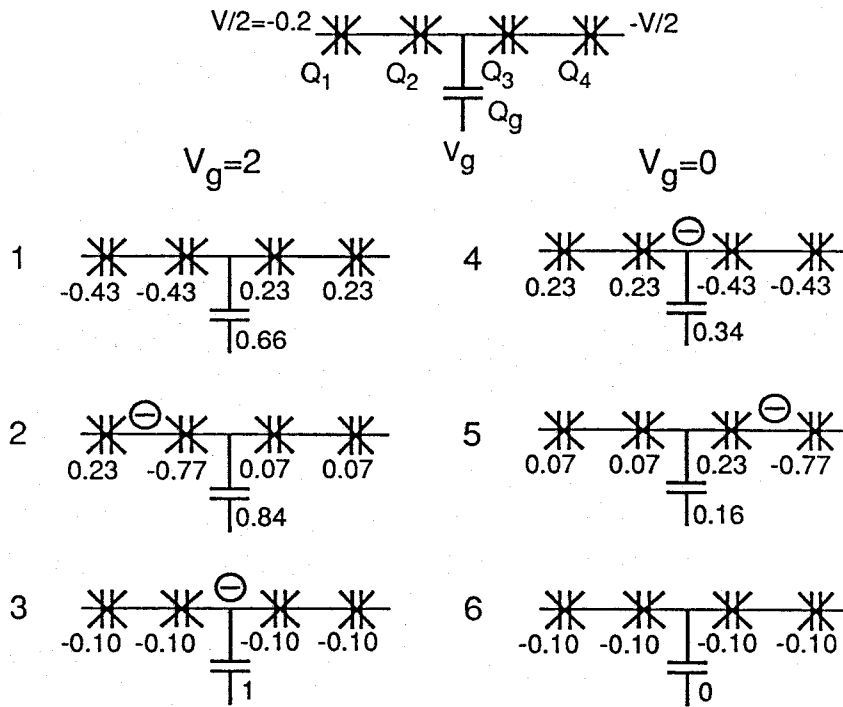


Fig. 1. Principle of controlled single electron transfer through a linear array of small tunnel junctions. Junctions, with capacitance C , are denoted by crossed capacitor symbols, the gate voltage V_g is applied via a true (non-tunneling) capacitance C_g . If $C_g = C/2$, tunneling across any junction can only occur if for that junction $|Q| > Q_c$, with $Q_c = e/3$. The voltages and charges are indicated in units of e/C and e . 1-6 indicate consecutive times in the cycle. Left: First half of the cycle, $V_g = 2$. An elementary charge (- in a circle) ends up trapped on the central electrode. Right: Second half of the cycle, $V_g = 0$. The charge can only leave on the right hand side. No further tunneling can occur in the emptied array.

$Q_{ck} = e/[2(1 + C_{ek}/C_k)]$ depends apart from the junction capacitance only on the equivalent capacitance C_{ek} of the circuit in parallel with junction k . With this concept of a critical charge Q_c the principle of the present experiment can be understood. It is illustrated in Fig. 1. A linear array of 4 junctions of capacitance C is biased by a drive voltage V , which is applied symmetric to ground. The central island, between junctions 2 and 3, is capacitively coupled to a gate voltage V_g . [2,5] If the gate capacitor C_g is chosen to equal $C/2$, all junctions have the same critical charge for tunneling, $Q_c = e/3$. For V and V_g within a certain window, the critical charge will be exceeded for the junctions in the left arm, but not for the junctions in the right arm. Once an elementary charge has entered the central island, part of it will polarize the gate capacitor, and the charge on all junctions will be lower than the critical charge. Therefore the elementary charge is trapped on

the central island until bias conditions are changed. It is also impossible for another charge to move to the central island. To make the charge leave by the right arm, the gate voltage is decreased. The junctions on the right arm will first exceed the critical charge because of the asymmetry caused by the bias voltage. Cyclically changing the bias conditions by applying an alternating voltage in addition to a dc voltage to the gate capacitor moves one electron per cycle through the chain. We emphasize that after an arbitrary long time, the total charge transferred will be known to within a single electron. The principle will work for a general T-shaped structure of $2n$ junctions with a gate capacitance of about C/n . However, at least two junctions on each side are needed to avoid the unwanted entering or leaving of a charge.

We will discuss why the stochastic nature of electron tunneling need not perturb the deterministic transfer of electrons through the device. At finite temperature T the tunneling rate is for arbitrary ΔE given by [1]

$$\Gamma = \frac{\Delta E/2E_C}{RC[\exp(\Delta E/k_B T) - 1]} \quad (2)$$

where R is the tunneling resistance of the junction. This shows the two main prerequisites for deterministic electron transfer. The ac cycle should last long enough to let tunneling to and from the central island happen with high probability, i.e. f must be much smaller than $(RC)^{-1}$ to avoid cycles being lost. On the other hand an electron trapped on the central electrode should have a negligible probability to escape by a thermally assisted transfer. At finite temperature there is a tradeoff between the two requirements: a thermally assisted escape will be more probable for lower frequencies. We will discuss the consequences of these limitations more quantitatively below. Finally, we note that eq. (2) is strictly valid only for negligible tunnel conductance. Quantum charge fluctuations associated with a tunnel resistance not much larger than h/e^2 [6,7] generally suppress the charging effects. We have not investigated the consequences of this aspect for the present experiment.

The physical layout of the device is very close to the circuit shown in Fig.1, with 4 junctions of about 0.5 fF and 340 kOhm ($(RC)^{-1} \approx 5$ GHz) and a gate capacitance C_g of 0.3 fF. The values of R and C were determined from the large scale I-V curve,[6] and C_g was determined from the period of the current modulation by the gate voltage. This period ΔV_g yields the gate capacitance as $C_g = e/\Delta V_g$. An important refinement over the circuit of Fig. 1 is the use of two small auxiliary gate capacitances (0.06 fF) to tune out non-integer trapped charges [5] on the remaining two islands. This device was fabricated with nanolithographic methods as described elsewhere,[6] with planar

aluminum-aluminum oxide-aluminum junctions. It was thermally anchored to the mixing chamber of a dilution refrigerator, and a magnetic field of 2 Tesla was applied to bring the junctions in the normal (i.e., non-superconducting) state. All leads were low pass filtered by a stage which was also thermally anchored to the mixing chamber. In addition, the gate voltages were strongly attenuated. The gate voltages were applied by room temperature dc voltage sources referenced to cryostat ground. In addition, an ac voltage could be applied to the central gate capacitor. The voltage bias was symmetric with respect to cryostat ground. The measurement was performed with a two-wire method: a FET-opamp circuit with virtually shorted input terminals, in series with voltage source and sample, was used to measure the current.

Fig. 2 shows I-V curves of the device, without ac gate voltage applied (dotted curve) and with ac gate voltage of different frequencies between 4 and 20 MHz. Without ac gate voltage, a large zero-current Coulomb gap is present. With ac gate voltage of frequency f , wide current plateaus develop inside the Coulomb gap at a current level $I=ef$. The plateaus even extend to voltages outside the gap. In Fig. 2 the dc gate voltages were the same for each curve, the ac amplitude was adjusted for the widest plateau, which required more power at higher frequencies. Thermometer temperature varied from 10 to 40 mK, depending on applied ac power. Good plateaus were observed up to 40 Mhz, but only for frequencies below about 10 MHz were part of the plateaus flat within experimental current noise (about 0.05 pA, DC to 1 Hz). Fig. 3 shows the dependence of the I-V curve on ac amplitude at a frequency of 5 MHz. Clearly, the height of the plateaus is not dependent on the ac amplitude, although the width is. For high amplitudes, we have observed a tendency to form plateaus at $I=2ef$. Another sample with $n=3$ junctions in each arm showed the same behavior, although with somewhat rounded plateaus. We attribute this rounding to the larger capacitances (about 2 fF) of the junctions in this device.

A gate voltage adjustment was necessary to obtain wide plateaus. A suitable procedure was to maximize the Coulomb gap without ac voltage, using the auxiliary gate voltages. Next the current versus dc gate voltage would be recorded at fixed bias voltage, with ac gate voltage applied. This shows an oscillating behavior with minima and maxima at $I=ef$, $I=2ef$ or even higher multiples, depending on the ac amplitude. An example is shown in the inset of Fig. 2. The I-V curves of Fig. 2 were obtained with dc gate voltage in the middle of a $I-V_g$ plateau at $I=ef$, corresponding to half the elementary charge induced on the gate capacitor. When misadjusting both auxiliary gates on purpose, we could still obtain plateaus in the I-V curve, but not as wide as in Fig. 2.

The dependence of the I-V curves on ac amplitude, as shown in Fig. 3, are very well simulated by numerical calculations based on eq. (1) and (2). Results are shown in the same figure as

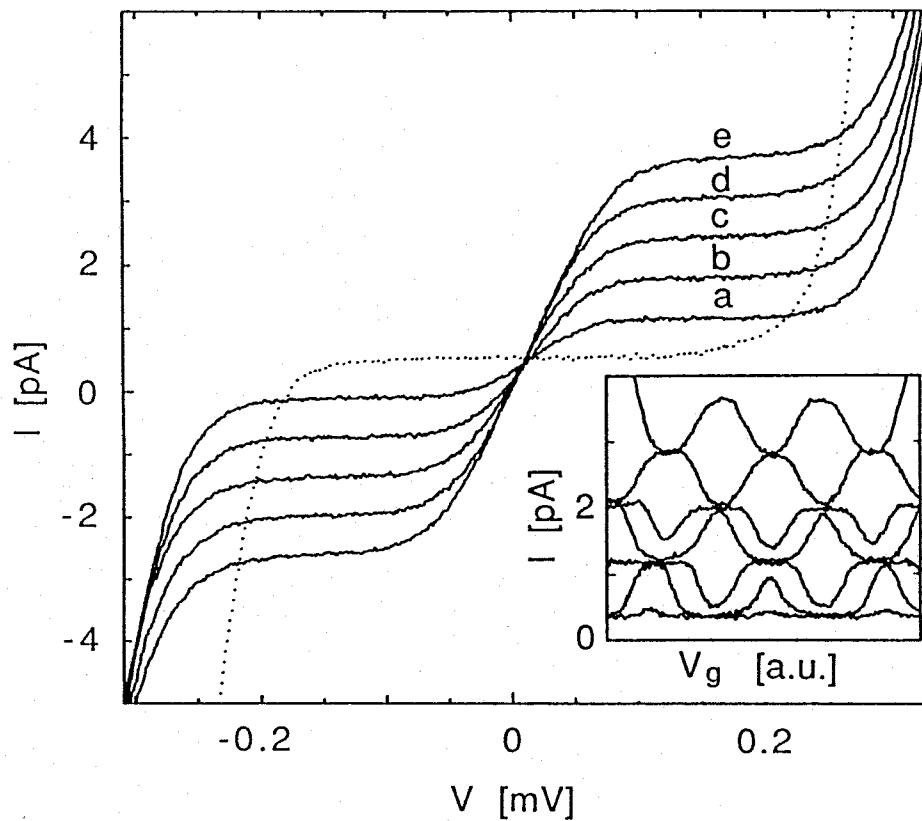


Fig. 2. Current-voltage characteristics without ac gate voltage (dotted) and with applied ac gate voltage at frequencies f from 4 to 20 MHz in 4 MHz steps (a-e). Current plateaus are seen at $I=ef$. The inset shows current versus dc gate voltage characteristics for $f=5$ MHz. The curves tend to be confined between levels at $I=nef$ and $I=(n+1)ef$, with n integer. The bias voltage was fixed at 0.15 mV. For the bottom curve, which is nearly flat, the ac gate voltage amplitude is 0. For the other curves the calculated ac amplitude at the sample increases from $0.60e/C$ for the lowest one to $3.4e/C$ for the upper one, where $e/C=0.30$ mV.

dashed curves on the right of the measurements. No fitting parameters were used. The only adjustments made were assuming 1 dB attenuation in the ac voltage line to be present in addition to the known attenuators, and introducing a higher temperature (50-75 mK) than the thermometer indicated during the experiments (10-20 mK) to roughly account for remaining noise or heating of the sample.

In Table 1 we compare the current step height I_S , obtained by taking half the measured current distance between the positive and the negative plateaus, with the prediction $I_S=ef$. Up to 10 MHz,

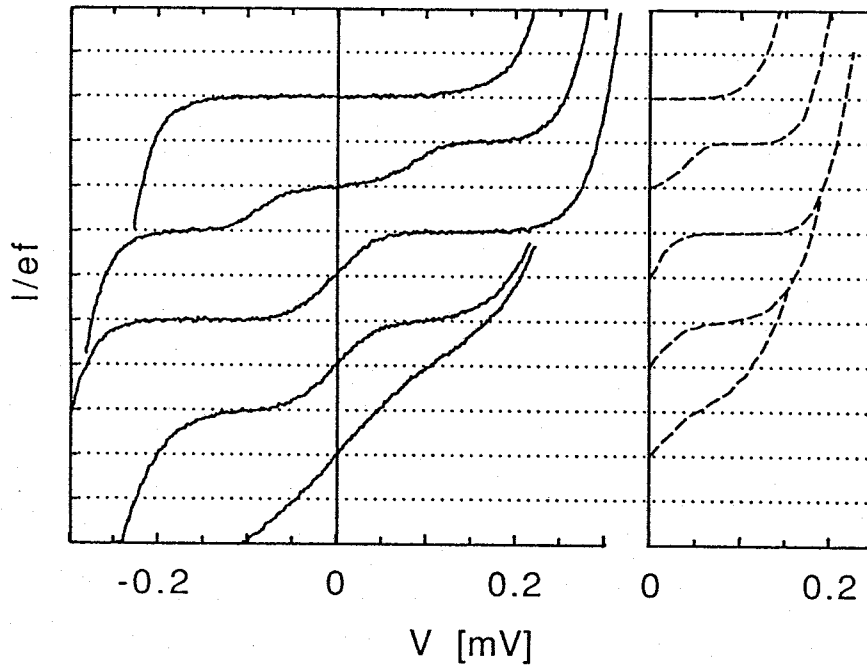


Fig. 3. Current-voltage characteristics at $f=5$ MHz for different levels of applied ac gate voltage. The dotted horizontal lines are at intervals $ef=0.80$ pA. The I-V curves have all been offset in x-direction by $15 \mu\text{V}$ to compensate for opamp voltage offset in the current measuring circuit, and individually in y-direction to display them more clearly. From top to bottom the calculated ac voltage amplitudes at the sample are 0, 0.60, 0.95, 1.50, and 1.89, expressed in units of $e/C=0.30$ mV. On the right, the corresponding simulated I-V curves are shown as dashed lines. For these calculations, 1 dB extra ac attenuation was assumed, and temperatures of 50 mK (upper 3 curves) and 75 mK (lower 2) were used.

regions could be found (around 0.15 mV) where the plateau was flat within the current noise. In those cases about 50 points were taken in the central parts of these regions to determine the average current with its standard deviation σ_m . Above 10 MHz, the current level at the inflexion point was taken in a similar way. The measured current step coincides with ef within experimental accuracy, which is around 0.3 %. We attribute the deviation of more than $3\sigma_m$ at 20 and 30 MHz to the difficulty of determining the inflexion point. To discuss the expected intrinsic accuracy of the current step height, we return to the example shown in Fig. 1. For an electron transfer in the circuit shown in Fig. 1 the first tunnel event of each half of the cycle ($\Delta E=-0.1e^2/C$) can occur in two junctions with a rate $\Gamma=(10RC)^{-1}$. For a square wave modulation this yields a probability to miss a cycle of about $\exp(-\Gamma/f)=\exp(-1/10fRC)$. For the device used in the experiments, $(RC)^{-1}\approx 5$ GHz, so at 5 MHz this probability is $\exp(-100)\approx 10^{-44}$, while at 50 MHz it is already about 10^{-5} .

f (MHz)	I_s (fA)	σ_m (fA)	$ef-I_s$ (fA)
4.012	635	2	8
6.011	967	2	-4
8.031	1287	2	0
10.040	1610	2	-1
12.029	1930	2	-3
14.028	2243	2	5
16.026	2560	3	7
18.063	2890	3	4
20.011	3196	3	10
30.036	4856	3	-44

Table 1. Comparison of the measured current plateau I_s with the relation $I_s=ef$. σ_m is the standard deviation of I_s .

Obviously, the required accuracy puts an upper limit to the allowed frequency. Next, to estimate the effect of thermal fluctuations, we compare the rate for unwanted tunneling events, $\tilde{\Gamma}$, with the one for favorable events, Γ . From eq. (2) we find that the ratio is of order $\exp(-\Delta E/k_B T)$. For an accuracy of e.g. 10^{-8} , it is necessary to have $\tilde{\Gamma}/\Gamma \approx 10^{-8}$, which combined with the requirement $\Gamma/f=10^3$ yields $\exp(-\Delta E/k_B T)=10^{-11}$, or $k_B T \approx \Delta E/25$. Since typically ΔE is on the order of $0.1e^2/C$, for the present device this corresponds to temperatures of about 15 mK. Comparable problems with unwanted transitions could arise from insufficient screening from noise and interference in the experiments. The simulations in Fig. 3 suggest that in the present experiment these disturbances seem to be described well by a temperature of not more than 50 mK, which is already close to the temperature requirement derived above. More careful screening is possible. These limitations are relaxed by the use of smaller junctions. For junctions of 0.1 fF with the same resistance, the requirement that $f < 10^{-3}/RC$ corresponds to $f < 30$ MHz and $k_B T < 0.1e^2/C$ to $T < 75$ mK.

In conclusion, we have fabricated a device producing a current clocked by an externally applied

high frequency voltage. Charge transfer is controlled at the level of single electrons. The theoretical limitations on the accuracy are very promising. The good agreement between the I-V curves and the theory shows that the dc and ac behavior of small capacitance normal metal tunnel junctions is well understood, and that device behavior can be reliably predicted.

This work was supported by the Dutch Foundation for Fundamental Research on Matter (FOM) and the Commissariat à l'Energie Atomique (CEA). We thank U. Geigenmüller, K. Likharev, M. Peters and G. Schön for valuable discussions, and P.F. Orfila for technical assistance.

REFERENCES

- (a) affiliation: Centre for Submicron Technology
1. D.V. Averin and K.K. Likharev, in "Quantum Effects in Small Disordered Systems", edited by B. Al'tshuler, P. Lee, and R. Webb (Elsevier, Amsterdam, to be published).
 2. T.A. Fulton and G.J. Dolan, *Phys. Rev. Lett.* **59**, 109 (1987).
 3. K.K. Likharev, N.S. Bakhvalov, G.S. Kazacha, and S.I. Serdyukova, *IEEE Trans. Magn.* **25**, 1436 (1989).
 4. P. Delsing, K.K. Likharev, L.S. Kuzmin, and T. Claeson, *Phys. Rev. Lett.* **63**, 1861 (1989).
 5. K.K. Likharev, *IBM J. Res. Develop.* **32**, 144 (1988).
 6. L.J. Geerligs, V.F. Anderegg, C.A. van der Jeugd, J. Romijn, and J.E. Mooij, *Europhys. Lett.* **10**, 1 (1989).
 7. G. Schön and A.D. Zaikin, Quantum Coherent Effects, Phase Transitions, and the Dissipative Dynamics of Ultra Small Tunnel Junctions, preprint submitted to Physics Reports, and references therein.

DEVIATION OF CURRENT QUANTIZATION DUE TO QUANTUM LEAKAGE

In the preceding paper we mentioned that quantum fluctuations of the charge, associated with a tunnel resistance not very large compared to h/e^2 , affect the applicability of orthodox theory for calculating the accuracy of the turnstile. In fact, quantum fluctuations decrease the accuracy of the quantization (to $I=ef$) of the current. In a comment to the preceding paper, Averin and Odintsov pointed this out and calculated a correction due to these fluctuations for a specific process: Inelastic macroscopic quantum tunneling of the electric charge (q-MQT, dealt with in the next chapter). This process opens the possibility for an electron which is trapped in a metastable position, to escape through virtual intermediate states of higher energy. For example, for the turnstile device this applies to the electron charge that is trapped on the central island during one half of the cycle.

If E_1 or E_2 is the increase in free energy after the first tunneling event in such an escape (in a 4-junction turnstile there are 2 junctions where this event can occur), and U the decrease after the second tunneling event, the rate of q-MQT is given by

$$\Gamma_{\text{MQT}} = \frac{hU}{(2\pi)^2 e^4 R_{t1} R_{t2}} \left[\left(1 + \frac{2E_1 E_2}{U(E_1 + E_2 + U)} \right) \ln \left(1 + \frac{U}{E_1} \right) \left(1 + \frac{U}{E_1} \right) - 2 \right] \quad (3)$$

Averin and Odintsov point out that for low bias voltage there is a leakage current in a direction opposite to the current flow of the turnstile. For higher voltage the current increases to a value higher than $I=ef$. At the cross-over region between negative and positive leakage current, at zero temperature the relation $I=ef$ would apply, but at finite temperature a positive leakage current due to thermally assisted macroscopic quantum tunneling arises.

We have performed calculations of the I-V curve (based on the algorithm that generates the simulations of the previous paper), including the possibility of macroscopic quantum tunneling through the left arm or right arm of the turnstile. These are based on the zero temperature rate eq. (3). There are at least two problems with the application of this equation. It diverges logarithmically at the Coulomb gap threshold voltage (where $E_1 \rightarrow 0$ or $E_2 \rightarrow 0$). Based on the measurements in the next chapter, we have limited this divergence to a maximum value of the logarithmic factor of 2. The q-MQT rate is in this way underestimated, which is not harmful because the divergence only occurs at bias conditions where q-MQT is actually a favorable process for the turnstile principle.

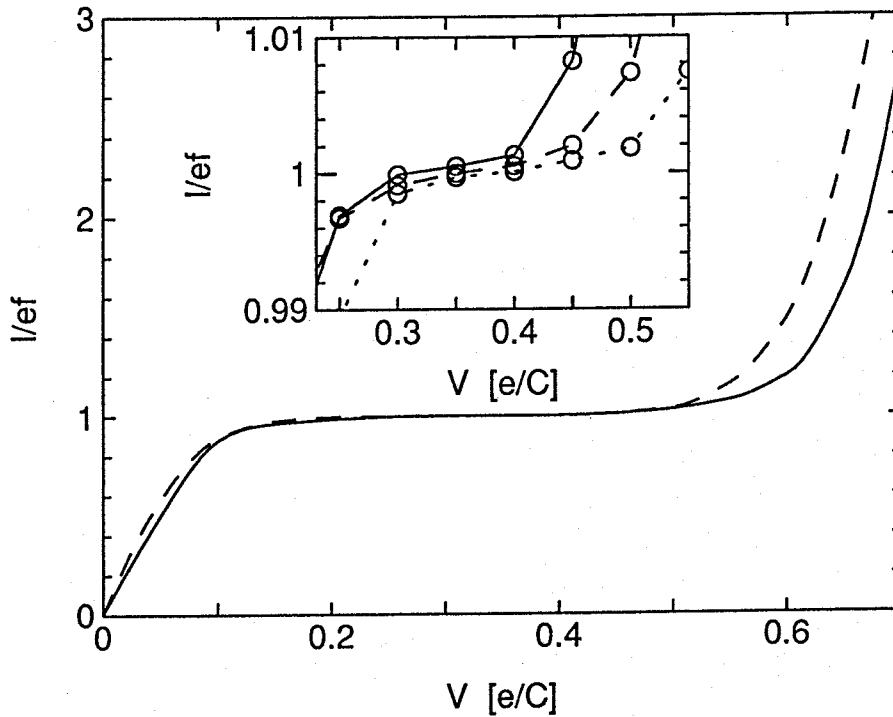


Fig. 4. Calculated I - V curves of a four-junction turnstile of the experimental parameters, at 60 mK without q -MQT (dashed curve) and at 50 mK with q -MQT (solid curve), at 5 MHz. The inset compares the q -MQT leakage at 5 (solid), 10 (dashed) and 20 MHz (dotted).

The second problem is that, although the zero-temperature fluctuations produce some rounding of the I - V curves, this rounding is much less than is experimentally observed (corresponding to about 60 mK, see the preceding paper). This indicates that thermal fluctuations, noise, or other yet unknown effects are important in the experiment. Since there are not yet simple equations for thermally assisted q -MQT available, as an approximation the calculations that we present are performed by summing the orthodox thermal rates at 50 mK and the q -MQT rates of eq. (3). These calculations show a small tilting and rounding of the plateaus, with a deviation from $I=ef$ of about 10^{-3} (Fig. 4). In Fig. 5 we compare a 6 MHz measurement with calculations. The experimental current noise is larger than the effect of q -MQT. However, the I - V_g curves of Fig. 6 show that the calculations reproduce an experimentally observed feature of quantum leakage, i.e. a significant leakage current in the absence of rf gate-modulation, which largely disappears when the gate is modulated. This means that the leakage in this device is worse for lower frequencies.

These preliminary calculations need to be elaborated before reliable statements with regard to the accuracy of turnstile devices can be made.

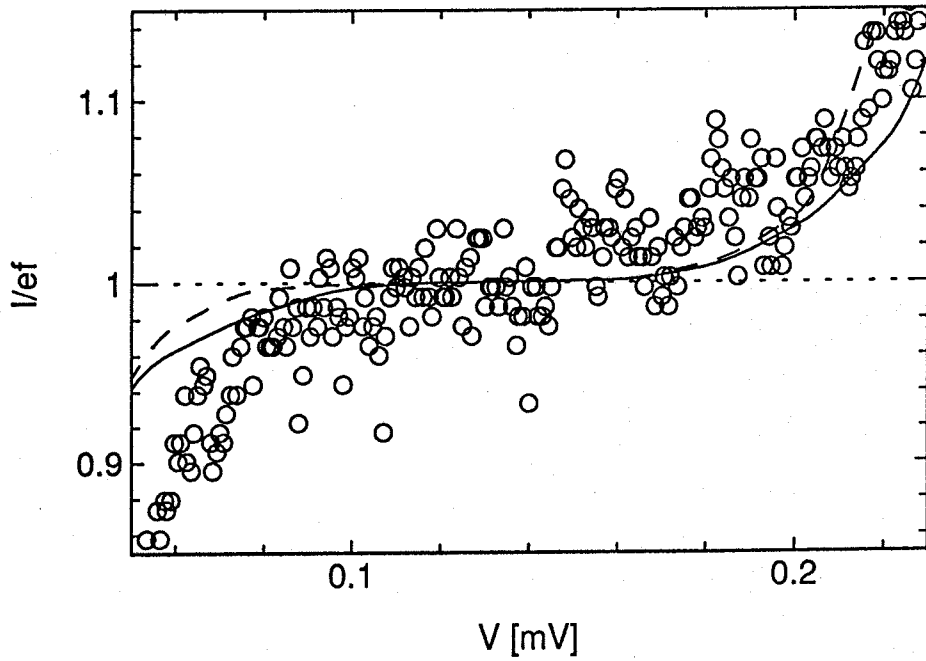


Fig. 5. Comparison of the experimental I - V curve at 6 MHz with a calculation (described in the text) including q -MQT.

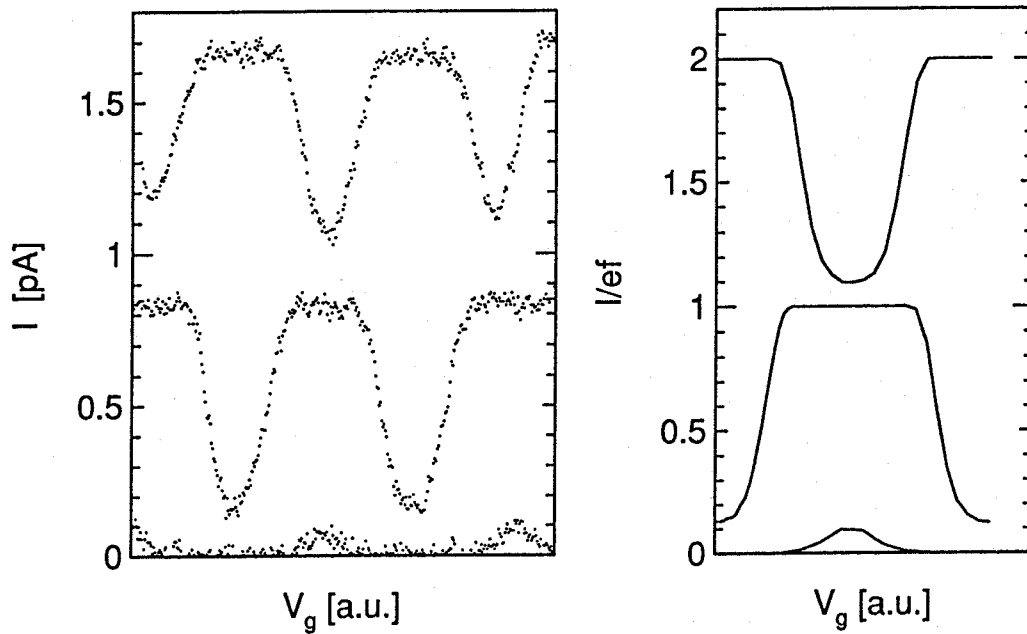


Fig. 6. Comparison of the experimental I - V_g curves without rf modulation and at (appr.) 5 MHz for different amplitudes (left) with calculations including q -MQT (right).

CHAPTER 5

OBSERVATION OF MACROSCOPIC QUANTUM TUNNELING OF THE ELECTRIC CHARGE

L.J. Geerligs, D.V. Averin,^(a) and J.E. Mooij

Department of Applied Physics, Delft University of Technology
Lorentzweg 1, 2628 CJ Delft, The Netherlands

ABSTRACT

The conductance of linear arrays of 2 and 3 normal-metal small tunnel junctions is studied, for bias voltages V below the Coulomb blockade threshold. At low temperature, we find evidence for macroscopic quantum tunneling of the electric charge (q-MQT) through the Coulomb energy barrier. For double junctions the tunneling rate scales as V^3 , and approximately as the product of the junction conductances, as predicted by the theory of inelastic q-MQT.

Quantum behavior of the macroscopic degrees of freedom of small tunnel junctions has recently attracted much attention.[1] Experimental investigations have been largely devoted to macroscopic quantum tunneling (MQT) of the Josephson phase difference φ , [2,3] that can take place in superconducting tunnel junctions with large quasiparticle conductance $R_T^{-1} \gg R_Q^{-1}$ ($R_Q \equiv h/4e^2 \approx 6.5 \text{ k}\Omega$). In such junctions φ behaves as an almost classical variable. In particular, for small bias current the phase can be trapped in a minimum of Josephson potential energy, resulting in a zero-voltage supercurrent. Quantum fluctuations of φ give rise to a nonvanishing probability of quantum tunneling through the Josephson potential barrier, and make the zero-voltage state metastable. This macroscopic quantum tunneling of φ (φ -MQT) has been convincingly demonstrated in several experiments.[3]

In the dual case of tunnel junctions with small conductance ($R_T^{-1} \ll R_Q^{-1}$) the electric charge q on the junction capacitance, conjugate to φ , evolves nearly classically.[1] At low temperature this results in Coulomb blockade of tunneling: for low bias voltage the tunnel current is suppressed, since tunneling would increase the Coulomb energy of the junction capacitance. However, small quantum fluctuations of the charge give rise to a nonvanishing probability of quantum tunneling through the Coulomb energy barrier, and thus make the zero-current Coulomb blockade state metastable. Only one electron (one Cooper pair for a superconducting junction) is transferred through the system in one act of this quantum tunneling. Nevertheless, it is an essentially macroscopic process, because the tunneling electron polarizes the junction electrodes in virtual states below the energy barrier, so that the Coulomb energy is given by usual macroscopic electrostatics. This implies that all free electrons of the junction electrodes do participate in the tunneling process. In this respect it is not the tunneling of a single electron but rather that of a macroscopic variable, the electric charge q of the junction. Apart from its fundamental importance, q -MQT has practical implications. Proper functioning of a number of 'single-electronic' devices [4] depends on the reliable trapping of an extra single electron charge between small tunnel junctions. The q -MQT process decreases the reliability of operation of these devices. For example, it is a source of possible inaccuracy of current quantization in the recently reported single-electron turnstile device.[5]

In this Letter we report for the first time on experimental observation of macroscopic quantum tunneling of the electric charge, in linear arrays of 2 and 3 normal metal junctions. In such systems an act of q -MQT consists of a finite number of consecutive tunneling events. In an array of two junctions an electron is transferred via one intermediate state, in which an extra electron or hole charges the central metal electrode between the two junctions. The Coulomb energy of this

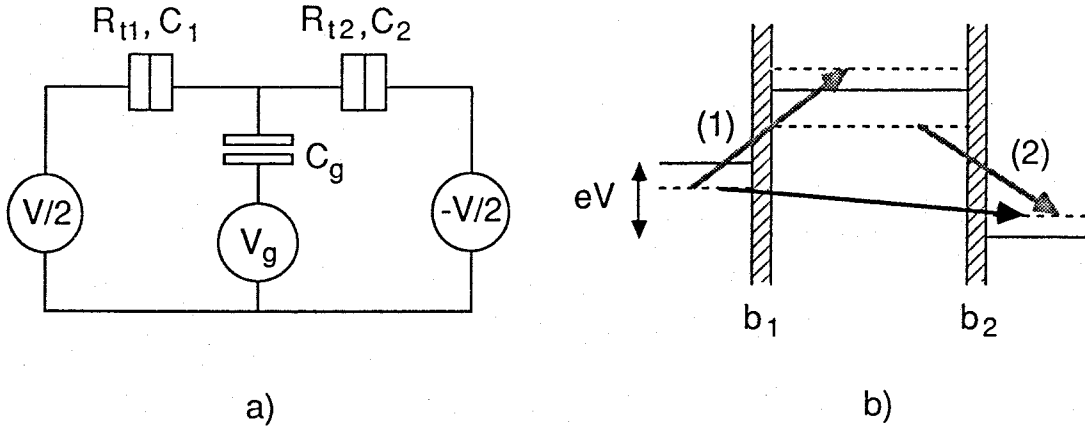


Fig. 1. (a) Equivalent circuit of a symmetrically biased two junction array, as used in the experiments. A square divided by a vertical line indicates a tunnel junction. (b) Macroscopic quantum tunneling of the charge occurs via occupation of a virtual intermediate state. An electron tunnels to an excited state in the central island (1). The resulting virtual state decays by a different electron tunneling across the second junction (2), leaving a hole and the excited electron, but decreasing the charging energy. b_1 and b_2 indicate the junction barriers, solid lines represent the Fermi levels in the electrodes.

intermediate state is equal to E_1 or E_2 if the first tunneling event occurs across the left or right junction, respectively:

$$E_1 = \frac{e}{C_\Sigma} [e/2 + Q_0 - V(C_2 + C_g/2)] \quad (1a)$$

$$E_2 = \frac{e}{C_\Sigma} [e/2 - Q_0 - V(C_1 + C_g/2)] \quad (1b)$$

where $C_\Sigma = C_1 + C_2 + C_g$, C_1 is the capacitance of the left junction, C_2 of the right one and C_g of the gate (Fig. 1a). Q_0 is the background charge of the central electrode which can be changed by the gate voltage V_g : $Q_0 = C_g V_g + \text{const}$. For bias voltage inside the Coulomb gap, $V < V_{th}$, the energy of the intermediate state is positive (this condition defines the threshold voltage V_{th}), and the thermally assisted classical consecutive tunneling is exponentially suppressed at low temperatures. However, even for $V < V_{th}$ there is a finite probability for an act of quantum tunneling with a virtual occupation of the central electrode.

For our metal junctions with relatively large electrodes, the main contribution to q-MQT is given by a process in which two different electrons tunnel through the two junctions. In this

inelastic process the q-MQT creates an electron-hole excitation on the central electrode (Fig. 1b).[6,7] In metal particles smaller than about 10 nm or semiconductor heterostructures, the energy level spacing in the central electrode need not be very small compared to the characteristic charging energy. In this case an 'elastic' contribution to q-MQT may become significant.[8,9]

The rate of q-MQT decreases with increasing tunnel resistance. It has been calculated in a perturbative approach, i.e. for $R_t \gg R_Q$. [6,7] For two junctions it is

$$\gamma_{\text{MQT}} = \frac{\hbar}{2\pi e^4 R_{t1} R_{t2}} \left\{ \left(1 + \frac{2}{eV} \frac{E_1 E_2}{E_1 + E_2 + eV} \right) \ln \left[\left(1 + \frac{eV}{E_1} \right) \left(1 + \frac{eV}{E_2} \right) \right] - 2 \right\} eV \quad (2)$$

and for a linear array of N junctions (with index i) at bias voltage low compared to V_{th} :

$$\gamma_{\text{MQT}} \propto V^{2N-1} \prod_{i=1}^N \frac{R_Q}{R_{ti}} \quad (3)$$

Eq. (2) is valid for $V < V_{\text{th}}$, except in the vicinity of the threshold voltage. As a result of the discreteness of charge transfer in an act of q-MQT, γ_{MQT} decreases only as a certain power of the relevant parameter, R_Q/R_t , that determines the strength of the quantum fluctuations of q . The rate of the quantum tunneling of a continuous variable, e.g. ϕ -MQT, or q-MQT in a single junction shunted by an ohmic conductance,[6] decreases exponentially.

We have studied q-MQT in four double junctions, with R_t between 41 and 347 k Ω . The junctions are made of overlapping aluminum strips, approximately 60 nm wide and 20 or 40 nm thick, and have an area of about (60 nm)². The resistance of the aluminum oxide barrier is controlled by varying the oxidation pressure. Inside an array, the junctions are about 1 μm apart. The metal electrodes between the junctions can be polarized (i.e. the background charge Q_0 can be controlled) by a gate electrode at 1.5 μm distance, with a coupling capacitance C_g of about 0.07 fF. The samples were thermally anchored to the mixing chamber of a dilution refrigerator. For all measurements low-pass filters were used that were also thermally anchored to the mixing chamber. However, we found no significant difference between filtering with RC-filters only, compared to more careful high-frequency filtering. A magnetic field of 2 Tesla was applied to bring the junctions in the normal state.

In Fig. 2 we show a typical I-V curve. The Coulomb gap is clearly visible, but even at the lowest temperatures (below 20 mK), the gap is rounded and there is significant current for voltages below V_{th} . The dashed line gives the asymptote to the I-V curve determined on a scale of a few mV. In the classical theory [5] this asymptote should intersect the zero current-axis at e/C_Σ ,

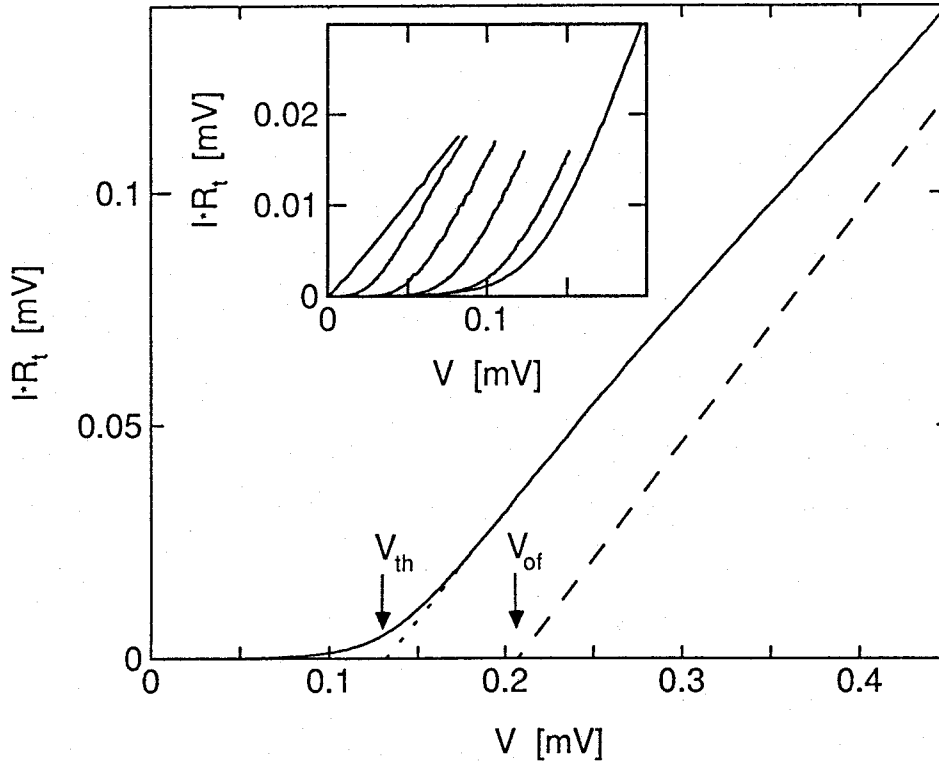


Fig. 2. I - V curves of a double junction with $R_t=78 \text{ k}\Omega$. The maximum Coulomb gap is obtained by adjusting V_g . The dashed line gives the asymptote to the I - V curve that is used to determine $R_\Sigma=2R_t$. V_{of} and V_{th} (see text) are indicated. The inset shows that the Coulomb gap can be continuously controlled with gate voltage (curves are given for, from right to left, $Q_0=0, 0.1e, 0.2e, 0.3e, 0.4e$ and $e/2$).

and have a slope $R_\Sigma=R_{t1}+R_{t2}$. The Coulomb blockade threshold voltage should also equal e/C_Σ , provided that it is maximized by adjusting Q_0 , [4] for instance with V_g . In Table 1 we give $R_t=R_\Sigma/2$ and C_Σ , the latter determined both from asymptote and threshold voltage, for all double junctions. The capacitances obtained from the high-voltage asymptote (e/V_{of}) are smaller by a factor of 1.5 than those obtained from V_{th} . Several reasons can account for this difference. First, the Coulomb gap could be partially suppressed by imperfect adjustment of the gate voltage, or by thermal and quantum fluctuations of the charge, leading to a smaller V_{th} , and thus larger capacitance e/V_{th} . Second, the I - V curve offset V_{of} at high voltages could be larger than the low-voltage offset, since additional channels of inelastic electron tunneling can become available with increasing voltage. [10] Another possible reason for decrease of the effective capacitance with increasing voltage is capacitance renormalization due to Coulomb blockade. At low voltages the capacitance is increased by $\delta C=(4/\pi)^2(R_Q/R_t)C$, [11] while at high voltages $\delta C \propto (V_{th}/V)^2 \rightarrow 0$.

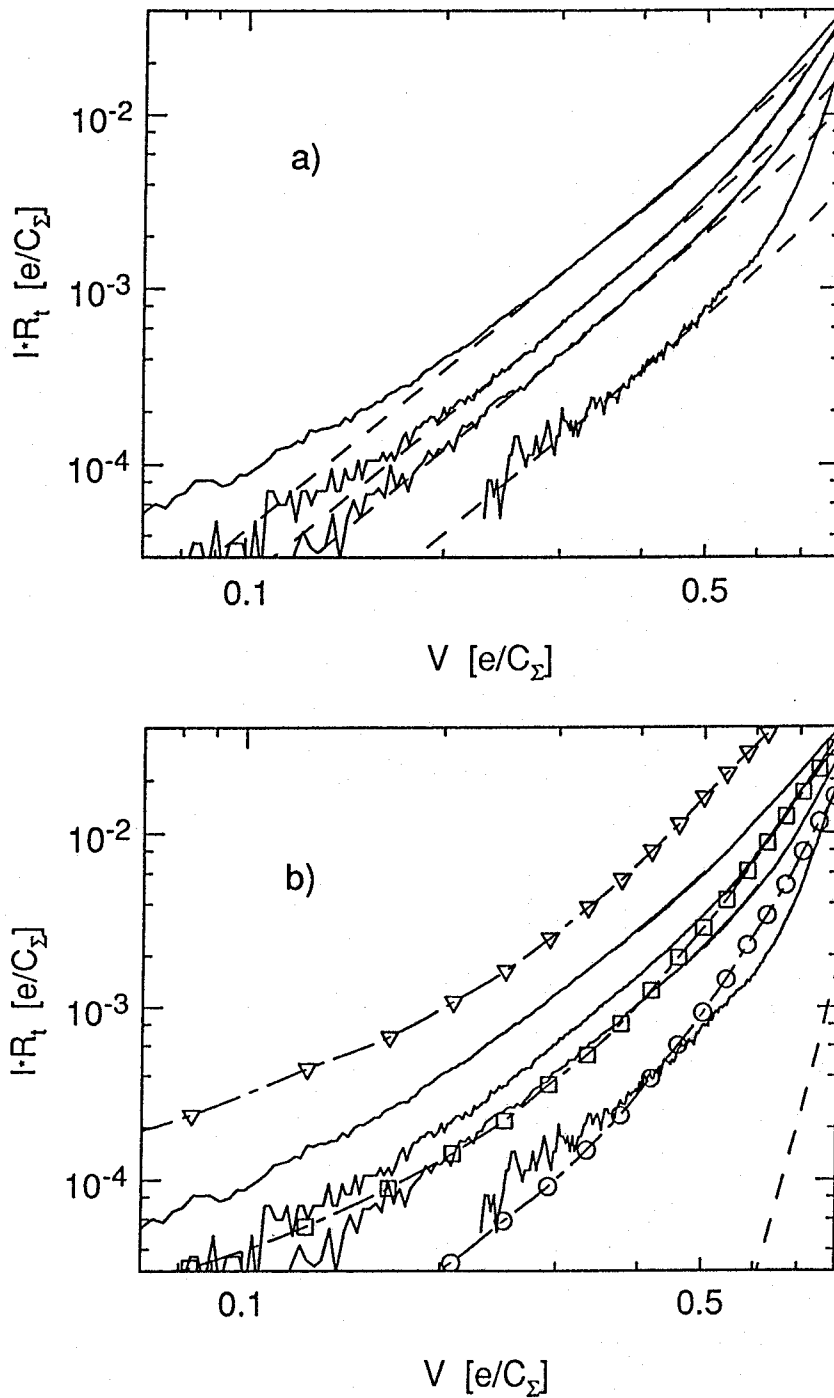


Fig. 3. Comparison of I-V curves with theory, for four double junctions. The measurements (solid curves) have been scaled with R_t and C_Σ , the latter being a fit parameter. The current increases with increasing R_t^{-1} , from top left to bottom right curve R_t equals 41, 78, 117 and 347 k Ω , and C_Σ equals 1.19, 0.95, 0.71 and 0.72 fF. (a) The dashed curves give the predictions from q-MQT (b) Comparison with predictions from thermally assisted tunneling. Dashed: $T=0.02e^2/C_\Sigma$ and $Q_0=0$. Dash-dotted: $T=0.04e^2/C_\Sigma$ and $Q_0=0$ (circles), 0.1e (squares) and 0.2e (triangles).

R_t (k Ω)	$C_{\Sigma}=e/V_{of}$ (fF)	$C_{\Sigma}=e/V_{th}$ (fF)	$C_{\Sigma, best fit}$ (fF)
41	0.92	1.38	1.19
78	0.77	1.21	0.95
117	0.63	0.88	0.71
347	0.68	0.91	0.72

Table 1. The parameters of the four double junctions.

The fact that the difference between the low-voltage and high-voltage capacitances is larger for junctions with lower R_t indicates that at least part of this difference can be attributed to the latter reason. We cannot quantitatively take into account all these factors, although it follows that the relevant capacitance for q-MQT should lie within the bounds set by V_{th} and V_{of} . For comparison with theory we will therefore use the capacitance as a fitting parameter.

In Fig. 3 we show the $\log(I)$ - $\log(V)$ curves for the four double junctions.[12] Classical tunneling current would increase exponentially with voltage. In contrast, the experimental $\log(I)$ - $\log(V)$ curves yield straight lines with a slope equal to 3, as expected for q-MQT (eq. 3), except for high or very low voltages. In Fig. 3a we compare the measured I-V curves with calculations for q-MQT from eq. (2), assuming both junctions to be equal. The measured current and voltage are scaled to $e/R_t C_{\Sigma}$ and e/C_{Σ} , respectively, making it possible to observe the effect of R_t on the q-MQT rate in one plot. All I-V curves can be very well fitted to theory in a broad voltage range inside the Coulomb gap, and the corresponding best-fit values of C_{Σ} lie (as they should) between the high-voltage and the low-voltage capacitances (Table 1). The smaller slope of the $\log(I)$ - $\log(V)$ curves at $V \rightarrow 0$ is probably caused by the fact that, if $eV \gg k_B T$ is no longer satisfied, crossover to a linear I-V curve occurs.[7,9] The larger slope for high voltages may be due to the crossover to thermally assisted charge transfer. In the regime where the classical tunneling rate becomes of order γ_{MQT} there will be more current than predicted from q-MQT. Inequality of the two junction capacitances or a not completely symmetric voltage bias would similarly increase the current at high voltages. We can not exclude that these effects play a role in the experiments.

The observed sub-Coulomb gap current could alternatively be explained by an effective sample temperature that is significantly higher than the mixing chamber temperature, e.g. because of noise and interference. Therefore in Fig. 3b we compare the same measurements with calculations for classical thermally assisted charge transfer, with the same scaling as in Fig. 3a. There is clearly

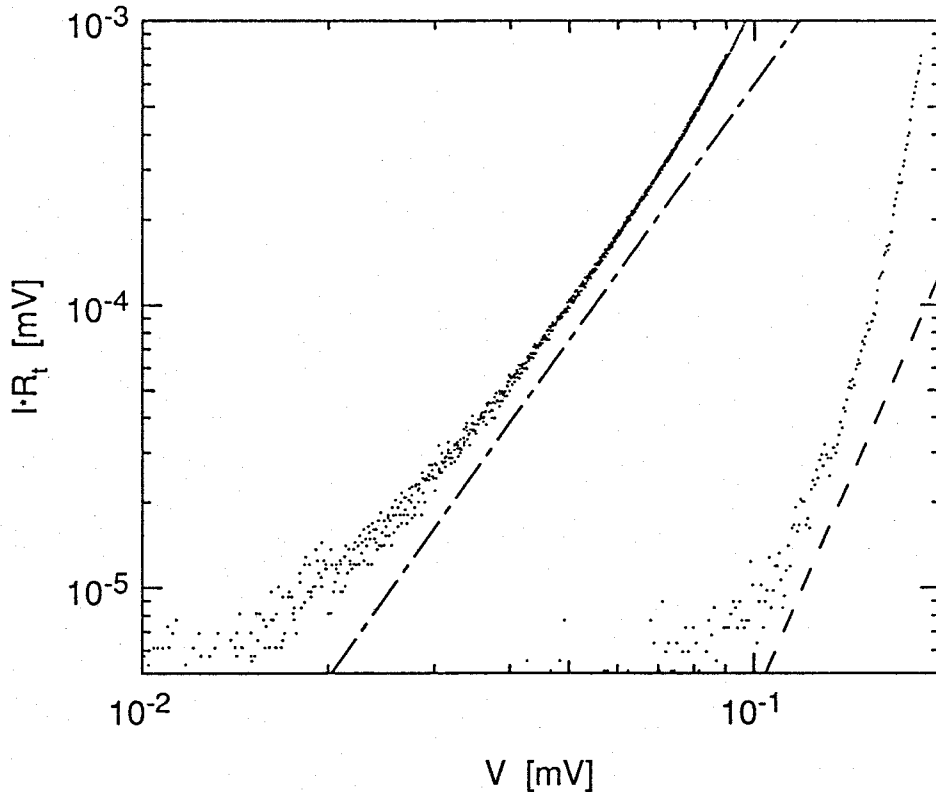


Fig. 4. I - V curves for a double junction with $R_t=78 \text{ k}\Omega$ and three junctions in series with $R_t=84 \text{ k}\Omega$. As a guide to the eye lines for which $I \propto V^5$ (dashed) and $I \propto V^3$ (dash-dotted) have been drawn, representing the q -MQT prediction for the slope of the $\log(I)$ - $\log(V)$ curves.

not a convincing agreement. To obtain rough similarity of calculations to measurements, it is necessary to assume a misadjustment of the gate voltage corresponding to a Q_0 of as much as $0.2e$, with in addition systematically more error for the lower R_t samples. Also, a high temperature of about 100 mK must be used to obtain a calculated curve that is at least in the range of the measurements. In previous experiments on similar devices [e.g. Ref. 5], using the same low pass filters, we have found that the noise temperature of our devices is not larger than about 50 mK.

Comparison of the $\log(I)$ - $\log(V)$ curves of a double junction and a 3-junction array of almost equal R_t , in Fig. 4, also provides support for q -MQT. The prediction from eq. 3 is that for a double junction $I \propto V^3$ whereas for 3 junctions $I \propto V^5$. As a guide to the eye, two lines give the expected slopes, which are in fair agreement with the results. Because of the higher exponent of I , the voltage range in which the current is not either unobservably small or for a significant amount due to thermally assisted transfer, is smaller for the longer array.

We conclude that for the first time we observed macroscopic quantum tunneling of the electric charge in linear arrays of two small tunnel junctions. As a result of this tunneling a finite current flows through the array even in the Coulomb blockade regime. The current is in quantitative agreement with theoretical predictions.

We gratefully acknowledge discussions with V. Anderegg, M. Devoret, D. Esteve, K. Likharev and C. Urbina. This work was supported by the Dutch Foundation for Fundamental Research on Matter (FOM). Part of the lithography was performed at the Delft Institute of Microelectronics and Submicron Technology.

REFERENCES

- (a) Permanent address: Department of Physics, Moscow State University
Moscow 119899 GSP, U.S.S.R.
1. See e.g. the review by G. Schön and A.D. Zaikin, to be published in *Physics Reports*.
 2. A.O. Caldeira and A.J. Leggett, *Ann. Phys.* **149**, 374 (1983).
 3. D.B. Schwartz, B. Shen, C.N. Archie and J.E. Lukens, *Phys. Rev. Lett.* **55**, 1547 (1985); J.M. Martinis, M.H. Devoret and J. Clarke, *Phys. Rev. B* **35**, 4682 (1987), and references therein.
 4. K.K. Likharev, *IBM J. Res. Develop.* **32**, 144 (1988).
 5. L.J. Geerligs, V.F. Anderegg, P.A.M. Holweg, J.E. Mooij, H. Pothier, D. Esteve, C. Urbina and M.H. Devoret, *Phys. Rev. Lett.* **64**, 2691 (1990).
 6. D.V. Averin and A.A. Odintsov, *Phys. Lett. A* **140**, 251 (1989).
 7. G. Schön and D.V. Averin, to be published in the proceedings of the NATO ASI on Coherence in Mesoscopic Systems, Les Arcs, France, April 1990 (Plenum, New York).
 8. L.I. Glazman and K.A. Matveev, *Pis'ma Zh. Eksp. Teor. Fiz.* **51**, 425 (1990) [*JETP Lett.*, to be published].
 9. D.V. Averin and Yu.V. Nazarov, Virtual electron diffusion at quantum tunneling of the electric charge, submitted to *Phys. Rev. Lett.*
 10. Yu.V. Nazarov, *Zh. Eksp. Teor. Fiz.* **95**, 975 (1989) [*Sov. Phys. JETP* **68**, 561 (1989)].
 11. E. Simánek, *J. Phys. Soc. Jap.* **54**, 2397 (1985).
 12. The measurements have been compensated for offset voltages by shifting the intersection of the $Q_0=0$ and $Q_0=e/2$ curves to the origin.

CHAPTER 6

INFLUENCE OF DISSIPATION ON THE COULOMB BLOCKADE IN SMALL TUNNEL JUNCTIONS

L.J. Geerligs, V.F. Anderegg, C.A. van der Jeugd, J. Romijn,^(a) and J.E. Mooij

Department of Applied Physics, Delft University of Technology

P.O. Box 5046, 2600 GA Delft, The Netherlands

ABSTRACT

Effects of charging energy were studied in small capacitance aluminum tunnel junctions in the normal state, with tunnel resistance R_t between 0.2 and 80 k Ω . Single junctions, chains and 2-dimensional arrays were fabricated. This allowed investigation of the influence of lead capacitance. For $R_t > 1$ k Ω the voltage offset ('Coulomb gap') determined from the I-V curve at high current is consistent with the capacitance calculated from junction area only. For single junctions with R_t near or below 10 k Ω at low current the charging effects are strongly suppressed. Results of chains with arbitrary R_t show the suppression of charging effects by dissipation. The $R(T)$ curves are in good agreement with theory and geometrical capacitance.

Coulomb blockade of single electron tunneling [1-3] becomes apparent in tunnel junctions of capacitance C when the temperature is near or below $E_C \equiv e^2/2C$. The energy change connected with transfer of a single electron then causes time coherence of the tunneling events. The small capacitance results in a voltage offset of magnitude $e/2C$ in the tunneling current-voltage characteristic, the so-called Coulomb gap. For single junctions, it is not trivial that a Coulomb gap can be seen at all, since the leads to the junction will add a large parasitic capacitance to the junction's geometrical capacitance. So far, only a few observations of the Coulomb gap in a single junction have been reported [4-6]. In Ref. 4 and 5 it is not clear whether impurities caused the experiments to actually look at more junctions in series. For junctions in series circuits, the inner junctions will be decoupled from the parasitic capacitance, so here the Coulomb gap should be better visible. Although various measurements on series circuits are reported in the literature [1,6-12], only Ref. 8 and 12 provide measurements on well-defined planar junctions, and indeed find agreement between geometrical capacitance and Coulomb gap. In this letter we present a comparison between single planar junctions, double junctions, and 1-D and 2-D arrays. We find a significant difference between the Coulomb gap in single junctions and in arrays, which is probably due to parasitic capacitance. The effect from parasitic capacitance turns out to vanish for high currents, and appears to be also affected by the junction resistance.

We have also investigated the influence of dissipation, which is controlled by R_t , the tunneling resistance in the absence of charging effects [13-17]. For a large resistance, $R_t \gg h/4e^2$, the charge on the junction can be treated classically, and the I-V curve is obtained from a perturbation analysis [3]. For low R_t , quantum fluctuations of the charge on the junction electrodes suppress the Coulomb blockade. The theoretical approach by Ambegaokar *et al.* [13] is applicable to both normal and superconducting tunnel junctions. It has been widely used in the extensive theoretical literature on the problem of dissipation in a macroscopic quantum system of the last few years. However, there has been very little direct experimental support for the results obtained. Two theoretical papers have been published which calculate properties of small normal tunnel junctions for not very low dissipation. Brown and Šimánek [16] use results of Ref. 15 and linear response theory to calculate the resistance versus temperature of a tunnel junction with arbitrary R_t . Odintsov [17] uses a formal analogy with the polaron problem to calculate I-V curves for high dissipation. We find detailed quantitative agreement with the predictions of Brown and Šimánek.

Patterning of the junctions is by electron beam lithography. The junctions are produced by shadow evaporation of the aluminum electrodes, with thermal oxidation of the first electrode in about 0.05 mbar O_2 gas to form the barrier. The electrode thicknesses are typically 30 and 60 nm,

sample	R_t (k Ω)	nr. junctions	area (μm^2)	C_p (fF)	C_{I-V} (fF)	$C_{R(T)}$ (fF)
A2	82	2	0.01 and 0.1	0.9	0.8	1.1
A3	51	3	0.01	0.9	0.9	-
B1	10.7	1	0.01	0.9	1.3	-
B2	11.8	2	0.01 and 0.1	0.9	0.9	-
B3	7.1	3	0.01	0.9	1.5	0.8
C	5.4	5	0.01	0.9	1.5	1.0
D	4.7	1	0.02	1.8	4.5	-
E	2.4	1	0.06	5.4	12.7	-
F1	1.3	10	0.02	2.0	1.8	0.8
F2	0.52	10	0.04	3.6	9.7	2.3
F3	0.24	10	0.06	5.6	37	3.7
G	129	190 x 60	0.04	3.6	2.3	-
H	15.3	190 x 60	0.01	0.9	1.0	-
I1	14.1	190 x 60	0.01	0.9	1.1	0.7
I2	8.0	190 x 60	0.02	1.8	2.8	-
J	9.7	190 x 60	0.01	0.9	1.2	-

Table 1. Sample parameters and measured capacitances. Names that start with the same character are for devices evaporated on the same substrate. C_p is the geometrical capacitance calculated from the junction area, C_{I-V} is the capacitance determined from the voltage offset in the I-V curve, and $C_{R(T)}$ is the capacitance determined from a fit to the $R(T)$ curve. Nr. junctions indicates single junctions (1), linear series arrays (single number > 1) and 2-D arrays ($L \times W$).

so that with a junction area starting at 100 nm x 100 nm the junction is a reasonable approximation of a parallel plate capacitor. For the parasitic capacitance to be as large as the junction capacitance we estimate that the connecting pattern within a radius of at least 10 μm should contribute. Superconductivity of the aluminum is suppressed by applying a magnetic field of 2 T. The Coulomb gap is also visible in zero field above T_c . The high quality of the tunnel barrier is manifested in the exponential temperature dependence of the subgap resistance in the superconducting state.

If we determine the asymptote of the I-V curve at currents around 1 μA we always roughly find the voltage offset expected from the geometrical capacitance, i.e. $C_p \equiv \epsilon A/t$, where A is the junction area and t the barrier thickness. In this way we have determined the junction capacitance for around 15 samples. Details are given in Table 1. For chains and arrays we have divided the offset by the number of junctions in series. For $R_t > 1 \text{ k}\Omega$ we find a capacitance per junction of around 1.1 fF per 0.01 μm^2 with a spread of about a factor two. This capacitance is in good agreement with the junction area for a parallel plate capacitor with barrier thickness and dielectric constant given by the expected ratio $t/\epsilon_T = 1 \text{ \AA}$. For low R_t the junctions are heated (see below), making high currents necessary to see the full voltage offset, which in turn heat the junction more. For $R_t < 1 \text{ k}\Omega$ this makes determination of capacitance from the I-V curve impossible.

In Fig. 1 we have plotted the measured I-V characteristics for two similar sets of samples, A and B, at low temperature. They contain the same circuits with R_t for 0.01 μm^2 junctions about 100 and 10 $\text{k}\Omega$ on samples A and B, respectively. Shown are the I-V curves of three 0.01 μm^2 area junctions in series (A3 and B3), and of a 0.01 μm^2 junction in series with a 0.1 μm^2 area junction (A2 and B2). The large junction in the latter configuration was included for experiments in the superconducting state. In addition the I-V curve for a single 0.01 μm^2 junction was recorded for the $R_t = 10 \text{ k}\Omega$ sample (B1). This figure shows two separate effects.

Firstly, there is a significant difference between the low R_t single junction B1 and chain B3. In the single junction the Coulomb gap is clearly suppressed. This effect was also observed in other samples. For the double junction B2, the Coulomb gap is somewhat better developed but still suppressed. The difference, as observed between B2 and B3, is much less in the comparable high R_t samples A2 and A3. In Fig. 2 the I-V curves up to high current are given for A2 and B1. Even for the low resistance single junction B1, a Coulomb gap is visible at high current. The contrast with the high resistance sample A2 is obvious. It is the capacitance determined from this high current gap that is given in Table 1.

The second effect in Fig. 1 is the difference in I-V curves of the chains, A3 and B3. For low R_t

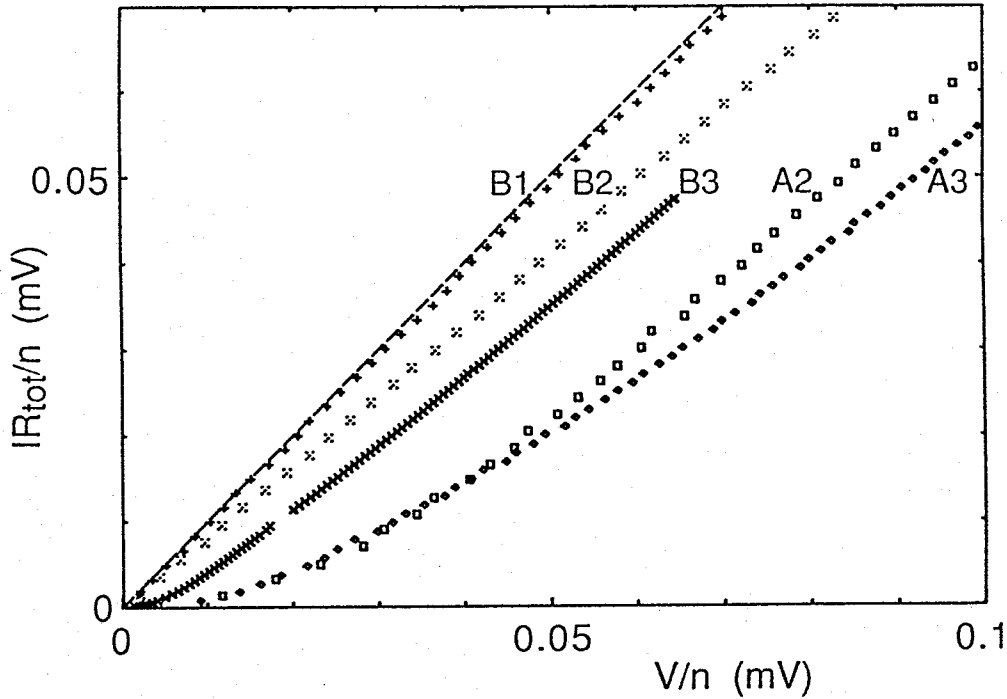


Fig. 1. I-V curves at about 10 mK of samples A and B, both with a series circuit of three $0.01 \mu\text{m}^2$ junctions (A3 and B3) and a single $0.01 \mu\text{m}^2$ junction in series with a $0.1 \mu\text{m}^2$ junction (A2 and B2). The R_t of the $0.01 \mu\text{m}^2$ junctions is roughly $80 \text{ k}\Omega$ for A, and $10 \text{ k}\Omega$ for B (see Table 1 for more details). The voltage axis is scaled to the voltage over one junction, the current axis in such a way (IR_{tot}/n) that a linear resistance yields a unity slope straight line (dashed line). R_{tot} is the total R_t of a device, n (number of junctions) is taken 1 or 3 for the two kinds of devices.

the Coulomb gap is suppressed, roughly as if the temperature were increased. This suppression of the charging effects for low R_t is also visible in the linear response of the junctions (Fig. 3).

In Fig. 3 we show the measurements (solid curves) of resistance versus temperature at low current, typically $\leq 0.1 \text{ nA}$, for chains of 5 or 10 junctions of various R_t and for the small high R_t junction (A2) of Fig. 1. Also shown (dashed) are the $R(T)$ curves calculated for a single junction as prescribed by Brown and Šimánek [16]. For this calculation only R_t and C need to be known, parameters that can be taken from the I-V measurements. However, to get an acceptable fit in Fig. 3 the capacitance is used as a fit parameter. For the highest resistance samples A2 and C this fitted capacitance is only 35 % different from the one determined from the Coulomb gap. For the lower R_t chains there is a deviation up to a factor 2.5 from the estimated geometrical capacitance. However, for these samples we do not know the area very accurately.

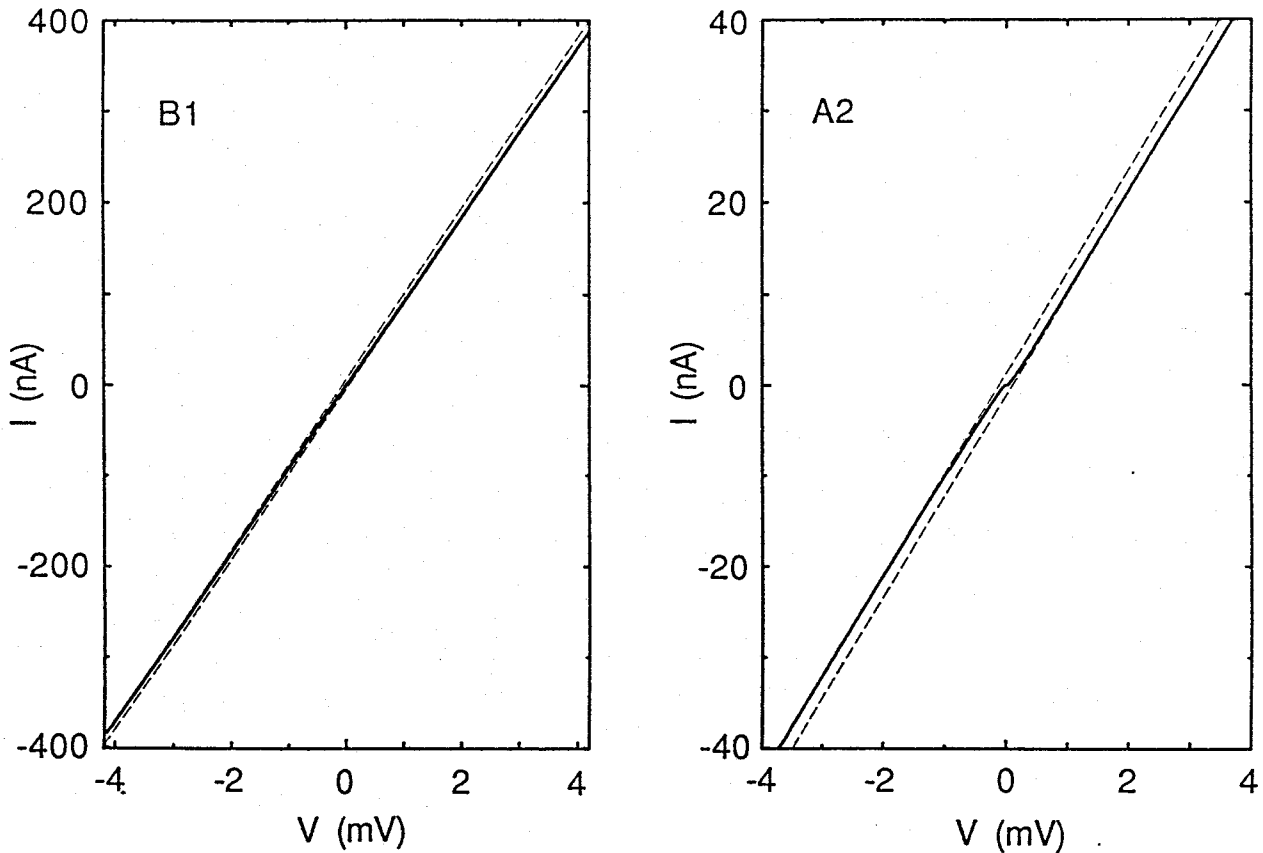


Fig. 2. I-V curves at about 10 mK showing the Coulomb gap for sample A2 and B1. At low currents the Coulomb gap is suppressed in the single low resistance junction B1, in contrast to the sample A2 (a small high resistance junction in series with a large junction).

For the interpretation of the results on chains, and the high R_t sample A2 we may apparently neglect parasitic capacitance. For a chain without electrode self-charging effects Geigenmüller and Schön showed that we can also use single junction calculations [18]. Likharev *et al.* have recently pointed out that if there is significant self-charging capacitance, solitons should be introduced in the description of the chains [19]. However, for our junctions with capacitance to ground $C_0 \approx 2 \cdot 10^{-17}$ F the length of the solitons $\sqrt{C/C_0}$ is equal to or larger than the chains and we expect the single junction theories to be applicable. We note that the $R(T)$ curves are in good quantitative agreement with the results of Brown and Šimánek [16]. This supports the present approach in treating dissipation [13], as well as the variational approximation made in Ref. 16. Comparison of the measured I-V curves with the calculations of Odintsov [17] is more complicated. Due to the heating effects at higher current levels mentioned before, the voltage is suppressed from the

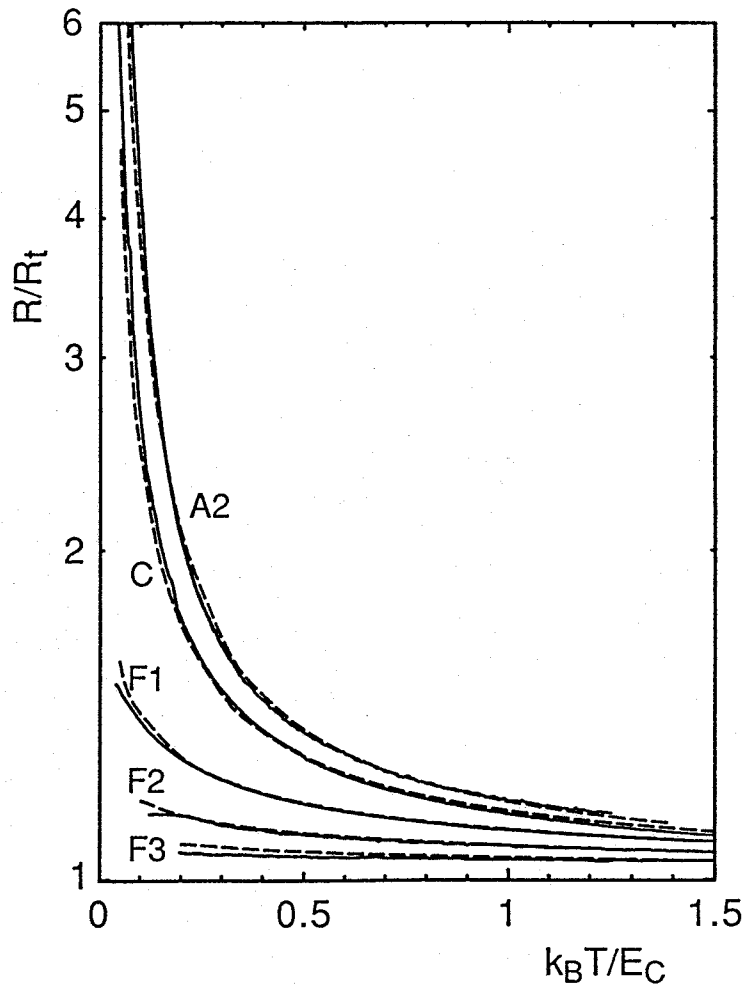


Fig. 3. Resistance as a function of temperature (solid lines) for several samples. Dashed lines are fits to theory of Brown and Šimánek [16] as described in the text. A2: $R_t=82 \text{ k}\Omega$ junction from Fig. 1. C: chain of 5 junctions with $R_t=5.4 \text{ k}\Omega$. F1-F3: chains of 10 junctions with $R_t=1.3, 0.52$ and $0.24 \text{ k}\Omega$, respectively.

expected value at substrate temperature to the value for a higher temperature. Relevant current and voltage magnitudes are of order $I_0 \equiv e/R_t C$ and $V_0 \equiv e/C$. So, the heating will be stronger for lower R_t . In addition non-equilibrium distributions of the electrons may be significant. We will not treat this problem here.

In order to explain the strong suppression of charging effects in the low R_t single junctions, the relevant capacitance for the Coulomb blockade must receive more consideration than it has been given so far. It has been suggested that the capacitance determining the Coulomb gap results from an area within a distance $c\tau$ of the tunneling site, where τ is the traversal time, $\tau \approx 10^{-15} \text{ s}$, and c is the propagation velocity of the electric field [20,4]. This distance amounts to roughly 100 nm, and

would therefore yield no difference between the Coulomb gap in arrays and single junctions. For tunnel junctions of dimensions larger than 100 nm, it would also predict a smaller effective capacitance than the geometrical one, in contradiction with Ref. 6 and 8, and our present results. A similar 'horizon' argument, where τ is taken to be the time between tunneling events, e.g. 10^{-13} s for $I=1.6 \mu\text{A}$, is in better agreement with our measurements on low R_t single junctions. It explains the necessity of a high current (of the order of μA 's) to see the Coulomb gap belonging to the geometrical capacitance. For high R_t junctions, however, comparing the results for samples A2 and B2, our measurements still suggest the concept of a very small area for the capacitance also at low current. We think this importance of R_t is a result of the higher probability of charge fluctuations connected with a low R_t . If for low R_t an electron can tunnel several times back and forth before it makes a real contribution to the dc current, charge redistributions can cover an area much larger than the tunnel junction, and thus increase the observed capacitance. The mean time between tunneling events e/I will be an upper limit of the time available for charge redistribution. The additional electron transitions can follow from several causes. They might e.g. be tunneling events to virtual states or a result of electron reflections against the electrode surface. In view of the latter mechanism note that at the experimental temperatures an electron that has tunneled will keep its excess energy for a long time. It will therefore have a relatively high tunneling probability if it reflects back to the tunnel barrier.

Recently, Nazarov [21] has evaluated another process which lengthens the relevant time scale. From the uncertainty principle he asserts that the electron after tunneling uses a probe time $\geq \hbar/eV$ to determine the relevant parameters like energy difference, capacitance and tunnel rate. Here, as far as we know, R_t is not important. This theory is compared more quantitatively with experiments by Delsing *et al.* [22].

We conclude that the behaviour of well-defined planar tunnel junctions can be described by geometrical capacitance and the quantum mechanical treatment of dissipation. We have only found a clear deviation of this rule for single junctions of low resistance, in which case the time between tunneling events may be determining the area that contributes to the capacitance. The effect of dissipation on quantum charge fluctuations is especially clearly observed in the linear response measurements on arrays.

We are indebted to U. Geigenmüller, G. Schön and K. Likharev for very valuable discussions. This work was supported by the Dutch Foundation for Fundamental Research on Matter (FOM).

REFERENCES

- (a) affiliation: Centre for Submicron Technology.
1. I. Giaever, and H.R. Zeller, *Phys. Rev. Lett.* **20**, 1504 (1968).
 2. E. Ben-Jacob, and Y. Gefen, *Physics Lett. A* **108**, 289 (1985).
 3. D.V. Averin and K.K. Likharev, *J. Low Temp. Phys.* **62**, 345 (1986).
 4. P.J.M van Bentum, H. van Kampen, L.E.C. van de Leemput, and P.A.A. Teunissen, *Phys. Rev. Lett.* **60**, 369 (1988).
 5. L.S. Kuzmin, and M.V. Safronov, *Pis'ma Zh. Eksp. Teor. Fiz.* **48**, 250 (1988) [*JETP Lett.* **48**, 272 (1988)].
 6. M. Iansiti, M. Tinkham, A.T. Johnson, W.F. Smith, and C.J. Lobb, *Phys. Rev. B* **39**, 6465 (1989).
 7. J. Lambe, and R.C. Jaklevic, *Phys. Rev. Lett.* **22**, 1371 (1969).
 8. T.A. Fulton and G.J. Dolan, *Phys. Rev. Lett.* **59**, 109 (1987).
 9. L.S. Kuzmin, and K.K. Likharev, *Pis'ma Zh. Eksp. Teor. Fiz.* **45**, 289 (1987) [*JETP Lett.* **45**, 495 (1987)].
 10. J.B. Barner, and S.T. Ruggiero, *Phys. Rev. Lett.* **59**, 807 (1987).
 11. P.J.M. van Bentum, R.T.M. Smokers, and H. van Kempen, *Phys. Rev. Lett.* **60**, 2543 (1988).
 12. L.J. Geerligs, and J.E. Mooij, *Physica B* **152**, 212 (1988).
 13. V. Ambegaokar, U. Eckern, and G. Schön, *Phys. Rev. Lett.* **48**, 1745 (1982).
 14. T.L. Ho, *Phys. Rev. Lett.* **51**, 2060 (1983).
 15. E. Ben-Jacob, E. Mottola and G. Schön, *Phys. Rev. Lett.* **51**, 2064 (1983).
 16. R. Brown and E. Šimánek, *Phys. Rev. B* **34**, 2957 (1986). In the transformation from eq. (16) to eq. (17) there is a numerical error. This has significant consequences if eq. (17) is used for quantitative purposes. We thank U. Geigenmüller for making us aware of it.
 17. A.A. Odintsov, *Zh. Eksp. Teor. Fiz.* **94**, 312 (1988) [*Sov. Phys. JETP* **67**, 1265 (1988)].
 18. U. Geigenmüller, and G. Schön, *Physica B* **152**, 186 (1988).
 19. K.K. Likharev, N.S. Bakhvalov, G.S. Kazacha, and S.I. Serdyukova, *IEEE Trans. Magn.* **25**, 1436 (1989).
 20. M. Büttiker and R. Landauer, *IBM J. of Res. and Develop.* **30**, 451 (1986).
 21. Yu. V. Nazarov, *Zh. Eksp. Teor. Fiz.* **95**, 975 (1989) [*Sov. Phys. JETP*, to be published].
 22. P. Delsing, K.K. Likharev, L.S. Kuzmin, T. Claeson, *Phys. Rev. Lett.* **63**, 1180 (1989).

CHAPTER 7

SINGLE COOPER-PAIR TUNNELING IN SMALL CAPACITANCE JUNCTIONS

L.J. Geerligs, V.F. Anderegg, J. Romijn,^(a) and J.E. Mooij

Department of Applied Physics, Delft University of Technology

P.O. Box 5046, 2600 GA Delft, The Netherlands

ABSTRACT

We present observations of charging effects for Cooper pairs in short linear arrays of small capacitance Josephson junctions. Current-voltage characteristics show a Coulomb gap for Cooper pair tunneling when the charging energy exceeds the Josephson coupling energy. In a double junction a zero-voltage current is observed that is modulated by a gate voltage applied to the metal island between the junctions. For longer arrays a crossover from Coulomb blockade of Cooper pair tunneling to a supercurrent is observed when the ratio of Josephson coupling to charging energy is increased.

In a tunnel junction with superconducting electrodes, a tunneling matrix element of magnitude $E_J/2$ couples states differing in junction charge by a Cooper pair.[1] The Josephson coupling energy E_J is determined by the junction resistance R_n and the BCS gap Δ of the superconducting metal: $E_J = \hbar\Delta/8e^2R_n$. For a junction of large capacitance, at zero bias voltage states differing by a large number of Cooper pairs are nearly degenerate in energy. Therefore, there is a large uncertainty in the charge on the junction. The eigenstates of the junctions are described by the phase difference ϕ of the superconducting electrodes,[2] conjugate to the charge of the junction. However, when the junction capacitance is reduced to a value where the typical energy of charging by a single Cooper pair becomes of order E_J the degeneracy of charge states is lifted, even for states differing by only one Cooper pair. The junction state is then well described by the charge, and single Cooper pair tunneling is an accurate concept to describe the conduction. Conventionally for normal metal tunnel junctions, the charging energy is expressed in units $E_C = e^2/2C$. Recently, sub-micron fabrication techniques have progressed to a level where junctions can be fabricated that have $E_C \gtrsim E_J$. This opens the possibility to investigate the tunneling of individual Cooper pairs, and thus study basic theory of Josephson junctions.

For normal metal tunnel junctions, a description in terms of the junction charge is allowed provided that R_n is larger than about \hbar/e^2 . In linear arrays of normal junctions with small capacitance the discreteness of charge transfer appears in several charging effects.[3,4] Firstly, the current-voltage (I-V) characteristic shows a threshold voltage for conduction, the Coulomb gap, with a magnitude $(n-1)e/2C$ for an array of n junctions. Secondly, by capacitively applying a gate voltage V_g to the metal island (with capacitance C_g) between two junctions, the I-V curve can be changed. This change has a periodicity e in the 'gate charge' $C_g V_g$ induced on the island, reflecting the equivalence of island charges $(C_g V_g - ne)$ that differ by an integer times e . Most reported experiments on junctions with superconducting electrodes also only show single electron effects, because of a very small ratio E_J/E_C .

Few experimental results have been published where interaction of charging effects with Josephson coupling was notable (E_J of order E_C). Iansiti et al. [5] published experiments on small junctions which were interpreted with theory based on macroscopic quantum phenomena [6] for a small Josephson junction, i.e. a description in ϕ -space. Fulton et al. [7] published experiments on a double superconducting junction and pointed out some aspects of charging effects for Cooper pair tunneling to interpret their results. Their device is quite similar to ours. However, they did not report on the low voltage region that we focus on in this Letter. Likharev and Zorin [8] and Averin and Likharev [4] have theoretically treated aspects of the double superconducting junction that are

relevant for the present work. In this Letter we present current-voltage (I-V) characteristics of small linear arrays of aluminum tunnel junctions. For low E_J , these show direct charging effects for Cooper pairs, for increasing E_J a crossover to more classical behaviour occurs.

Fig. 1 shows I-V curves of a double Al-AlO_x-Al junction with $R_n=58$ k Ω , and a capacitance derived from the Coulomb gap of about 1 fF ($E_J/E_C=0.13$), in normal and superconducting state. In both cases the I-V curves for two different gate voltages are shown. The junctions, with an area of 0.01 μm^2 , were patterned by e-beam lithography and produced by shadow evaporation on an oxidized silicon substrate.[9] A junction is formed of two aluminum strips, of width 100 nm and thicknesses 20 and 40 nm, overlapping for about 100 nm. The two junctions are 1 μm apart. The sample was thermally anchored to the mixing chamber of a dilution refrigerator. The leads to the junctions were filtered by low-pass filters which were also thermally anchored to the mixing chamber. Normal state measurements were performed in a magnetic field to suppress superconductivity. The inset of Fig. 1a shows the device and measurement layout. In the normal state (Fig. 1a) a Coulomb gap of about 70 μV is visible, which can be completely suppressed with gate voltage.

In the superconducting state (Fig. 1b) the curves show a current peak at zero voltage. In the following we will call this a supercurrent. We also see current peaks at multiples of about 20 μV , and for a voltage about equal to $2\Delta/e$ (0.4 mV for aluminum). Fulton et al. have previously considered the peak at $2\Delta/e$ [7]. Here we want to emphasize two novel features. Firstly, the current peaks in the first 150 μV , including the supercurrent, can be largely suppressed with the gate voltage, a clear indication of charging effects for Cooper pairs. Gate voltage experiments will be described in more detail below. The second new feature in Fig 1b is the voltage gap of about 150 μV (indicated by the arrow) that is visible if the supercurrent is suppressed with the gate voltage. The width of 150 μV is twice as large as the Coulomb gap in the normal state. This doubled width indicates Coulomb blockade of Cooper pair tunneling as the origin of the gap. We will therefore call it a Cooper pair gap. Fig. 2a shows I-V curves for a linear array of 5 junctions, with $R_n=60$ k Ω and $C=2$ fF ($E_J/E_C=0.3$). This device also exhibits a Cooper pair gap, equal to about two times the normal state Coulomb gap. With increasing temperature the gap first decreases in width and then changes into a supercurrent-like feature. Omission of the low-pass filters on the mixing chamber caused the high temperature I-V curve to persist at the lowest temperature, thus hiding the Cooper pair gap. On a larger scale (inset) 4 current peaks of increasing height are visible at voltages around multiples of $2\Delta/e$. In Fig. 2b we show the I-V curve of an array of 5 junctions with high E_J ($R_n=5.5$ k Ω) and $C=1$ fF ($E_J/E_C=1.5$). Instead of a

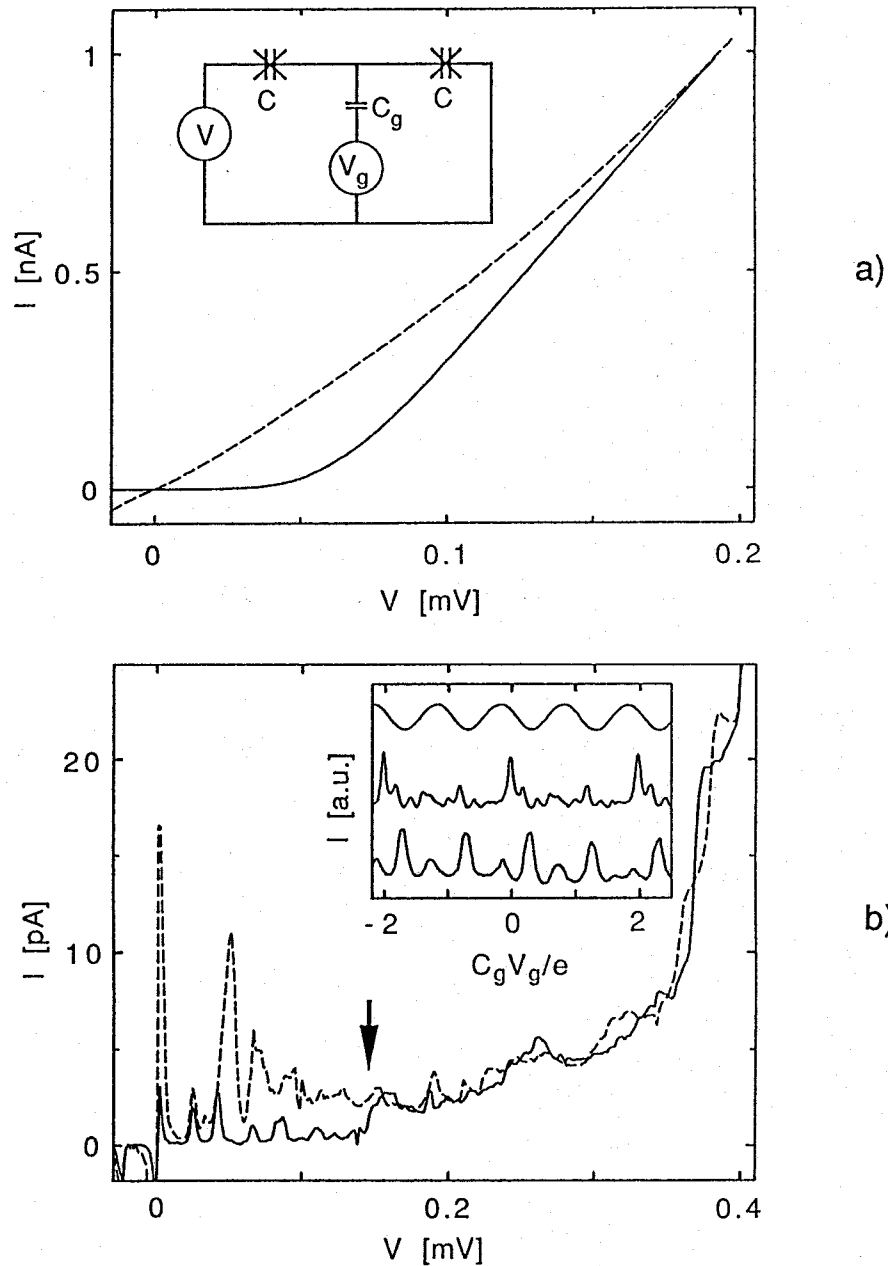


Fig. 1. I - V curves of a double junction with $R_n=58 \text{ k}\Omega$ ($E_J/E_C=0.13$) for two different values of the gate voltage V_g at 10 mK . (a) In the normal state, realized by applying a magnetic field of 2 Tesla. The Coulomb gap with a maximum value of about $70 \text{ }\mu\text{V}$ (solid curve) can be suppressed with the gate voltage (dashed curve). The inset shows the device and measurement layout. The junctions are denoted by crossed capacitor symbols, $C_g \approx 0.01C$. (b) In the superconducting state a Cooper pair gap of about $150 \text{ }\mu\text{V}$ arises (arrow). Coulomb gap and supercurrent are strongly dependent on gate voltage (compare solid and dashed curve). The inset shows I - V_g curves for the normal state (top), the current peak at $20 \text{ }\mu\text{V}$ (middle) and the supercurrent at $V=0$ (bottom).

Cooper pair gap, at low temperatures a supercurrent arises. On a large scale, we find again 4 current peaks at multiples of $2\Delta/e$, and negative differential resistance regions. These results were reproduced in the other samples that we examined. We have observed a Cooper pair gap such as shown in Fig. 2a in arrays of 5 junctions with E_J/E_C up to 0.43. We have also examined other double junctions with small E_J . For these, as in Fig. 1b, generally this gap was difficult to discern between the structure (resonances) in the I-V curve.

Three I- V_g curves for the double junction are given in the inset of Fig. 1b. The height of the supercurrent is periodic in gate voltage, with the same period e/C_g as in the normal state. The current just outside the Cooper pair gap also oscillates with this single electron period. It is important to note that if the voltage bias is increased the curves invert. At a gate voltage where the supercurrent and the current just outside the Cooper pair gap are at a maximum, the current near the first BCS gap and the current in the normal state (for arbitrary bias) are at a minimum. For the first two 20 μ V resonances in Fig. 1b a doubled modulation period was observed, corresponding to $2e$ periodicity in gate charge.

Since several of the concepts of single electron tunneling in small junctions [4] are also useful to describe Cooper pair tunneling,[7,8] we will first shortly discuss the extensively verified theory for normal metal tunnel junctions. At zero temperature the single electron tunneling rate is proportional to the change ΔE in in the relevant (Gibbs) free energy, the sum of the capacitive energies and the work performed by the voltage sources. For a single voltage biased junction $\Delta E = -eV$, hence a Coulomb gap (or Cooper pair gap) does not arise. In an array of junctions charge transfer occurs via intermediate states, where the charge resides on an electrode between the junctions. For low voltage, these states are higher in energy (by an amount of order E_C) than the initial state, so that tunneling is blocked and a Coulomb gap arises. With an externally applied gate voltage, the Coulomb gap can be suppressed. In two serially coupled junctions with island charge $e/2$, the energy change of a tunneling step is always smaller than zero for all finite voltages. Therefore no threshold voltage for conduction is observed. For n serially coupled junctions, this complete suppression of the Coulomb gap is usually impossible due to random offset charging of the junctions [4,9], e.g. by trapped charges near a junction barrier.

One essential difference between Cooper pair tunneling (in the following abbreviated to CPT) and single electron tunneling is the dependence of the tunnel rate on the energy change. Generally, Cooper pairs can only tunnel non-dissipatively. Therefore, dc conduction by CPT can only be obtained if $\Delta E = 0$ for the tunneling event. If $\Delta E \neq 0$ an oscillating charge state is obtained, comparable to the ac supercurrent for a large capacitance junction under voltage bias. Coherent

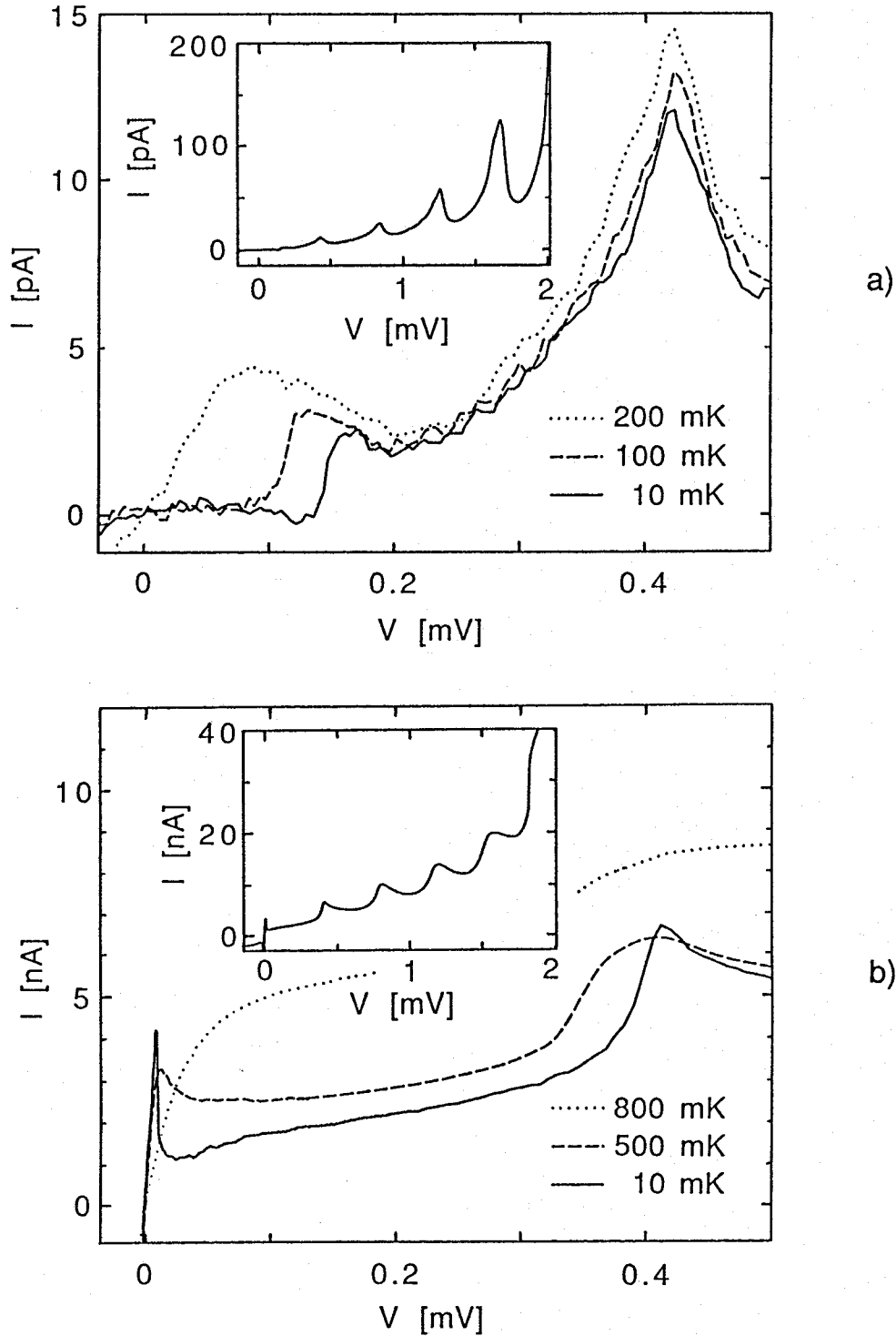


Fig. 2. I-V curves of linear arrays of 5 junctions. The insets show the I-V curves at 10 mK on a larger scale. (a) $E_J/k_B \approx 0.13$ K and $E_C/k_B \approx 0.45$ K. A clear Cooper pair gap arises. (b) $E_J/k_B \approx 1.4$ K and $E_C/k_B \approx 0.9$ K. At low temperature the resistance in the origin is zero (the finite slope in this figure is caused by the two-wire measurement method).

Cooper pair tunneling across more than one junction (e.g. an array) can be usefully described as tunneling across an equivalent single junction with a smaller Josephson coupling.[8,10] Each intermediate tunneling step with energy change ΔE_i contributes to the decrease of the coupling by a factor of order $E_J/\Delta E_i$. In the present small capacitance junctions, the intermediate states will typically differ by an amount of order E_C in energy. Obviously, the coherent transfer of Cooper pairs through an array of junctions is therefore strongly dependent on the ratio E_J/E_C and the number of junctions. Only for gate charge e in a double junction at small voltage the coupling between initial and final state will be of order E_J .

We can now proceed to discuss the results for the double junction of Fig. 1 in the superconducting state. If a gate charge e is induced on the central electrode, at zero drive voltage the energy change for CPT is zero for either of the junctions. Therefore a supercurrent develops as an equivalent of the complete suppression of the Coulomb gap in the normal state for a gate charge $e/2$. This is the situation of the dashed curve. One might expect that the height of the supercurrent is periodic in the gate voltage with period $2e/C_g$. [4] However, the observed periodicity is e/C_g because all states differing in gate charge by a multiple of e are equivalent due to the possibility of quasiparticle tunneling. This is true even if the number of quasiparticles is very small. States with gate charge equal to a multiple of e will relax by quasiparticle tunneling to the lower energy state of island charge 0, which suppresses CPT. We propose that the supercurrent is at a maximum for all gate charges equal to an integer times e because occasionally a quasiparticle tunneling event produces the situation with island charge e , and thus catalyzes conduction by CPT. The supercurrent is limited by the duration of this situation, which only lasts until relaxation to the gate charge 0 occurs again. The probability of a tunneling event from island charge 0 to e is strongly dependent on temperature. Indeed, in our experiments the supercurrent was found to increase strongly for increasing temperature. At a gate charge e the Coulomb gap in the normal state is maximized, which explains the inversion of the current versus gate-voltage characteristics and in this way confirms conduction by CPT.

The other I-V curve of Fig. 1b (solid line) corresponds to the situation with a non-integer gate charge on the central island. Current by coherent CPT through both junctions is now smaller by a factor of about E_J/E_C . Inside the Cooper pair gap, for voltages larger than the normal state Coulomb gap, conduction takes also place by quasiparticle tunneling with a very small rate, proportional to the subgap conductance. At the Cooper pair gap Cooper pairs are mixed across one junction ($\Delta E=0$) so that the quasiparticle tunneling events across that junction can be replaced by CPT. Therefore CPT across this junction alternates with quasiparticle tunneling across the

other, resulting in an increase of current. Fulton et al. [7] have shown that a similar process accounts for the current peak around the BCS gap voltage. They explained that for such a voltage CPT across one junction alternates with quasiparticle tunneling with a higher rate across the other. Because the energy gain of the quasiparticles is larger than 2Δ , the tunneling rate is in that case determined by the normal state resistance.

For the interpretation of the current peaks at small nonzero voltages we use again the equivalence of a double junction to a single junction with coupling dependent on gate charge. For a single junction under voltage bias, current resonances arise if the ac Josephson frequency $2eV/\hbar$ is in resonance with an environmental mode.[11] These resonances cause the current peaks in Fig. 1b. Experiments have shown that the resonant modes are specific for our experimental circuit. They cause current peaks at the same voltages in the I-V curve of a single high- E_J junction. It is puzzling that in contrast to the situation for the supercurrent here a $2e$ -periodicity in gate charge is observed.

In Fig. 2a for the array of low E_J/E_C junctions we observe a Cooper pair gap as in Fig. 1b. However, now Josephson coupling across the 5 junctions will generally be attenuated by a factor of order $(E_J/E_C)^4$. Because of random offset charging it is not possible to obtain a higher coupling using a gate charge. This is the reason for the absence of a supercurrent (similar to the impossibility in the normal state to suppress the Coulomb gap in this array completely) and for the absence of the $20 \mu\text{V}$ resonances. Again at the Cooper pair gap the current increases because of the possibility of CPT alternating with quasiparticle tunneling. The current peaks at multiples of the BCS gap are, as for the double junction, probably a result of the combination of CPT with quasiparticle tunneling with a rate determined by the normal state resistance. Finally, in the case of the array of Fig. 2b, $E_J=1.4 E_C$. Therefore all states with Cooper pairs on the central islands are mixed and there is strong coupling across the array. At zero voltage the Cooper pairs can transfer coherently through the complete chain.

In conclusion we have observed features of localization of the charge on Josephson junctions due to small capacitance. The charge transfer unit is $2e$, but quasiparticles also play a role. For $E_J > E_C$ coherent mixing of the Cooper pair states can occur despite the still appreciable charging energy, resulting in a supercurrent. In a double junction coherent Cooper pair tunneling is modulated by charging of the central island through a gate voltage.

We are much indebted to D.V. Averin, M.H. Devoret, D. Esteve, M. Peters, U. Geigenmüller, G. Schön, B. van Wees and P. Hadley for enlightening discussions. We thank the Commissariat à l'Energie Atomique for hospitality during several visits. This work is supported by the Dutch

Foundation for Fundamental Research on Matter (FOM).

REFERENCES

- (a) affiliation: Delft Institute of Microelectronics and Submicron Technology.
1. B.D. Josephson, *Phys. Lett.* **1**, 251 (1962).
 2. R.A. Ferrell and R.E. Prange, *Phys. Rev. Lett.* **10**, 479 (1963). See also de P.G. de Gennes, *Superconductivity of Metals and Alloys*, (Benjamin, New York, 1966) p. 118.
 3. T.A. Fulton and G.J. Dolan, *Phys. Rev. Lett.* **59**, 109 (1987).
 4. See the review by D.V. Averin and K.K. Likharev, *Single Electronics*, in: *Quantum effects in small disordered systems*, eds. B.L. Altshuler, P.A. Lee and R.A. Webb (Elsevier, Amsterdam) to be published.
 5. M. Iansiti et al., *Phys. Rev. B* **39**, 6465 (1989).
 6. See the review by G. Schön and A.D. Zaikin, *Quantum coherent effects, phase transitions, and the dissipative dynamics of ultra small tunnel junctions*, submitted to *Phys. Reports*.
 7. T.A. Fulton et al., *Phys. Rev. Lett.* **63**, 1307 (1989).
 8. K.K. Likharev and A.B. Zorin, *Jap. J. Appl. Phys.* **26**, Supplement 26-3, 1407 (1987). See also Ref. 4, section 3.1.2.
 9. L.J. Geerligs and J.E. Mooij, *Charging effects and 'turnstile' clocking of single electrons in small tunnel junctions*, to be published in the proceedings of the NATO Advanced Study Institute on Granular nanoelectronics, Il Ciocco, Italy, July 1990 (Plenum Press, New York).
 10. D.V. Averin, private communication
 11. L.Kuzmin, H.Olsson and T. Claeson, p. 1017 and V.Yu. Kistenev et al., p. 113, in: *SQUID'85, Proceedings of the Third International Conference on Superconducting Quantum Devices*, Berlin, 1985, Eds. H.D.Hahlbohm and H. Lübbig (Walter de Gruyter, Berlin, 1985).

CHAPTER 8

UNBINDING OF CHARGE-ANTICHARGE PAIRS IN TWO-DIMENSIONAL ARRAYS OF SMALL TUNNEL JUNCTIONS

J.E. Mooij, B.J. van Wees, L.J. Geerligs and M. Peters

(solid state group)

and

R. Fazio ^(a) and G. Schön

(theory group)

Department of Applied Physics, Delft University of Technology

Delft, The Netherlands

ABSTRACT

We describe behavior of charges in 2-dimensional arrays of normal metal tunnel junctions with very small capacitance. A Kosterlitz-Thouless-Berezinskii phase transition with unbinding of charge-anticharge pairs occurs at a transition temperature of about $T_c = e^2/8\pi Ck_B$, with C the junction capacitance. We calculate the influence of tunneling conductance. T_c is reduced with increasing conductance, no transition occurs for junction conductance above $(14 \text{ k}\Omega)^{-1}$. In the superconducting state a similar transition occurs at a 4 times higher T_c . We present first experimental results on the conductive transition of an array in the normal and superconducting states.

With modern lithographic techniques it is possible to fabricate metal-insulator-metal tunnel junctions with an area below $(100 \text{ nm})^2$, and consequently a capacitance of less than 10^{-15} F . When one electron crosses the tunneling barrier, the charging energy $E_C = e^2/2C$ is about 1 K and cannot be neglected at low temperatures. This has given access to a new area of mesoscopic physics. A series of effects has been predicted theoretically, some have recently been observed. A review is given by Averin and Likharev¹. Most experimental effort has been directed at single junctions, circuits with 2 or 3 junctions and longer linear arrays. Only one experimental paper² has appeared on fabricated 2D arrays of small junctions. In that paper a transition is reported, similar as seen in granular films, between insulating and superconducting behavior at $T=0$ for samples with a normal state sheet resistance above or below the quantum resistance. A large number of theoretical papers have been devoted to this subject³. In the present article, we discuss a different aspect of 2D arrays: for certain reasonable values of the parameters the interaction between single charges on islands depends logarithmically on their separation. A real Coulomb gas with 2D interaction can be realized, and a Kosterlitz-Thouless-Berezinskii (KTB) phase transition⁴ should occur at a critical temperature T_C . Below T_C , only bound charge-anticharge pairs are present, above T_C free charges $+e$ and $-e$ are generated. We calculate the influence of dissipation on this charge unbinding transition. It leads to a suppression of T_C when the tunnel junction resistance is lower than the quantum resistance. As we will discuss later, present day techniques only allow fabrication of samples in which the logarithmic interaction extends over a limited number of cell distances (10-100), with a consequent rounding of the transition. In the superconducting state a similar transition is expected at a 4 times higher temperature, where bound $+2e / -2e$ pairs unbind. The possibility of a charge KTB transition in superconducting 2D granular materials has been indicated by Sugahara and Yoshikawa⁵ and by Widom and Badjou⁶.

Single electron charge solitons in 1D chains have been discussed in detail by Averin and Likharev¹ and others⁷. A simple exact solution is available for the dependence of the island potential on position. When the nearest neighbour capacitance is C and the self-capacitance of an island is C_0 , the screening length is $L=(C/C_0)^{1/2}$. When Λ is small, the solitons are independent for low density. Solitons repel/attract each other when they have equal/opposite charge. We adopt a similar picture for the 2D array, concentrating on the behavior within the screening length. It should be noted that the 1D array does not show a phase transition at a finite temperature.

Consider a square 2D array of small tunnel junctions (see Fig. 1) with capacitance C , connecting 'islands' (x,y) with their nearest neighbors at distance 1 (lengths are dimensionless). Each island in addition has a capacitance C_0 to ground. The non-nearest-neighbour elements of the

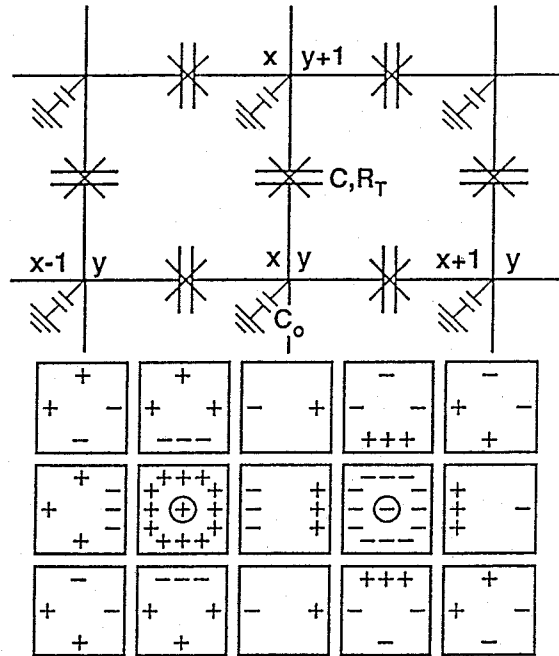


Fig. 1. Top: Approximation scheme of a square 2D network. Tunnel junctions are represented as crossed capacitances. 'Islands' are positioned at integer values (x,y). Bottom: Schematic distribution of charges in the neighborhood of a charge-anticharge pair. Only two islands in the picture contain a net charge.

capacitance matrix are neglected. The electrical potential of island x,y is indicated as $\Phi_{x,y}$. The charge distribution for the case of a positively charged island near a negatively charged island is schematically indicated in Fig. 1. The charge on island x,y is equal to:

$$q_{x,y} = C_0\Phi_{x,y} + C(4\Phi_{x,y} - \Phi_{x-1,y} - \Phi_{x+1,y} - \Phi_{x,y-1} - \Phi_{x,y+1}).$$

When $q_{0,0} = e$ and all other $q_{x,y}$ are zero, the potential for $r=(x^2+y^2)^{1/2} \gg 1$ can be approximately solved in a quasi-continuous approximation from $\nabla^2\Phi(r) - (C_0/C)\Phi(r) = 0$, with the solution:

$$\Phi(r) = \alpha K_0(r/\Lambda) , \quad \Lambda = (C/C_0)^{1/2} \tag{1}$$

The modified Bessel function $K_0(r/\Lambda)$ falls off exponentially for $r/\Lambda \gg 1$. For $r/\Lambda \ll 1$ it is approximately equal to $-\ln(r/\Lambda)$. In this regime we have: $\Phi(r) = -\alpha \ln(r/\Lambda)$, which is the same potential as for the 2D Coulomb gas. From Gauss's law in the 2D medium with effective dielectric constant C we find $\alpha=e/2\pi C$. The free energy of a pair of charges +e and -e at a mutual distance r,

for $1 \ll r \ll \Lambda$, is equal to

$$U_p = 2\mu_{\text{core}} + (E_C/\pi) \ln r \quad (2)$$

The constant $2\mu_{\text{core}}$ is the free energy of a pair with separation 1 and includes an entropy term. Without the latter it has a value of about $0.42 E_C$. The form of (2) is the same as for vortex-antivortex pairs in the 2D X-Y model⁴ or in arrays of superconducting Josephson junctions⁸. The ratio between μ_{core} and the prefactor of the logarithmic term in (2) is also very similar to the ratio in those systems. A KTB phase transition occurs at a temperature:

$$k_B T_c = \frac{1}{4\pi\epsilon_c} E_C \quad (3)$$

where ϵ_c is a non-universal constant slightly larger than 1. Above T_c , free charges of either sign, $\pm e$, will be present. Near T_c , their density should be given by the well-known square root cusp formula: $n_e = K \exp\{-2b(T/T_c - 1)^{-1/2}\}$ where K and b are constants of order 1.

Above we concentrated on the interactions between the charges. We did not account explicitly for the tunneling of electrons between the islands, except that we assumed that it establishes the equilibrium charge distribution. However, if the tunneling conductance, characterized by the parameter $\alpha_T = (h/4e^2)/R_T$ where R_T is the junction resistance, is not small this picture is no longer sufficient. We can investigate the influence of arbitrarily strong tunneling by means of the microscopic theory⁹. The partition function $Z = \int \prod_i D\varphi_i \exp\{-A[\varphi]\}$ can be expressed as a path integral over the fields φ_i , which are related to the electric potential by $d\varphi_i/dt = e\Phi_i$. The action is⁹

$$A[\varphi] = \frac{1}{4E_C} \sum_{\langle ij \rangle} \int_0^\beta d\tau \left(\frac{d\varphi_{ij}}{d\tau} \right)^2 - \sum_{\langle ij \rangle} \int_0^\beta d\tau \int_0^\beta d\tau' \alpha(\tau - \tau') \cos[\varphi_{ij}(\tau) - \varphi_{ij}(\tau')] \quad (4)$$

The first term represents the charging energy (here for simplicity we drop the self-capacitance and put $\hbar = 1$, $\beta = 1/k_B T$), the second is due to the tunneling. The islands are labeled by the subscripts i , and $\varphi_{ij} = \varphi_i - \varphi_j$ refers to nearest neighbors. The dissipative kernel is $\alpha(\tau) = \alpha_T [\beta \sin(\pi\tau/\beta)]^{-2}$. The fields φ_i are conjugate to the charges and the limits of the integration in the partition function depend on the allowed charge states of the system. Since here the total charges on the islands are quantized the integrals include a summation over the winding numbers $\varphi_i(\beta) = \varphi_i(0) + 2\pi n_i$. To proceed we decompose the phase as $\varphi_i(\tau) = \varphi_i(0) + \vartheta_i(\tau) + 2\pi n_i \tau/\beta$ where $\vartheta_i(0) = \vartheta_i(\beta) = 0$. In lowest order we consider the charging energy only. The winding

number contribution then leads to the so called "Discrete Gaussian Model" (DGM). This model exhibits the KTB transition at the critical temperature given by (3). This result was also obtained (by a different method) in reference 6 where the case of a 2-D Josephson array was considered. The present method allows us to extend the analysis to evaluate the influence of the dissipation by tunneling on the transition temperature. Details of the calculations will be presented elsewhere¹⁰. For small α_T the dissipation can be treated perturbatively. The first order correction to the transition temperature is:

$$T_c(\alpha_T) = (E_C/4\pi\epsilon_c) (1 - 0.1\alpha_T) \quad (5)$$

On the other hand, for strong dissipation T_c is almost reduced to zero. In this limit it is possible to map the problem onto the 'absolute solid on solid' (ASOS) model¹¹, in which the coupling constant (in the limit $T \rightarrow 0$) is proportional to α_T . The critical value of dissipation determined from Monte Carlo calculations¹² is:

$$\alpha_{T,crit} \approx 0.45 \quad (6)$$

Above this critical value the Coulomb gas is always in the disordered phase. All roughening models (such as the DGM and ASOS models) belong to the same class of universality so that the transition is of the KTB type everywhere in the phase diagram (Fig. 2). The value 0.45 corresponds to a critical junction resistance of 14 k Ω .

The mobility of the charges is determined by the tunneling rate in the junctions. Applying the 'global' rules, where the energies of the whole system before and after tunneling count, in a large system at low density the charge energy is independent of position and the charges should be mobile. Without driving voltage, they will diffuse around. With a voltage V over the length L of the array, the net tunneling rate is $r_t = (eR_T)^{-1}(V/L)$, as long as $L \ll \Lambda$. This leads to a current $I = n_e W e r_t$, where W is the array width. Consequently the conductance of the whole array is:

$$G = (W/L) R_T^{-1} n_e = (W/L) R_T^{-1} K \exp\{-2b/(T/T_c - 1)^{1/2}\} \quad (7)$$

Below T_c , $G=0$. Above T_c , the conductivity should start to rise according to eq. (7). In practice, the screening length Λ or the array size will limit the scale over which charge-anticharge pairs exist. To have an ideal KTB transition, one needs conditions in which the logarithm of the

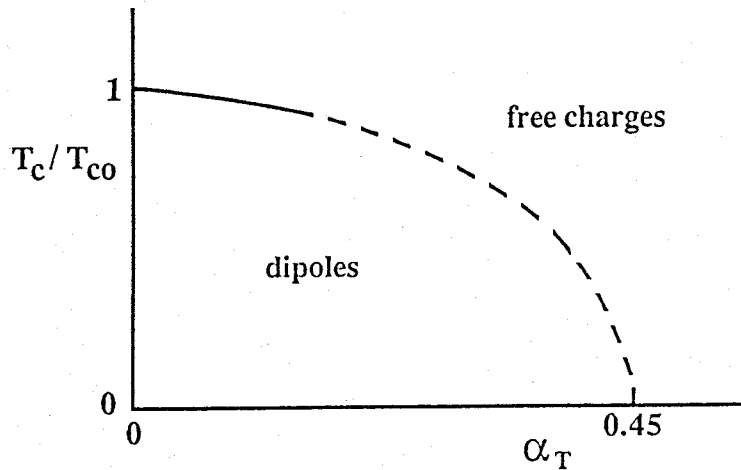


Fig. 2. Phase diagram of the normal metal tunnel junction array. T_c is the transition temperature, $\alpha_T = (6.45 \text{ k}\Omega)/R_T$. Values of T_c have been calculated on both axes and close to the temperature axis.

pair separation can be much larger than 1. For finite array size or finite screening length, the transition will be rounded-off.

Due to the complementarity of phase and charge as well as the similarity of the Hamiltonians involved, a high degree of correspondence exists between charges in arrays of low capacitance superconducting or normal metal tunnel junctions and vortices in arrays of superconducting junctions where charging effects can be ignored. In classical two-dimensional Josephson junction arrays, a KTB transition occurs where vortex-antivortex pairs dissociate. The resistance is zero below T_c and grows with a square root cusp equation similar to eq. (7) above T_c . Voltage, conductance and charge are replaced by current, resistance and vortex.

When the potential of both end electrodes is increased to V_g with respect to ground (V_g is much larger than V used for measuring G) and the array is shorter than Λ , the capacitive coupling to ground leads to an induced charge $C_0 V_g$ on each island. The effect of this induced charge is a 'frustration', similar to the frustration induced in classical Josephson junction arrays by a perpendicular magnetic field. There f is equal to the flux per cell divided by the superconducting flux quantum $h/2e$. In the 2D charge system the frustration is

$$f = C_0 V_g / e \quad (8)$$

The properties of the array should be periodic in f with period 1. In practical fabricated arrays

random fractional charges will sometimes be induced on islands by trapped charges in the barriers or on the film surfaces. Their presence leads to a random initial additional value of f for each island.

In the superconducting state, if there are no quasiparticles, the unit of charge is $2e$ and the charging energies are larger by a factor 4. This is also true for the KTB temperature, which should now be: $k_B T_{CS} = E_C / (\pi \epsilon_c)$. Because of the presence of Josephson tunneling, and because the charges have equal energy on all islands, the charges will not be localized. However, the calculation of the conductance in the highly correlated superconducting state is more complicated. Also the influence of dissipation on T_{CS} is different from the normal state case. Widom and Badjou⁶ previously indicated the possibility of a charge-KTB transition in granular superconducting films, and gave the same (unrenormalized) transition temperature. From the correspondence with classical 2D Josephson junction arrays, Sugahara and Yoshikawa also qualitatively predicted the charge transition in superconducting films. It is clear that for large Josephson coupling energy E_J , the superconducting phase coherence dominates at low temperatures and the resistance is zero. When $E_c \gg E_J$, on the other hand, the conductance is zero at low T . This implies that a zero temperature transition should occur between a superconducting and an insulating phase when E_C is of order E_J . This is exactly the type of transition that we reported on in reference 2, which had to be studied by fabricating a series of samples with varying resistance and E_J . In those samples that become insulating at $T=0$, we expect the charge-pair-unbinding transition to occur when the temperature is increased to T_{CS} .

We have experimentally investigated this transition in an aluminum array with $(100 \text{ nm})^2$ junctions, an island size of about $(0.5 \mu\text{m})^2$ and a cell size of $(2 \mu\text{m})^2$. The junction resistance R_T is $15.3 \text{ k}\Omega$. The array length is 190 cells, the width 60 cells. We estimate the self-capacitance to ground to be about $3 \cdot 10^{-18} \text{ F}$. The junction capacitance is near 10^{-15} F , so Λ is about 18 cells. The array is considerably larger than Λ , which should lead to significant rounding of the transition. According to Eq. (3) the normal state T_{CO} should be near 60 mK (for ϵ_c about 1.2). For this array, with a junction resistance such that α_T is just above the critical value (6), we expect the normal state transition temperature to be considerably reduced below T_{CO} . For the same sample, the conductance in the normal state and in the superconducting state is given in Fig. 3. The normal state is achieved by application of a 3 T magnetic field. As shown, the conductance is zero at low temperatures and increases sharply above about 20 mK in the normal state and 160 mK in the superconducting state, clearly showing the 'conductive transition'.

We consider the value of the transition temperature in the normal state to be in good agreement

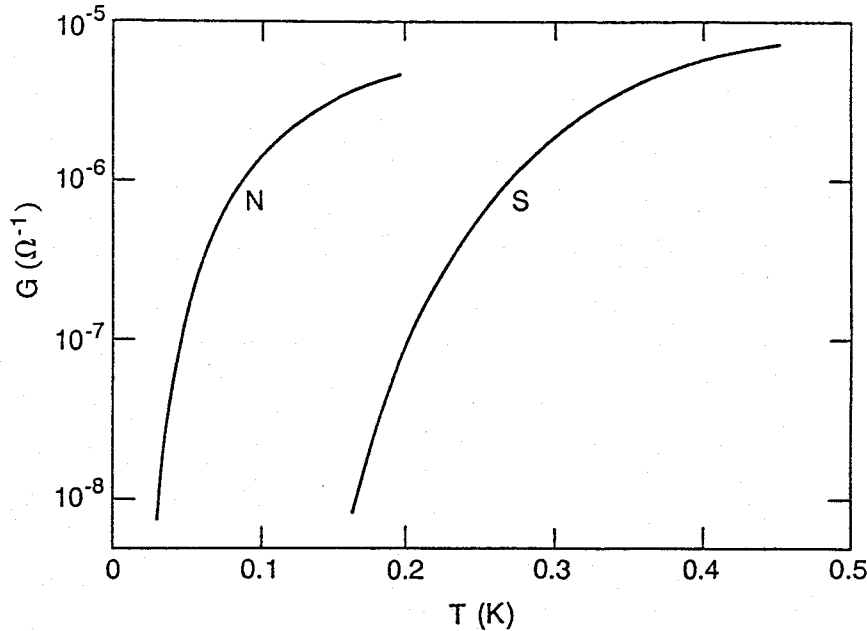


Fig. 3. Measured conductance of an array of $(100\text{nm})^2$ aluminum tunnel junctions, 190 cells long and 60 cells wide. N is in the normal state (magnetic field of 3T applied), S in the superconducting state.

with the theoretical prediction, including effects of dissipation. The functional dependence of G on T does not follow the square-root cusp dependence, due to the limited screening length. The transition in the superconducting state at 160 mK is to be compared with the theoretical value T_{CS} , about 240 mK without taking dissipation into account. It appears from the experiment that the influence of dissipation is smaller in the superconducting state (no theoretical calculation is available as yet).

We want to draw attention to the remarkable fact that the conductance is orders of magnitude smaller in the superconducting state, compared with the normal state. This directly demonstrates that charging effects are dominating. We expect that it is possible to fabricate arrays with smaller islands and an order of magnitude smaller junction capacitance. The increased screening length will allow a closer test of the theory.

We thank K.K. Likharev, U. Geigenmüller and H.S.J. van der Zant for discussions. This research was supported by the Foundation for Fundamental Research on Matter FOM.

REFERENCES

- (a) on leave from: Institute of Physics, Faculty of Engineering, Catania.
1. D.V. Averin and K.K. Likharev, *Single-Electronics*, to be published in "Quantum Effects in Small Disordered Systems", eds. B.L. Al'tshuler, P.A. Lee and R.A. Webb (Elsevier, Amsterdam, 1990).
 2. L.J. Geerligs, M. Peters, L.E.M. de Groot, A. Verbruggen and J.E. Mooij, *Phys. Rev. Lett.* **63**, 326 (1989).
 3. see Proceedings of the NATO Advanced Research Workshop on Coherence in Superconducting Networks, edited by J.E. Mooij and G.B.J. Schön, *Physica B* **152**, 1-302 (1988).
 4. J.M. Kosterlitz and D.J. Thouless, *J. Phys.* **C6**, 1181 (1973); V.L. Berezinskii, *Zh. Eksp. Teor. Fiz.* **59**, 907 (1970) [*Sov. Phys. JETP* **32**, 493 (1971)].
 5. M. Sugahara and N. Yoshikawa, Extended Abstracts of 1987 International Superconductivity Electronics Conference (ISEC '87), p. 341; N. Yoshikawa, T. Akeyoshi, M. Kojima and M. Sugahara, *Jpn. J. Appl. Phys.* **26**, 949 (1987).
 6. A. Widom and S. Badjou, *Phys. Rev. B* **37**, 7915 (1988).
 7. M. Amman, E. Ben-Jacob and K. Mullen, *Phys. Lett.* **142**, 431 (1989).
 8. C. J. Lobb, D.W. Abraham and M. Tinkham, *Phys. Rev. B* **27**, 150 (1983).
 9. V. Ambegaokar, U. Eckern and G. Schön, *Phys. Rev. Lett.* **48**, 1745 (1982); E. Ben-Jacob, E. Mottola and G. Schön, *Phys. Rev. Lett.* **51**, 2064 (1983); G. Schön and A.D. Zaikin, *Physica B* **152**, 203 (1988).
 10. R. Fazio, U. Geigenmüller and G. Schön, to be published.
 11. Y. Saito and H. Müller-Krumbhaar in: *Applications of the Monte Carlo Method*, edited by K. Binder (Springer Verlag 1984).
 12. R. H. Swendsen, *Phys. Rev. B* **15**, 5421 (1977).

CHAPTER 9

CHARGING EFFECTS AND QUANTUM COHERENCE IN REGULAR JOSEPHSON JUNCTION ARRAYS

L.J. Geerligs, M. Peters, L.E.M. de Groot,^(a) A. Verbruggen,^(a) and J.E. Mooij

Department of Applied Physics, Delft University of Technology
P.O. Box 5046, 2600 GA Delft, The Netherlands

ABSTRACT

2-dimensional arrays of very small capacitance Josephson junctions have been studied. At low temperatures the arrays show a transition from superconducting to insulating behaviour when the ratio of charging energy to Josephson coupling energy exceeds the value 1. Insulating behaviour coincides with the occurrence of a charging gap inside the BCS gap, with an S-shaped I-V characteristic. This so far unobserved S-shape is predicted to arise from macroscopic quantum coherent effects including Bloch oscillations.

In the last few years the effects of the charging energy in small Josephson junctions have been the subject of intensive theoretical study.[1] As noted by several authors [2] experiments on very small junctions can provide important information about the validity of quantum mechanics on a macroscopic scale. From microscopic theory it has been derived [3] that a Josephson junction can be described as a quantum particle of mass $\hbar^2/8E_C$ in a periodic potential $-E_J\cos(\phi)$. Here the charging energy $E_C \equiv e^2/2C$, C is the capacitance of the junction, E_J is the Josephson coupling energy and ϕ is the phase difference across the junction. With increasing ratio $x \equiv E_C/E_J$ the quantum mechanical behaviour of the junction (delocalization in phase-coordinate space) should become more noticeable. So far only low x effects, i.e. macroscopic quantum tunneling and energy level quantization,[4] have been observed convincingly. For high x the behaviour of a junction should be governed by a band energy spectrum. External current causes a sweep of the junction Bloch state through this band spectrum. For increasing current the voltage is subsequently dominated by single electron tunneling, Bloch oscillations and finally Zener tunneling, resulting in a characteristic S-shape of the I-V curve.[5] Although high x junctions have been fabricated before,[6-8] this S-shape was not observed. Yoshihiro *et al.* [9] reported on microwave-induced voltage steps in granular superconducting films which they interpreted as due to Bloch oscillations. Owing to the undefined nature of their samples this interpretation has not been generally accepted. Iansiti *et al.* [7] find in superconducting junctions a knee in the I-V characteristic which may be related to the above effects. The knee only occurs when E_J is suppressed by a magnetic field.

In this letter experiments are reported on two-dimensional arrays of well-defined high x junctions that prominently exhibit the predicted current-voltage dependence. We consider this as the clearest observation so far of macroscopic quantum coherent effects. The prominent negative slope is also a manifestation of the more general phenomenon of Bloch oscillations.

In addition the arrays provide the opportunity to test the effects of charging energy on coherence in 2-dimensional systems. Generally quantum fluctuations of the phase destroy global superconductivity for high x . [10] Experiments on granular films [11] suggested that apart from the parameter x the junction dissipation, i.e. coupling to external degrees of freedom which is proportional to the quasiparticle conductance, has a strong influence on macroscopic quantum effects. It appeared that whether or not a granular film became superconducting depended on dissipation only, and not on x . In this letter we compare our experimental results with predictions of phase diagrams for 2-D systems.[10,12-14] Owing to the fabrication by nanolithographic methods, reliable estimates of E_J and E_C are available and percolation effects are absent. In short,

results for $T=0$ show a phase transition from insulating behaviour at high x to superconducting at low x , with at most a small dependence on dissipation. Preliminary results were published in Ref. 15.

The junctions in the arrays are arranged in a square network. The arrays are 190 junctions long and 60 junctions wide. The junctions are made of aluminum, and have an area of 0.01 or 0.04 μm^2 . The area of the aluminum islands is approximately 1.9 μm^2 . Since we found shielding of magnetic and electrical interference to be critical we give some details of our experimental setup. The experiments on the arrays in the superconducting state were performed inside a magnetic shield. A magnetic field of 4.1 G corresponded to a flux quantum $\Phi_0=h/2e$ per unit cell. (The area of the elementary cell is 4.9 μm^2 .) The typical remanent field was between 0.04 and 0.004 G. In this paper the field is indicated as the frustration f , the flux per cell divided by Φ_0 . The leads to the arrays were filtered at the entrance to the cryostat with rfi feedthrough filters. At mixing chamber temperature the leads were filtered by RC-filters and microwave filters [4] before entering the electrically shielded case containing the arrays. For recording the charging gap, in a separate experiment we put 10 M Ω resistors in the leads close to the arrays. All the measuring methods were standard except for the addition of analog optical decoupling between current source/preamplifier and the rest of the equipment.

As the critical current was too small to be measured directly, we calculated E_J with I_c given by the Ambegaokar-Baratoff equation, i.e. $E_J=\pi\hbar\Delta/4e^2R_n$ at zero temperature, using experimental values of the normal state resistance R_n and the critical temperature T_c and assuming $\Delta(0)=1.76k_B T_c$. Results on larger single junctions justify this procedure.

For $T>T_c$ or in a large magnetic field, i.e. in the normal state, the arrays show the effect of charging energy as the 'Coulomb gap' in the I-V curve. This is a voltage offset of magnitude $e/2C$ for a single junction and $Le/2C$ for an array, where L is the length of the array. For details we refer to Ref. 15. From this offset the capacitance is calculated. It is about 1.1 fF for a 0.01 μm^2 junction, and proportionally larger for the larger junctions.

Fig. 1 shows $R(T)$ curves for several arrays in zero magnetic field, measured with a lock-in amplifier and current bias. The current was chosen small enough that the resistance was linear for increasing current, typically 0.1 to 1 nA. The resistance given is the measured resistance divided by the length/width ratio 3.14 of the array. For the five arrays shown, $E_C=0.84$ K is constant and R_n varies from 4.8 to 36 k Ω . Since the critical temperature of the aluminum was also approximately constant, $T_c=1.37$ K, this causes x to vary from 0.53 to 3.9. In the figure caption the relevant data are given for each array. The arrays with the smallest x , which are not all

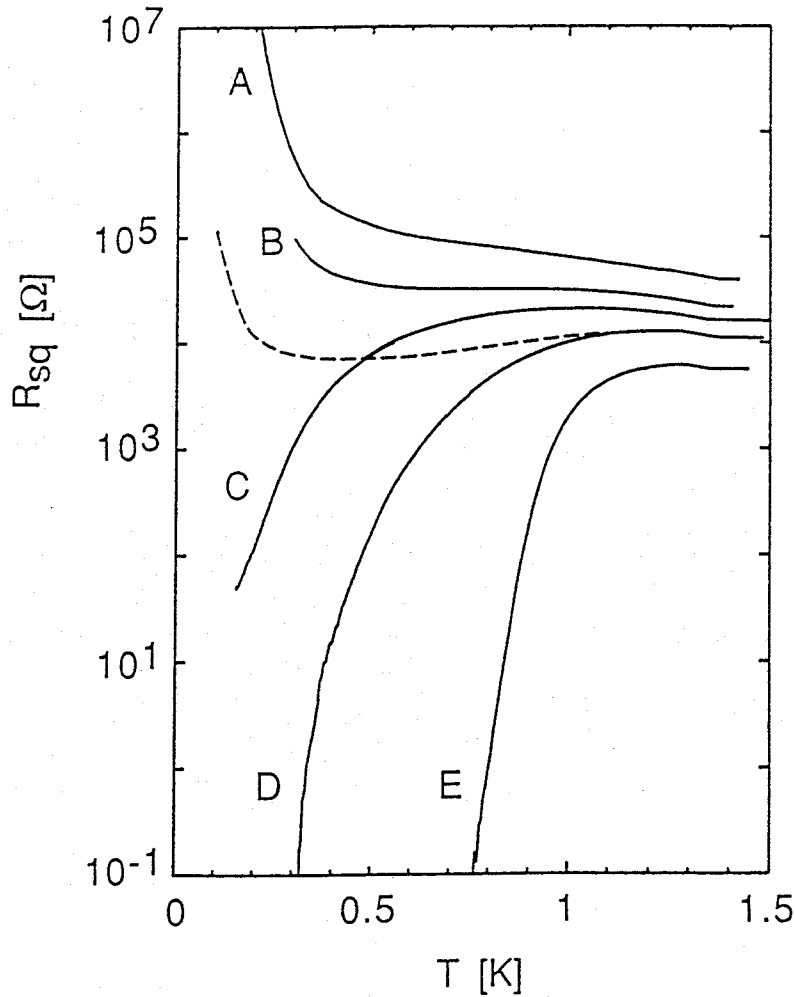


Fig. 1. $R(T)$ curves for arrays of $0.01 \mu\text{m}^2$ junctions ($E_C \approx 0.84$ K). R_{sq} is the resistance divided by the length/width ratio 3.14. Each solid curve corresponds to an array with a particular normal state resistance R_n in zero field. The dashed curve is for array D with $f \approx 1/2$. Values of R_n in $\text{k}\Omega$, E_J/k_B in K and $x = E_J/E_C$ are: sample A: 36, 0.22, 3.9; B: 15.3, 0.51, 1.8; C: 14.1, 0.55, 1.5; D: 9.7, 0.80, 1.0; E: 4.8, 1.6, 0.53.

included in Fig. 1, show the Kosterlitz-Thouless transition in the form of the square-root cusp behaviour $R(\tau) = R_{qp} \exp\{-b/(\tau - \tau_c)^{0.5}\}$, [16] where $\tau = kT/E_J(T)$, and R_{qp} is the temperature dependent quasiparticle resistance. The $R(T)$ curves for the arrays with significant charging energy show deviations from a Kosterlitz-Thouless transition. For arrays with $x \lesssim 1.0$ (D and E in Fig. 1) the resistance decreases to zero within experimental accuracy (about 0.01Ω), but the transition temperature is significantly lower than the Kosterlitz-Thouless temperature. For array C, with $x \approx 1.5$, the resistance decreases in a similar way down to 0.1 K. At that temperature the 'supercurrent' in the I-V curve becomes noisy with voltage spikes, the effect getting worse for

lower temperature. It is therefore impossible to attribute a resistance to this array below 0.1 K. Arrays with still higher x show at low temperatures a strongly increasing resistance with no sign of flattening off.

In earlier experiments [15] we found a flattening off of the resistance at low temperatures. This feature has completely disappeared with the addition of the special cryogenic microwave filtering to the experiments.

At first sight all I-V curves show the same general features, similar to those of classical arrays. Fig. 2a gives an example for $x \approx 3.9$ (array A). For increasing current there is first a supercurrent-like part. Then the voltage increases from near zero to a value equal to the length of the array times the single junction BCS sum gap. Finally, after the gap edge, the voltage increases with the normal state resistance of the array.

The new phenomenon of these quantum arrays, with $x > 1$, is the existence of a small second gap, in the supercurrent-like part of the I-V characteristic at low temperatures. This gap, of order 1 mV, is situated *inside* the BCS gap (80 mV in our 190 junctions long arrays). In the following we indicate it as the charging gap. Fig. 2b shows it for $T \approx 20$ mK. At this temperature the resistance in the gap is larger than $5 \text{ G}\Omega$. The occurrence of the charging gap is responsible for the strong increase of resistance at low T for the high x arrays in Fig. 1. In arrays with $E_C \approx 1$ K the charging gap becomes visible below 0.5 K, for $E_C \approx 0.4$ K below 0.2 K. Below 0.1 K the gap edge of the high x arrays develops a negative resistance region. In an array with Hall contacts we verified that the gap is present proportionally in both halves of the array. This indicates that the gap is distributed over the length of the array, instead of being localized in certain crossrows. The charging gap is present in the I-V curves of the highest x arrays at zero magnetic field. It is also present in arrays with smaller x (down to 0.5) at low temperatures if the array is frustrated in a magnetic field. For frustrated arrays the gap can cause quasi-reentrant behaviour of the $R(T)$ curve (dashed curve in Fig. 1). No quasi-reentrant behaviour was found in zero field. The width of the charging gap is modulated by the frustration with period 1. For large fields the width gradually increases and the gap changes into the normal state Coulomb gap as the superconductivity in the islands is destroyed. This behaviour is shown in Fig. 3.

Macroscopic quantum behaviour of single high x junctions is predicted to yield an S-shaped I-V curve because of band spectrum effects.[5] For low current quasiparticle tunneling confines the junction to the centre of the first Brillouin zone, and the I-V curve follows a high resistance branch. For higher currents Bloch oscillations, which can be regarded as coherent Cooper pair tunneling, become important, decreasing the mean voltage. The resulting low current part of the

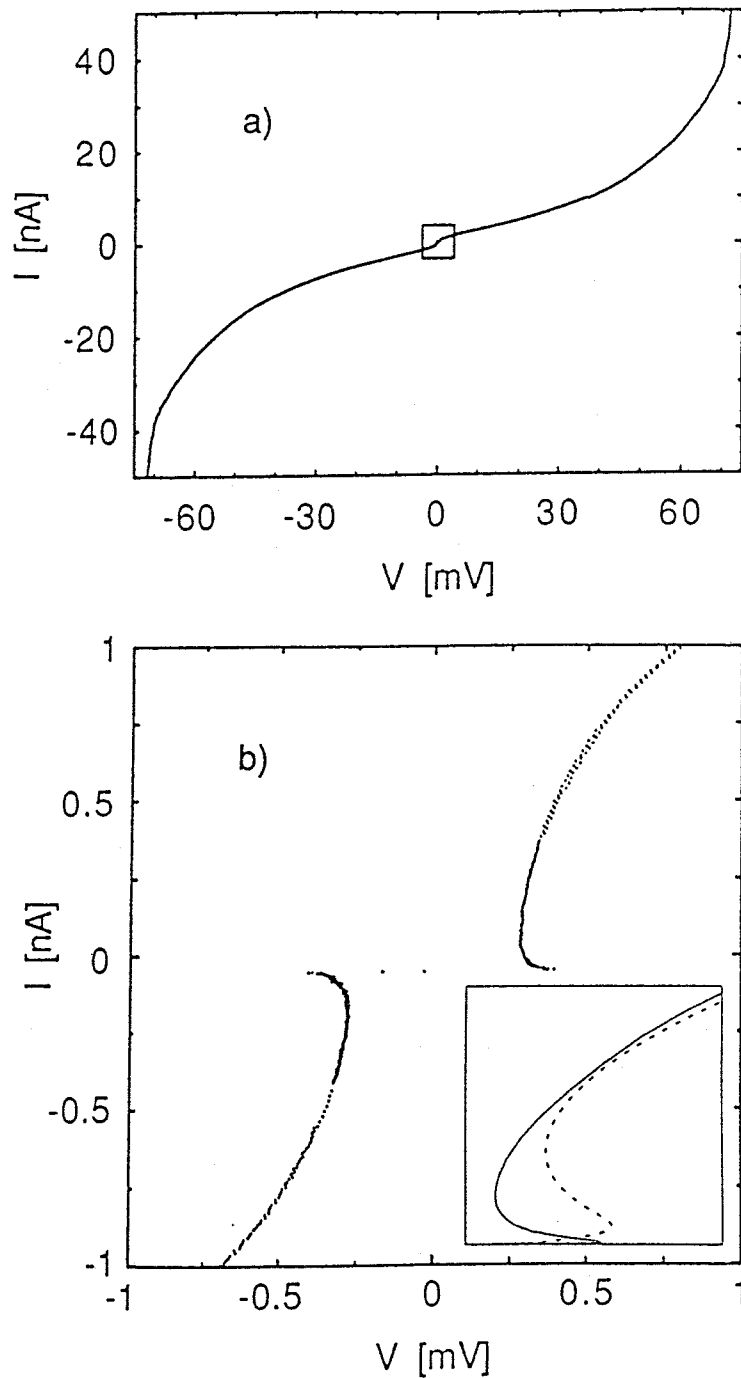


Fig. 2. I-V characteristic for sample A at 20 mK. (a). large scale showing the BCS sum gap of the array, with a small 'supercurrent'. (b). Small current region (box in (a)) with voltage measured over 95 junctions, showing effects of Bloch oscillations and Zener tunneling. The inset shows calculated I-V curves [17] for a single junction (dashed curve) and of a circuit of one junction parallel to two junctions (solid curve). The junction parameters are chosen to be the estimated parameters for sample A. The axes are in arbitrary units but identical for the two calculated curves.

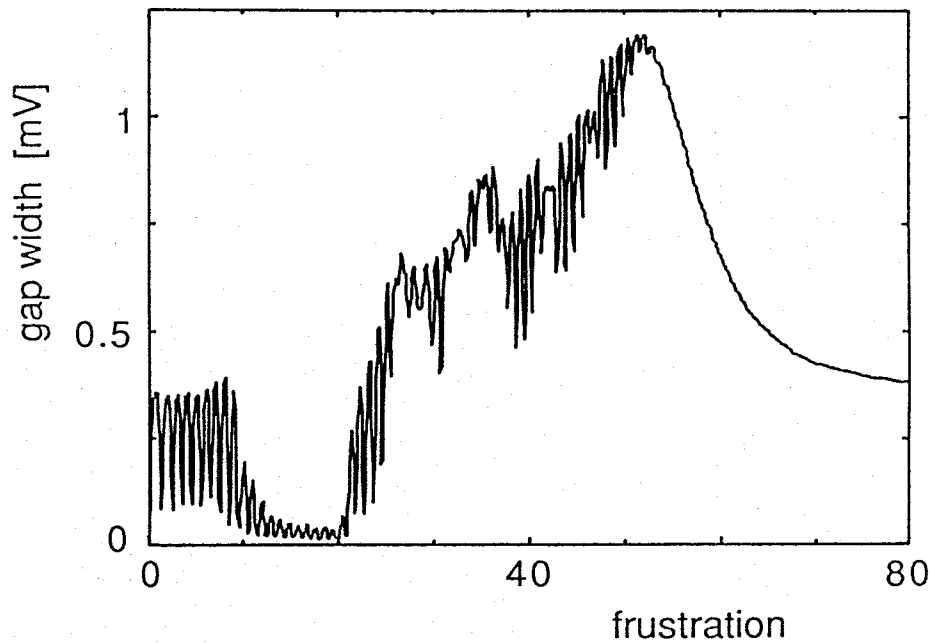


Fig. 3. Voltage for $I=10$ pA in array C. This voltage is indicative for the charging gap and oscillates with a period of one flux quantum per cell.

I-V curve is known as the 'Bloch nose'. For qualitative comparison, the inset of Fig. 2b shows calculated I-V curves [17] for a single junction and a series/parallel arrangement of three junctions. The trend of sharpening-up of the Bloch nose with increasing number of degrees of freedom is consistent with the experimental I-V curve. A quantitative comparison will have to wait for a more similar theoretical system.

The superconductor-insulator transition of Fig. 1 can be compared with theory. Quantum XY models which do not include dissipation [10] generally predict a transition from superconducting to non-superconducting behaviour near $x=1$. Several theoretical calculations [12] have shown that quasiparticle dissipation significantly influences superconductivity in Josephson junction arrays. Quasiparticle tunneling in addition leads to a renormalization of the capacitance [18,13,14] which even at low temperatures depends on the *normal state* resistance. In our junctions the subgap resistance is very high so that quasiparticle dissipation is negligible. This leaves only capacitance renormalization to be considered in addition to bare charging effects.

Array D, clearly showing superconducting behaviour, has a value $x=1.04$, calculated from the normal state Coulomb gap. Possibly this Coulomb gap is suppressed by heating.[15] We estimate that x is between 1.0 and 1.3. Similarly, array C has $1.5 < x < 2.0$. It appears to go superconducting but develops the above described noisy supercurrent below 0.1 K. Array B, the

first insulating sample, has $1.8 < x < 2.5$. So, the experimental transition is close to $x=1.5$. The variation in the prediction for the critical x from various bare charging theories is large and $x=1.5$ lies in their range. In contrast, the transition observed in granular films [11] occurred at $x \gg 1$.

The phase diagram of a 2-D array of Josephson junctions, influenced by capacitance renormalization, was evaluated by Chakravarty *et al.* [13] and Ferrell and Mirhashem.[14] The experimental results for granular films, where the capacitance can only be estimated, are in reasonable agreement with that phase diagram. In our arrays the capacitance is well known. Applying the phase diagram of Ref.13, the transition should occur for $R_n=13 \text{ k}\Omega$. This is in excellent agreement with our experimental data. The same holds for the similar treatment in Ref. 14.

We thank J. Martinis and M. Devoret for explaining details of their cryogenic filtering, U. Geigenmüller for providing his results of I-V calculations, H. van der Zant, G. Schön, U. Geigenmüller and H. Jaeger for valuable discussions. This work was supported by the Dutch Foundation for Fundamental Research on Matter (FOM).

REFERENCES

- (a) affiliation: Centre for Submicron Technology.
1. See, e.g., A. Widom *et al.*, J. Phys. A **15**, 3877 (1982); K.K. Likharev and A.B. Zorin, J. Low Temp. Phys. **59**, 347 (1985); E. Ben-Jacob and Y. Gefen, Phys. Lett. A **108**, 289 (1985); F. Guinea and G. Schön, J. Low Temp. Phys. **69**, 219 (1987); M. Büttiker, Phys. Rev. B **36**, 3548 (1987); S.V. Panyukov and A.D. Zaikin, J. Low Temp. Phys. **73**, 1 (1988).
 2. A.J. Legget, Progr. Theor. Phys. Suppl. **69**, 80 (1980); A.I. Larkin, K.K. Likharev, and Yu.N. Ovchinnikov, Physica B **126**, 414 (1984).
 3. V. Ambegaokar, U. Eckern, and G. Schön, Phys. Rev. Lett. **48**, 1745 (1982); U. Eckern, V. Ambegaokar, and G. Schön, Phys. Rev. B **30**, 6419 (1984).
 4. J.M. Martinis, M.H. Devoret, and J. Clarke, Phys. Rev. B **35**, 4682 (1987).
 5. D.V. Averin, A.B. Zorin, and K.K. Likharev, Zh. Eks. Teor. Fiz **88**, 692 (1985) (Sov. Phys. JETP **61**, 407 (1985)); U. Geigenmüller and G. Schön, Physica B **152**, 186 (1988); A.D. Zaikin, and I. N. Kosarev, Phys. Lett. A **131**, 125 (1988).
 6. T.A. Fulton, and G.J. Dolan, Phys. Rev. Lett. **59**, 109 (1987).
 7. M. Iansiti *et al.*, Phys. Rev. Lett. **59**, 489 (1987); Phys. Rev. Lett. **60**, 2414 (1988).

8. L.S. Kuzmin *et al.*, Phys. Rev. Lett. **62**, 2539 (1989).
9. K. Yoshihiro *et al.*, Jap. J. Appl. Phys. **26**, Suppl. 26-3, 1379 (1987).
10. B. Abeles, Phys. Rev. B **15**, 2828 (1977); K.B. Efetov, Sov. Phys. JETP **51**, 1015 (1980); S. Doniach, Phys. Rev. B **24**, 5063 (1981); E. Simanek, Phys. Rev. B **25**, 237 (1982); L. Jacobs and J.V. José, Physica B **152**, 148 (1988); R. Fazio, G. Falci, and G. Giaquinta, Physica B **152**, 257 (1988).
11. B.G. Orr, H.M. Jaeger, and A.M. Goldman, Phys. Rev. B **32**, 7586 (1985); A.E. White, R.C. Dynes, and J.P. Garno, Phys. Rev. B **33**, 3549 (1986); H.M. Jaeger *et al.*, Phys. Rev. B **34**, 4920 (1986); N. Yoshikawa *et al.*, Jap. J. Appl. Phys. **26**, Suppl. 26-3, 949 (1987); S. Kobayashi, Physica B **152**, 223 (1988).
12. See, e.g., M.P.A. Fisher, Phys. Rev. B **36**, 1917 (1987); A. Kampf and G. Schön, Phys. Rev. B **36**, 3651 (1987); Physica B **152**, 239 (1988); S. Chakravarty *et al.*, Phys. Rev. B **37**, 3283 (1988); W. Zwerger, J. Low Temp. Phys. **72**, 291 (1988); A.D. Zaikin, Physica B **152**, 251 (1988); S.E. Korshunov, Physica B **152**, 261 (1988); A.I. Larkin, Yu.N. Ovchinnikov, and A. Schmid, Physica B **152**, 266 (1988).
13. S. Chakravarty, S. Kivelson, G. Zimanyi, and B.I. Halperin, Phys. Rev. B **35**, 7256 (1987).
14. R.A. Ferrell and B. Mirhashem, Phys. Rev. B **37**, 648 (1988); B. Mirhashem and R.A. Ferrell, Physica C **152**, 361 (1988).
15. L.J. Geerligs, and J.E. Mooij, Physica B **152**, 212 (1988).
16. C.J. Lobb, D.W. Abraham, and M. Tinkham, Phys. Rev. B **36**, 150 (1983).
17. U. Geigenmüller, and G. Schön, in Ref. 5, and private communication.
18. V. Ambegaokar, in Percolation, Localization, and Superconductivity, Proceedings of the Nato Advanced Study Institute, Les Arcs, France (1983), eds. A.M. Goldman and S.A. Wolf (Plenum Press, New York, 1984), p. 43.

CORRECTION DUE TO CAPACITANCE RENORMALIZATION ON THE SUPERCONDUCTOR-INSULATOR PHASE TRANSITION.

In a comment to the preceding paper,[1] Ferrell and Mirhashem [2] considered the effect of capacitance renormalization on the exact value of $x=E_C/E_J$ at which the phase transition between superconducting and insulating behavior should occur, more thoroughly than we did in the last paragraph. Virtual quasiparticle tunneling screens the Coulomb interaction of the Cooper pairs, to an extent depending on normal state resistance, and thus results in a larger effective capacitance. As quoted in the preceding paper, theory for "bare" charging effects predicts a threshold x approximately equal to 1. This is a general statement that applies both to theories that take into account Coulomb energy due to charging of the self-capacitance and theories that take into account charging of the nearest-neighbour capacitance. For the latter possibility (i.e., only nearest neighbour charging), Ferrell and Mirhashem calculated that in mean-field theory the threshold value for E_C/E_J is approximately 1.54,[3] in a second order expansion in $1/z$ ($z=4$ is the number of nearest neighbours). However, we want to note that they assume the effective nearest-neighbour capacitance to be a factor two smaller than the capacitance that is experimentally measured in the Coulomb gap.

This calculated threshold value is close to the experimentally observed one. The point that Ferrell and Mirhashem make is that the capacitance renormalization due to quasiparticle tunneling [4] accounts for the small deviation between the two. If the superconducting phase difference varies only slowly in time, this correction takes the form of an extra capacitive charging term in the imaginary-time action of the system,

$$\Delta C = \frac{3h}{64\Delta_{\text{BCS}}R_n}$$

is added to the nearest neighbour capacitance, and lifts the transition line somewhat from array C (superconducting), to precisely midway arrays B and C (insulating and superconducting, respectively). We advise not to draw any conclusions from this marginal effect. We fully agree with the authors that further miniaturization is necessary to establish the role of virtual quasiparticle tunneling and think that this would yield very interesting information.

REFERENCES

1. L.J. Geerligs *et al.*, Phys. Rev. Lett. **63**, 326 (1989).
2. R.A. Ferrell and B. Mirhashem, Phys. Rev. Lett. **63**, 1753 (1989).
3. ref. 14 of the preceding paper.
4. refs. 18,13 and 14 of the preceding paper.

SUMMARY

This thesis presents an experimental study of the effects of a small capacitance on the electrical conduction in systems of small tunnel junctions. In zero magnetic field we study the characteristics of the junctions with superconducting electrodes. By applying a magnetic field the superconductivity of the electrodes is quenched and the normal state characteristics can be studied for the same devices, in the same setup, without thermal cycling the sample.

In normal and in superconducting state the characteristics of arrays of high resistance junctions show clear Coulomb blockade of single electron and Cooper-pair tunneling, respectively. Due to incorporation of the junctions in arrays, stray capacitance is suppressed and the junction capacitance turns out to be close to the simple geometrical parallel-plate value. The results can in normal as well as superconducting state be interpreted by classical charge dynamics. In the normal state, there is detailed quantitative agreement with simple ("orthodox") theory, based on thermal equilibrium in the junction electrodes and first order perturbation theory for electron tunneling. In the superconducting state there is no such quantitative agreement, but a qualitative description based on Coulomb blockade of Cooper-pair tunneling is possible. For single junctions Coulomb blockade is strongly suppressed due to stray capacitance shunting the junctions. The only remaining feature is a voltage offset in the current-voltage characteristic at high currents. By making connection to these single junctions via arrays of similar small junctions, in the normal state a clear Coulomb blockade is observed. In the superconducting state the same devices do not show indications of classical charge dynamics.

In the normal state, a frequency-controlled turnstile-device for single electrons has been operated, based on a small array of high-resistance junctions. Applying an alternating voltage to a gate causes one electron to be transferred through the device per cycle. It can yield a high-accuracy charge or current source. Limitations to the accuracy are discussed.

Some possible mechanisms to operate a turnstile-device for Cooper-pairs are discussed, with preliminary results. Part of the importance of testing these mechanisms is that they probably provide the better means to test hypotheses on Cooper-pair tunneling and dissipative band dynamics.

The effects of finite barrier transparency on charge dynamics are studied for junctions with well-defined capacitance, i.e. those incorporated in arrays. In the normal state the suppression of Coulomb blockade due to quantum charge fluctuations, increasing with decreasing tunnel resistance, is in quantitative agreement with theory. For tunnel resistances high compared with the

resistance quantum $R_q \equiv h/4e^2 \approx 6.5 \text{ k}\Omega$ the charge behaves semi-classically. Charge leakage (i.e., violation of the Coulomb blockade) is possible due to successive tunneling events through the junctions in the array, and can be described by higher order perturbative treatment of electron tunneling. For tunnel resistances around or below R_q a strong suppression of Coulomb blockade occurs, due to quantum charge fluctuations. The small-signal resistance can be evaluated with the Kubo-formula. In the superconducting state the ratio of Josephson coupling to charging energy is crucial for the sample characteristics. If the Josephson coupling is the larger one, zero-voltage transfer of Cooper pairs is possible. If the charging energy is the larger one Coulomb blockade is observed, but the probability of zero-voltage Cooper-pair tunneling through double junctions is still significant, supposedly only decaying linearly in this ratio. In general, for junction arrays with superconducting electrodes if both energies are comparable there is a complicated combination of features belonging to classical phase dynamics (such as sensitivity to an environmental resonance of the Josephson frequency) and classical charge dynamics (such as gate voltage modulation of the Cooper-pair tunneling rate).

The excess charges on the normal metal electrodes of a 2-dimensional junction array interact as a two-dimensional Coulomb gas. They are expected to show a Kosterlitz-Thouless charge unbinding transition at a critical temperature scaling with the charging energy. However, if the junction conductance exceeds a critical value $0.45 R_q^{-1}$ charge pairs unbind even at zero temperature because of quantum charge fluctuations. Preliminary results are in rough agreement with this theory. In arrays with superconducting electrodes the ratio of Josephson coupling to charging energy is important for the charge fluctuations. There is a duality between excess charges and vortices in these arrays. If the Josephson coupling dominates, the vortices are bound at low temperature and global phase coherence in the array yields a superconducting state. If the charging energy dominates, charges are bound and an isolating state results at low temperature. The crossover occurs at the predicted value of the ratio of the two energies, possibly even showing the effect of capacitance renormalization due to quasiparticle tunneling.

In the charging-energy dominated arrays the moving excess charges are expected to repel each other and keep at regular distances, causing each junction to be current biased. This results in the I-V characteristic showing a characteristic negative differential resistance: quasiparticle tunneling is replaced by coherent Cooper-pair tunneling (Bloch oscillations) as the current increases. The significance of this observation lies in the quantum behavior of the macroscopic degrees of freedom which describe the junctions.

SAMENVATTING

In dit proefschrift wordt een experimenteel onderzoek gepresenteerd naar de effecten van een kleine capaciteit op de elektrische geleiding in systemen bestaande uit kleine tunnel-juncties. In afwezigheid van een magnetveld kunnen de eigenschappen van de juncties met supergeleidende elektroden bestudeerd worden. Door een magnetveld aan te leggen wordt de supergeleiding in de elektroden onderdrukt, zodat de eigenschappen van dezelfde juncties in normale toestand onderzocht kunnen worden, in dezelfde opstelling en zonder te hoeven opwarmen.

Zowel in normale als in supergeleidende toestand vertonen netwerken van juncties met hoge weerstand duidelijk Coulomb blokkade van respectievelijk elektron- en paar-tunneling. Door de juncties in een netwerk op te nemen is het mogelijk parasitaire capaciteit te onderdrukken. De capaciteit van de juncties blijkt dan de waarde te volgen die wordt verwacht voor een vlakke-plaat condensator van de junctie-afmetingen. In zowel normale als supergeleidende toestand gedraagt de junctie-lading zich als een klassieke variabele. In normale toestand is er kwantitatieve overeenstemming tussen experiment en de eenvoudige theorie die thermisch evenwicht in de elektrodes veronderstelt, en de electron tunneling in eerste orde storingsrekening bepaalt. In de supergeleidende toestand is een dergelijke kwantitatieve overeenstemming afwezig, maar de resultaten kunnen wel kwalitatief begrepen worden op een basis van Coulomb blokkade van paar-tunneling. Voor enkele (d.w.z. niet in een netwerk opgenomen) juncties staat een grote parasitaire capaciteit parallel aan de junctie capaciteit, waardoor Coulomb blokkade onderdrukt wordt. Alleen een verschuiving van de stroom-spannings-karakteristiek in spannings-richting wijst nog op Coulomb blokkade. Als een enkele junctie doorgemeten wordt via netwerken van vergelijkbare kleine juncties, is in de normale toestand wel duidelijk Coulomb blokkade aanwezig. In de supergeleidende toestand kan in ieder geval niet duidelijk geconcludeerd worden dat de junctielading zich klassiek gedraagt.

Er is aangetoond dat in de normale toestand een schuifregister voor enkele electronen kan worden gemaakt met deze kleine juncties. Een wisselspanning bepaalt de passage van electronen, tot precies één electron per periode. Op deze wijze kan een stroom- of ladings-generator van hoge nauwkeurigheid gecreëerd worden. Wat de vereisten voor de hoge nauwkeurigheid zijn wordt behandeld.

Er zijn verschillende ideeën om een schuifregister te laten werken met paartunneling in de supergeleidende toestand. Voorlopige metingen geven goede hoop op realisatie hiervan. Een interessant aspect van deze experimenten is de mogelijkheid die ze bieden om veronderstellingen

over paar-tunneling en bandbeschrijvingen van deze systemen te testen.

Voor juncties waarvan de capaciteit goed bepaald is, doordat ze in een netwerk zijn opgenomen, is het effect van variatie van tunnelbarrière onderzocht. In de normale toestand wordt bij dunne barrières (de schaal om dat aan af te meten is de verhouding van tunnelweerstand tot quantumweerstand $R_q = h/4e^2 \approx 6.5 \text{ k}\Omega$) de Coulomb blokkade onderdrukt; er treden quantumfluctuaties van de lading op. De experimenten laten goede overeenstemming met theorie zien. Als de tunnelweerstand hoog is, is de lading van de junctie bijna-klassiek. Lading lekt door een netwerk - niettegenstaande de Coulomb-blokkade - in een opeenvolging van tunneling-gebeurtenissen die volgen uit hogere-orde storingsrekening. Is de tunnelweerstand kleiner dan R_q , dan wordt Coulomb-blokkade sterk onderdrukt. In dit geval is de weerstand bij kleine excitatie goed beschreven door de Kubo-formule. In supergeleidende juncties is de verhouding tussen Josephson koppelings- en ladings-energie doorslaggevend. Is de Josephson koppeling de grootste, dan is een "superstroom" door paar-tunneling mogelijk. In het andere geval wordt Coulomb-blokkade waargenomen, maar in dubbele juncties is er nog steeds een mogelijkheid tot paar-tunneling zonder aangelegde spanning, welke afneemt met afnemende verhouding van de karakteristieke energieën. Als de energieën vergelijkbaar zijn wordt een gecompliceerde mengeling zichtbaar van gedrag dat wijst op een klassieke fase en gedrag dat wijst op klassieke lading.

De lading op electrodes van normaal metaal in een 2-dimensionaal netwerk van tunneljuncties, gedragen zich als een 2-dimensionaal Coulomb gas. Er zou daarom een Kosterlitz-Thouless fase-overgang moeten plaatsvinden, waarbij ladingen vrijkomen uit een gebonden dipool-toestand voor temperatuur hoger dan een kritische temperatuur, welke schaal met de ladingsenergie. Als de junctieweerstand kleiner is dan $R_q/0.45$ zorgen quantumfluctuaties voor opbreken van dipolen bij willekeurig lage temperatuur. Voorlopige resultaten ondersteunen deze theorie. Als de netwerken supergeleidende electrodes hebben, wordt verhouding van de karakteristieke energieën - Josephson koppelings- en ladingsenergie - belangrijk. De dualiteit tussen vortices en ladingen in deze arrays helpt bij het begrip. Als de Josephson koppelingsenergie de grootste is, vindt binding van vortices plaats bij afkoeling, resulterend in een supergeleidende toestand. In het andere geval worden ladingen gebonden bij afkoeling, resulterend in een isolerende toestand. De overgang tussen deze twee soorten gedrag is waargenomen bij de voorspelde verhouding van de karakteristieke energieën, met enige aanwijzing voor het optreden van renormalisatie van de junctie-capaciteit.

In de netwerken waar ladingsenergie overheerst, bewegen de elkaar afstotende ladingen op regelmatige afstand, resulterend in een stroomsturing van de juncties in het netwerk. Het resultaat

is dat de stroom-spannings-karakteristiek een negatieve differentiële weerstand laat zien: electron-tunneling wordt verdrongen door coherente paar-tunneling (Bloch-oscillaties) bij toenemende stroom. Het belang van deze waarneming is dat het quantum gedrag van de macroscopische junctie-variabelen laat zien.

VITALS

L.J. Geerligs

- 16 December 1962 Born at Rotterdam
- 1975 - 1981 Atheneum b
at the Willem de Zwijger Scholengemeenschap (Papendrecht)
- 1981 - 1982 Propaedeutics Medicine
at Rotterdam Erasmus University
- 1982 - 1986 Physics at Utrecht University
graduate research on ionic conductors with puls-nmr
in the Condensed Matter Physics group of prof. dr. H.W. de Wijn
- 1986-1990 Ph.D. research at Delft
in the Solid State Physics group, section Superconductivity of
prof. dr. ir. J.E. Mooij